School of Petroleum Engineering

DIFFERENT SCALES AND INTEGRATION OF DATA IN RESERVOIR SIMULATION

By

Lina Hartanto

This thesis is presented for the Degree of
Doctor of Philosophy
of
Curtin University of Technology

October 2004

This thesis contains no material, which has been accepted for the award of any other degree or diploma in any university.

To the best of my knowledge and belief this thesis contains no material previously published by any other person except where due acknowledgment has been made.

Signature: …….

Date: ……...

BORROWER'S PAGE

Curtin University of Technology requires the signatures of all persons using or photocopying this thesis. Please sign below, and give address and date.

ACKNOWLEDGEMENTS

I would like to thank my family and friends for their support.

Special thanks go to Professor Robert Amin from the Woodside Research Foundation for his tireless assistance during this period of research.

I would also like to thank Roxar Pty Ltd for their contribution in providing the support and technical software used throughout this research.

There is no failure except in no longer trying.

Elbert Hubbard

ABSTRACT

The term upscaling and determination of pseudo curves, or effective parameters, used on a coarse-scale simulation grid are related to the complex and extensive problems associated with reservoir studies. The primary strategy mainly focuses on having a good physical and practical understanding of the particular processes in question, and an appreciation of reservoir model sensitivities. Thus the building of the reservoir simulation models can be optimally determined.

By concentrating on the modelling and upscaling gas injection for Enhanced Oil Recovery (EOR) process, which includes Interfacial Tension (IFT) and the amicability effect, a new effective and efficient algorithm of upscaling will be investigated and determined by using several upscaled parameters. The sensitivities of these determined coarse scale parameters (i.e. porosity, absolute and relative permeability and capillary pressure), will also be studied through a history matching of the existing field.

NOMENCLATURE

d/2	the mean horizontal extension of stream tube (average shale continuity) (m)
f_d	the number of shales per unit length (m^{-1})
F_s	shale fraction (dimensionless)
k	absolute permeability in fine cell
K	effective absolute permeability in coarse cell
k_v	vertical perm
k_h	horizontal perm
Q	the flow rate
A	cross sectional area
P	pressure
P_c	capillary pressure
X	length in x direction
μ	viscosity
V	electrical voltage
I	electrical current
R	electrical resistance
K_r	relative permeability obtained by normalizing the effective permeability curves by dividing by the absolute permeability
K'_r	end point relative permeability
K_{rg}	relative permeability of gas
K_{rog}	relative permeability of gas in the presence of oil
K_{row}	relative permeability of water in the presence of oil
K_{rw}	relative permeability of water
K_{rg}*	K_{rg} at the end point
K_{rog}*	K_{rog} at the end point
K_{row}*	K_{row} at the end point
K_{rw}*	K_{rw} at the end point
h	reservoir thickness

L	reservoir length
ϕ	potential of phase i by counting into consideration the gravitational effects [$\phi = P_i - \gamma_i(\Delta z)$]
γ_i	pressure gradient
Δz	depth from the datum
l	reservoir length
$\Delta P/\Delta L$	pressure change across reservoir length
$\Delta \rho g$	density difference
α	dip angle
g	gravitational acceleration
z	elevation potential
PV	pore volume
Vbulk	bulk volume (grid block volume)

Subscript

n, m, p	number of blocks in x, y, z direction
i, j, k	block index
x, y, z	directional indication (x, y, z direction)
A	arithmetic average
AH	arithmetic-harmonic average
G	geometric average
H	harmonic average
HA	harmonic-arithmetic average
g	gas
gc	connate gas
w	water
wc	connate water
orw	residual oil
org	residual gas
i	fluid phase i

xy, xz, yz	direction of the fluid flow i.e. xy is from x to y direction, xz is from x to z direction and yz is from y to z respectively
fine	properties at fine scale
coarse	properties at coarse scale

TABLE OF CONTENTS

LIST OF FIGURES

LIST OF TABLES

Chapter 1.
INTRODUCTION

Prediction of reservoir performance is normally carried out by reservoir simulation. A numerical reservoir simulator approximately solves the equations of fluid flow in the reservoir, based on partitioning of the reservoir into a set of numerical grid blocks. Each grid block is assumed to be homogeneous. In the full field reservoir geological models, grid blocks are typically in the regions of 50m by 50m by 1ft, which is then upscaled to the appropriate size to be used for the reservoir simulation. Consequently, there is a need to 'average' the laboratory data (10cm x 10cm x 10cm) / geological model before using it in the simulators. Herein lies the upscaling problem, as some rock properties, like permeability and relative permeability, cannot simply be averaged arithmetically. The rock properties that need to be upscaled are porosity, absolute and relative permeability and capillary pressure.

Except in the case of truly homogeneous reservoirs, upscaling must always be carried out, although present day practice does not always recognise this as such. For instance, plotting measured relative permeability as a function of normalised saturation, and choosing an average curve as representative, are forms of upscaling which are often used. Such procedures do not take into account the spatial arrangement of the different rock types, and will therefore be unreliable. In media where the ratio between horizontal and vertical correlation lengths is large, for example, the proper upscaled relative permeability may be significantly different from their rock counterparts, even if all participating rock types have identical relative permeability curves.

In history matching reservoir performance, relative permeability is perhaps the first parameter to be adjusted. Somewhat simplistically, this process should be interpreted as 'posteriors upscaling'. The willingness to sacrifice relative permeability signals a perceived unreliability of the priori upscaling originally carried out.

Upscaling is a broad term, also encompassing techniques to increase numerical accuracy at the passage of sharp saturation fronts. The main interest here is more specific: if heterogeneities are small relative to the distance between wells, one can define effective properties of the heterogeneous medium, (effective absolute & relative permeability and capillary pressure). Effective properties are physical parameters valid on the larger scale, and capture the average effect of small-scale heterogeneity.

The software called IRAP RMS provides the necessary upscaling tools to easily coarsen very large reservoir models to sizes acceptable to commercial fluid reservoir simulators. These large models can be manipulated quite easily. The flexibility to create models gives the user the ability to carry out upscaling optimally for the given situations. However, there are several varieties of algorithms for determining the upscaled grid and calculating the upscaled reservoir properties, which are less understood in each algorithm's application.

Furthermore, through personal experiences dealing with geologists and engineers from several different oil & gas companies, an understanding of upscaling methods seems to be very limited. Simple analytical methods (e.g. the harmonic method used for upscaling the permeability and the arithmetic method for porosity) are normally used without knowing the availability of different algorithms and pros and cons of each individual algorithm. In this way, a new effective and efficient algorithm, which will be better understood by our petroleum or oil and gas industries, will be developed through an understanding of the existing upscaling algorithms.

1.1. PROBLEM STATEMENT

In this research, the new effective and efficient upscaling algorithm and procedure will be investigated and proposed throughout the upscaling investigation. The prediction of the reservoir performance at the fine scale with the reservoir simulation model will then be compared against its coarser scale's reservoir performance at

various different reservoir models. These comparisons will then be used to judge how well the new upscaling algorithm, in comparison to the existing upscaling algorithms, is in representing the effective and efficient method of upscaling.

1.2. OBJECTIVES

The objectives of the research are:

- To investigate and to review the available existing algorithms for upscaling by using the existing field throughout the modelling (this includes building an efficient and economical simulation grid) and upscaling gas injection for EOR processes.
- To history match each individual upscaled model and to conclude the efficient and effective upscaled algorithms from the available upscaling algorithm in any given situation.
- To develop and to determine a new efficient and effective algorithm of upscaling by using several upscaled parameters from the reservoir model and test it by history matching the existing field.

1.3. RESEARCH METHODOLOGY

The research will focus in particular on modelling and upscaling gas injection processes. In the course of the research program, a new algorithm for upscaling of the reservoir properties (e.g. porosity, absolute permeability, fluid saturation, relative permeability and capillary pressure) based on a fine grid compositional, or black oil simulation, will be developed. The algorithm will then be implemented as programming script based on Internal Programming Language (IPL) script within IRAP RMS, which will then be tied to the black oil/compositional simulator MORE/Roxar.

In any reservoir study, the upscaling algorithm used is often based on the dimension of the coarse reservoir simulation grid and its dimension of the fine geological grid. The initial step prior to investigating the upscaling algorithm is to create the coarse grid simulation for the full field reservoir study. This step has often become a critical step in determining the effective and efficient upscaling procedure, since the upscaling properties are often related to the dimensional flow within the coarse grid cell. Ideally, for optimum coarse grid buildings, single well models around each individual well are required to be performed so that the understanding of a single well performance (a history match of each individual well in the reasonable coverage drainage reservoir area) can be studied more thoroughly. By examining these single well models, similar characteristics of the geological model may then be grounded into sector models within the full field simulation model. However, this procedure can become time consuming. Therefore, the streamline simulation method will be used to give an indication for fluid flow movement within the particular reservoir units for a further building of the representative of the coarse scale full field model. Each cell within the coarse gridded model will then be filled with its petrophysical properties by using the appropriate upscaling algorithms.

The appropriate upscaling algorithm is normally based on mass conservation, the determination of the coarse scale absolute and relative permeability, porosity, fluid saturation and capillary pressures that minimise the error in the mass (mole number) of each component in all grid blocks at the end of a coarse scale time step. The algorithm differs from other approaches in three main aspects:

- Time steps may be different (longer) in the coarse scale simulation compared to the fine scale simulation. This reflects the true situation, and tends to smooth out noise in the generated pseudo.
- The optimisation is performed on the whole coarse scale model, that is, in all grid blocks simultaneously and not in individual grid blocks.
- Compositional information is utilised. This opens the possibility for simultaneously upscaling phase behaviour and relative permeability. This

possibility has not yet been fully implemented in the code. The necessary additions may, however, be easily implemented.

The selection for effective and efficient algorithms will be mainly based on the conservation of the reservoir heterogeneities (reducing the uncertainties of reservoirs throughout the reservoir geological model and laboratory data) and also the capability of the upscaled parameter data used to match the history of the productions. Furthermore, the accuracy of such effective properties as applied to flow through porous media will be judged by how well the fluid flow prediction made at the coarser (macro-scale) level mimic predictions made at the finer (micro-scale) level. Thus, the research will be based on a data analysis of data from the geologists (reservoir model with its petrophysical parameters), rock laboratory data (PVT, capillary pressure and also the relative permeability curves), and also the study of the flow characteristics of the reservoir.

Chapter 2.
LITERATURE REVIEW

2.1. BACKGROUND OF UPSCALING

In the gas and oil industry, the prediction for hydrocarbon recovery in any oil and gas field generally involves the following modelling cycle:

- Understanding the rock properties through core samples.
- Deriving the well representative of rock properties in log curves based on the understanding of the core.
- Generating the most representative of its log/core understanding in the reservoir geology.
- Quantification of the geological and other relevant static data, into a system of numerical grids.
- Performing and understanding the fluid flow behaviour through static and dynamic reservoir properties with the reservoir computer simulation.

In each of the modelling steps, integrating different scales of data and implementing them accurately can lead to an improvement in reservoir performance prediction.

The first hierarchy for integrating data is to have an understanding of the rock properties through core samples from the well logging. The core sample is typically in the micro scale measurement of 10cm by 10cm by 10cm. From this core sample, an understanding of rock geological characteristics and analysis, such as relative permeability & capillary pressure, are performed. Well logging is then performed to gain an understanding of the reservoir properties (e.g. resistivity, neutron density, etc) along the well trajectory of the log samples. These reservoir properties are then interpreted to relevant reservoir properties for static and dynamic reservoir models.

Through an understanding of the core sample(s), well logs and a geological understanding of the depositional environment, the geologist then builds the geological model. This geological model is typically in the fine scale of 50m by 50m by 1ft, in order to capture the heterogeneity of the reservoir in such detail as represented by numerical grids. Fine scale reservoir models often have between one to 100 million grid cells. However, with the current computing power and further development of current reservoir characterisation technology, the reservoir modeller(s) who is/are normally a group of integrated teams consisting of a petrophysicist, geophysicist, geologists and reservoir engineer, tends to build in much finer scale than before to capture every detail of the heterogeneity in order to reduce the uncertainties.

The next modelling sequence is to perform and understand the dynamic aspect of a reservoir model. This is basically done by integrating an understanding of the static geological model and dynamic fluid flow properties (Fluid Pressure-Volume-Temperature (PVT) relationship, fluid-to-fluid interaction, well inflow performance, etc) in order to predict the reservoir behaviour dynamically. These data are normally integrated by using the reservoir computer dynamic simulation.

However, due to implicit and iterative procedures in this dynamic simulation, the finer details of the geological model cannot be captured due to computer power limitations and required turn around time for any Asset reservoir management decision. Current computing power allows a reservoir simulation to handle only 10 to half million cells depending on the number of components (up to three components of gas, oil, and water in black oil simulation and multi components for Compositional (Equation of State – EOS) simulation) used in the simulation. Thus, the fine scale geological model has to be upscaled to a coarser model that can be handled efficiently by reservoir simulators.

A typical workflow for the reservoir modelling is shown in Figure 2-1.

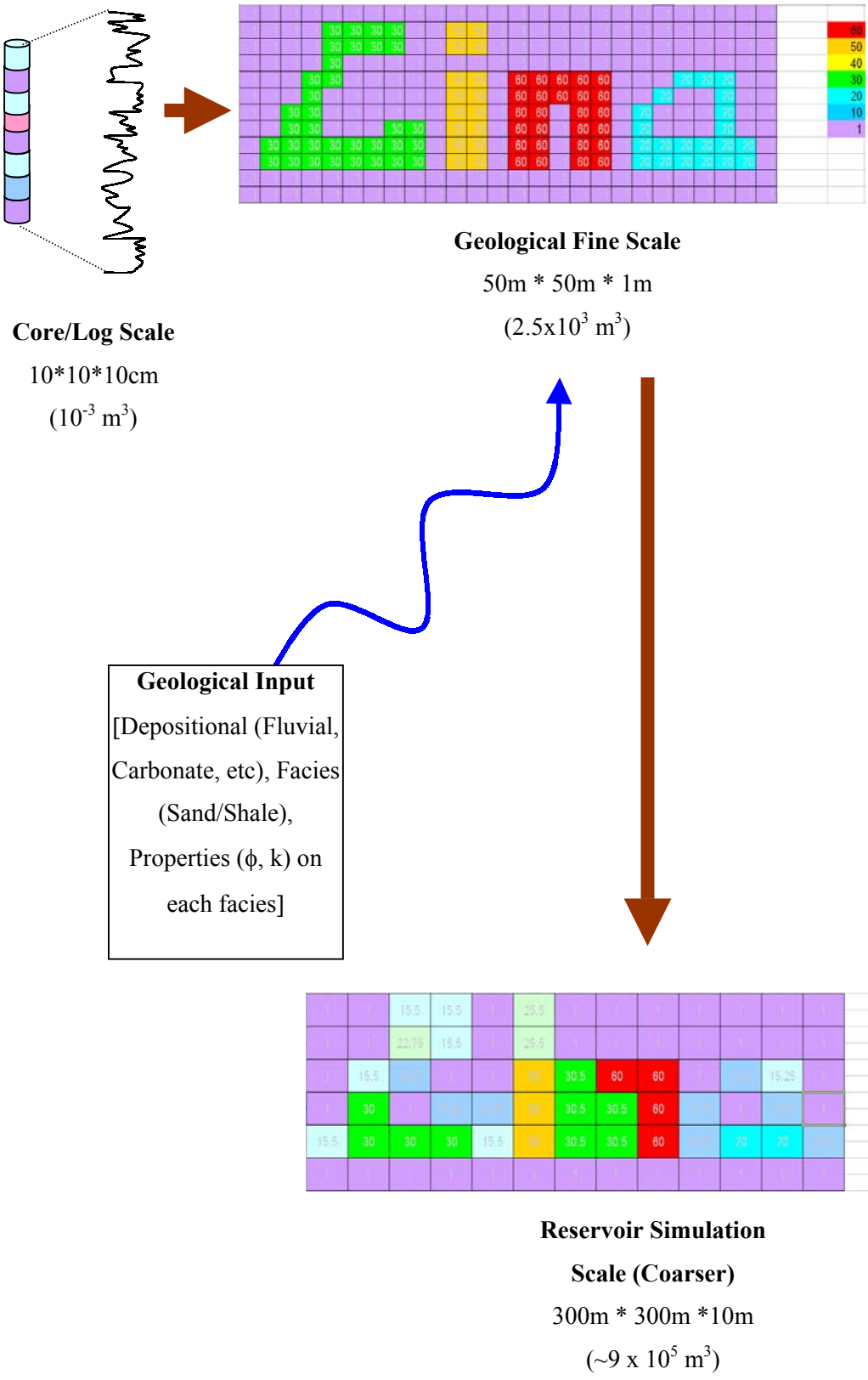

Figure 2-1 Integrating reservoir modelling at different scales for reservoir simulation

Table 2-1 An example of upscaling from core to reservoir simulation model (Reservoir size of 9km x 5km x 0.3km)

Reservoir Size: 9-km x 5-km x 0.3-km					
Scale	**Size**	**No of cells**	**Ratio to Core Scale**	**Ratio to Log Scale**	**Ratio to Geo. Scale**
Core	10*10*10cm (10^{-3} m^3)	$13.5x10^{12}$	1: 1	1: $2x10^{-1}$	1: $4x10^{-7}$
Log data	10cm*10cm*0.5m ($5x10^{-3}$ m^3)	$2.7 x10^{12}$	1: 5	1: 1	1: $2x10^{-6}$
Geological model	50m * 50m * 1m ($2.5x10^3 m^3$)	$5.4 x 10^6$	1: $2.5x10^6$	1: $5x10^5$	1: 1
Simulation model	300m * 300m *10m ($9x10^5 m^3$)	$15 x 10^3$	1: $9x10^8$	1: $1.8x10^8$	1: 360

In the integration of different scales for the reservoir simulation, upscaling from a core scale to the required scale of reservoir simulation is involved. As shown in Table 2-1, a single cell in the geological model represents in the order of a quarter of a million core samples as a single value. This core/log data will be upscaled at the well locations of the reservoir model to represent the single cell of the geological model. Properties along the well locations and an understanding of the geological depositional in the reservoir will then be used to represent the entire area of the reservoir. Thus, most of the heterogeneity properties along the well location will be smoothed and homogenised to represent the size of the reservoir. Also, around a few hundred of the geological scale cells will then be upscaled and smoothed further to represent a single cell in the reservoir simulation model. In this way, properties with correlation lengths less than the size of the reservoir simulation scale disappear, while the long-range correlation lengths remain in the model.

In any reservoir predictions, either in geological or reservoir simulation scales, a realistic description of reservoir behaviour under any depletion scheme is probably the most important factor. Permeability, which describes the ability of fluid to flow

through the connectivity of the pores of the rock in the porous media, is the major parameter that affects reservoir behaviour. In upscaling, permeability is really a complicated matter, as it is not an additive variable (i.e. the equivalent permeability in the reservoir scale cannot be represented by arithmetic means). The expected permeability values have in general decreased and permeability variance has also decreased in reservoir simulation scales compared to much finer scales such as geological or core scales. Consequently, reducing the number of cells in any scale results in reducing the accuracy of the parameter model and also smoothing the ability to describe the heterogeneity flow behaviour in the reservoir model. Therefore, a balance is required between the loss of accuracy due to the smoothing (averaging) process and the gain in computer speed due to fewer numbers of grids.

Another important concept in upscaling is finding the most representative of the effective grid cell values at larger reservoir simulation modelling scales. The degree of its accuracy is normally judged by how well the fluid flow predictions made at its coarser (macro scale) level mimic the predictions made at its finer (micro scale) level. If at all possible, the upscaling methodology should not be applied directly to the solution at the fine scale, as the purpose of upscaling is to avoid conducting such time-consuming flow simulations.

With recent developments on the geo-statistical stochastic simulation, the geological model can then be generated in high resolution for capturing any details of the reservoir heterogeneity by integrating data from core measurements, well logs, seismic and geological features, covering a broad range in the scale of measurements. In this way, no matter how fast the computer and technology used will be, upscaling from the fine geological model to the reservoir simulation model will be intensive and will remain a challenge in providing answers to the most representative effective permeability at the macro level.

2.2. CLASSIFICATION OF UPSCALING METHOD

Research has been on going to find and develop a new algorithm that gives the best representation for calculating the effective properties of fluid flow. Several of these algorithms are publicly and commercially available for upscaling by using either analytical or numerical approaches and even generating pseudo functions (pseudo relative permeability and capillary pressure) based on the reservoir simulation of the fine grid model. Simple methods, such as arithmetic, geometric and harmonic averages to the more complicated tensor methods, such as diagonal and full tensor methods, have been developed and exist commercially. Pseudo generation methods such as those Hearn, Kyte & Berry and Stiles methods are also available in determining the pseudo fluid properties to be represented at the coarser scale based on the fine scale of the reservoir simulation properties.

In this section, different existing upscaling algorithms, which mainly focus on the available algorithms in Roxar's IRAP RMS, will be discussed further. Each individual algorithm's function, advantages and disadvantages and also usefulness to a specific case will be captured in the discussion.

2.2.1. Analytical method

2.2.1.1. Arithmetic, geometric and harmonic averages

The analytical methods such as arithmetic, geometric and harmonic averages, have been regarded as the fastest and intuitively simple methods for upscaling. Earlier research by Warren and Price in 1961 and Bower in 1969 indicated that the effective permeability behaved geometrically based on a Monte Carlo simulation and analog simulation in 2D flow field respectively. Further analysis by Freeze in 1975 indicated that the harmonic mean is representative of the homogeneous conductivity

based on the steady state and 1D transient ground water flow in non-uniform media (Mansoori, 1992, p.67).

The arithmetic, harmonic and geometric averages can be expressed as shown in Equation 2-1, Equation 2-2 and Equation 2-3 respectively.

$$K_{x,A} = \frac{1}{nmp} \sum_{i,j,k} k_{xi,j,k}$$

Equation 2-1 Arithmetic Average

$$K_{x,H} = \frac{nmp}{\sum_{i,j,k} k_{xi,j,k}^{-1}}$$

Equation 2-2 Harmonic Average

$$K_{x,G} = \left[\prod_{i,j,k} k_{xi,j,k} \right]^{1/nmp}$$

Equation 2-3 Geometric Average

Some of these methods (e.g. harmonic and geometric methods), however, would be disadvantageous if there was a nil value present in the fine scale system, which is sometimes defined as a non-flow or barrier in the system (shale or undefined/non-active cells in the system). With any nil value present in the system, the effective permeability would create an undefined heterogeneity of the reservoir. Thus, it is resulting in a limited range for validity. Furthermore, any undefined heterogeneity of the reservoir needs to be reported, such that a treatment in barrier preventing any vertical communication through it and a vertical permeability (Kv) determination for blocking the wells can be treated appropriately.

In addition to these nil value limitations, these methods can only solve a single direction of the effective permeability for determining the effective permeability (i.e.

a simple 1D or 2D reservoir model). This is not the case in real life, as permeability is a directional property of fluid flow in porous media. It therefore requires more complex calculations than that of the three-dimensional approach. Furthermore, it suffers from some limitations in applicability. (Beggs *et al*., 1993, p. 143-148, Durlofsky *et al*., 1995, p. 53-66)

Most reservoirs are generally more laterally homogeneous compared to their vertical direction. Therefore, due to the reservoir's heterogeneity nature, arithmetic average, as it is derived based on parallel sequences of layered reservoir beds, is believed to represent the upper bound of the effective permeability value. On the other hand, on the vertical direction of the reservoir bedding, it is more heterogeneous compared to its lateral directions. Therefore, harmonic average, as it is derived based on serial sequences of beds or perpendicular to the bedding, is believed to represent the lower bound of the effective permeability values by taking into consideration the lowest permeabilities as the dominant ones. Derivations of these algorithms are summarised in Appendix A.

According to Dagan in 1979, this theory holds true, as the effective permeability is between the arithmetic and harmonic mean of the heterogeneous reservoir. Furthermore, Dagan (1982) also states that under unsteady states, the effective hydraulic conductivity is time dependent and shows a deviation from arithmetic means at an early time. Thus, the reservoir will first flow laterally compared to its vertical direction as they are behaving more homogeneously and more connected compared to the vertical flow. (Mansoori, 1992, p. 69)

The geometric average algorithm is also believed to take into consideration both harmonic and arithmetic effects of the effective permeability (i.e. the mid point between the upper and lower bound of the effective permeability values). It is a good estimator for lognormal isotropic fine scale permeability when the range is smaller than the size of the coarse scale block. Also, when the permeability is distributed randomly to flow direction, that is, in a heterogeneous, unstructured

reservoir, this geometric average will be a good estimator. Thus, it is often used conventionally as the effective permeability value for numerical simulations.

The above statement concurs with Smith and Freeze's (1979) findings. They stated that the geometric mean would accurately predict the average behaviour of hydraulic conductivity, which statistically would behave homogeneously with isotropic covariance function. However, in 2D and 3D, this simple algorithm can become less accurate as the effective conductivity is a function of spatial distribution and system dimensionality. Furthermore, this tends to influence the lower permeabilities in many reservoirs and disregard the potentially significant high permeability streaks, which will be the main preferential path in the reservoir. (Mansoori, 1992, p. 67)

The selection for these mentioned algorithms is normally based on the rock fabric and fluid flow direction. However, this is only realistic if certain conditions are met, such as single-phase fluid in homogeneous, or simple heterogeneous, reservoirs with continuous layers. For complex reservoirs, these algorithms are no longer valid and upscaling with numerical simulations will be required which involves running the fine grid simulation to calculate the effective permeability at a coarser scale.

2.2.1.2. Power average

Another analytical algorithm that can be used is the power average. It is a fast and simple intuitive method similar to any other analytical algorithm. Journel *et al*. (1986) based his experiment on the indicator approach to generate realisation of sand shale proportion in the system. He generated the permeability field, which was highly variable, highly anisotropy and whose spatial distribution and correlation covered multiple scales of variability. It was found that the effective permeability, based on a Monte Carlo simulation for various shale/sand proportions, could be fitted using the power average model. (Mansoori, 1992, p.67)

The equation of power average is shown below in Equation 2-4.

$$k_{x,P,\omega} = \left[\frac{1}{nmp} \sum_{i,j,k} k_{xi,j,k}^{\omega} \right]^{\frac{1}{\omega}}$$

Equation 2-4 Power average

The power average model requires the power factor, which should be in the range of between –1 and 1. The power factor of –1 (ω=-1) basically represents the harmonic average, while the power factor of 1 (ω=1) represents the arithmetic mean. The power factor of 0 (ω=0) represents the geometric mean of the heterogeneous system. From Journel *et al.*'s (1986) experiments, it was also found that a power factor of 0.57 (ω=0.57) is the best-characterised horizontal flow in shale-sand environments, and a power factor of 0.12 is the best characterised for vertical flow (Mansoori, 1992, p. 67).

The drawback of the power average is similar to the rest of the analytical methods, which are limited to solving only in 1D or 2D directions and also misleading with the presence of nil values for power factors less than 0. Choice of the power parameter is normally very tedious as we are never sure what the appropriate value of this parameter will be. This factor, however, is quite sensitive to such factors as the shale geometry, dimensions of blocks relative to correlation range and its nature to multi model distribution.

Gomez-Hernandez and Gorelick in 1989 found that the effective hydraulic conductivity could be determined based on power average models using exponents between harmonic and geometric mean distribution. They based their research on the investigation of spatial variability of aquifer hydraulic conductivity influences on hydraulic head, under steady state flow for a stochastic approach with conditional and unconditional simulation. They also stated that the effective hydraulic conductivity is a function of distribution type, anisotropy, correlation length and boundary conditions. (Mansoori, 1992, p. 67-68)

Deutsh in 1989 compared the power average and percolation model to correlate the relationship between effective permeability and volume fraction of 'shale and shale' anisotropy. The graphical procedure was developed for determining the power exponent from shale aspect ratio, shale volume fraction and shale/sand permeability. Both methods are equally suitable for fitting the observed correlation. This power average could be very superior due to its simplicity and only requires a single exponent parameter to be determined to fit into the power average model for calculating the effective parameter, as opposed to three parameters required for the percolation model (Mansoori, 1992, p. 67).

Furthermore, the power exponent is often calculated to replicate the performance of the more computing extensive fluid flow based methods and to determine a proper chosen exponent. In this way, it becomes particularly useful and less time consuming for upscaling a large number of realisations of a reservoir.

2.2.2. Directional dependent averages (arithmetic-harmonic and harmonic-arithmetic averages)

Directional dependent averages (arithmetic-harmonic and harmonic-arithmetic methods), have been developed in order to simplify the determination of effective properties in three-dimensional models.

These directional dependent averages were derived based on an understanding of how the arithmetic and harmonic averages were derived. As mentioned earlier in Section 2.2.1.1, the arithmetic average should apply to parallel sequences of the reservoir beds in a particular direction, while the harmonic average should apply to the vertical direction perpendicular to the reservoir bedding.

In determining the effective permeability in the x-direction using the arithmetic-harmonic average, the arithmetic is firstly applied within the plane and then followed by the harmonic mean of the plane's values of the series of arithmetic averages. This

determination of effective permeability is then applied to the y and z directions to obtain the cell's effective permeability in x, y and z directions. According to most published papers and research, the arithmetic-harmonic average is believed to represent the upper bound of the effective properties.

The harmonic-arithmetic average is derived similarly to the arithmetic-harmonic average. However, the harmonic average along the 1D stack in the particular direction will be applied first, before applying the arithmetic average of all the stacks. Also, similarly to arithmetic-harmonic averages, y and z directions are then applied accordingly to the principal direction with the same derivation of algorithms. This algorithm is believed to represent the lower bound of the effective permeability.

These directional dependent averages are illustrated in Equation 2-5 and Equation 2-6 for arithmetic-harmonic and harmonic-arithmetic averages respectively.

$$K_{x,AH} = \frac{1}{nm} \sum_{i,j} \frac{p}{\sum_{k} k_{xi,j,k}^{-1}}$$

Equation 2-5 Arithmetic-harmonic average

$$K_{x,HA} = \frac{p}{\sum_{k} \frac{nm}{\sum_{i,j} k_{xi,j,k}^{-1}}}$$

Equation 2-6 Harmonic-arithmetic average

However, similar to harmonic averages, these directional methods would still suffer with the nil values. Also, the effective properties may not always lead to accurate results, but they are generally honour detailed reservoir descriptions.

With the knowledge of how these directional dependent averages were derived, the effective permeability was found to be bounded between arithmetic-harmonic and harmonic-arithmetic averages as the upper and lower bound of the effective

permeability values respectively. These bounds are known as the Cardwell and Parsons (1945) bounds. (Renard *et al*., 1997, p. 256)

2.2.2.1. Renormalisation

In addition to these analytical averages, a renormalisation method has been developed and used in many reservoir studies. It is based on the analog electrical network principal and successful star-triangle transformation. The effective permeability was estimated by averaging over small regions (2x2x2 of the fine scale block) to form a new 'average permeability' distribution with lower variance (reducing the variance) than the original scale. Further reduction in variance at the intermediate scale is then carried out before ending up with the coarse block size. Each step is upscaled using the appropriate method, such as single-phase flow simulation, with the effective medium conductivity calculation. (King *et al.,* 1988, p.217-234)

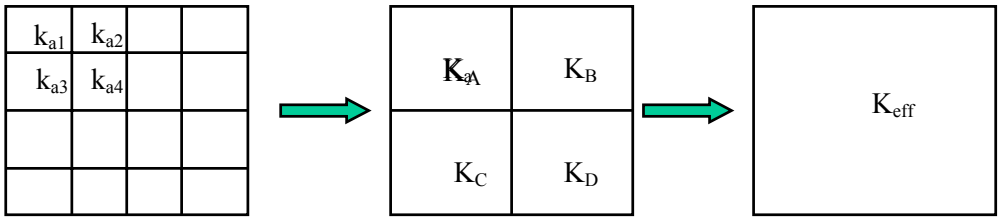

Figure 2-2 Renormalisation method

This renormalisation algorithm is based on a successive upscaling to obtain the properties at the required scale. It is faster than upscaling in one step iteration, but can become less accurate. In general, this method has been regarded as the fastest way to estimate effective properties by carrying out successive upscaling to obtain properties at the required scale. It is more accurate compared to simple averaging methods, but it is slower in terms of its CPU performance. It is a good estimator as it takes into account heterogeneity on several length scales, but this algorithm cannot be used with a 'skin' region to account for flow outside each coarse grid.

This renormalisation algorithm is also good for taking large problems and breaking them down into a hierarchy of manageable problems, as has been proven successfully in theoretical physics areas. It imposes a diagonal pressure gradient, which results in significant fluxes across all block interfaces, allowing flow accuracy to be tested on a block-by-block basis (Lozano *et al*., 1996, p. 328-338). However, this upscaling method is only a local upscaling procedure. It is poor for highly anisotropy media and probably unreliable due to unrealistic boundary condition effects. (Beggs *et al.,* 1993, p. 143-148, Christie, 1997, p. 105-113, Christie *et al.,* 1995, p. 353-361, Durlofsky *et al*., 1995, p. 53-66, Lemouzy *et al.,* 1993, p. 1-8)

Further developments of this renormalisation method have also been carried out by Le Loch (two meshes with simplified renormalisation), Kruel-Romeu (direct formulation with permeability assigned to each link between two nodes rather than block surrounding nodes), Gautier and Noetinger (complete tensor by periodic boundary conditions) and Hinrichsen et al. (directional permeability). (Renard *et al.,* 1997, p. 260-261)

2.2.3. Numerical method

Several numerical methods, such as the diagonal and full tensor methods, are also available based on Darcy's law of flow equation and the law of mass conservation on each volume represented by a coarse grid block. Thus, this method represents the solution of flow equation and yields the diagonal tensor of the permeability in nature. By applying the relevant boundary conditions for the calculations, the directional effective permeability, the x, y and z directions, can be determined. Nil values can also be delimited by using these methods.

For these numerical methods, can these boundary conditions approximate the true reservoir conditions? (Aasum *et al.,* 1993, p. 679-692, Durlofsky *et al.,* 1995, p. 53-66, Mansoori, 1992, p. 66-68, Renard *et al.,* 1997, p. 272-275)

2.2.3.1. Diagonal tensor based on periodic boundary conditions

The diagonal tensor algorithm is basically based on Darcy's law fluid flow equation and the law of mass conservation. The following diagram in Figure 2-4 is the basic principle of the diagonal tensor algorithm.

The geometry of the fine scale cells is firstly calculated and determined in the calculation. The appropriate pressure drop and the boundary conditions in the specific directions are then applied and calculated to determine the effective properties. This basically applies some pressure on the inlet to force the fluid flow from left to right in the x direction, while assuming that there is no flow across to the other directions, as shown below as a solid line. The boundary condition is specified to be at a constant pressure of one at the inlet stream and a constant pressure of 0 at the outlet stream.

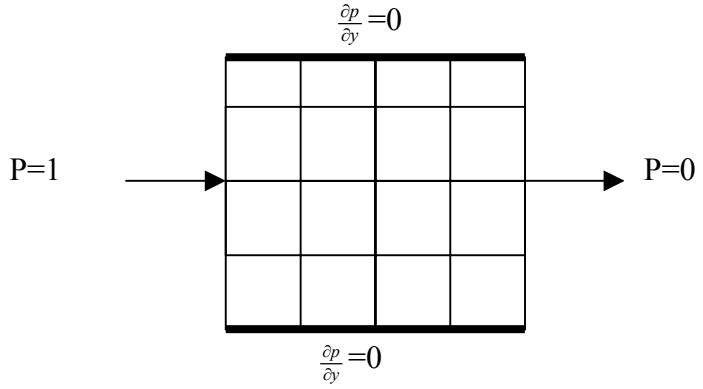

Figure 2-3 Pressure & boundary condition assumptions for diagonal tensor

The pressures in each fine scale grid inside the coarse grid block and the mass flux across the system are solved by applying appropriate Darcy's law fluid flow equation and the mass conservation equation as shown below:

$$q = \frac{k.A}{\mu}\nabla P \qquad \textbf{\textit{Or}} \qquad \upsilon = k.\nabla P$$

Equation 2-7 Darcy's law of fluid flow equation

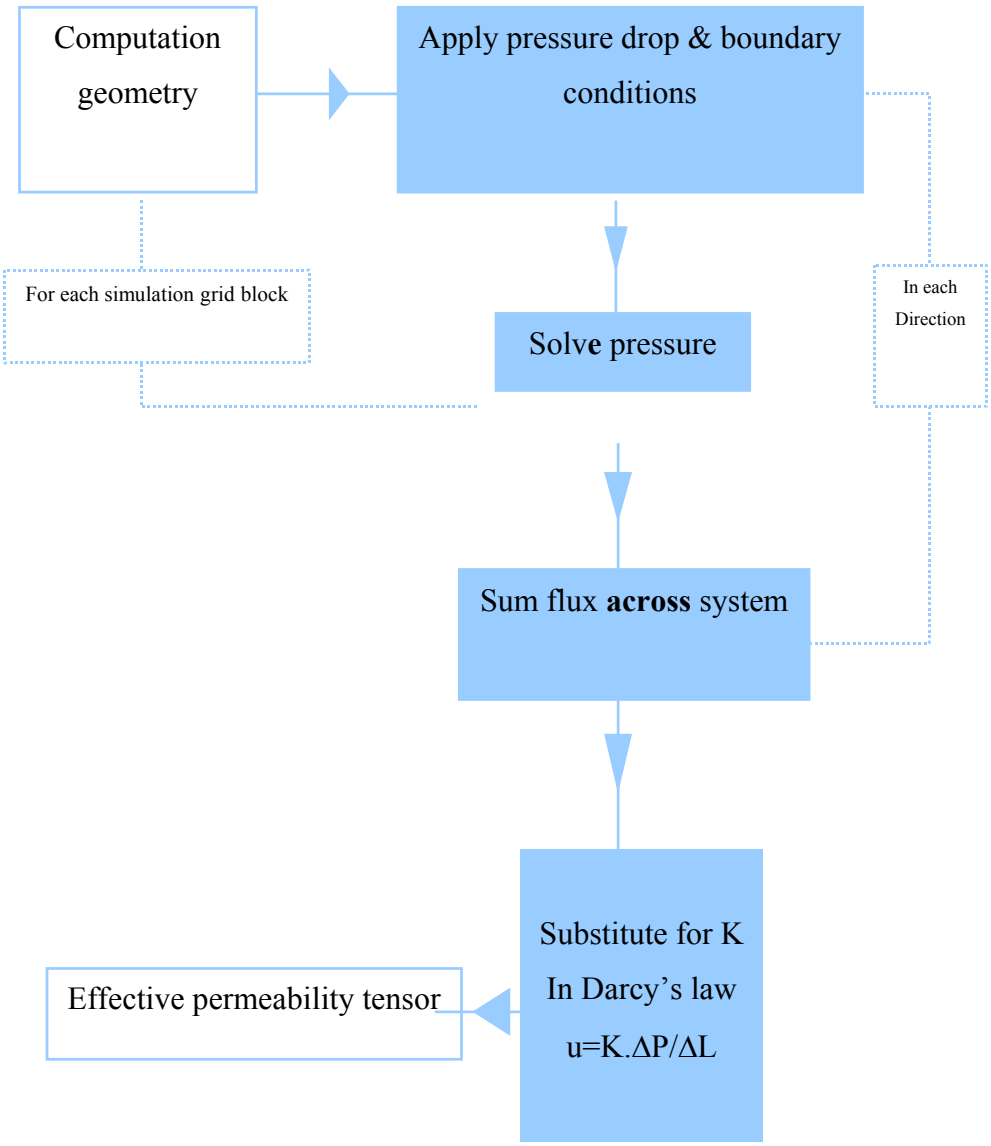

Figure 2-4 Process flowchart on how diagonal tensor is derived

In reality there should not be a change in flux between the fine grid system and the single coarse grid system. Hence, the flux across the system is then summed up to obtain the single value flux at the coarse grid.

By using Darcy's equation again, the effective permeability can then be obtained.

$$k_{eff} = q_{finescale} \Delta x / A$$

Equation 2-8 Effective permeability by rearranging the Darcy's law equation

The above procedures are then repeated to obtain the diagonal tensors permeability (k_{xx}, k_{yy}, k_{zz}) by applying a periodic boundary to the appropriate directions.

2.2.3.2. Full tensor based on periodic boundary conditions

Diagonal tensor can only determine in the principal directions of the effective permeability (x-x, y-y and z-z directions). In reality, the bedding of the reservoir rock is not parallel or in series. The alignment of the bedding could be cross flow and parallel in an angle to the directional of pressure gradient. Thus, diagonal directions (x-y, y-z, and x-z) of permeability are required. These diagonal principal directions of effective permeability can be determined by using the full tensor method, where the various terms reflect the spatial variations of permeability in both magnitudes and directions.

A full tensor algorithm is basically derived on a similar principal to the diagonal tensor. The full permeability tensor is redefined with Darcy's law as follows:

$$\upsilon = k_F.\nabla P = \begin{bmatrix} k_{xx} & k_{xy} & k_{xz} \\ k_{xy} & k_{yy} & k_{yz} \\ k_{xz} & k_{yz} & k_{zz} \end{bmatrix}.\nabla P = k_D.\nabla P$$

Equation 2-9 Full tensor effective permeability based on Darcy's law equation

The input permeability tensor must be symmetrical and positive definite. Since K_F is positive definite, the equation $\upsilon = K_F.\nabla P$ can be solved, in principle exactly with respect to ∇P. Since the dimensions of this equation are only three, and the program finds the solutions from a direct method. Certain ill-conditioned full tensor permeabilities can however give significant errors in this procedure. Given the gradient pressure ∇P, the diagonal permeability tensor is then calculated.

The above Equation 2-9 can then be simplified to a diagonal tensor algorithm as it only considers the principal directional flow of permeability.

$$k_{D\cdot}=\begin{bmatrix} k_{xx}+k_{xy}\dfrac{\partial_y p}{\partial_x p}+k_{xz}\dfrac{\partial_z p}{\partial_x p} & 0 & 0 \\ 0 & k_{yy}+k_{xy}\dfrac{\partial_x p}{\partial_y p}+k_{yz}\dfrac{\partial_z p}{\partial_y p} & 0 \\ 0 & 0 & k_{zz}+k_{xz}\dfrac{\partial_x p}{\partial_z p}+k_{yz}\dfrac{\partial_y p}{\partial_z p} \end{bmatrix}$$

Equation 2-10 Diagonal tensor effective permeability as a result of simplifying full tensor (If $\partial p/\partial x = \partial_x p \neq 0, \partial_y p \neq 0, \partial_z p \neq 0$)

The effective permeabilities on the principle diagonal directions, i.e. x-y, x-z, y-x, y-z, z-x and z-y have been neglected. However, these principal directions of effective permeability will be neglected by the reservoir simulators, as there is no available simulator to handle these principal direction permeabilities. (Aasum *et al.,* 1993, p. 679-692, Christie, 1997, p. 105-113)

2.2.3.3. Rate equivalent upscaling and rate equivalent upscaling to tensor

Other known upscaling methods are ‘rate equivalent upscaling’ and ‘rate equivalent upscaling to tensor’. Both methods use a similar method to diagonal/full tensor methods by utilising Darcy’s law and finite element solver for three diagonal elements of tensor. However, they use the iterative linear finite element solver to solve three linear elements simultaneously based on finite difference and a preconditioned conjugate gradient method. Irregularity of flow within a simulation block is approximated and full (symmetric) permeability tensor is used.

The difference between these two rate equivalent upscaling methods is that rate equivalent upscaling uses the mass conservation for pressure within a large scale block, while the rate equivalent upscaling to tensor uses the similarity of energy dissipation through large-scale as through fine-scale blocks.

Furthermore, these methods are often more time consuming than other upscaling methods.

2.2.4. Inequalities theoretical bounds and its averaging mean for equivalent permeability

Several inequalities for determining the equivalent effective permeability have been known and published. In this section, several algorithms based on the averaging means of the theoretical bound will be discussed here.

2.2.4.1. Theoretical bound of effective permeability

The fundamental inequality is known as Wiener bounds as this inequality is always valid. The effective permeability is bounded by the harmonic mean and the arithmetic mean of the fine grid permeabilities.

$$k_H < k_{eff} < k_A$$

Equation 2-11 Wiener bounds

The above inequality is then developed further with the directional dependent averages (arithmetic-harmonic mean and the harmonic-arithmetic mean). It is stated that the harmonic-arithmetic mean is the lower bound of the effective permeability, while the arithmetic-harmonic mean is the upper bound of the effective permeability. Therefore, the upscaled effective permeability can be found within the following theoretical bounds in Equation 2-12.

$$k_H < k_{HA} < k_{eff} < k_{AH} < k_A$$

Equation 2-12 Inequality for the effective permeability

2.2.4.2. Averaging mean of the theoretical bounds for determining the effective permeability

In determining the effective permeability, some algorithms have been developed based on the averaging mean of the theoretical bounds Equation 2-12. These algorithms are normally easy to implement for upscaling the effective permeability at the coarser scales. They also tend to be very fast in term of computational speed in comparison with numerical upscaling methods.

Matheron (1967) published the effective permeability as being determined from the power average of the two theoretical bounds (harmonic and arithmetic means) as shown in Equation 2-13. (Renard *et al.,* 1992, p. 257)

$$k_{eff} = k_A^{\alpha} k_H^{(1-\alpha)} \quad ; \quad \alpha \in [0,1]$$

Equation 2-13 Matheron bounds

If the permeability field in the fine scale is homogeneous and isotropic, then the power parameter, α, can simply be defined in the following equation:

$$\alpha = \frac{(D-1)}{D}$$

Equation 2-14 Matheron's α parameter for isotropic and homogenous medium, where D is the space dimension i.e. in 3D, $\alpha = 1/2$

If the permeability is in three-dimensional fields, then α parameter is equal to 1/2. The above Equation 2-14, has then become the geometric mean of the two theoretical bounds, which is also well known as Cardwell Parson's equation. A similar equation has also been known as Kruel–Rumeu (1994) or Guerillot (1990)'s equation.

$$k_{eff} = \sqrt[2]{k_H k_A} \quad \text{or} \quad k_{eff} = \sqrt[2]{k_{HA} k_{AH}}$$

Equation 2-15 Cardwell Parson equation

Ababou (1995) has also developed an alternative equation for determining the α parameter in isotropic and homogeneous media (Renard *et al.,* 1992, p. 257). It is shown in the following equation:

$$\alpha = \frac{(D - L_h / L_r)}{D}$$

Equation 2-16 Ababou equation, where Lh is the harmonic mean of the correlation length in principal direction and Lr is the harmonic mean of the correlation length in the relevant direction

Another method that is the averaging mean of the theoretical bound is Lemouzy's equation. The equation is shown below:

$$k_{eff} = \sqrt[b]{k_1^2 k_2^2 k_3^2 k_4^2}$$

where

$$k_1 = k_{\mathrm{h}}^{\mathrm{x}}(k_{\mathrm{a}}^{\mathrm{y}}(k_{\mathrm{a}}^{\mathrm{z}})) = k_{\mathrm{h}}^{\mathrm{x}}(k_{\mathrm{a}}^{\mathrm{z}}(k_{\mathrm{a}}^{\mathrm{y}}))\ ;$$

$$k_2 = k_{\mathrm{a}}^{\mathrm{y}}(k_{\mathrm{a}}^{\mathrm{z}}(k_{\mathrm{h}}^{\mathrm{x}})) = k_{\mathrm{a}}^{\mathrm{z}}(k_{\mathrm{a}}^{\mathrm{y}}(k_{\mathrm{h}}^{\mathrm{x}}))\ ;$$

$$k_3 = k_{\mathrm{a}}^{\mathrm{x}}(k_{\mathrm{h}}^{\mathrm{y}}(k_{\mathrm{a}}^{\mathrm{z}}))\ ; k_4 = k_{\mathrm{a}}^{\mathrm{z}}(k_{\mathrm{h}}^{\mathrm{y}}(k_{\mathrm{a}}^{\mathrm{x}}))$$

Equation 2-17 Lemouzy equation

A similar equation to Lemouzy (1991)'s equation has been developed by Kruel and Rumeu (1994) by using variable exponents that influence the anisotropy of the media.

These averaging methods of the theoretical bounds are only used for estimating the effective permeabilities. Furthermore, if there are any undefined values due to the presence of nil values, the invalid results obtained will be based on the averaging means of the theoretical bounds.

2.2.5. Pseudo method

There are also several multiphase upscaling algorithms, which have been used widely for the reservoir upscaling. It is relatively complicated compared to the single-phase upscaling as it involves a complex solution for non-linear with coupling between rock properties and fluid flow effects. There are two categories for pseudo methods, which are static and dynamic pseudo methods. Each method will be discussed in detail.

2.2.5.1. Static pseudo method

The static pseudo method is possibly the simplest form of the pseudo methods. Pseudo properties are normally generated for inputs to the reservoir simulation and dynamic impacts such as the variability of pressure with respect to time and other properties are ignored in this method. The most widely used static pseudo methods are probably the Coats, Hearn, Stiles and Dykstra/Parson methods.

Prior to use of any of the above mentioned static pseudo methods, the following constant ratios are normally determined in order to choose the appropriate fluid movement criteria (capillary, viscous or gravity domination).

$$N_{Pc/\mu} = \frac{k_v \Delta PcL}{k_h \Delta Ph}$$

Equation 2-18 Capillary to viscous number

$$N_{\rho/\mu} = \frac{k_v \Delta \rho g \cos\alpha L}{k_h \Delta P}$$

Equation 2-19 Gravity to viscous number

Another parameter to be determined is the vertical equilibrium (VE) number, which indicates the dominated redistribution of the fluid in dip normal direction compared to the fluid movement in the areal directions.

$$N_{VE} = N_{\rho/\mu} + N_{Pc/\mu}$$

Equation 2-20 Vertical equilibrium number

The fluid in the reservoir will be vertically segregated when the VE number is considerably larger than one and the capillary to viscous number is significantly smaller than one. In that case, the Coats' method can be applied with zero capillary pressure. It is applied for reservoirs with two to three phases. It assumes that the intermediate phase (second phase for a two phase reservoir) is a reference phase of capillary pressure (usually oil phase).

The following table summarises the criteria of selection for the appropriate static pseudo method.

Table 2-2 Criteria for selecting the appropriate static pseudo method

Method	**Criteria**
Coats	Vertical equilibrium, segregated flow ($N_{VE} > 1$, $N_{pc/\mu} < 1$)
Hearn	Vertical communication, piston like displacement, viscous dominated ($N\rho_{g/\mu} < 1$)
Stiles	Non communicating layer, piston like displacement, mobility ratio = 1 ($N_{VE} < 1$)
Dykstra/Parson	As Stiles, mobility ratio not equal to 1 ($N_{VE} < 1$)

Coats started the static pseudo method with the assumptions of vertical equilibrium and segregated flow (i.e. Vertical equilibrium number > 1 and capillary to viscous number < 1).

For a reservoir with good vertical communication within layers and dominated by viscous forces (small gravity to viscous number), there should be a 'piston like' displacement in each layer. In this case, the Hearn method is suitable for use.

In the case where a reservoir has low permeability and/or a barrier to vertical flow (non-communication within reservoir layers), it may have a vertical fluid distribution that is independent of gravity and capillary effects. The displacement process in these types of reservoirs will be characterised by a small value of vertical equilibrium number. When displacement is piston like and the mobility ratio is equal to one, the Stiles' method can be used to generate pseudo relative permeability. For mobility not equal to one (no restriction with mobility ratio), the Dykstra/Parson method, which is an extension of Stiles' method, can then be used.

2.2.5.2. Dynamic Pseudo Method

The multi phase upscaling procedure normally involves the following steps:

- Generating the fine grid simulation of a (small) representative area of the reservoir.
- Performing an averaging step(s) to obtain the averaged rock properties (porosity, absolute permeability, reservoir pressure) at each time step.
- Creating a pseudo relative permeability table and pseudo capillary pressure table at each time step.

This method is normally referred to as the 'dynamic pseudo' method. The result at a coarse grid with the average properties should give comparable results to the fine grid simulation. However, this multiphase upscaling can become very time consuming, as it requires the generation of the fine grid cell simulation prior to obtaining information required at the coarse cell. Due to the involvement with much finer scales and huge numbers of grid block cells, it would also require extensive computer power to solve the simulation at the fine scale. Furthermore, the set of

pseudo functions generated for the coarse scale is problem specific. Thus, for new requirements at the coarse scale, the whole procedure must be repeated to obtain the necessary information. Also, this method makes it hard to generate any other flow geometries.

Another well known problem associated with generating pseudo relative permeabilities, is that the values can become greater than one, or negative or infinite. The values greater than one can be attributed to discrepancies in the averaging of relative permeability or transmissibility and can become the correction for this discrepancy. Negative pseudo relative permeability is inherent in results of the dynamic pseudo algorithm and the coarsening of the chosen grid. This could be due to flow alignment to the predominant flow parallel to other grid directions, or the net flow of a phase to be in the reverse direction to the average potential difference. The infinite values of pseudo relative permeability are due to non-zero net flow with the zero value of the average potential difference. Should any of the above-mentioned problems occur, the pseudos generated by this method could become impractical and a different coarsening pattern with the repeated procedures would be required.

The Kyte and Berry (1975) method is very well known and widely used for generating pseudo properties, but it is also widely believed to be unreliable, although there is little published evidence for this. A similar method is the 'pore volume weighted' method, which differs from Kyte and Berry's only in the use of a different formula to determine average pressure. (Kyte & Berry, 1975, p. 269, Barker *et al.,* 1997, p. 138-143)

All the relevant fine grid variables such as reservoir properties, fluid properties, flow variables and transmissibility are required to be averaged for the coarse grid cell. The transmissibility is normally averaged with either arithmetic and/or harmonic algorithm(s) depending on the considered component of the absolute permeability. For most other variables, such as density and viscosity, the pore volume weighted average is normally applied.

With the Kyte and Berry method, pseudo relative permeabilities are normally averaged by substituting the fine grid simulation with Darcy's law of equation for reproducing the fine grid flows at the coarse grid level. The pseudo relative permeabilities at a coarse grid block boundary face are averaged with the transmissibility weighted average to obtain the pseudo relative permeability table(s) as shown in the following equation.

$$q = T_r k_r (\Delta P + \rho g h) / \mu$$

$$q = q_1 + q_2 + q_3 + q_4$$

$$\frac{1}{T_r} = \sum \frac{1}{\sum T_r}$$

$$k_r = \frac{\sum k_r T_r}{\sum T_r}$$

Equation 2-21 Kyte and Berry method for pseudo relative permeabilities

For the pseudo capillary pressure of a face, it is found by subtracting the average reference pressure from average pressure of the considered phase. Averaging methods for potential difference are:

- Original Kyte and Berry method.

$$P = \frac{1}{K k_r A} \sum P_i K_i k r_i A_i$$

- Pore volume weighted average method.

$$P = \frac{1}{V} \sum P_i V_i$$

- Pore volume phase saturation weighted average.

$$P = \frac{1}{SV} \sum P_i S_i V_i$$

This method favours grid blocks where a high rate is expected.

In practice, several problems may occur. The net flow in opposite direction to the average calculated pressure may result in a negative pseudo relative permeability. When the net flow is non-zero and the average pressure gradient is zero, this could result in the infinite value of the pseudo relative permeability. Multiple values of the pseudo relative permeability may also result due to multiple occurrences of the same average saturation. (Azoug *et al.,* 2003, p.1-19, Barker *et al.,* 1997, p. 138-143)

Another method that avoids average pressure problems is Stone's method. It uses the average total mobility in a way that determines the net fractional flow. The relative permeability can then be calculated by neglecting the gravity and capillary pressure. A problem with this method is inadequate average mobility is experienced when significant variations in total mobility occur. This is due to significant gravity and capillary pressure effects, which result in poor determined pseudo functions. (Azoug *et al.,* 2003, p.1-19, Barker *et al.,* 1997, p. 138-43)

2.2.5.3. Capillary equilibrium limit and viscous limit pseudo methods

The other two common pseudo methods are the 'capillary equilibrium limit' and 'viscous limit' methods. The capillary equilibrium limit method is based on the assumption that the capillary pressure is in equilibrium within the coarse scale block that is to be upscaled, while the viscous limit method is based on the assumption that the flow rate is large and viscous in terms that the flow equations dominate the flow. The fraction between the oil and water flow rate is assumed to be constant for all fine scale blocks within a coarse scale block and this determines implicitly that the water saturation for all fine scale grid blocks are in the coarse scale block. Upscaling is done by calculating the fine scale water saturation for different constant values of capillary pressure, and water to oil flow fractions for the capillary equilibrium and viscous limit methods, respectively.

2.2.5.3.1 Capillary equilibrium limit method

The capillary equilibrium limit method is based on the assumption that the capillary pressure is in equilibrium within the coarse scale block that is to be upscaled. This is true for sufficiently slow flow velocity, where the capillary pressure changes so slowly within space and can be assumed to be constant over a volume corresponding to the size of a grid block used in the reservoir fluid flow simulation.

The capillary pressure is then treated to be constant for all fine scale grid blocks within the coarse scale block. For any given capillary pressure value with the corresponding water saturation, the water saturation can then be used to determine the fine scale water and oil phase permeability, where phase permeability is the product of the relative permeability and absolute permeability. The fine scale water and oil phase permeability for a given saturation distribution at the fine scale can then be scaled up using the same techniques as if they were absolute permeability. Diagonal tensor is often used to solve the incompressibility stationary one phase flow equation locally within the coarse grid block. The water saturation for the coarse block is scaled up by using the porosity weighted arithmetic average of the fine scale saturation. Different points on the upscaled relative permeability curves are then found by choosing different values of capillary pressure.

In summary, the upscaled relative permeability is a function of capillary pressure, which corresponds to the upscaled critical saturations with the corresponding relative permeability values. The end point of the upscaled relative permeability is then based on the binary search of upscaled endpoints for the capillary pressures. The relative permeability of water at the water saturation should be between zero and the specified tolerance.

The problem encountered with this method, is that an infinite number of permeability classes for the relative permeability curves may result. If the capillary pressure is not a Leverett J function, the relative permeability curves will not be equal to the fine scale curves regardless of the heterogeneity of the absolute permeability.

Furthermore, the capillary pressure is a function of absolute permeability, porosity and J function, which will then correspond to the infinite number of permeability classes for relative permeability curves.

2.2.5.3.2 Viscous limit method

The viscous limit method is based on the assumptions that the flow rate is large and viscous in terms that the flow equations dominate the flow. In this case, the fraction between the oil and water flow rate is assumed to be constant for all fine scale blocks within a coarse scale block, which is then used to determine implicitly the water saturation for all fine scale grid blocks in the coarse scale block.

For two phase incompressible stationary flow of fluids with the same density, the viscous limit equations are:

$$\nabla.k.k_{rw} / \mu_w.\nabla P = 0$$
$$\nabla.k.k_{ro} / \mu_o.\nabla P = 0$$

For a small distribution where krw (Sw) is proportional to kro (Sw), the same pressure solution can be obtained for both equations. In this way, the ratio between water flow rates to the total flow rate is constant. Thus, possible fine scale saturation can be determined by:

$$\frac{[k_{rw}(S_w)/\mu_w]}{[k_{rw}(S_w)/\mu_w + k_{ro}(S_o)/\mu_o]} = \text{constant}$$

In this method, a constant value between zero and one is selected to represent the fraction between the water and total flow rate of all fine scale grid blocks within a coarse scale grid block. The water saturation can then be determined by solving flow rates with respect to the saturation and its phase of relative permeabilities. The fine scale water and oil phase permeability for a given constant fraction of water to its

total flow rate can then be scaled up by using the same techniques as the absolute permeability upscaling. Different points on the upscaled relative permeability curves can be determined by selecting different constant value between zero and one. The constant end point of zero and one is then determined by the critical water saturation and critical oil saturation respectively.

The difference between this method and the capillary equilibrium method is that the fine scale saturation is defined and there is no requirement to search for endpoints. The upscaled phase permeability is positive and does not depend on the distribution at its fine scale, which may happen to have the saturation greater than the critical saturation as defined by the capillary equilibrium method. For the capillary equilibrium method, the upscaled mobile interval is in general less than the interval defined by taking the porosity weighted arithmetic average of fine scale critical saturation; while for the viscous limit method; the upscaled critical saturation is identical with the porosity weighted arithmetic average of the fine scale critical saturation.

This method is not useful in the case of having only one facies defined within a coarse scale and only a single permeability class for facies, since the upscaled relative permeability will be equal to the fine scale curves regardless of the heterogeneity of the absolute permeability. This is also applied to the homogeneous block, which will of course have upscaled relative permeability curves equal to fine scale curves. Therefore, more than one permeability class must be defined and fine scale absolute permeability must have large enough variability such that not all fine scale blocks must belong to the same permeability class.

2.2.6. Other methods

The other upscaling method, proposed by Beggs *et al.* in 1985 for calculating the vertical permeability, is for reservoirs in which layers are not laterally extensive and dispersed shale bodies are present. This method is based on the single-phase flow of

incompressible fluids through tortuous paths within a simulation grid block determined by shale dimensions. The number of shales per unit length, vertical and horizontal sand permeabilities, mean of shale continuity and shale fraction should be supplied. Effective vertical perm is then calculated as:

$$k_{v,eff} = \frac{(1-F_s)}{(1-\frac{f_d}{2})(\frac{1}{K_V}+\frac{f_d}{2K_h})}$$

This method is consistent with the findings of Prats in 1972, who believes that the effective permeability is a function of width, vertical spacing and degree of overlapping shale string for large numbers of very thin and impermeable horizontal shale strings with uniform distribution. Weber in 1982 also states that for the same potential difference in sand body, the ratio of the total flux in the presence of shale and the total flux in sand only is a strong function of the horizontal to vertical permeability ratio (Kv/Kh). (Mansoori, 1992, p.68, Renard *et al.*, 1997, p. 253-278)

Haldorsen and Lake in 1984 further state that the effective permeability is determined by calculating the effective cross sectional area from stochastic distribution of shale strings within the coarse grid block, based on the combined analytical method with statistical information on shale lateral continuity and spatial deposition to estimate the effective permeability of the sand shale depositional environment. Only for two-dimensional models where the ratio of lateral to vertical permeability is less than or equal to 10, this implies that the impermeable shale and homogeneous sand body rely heavily on a deterministic knowledge of spatial distribution of shales within a homogeneous sand body. The restriction to 2D and the grid ratio were then removed by Begg and King in 1985, based on the statistical technique by directly calculating effective permeability of mediums using a histogram of shale length and volume fraction. In this finding, zero permeability cannot be relaxed; however, it indicates that there is a strong dependency of effective permeability to system dimensions, and density and thickness of shale barriers (Mansoori, 1992, p. 68-69, Renard *et al.*, 1997, p. 253-278).

Beggs *et al*. in 1985 generalised further from Beggs and King (1985), for layered mediums in which shale frequency and dimension, and sand permeability anisotropy, vary from layer to layer. The effective permeability in three-dimensional models always has a greater uncertainty than in two-dimensional models. The effective permeability becomes negligible as Kv decreases.

Desbarats in 1987 stated that the effective permeability in finite flow fields was correlated with shale volume fraction, spatial structure and flow field dimensions based on the Monte Carlo stochastic distribution of sand shale sequence and numerical techniques to estimate sand/shale formation under saturated and steady state flow condition.

King in 1987 also stated that if the permeability fluctuations were small (rare case), then the perturbation theory or effective medium theory (EMT) would give reliable estimates of the effective permeability. However, for systems with a more severe permeability variation, or for those with a finite fraction of non-reservoir rock, all the simple estimates would be invalid as well as the EMT and perturbation theory. Also, many reservoirs contain significant amounts of impermeable material (or material of very low permeability). This situation is not as simple as is treatment by simple methods and estimates like the geometric mean become invalid.

A significant amount of zero (or very low) permeability regions may also be present, which may reduce the flow path. This makes it difficult to assign a single effective value to this property, to give the same flow path. Many attempts have been carried out to address the above-mentioned problem such as in numerical methods by Warren and Price 1963, Freeze 1975, Smith and Freeze 1979, Smith and Brown 1982, and other analytical methods such as the effective medium theory (EMT) or perturbation expansion by Baker *et al*. (1978), Gutjahr and Gelhar (1981), Gelhar (1974), Mizell *et al*. (1982), Dagan (1981 and 1982), King (1987). (Mansoori, 1992, p. 68-69, Renard *et al.*, 1997, p. 253-278)

2.3. REMARKS ON AVAILABLE UPSCALING METHODS

As stated above, there have been several investigations, based on the simplest form of mathematical algorithms to highly complex algorithms, for determining the effective properties within the heterogeneous reservoirs. Overall, the main limitation of upscaling is the lack of validation of assumptions made. There have been limited attempts in analysing the upscaling process, but there is no logical theory that exists to state whether the upscaled values are good or bad approximations (Beggs *et al.*, 1993, p. 143-148).

In some situations, such as in composite materials with effective properties which can be measured directly, the simplest analytical upscaling methods will be sufficient. However, we are not so fortunate in our business, since measurements can only be practically made on a centimetre scale in the laboratory and some reservoirs can only be represented with heterogeneous models. Thus, the determination of effective properties is, in practice, a mathematical problem.

Chapter 3.
EXPERIMENTAL RESEARCH WITH EXISTING ALGORITHMS

In order to gain an understanding of the upscaling process, the following three different reservoir models will be used throughout this research.

- Model A: A quite homogeneous sector model with 100,000 grid cells. (Refer to Section 3.1 for more detail.)

- Model B: 2D heterogeneous reservoir model (i.e. Vertical cross sectional flow model with 2000 cells (100x1x20 cells)) of an oil reservoir. (Refer to Section 3.2 for more detail.)

- Model C: 3D water-flood heterogeneous reservoir model with 1.1 million cells (60x220x85 cells). (Refer to Section 3.3 for more detail.)

Prior to upscaling, the coarse grid cells for each model will be generated based on the engineering judgment to capture the desired resolution. Details on the treatment of each model will be described in later sections.

Several single phase upscaling algorithms will be used and tested against the current theories of upscaling.

- For porosity, the volumetric weighted arithmetic average was selected in order to preserve the pore volume locally and globally throughout the reservoir.

- For permeability, however, several algorithms were selected and studied. They are:
  - Arithmetic average

- Harmonic average
- Geometric average
- Arithmetic-harmonic average
- Harmonic-arithmetic average
- Renormalisation
- Diagonal tensor methods with sealed and open boundary conditions.

The dynamic reservoir simulation will then be used to predict the fluid flow performance at the fine grid and coarse grid levels. Apart from the grid cells with porosity and permeability parameters, any data required for the simulation (i.e. relative permeability, capillary pressure, initial fluid distribution, fluid PVT properties and well inflow/outflow parameters) will be treated the same at the fine and coarse scales. This treatement is valid, if any data assigned to the model has no dependency to other parameter, i.e. a single relative permeability, used for most models is assigned to the entire model. If the dependency i.e relative permeability based on various permeability classes / rock type is assigned to the model, careful consideration is required, since this assigned data will be influenced by its dependency parameter for both fine and coarse scales. For relative permeability, the breakthrough time and cumulative production could be influenced the results for both fine and coarse scaled models. The results of the fluid flow performance at the coarse grid model will then be compared against its fine grid fluid flow. The selection of the appropriate upscaling algorithm for each model will be judged according to how well the fluid flow prediction made at the coarser (macro-scale) level mimics the prediction of field performance at the finer (micro-scale) level.

In this research, the upscaling from the geological model (finer scale) to the reservoir simulation model (coarser scale) will be the main focus. Any uncertainties with regards to the geological model (reservoir model built by the geologist) and accuracy of the laboratory data (the analysis of the PVT, capillary pressure and also the relative permeability curves) will not be discussed in this research.

3.1. MODEL A

Model A, which represents quite a homogeneous reservoir, has characteristics as shown in Figure 3-1 and Figure 3-2 for the porosity and permeability 3D parameters respectively. The fine scale Model A has 100,000 grid cells (28 x 36 x 90 cells).

Model A is a typical reservoir model which illustrates the interpolation between well logs with known anisotropy throughout the reservoir. From the available well logs data, the reservoir properties are distributed homogeneously in lateral directions with wide correlation lengths, while the vertical heterogeneity found on the well logs data is captured and distributed with the fine scale resolution.

In this reservoir, the depletion drive, via a single producer which is located in the middle of the area of drainage, is used for the ultimate recovery of the reservoir volume.

Throughout the research, this model will be referred to as Model A.

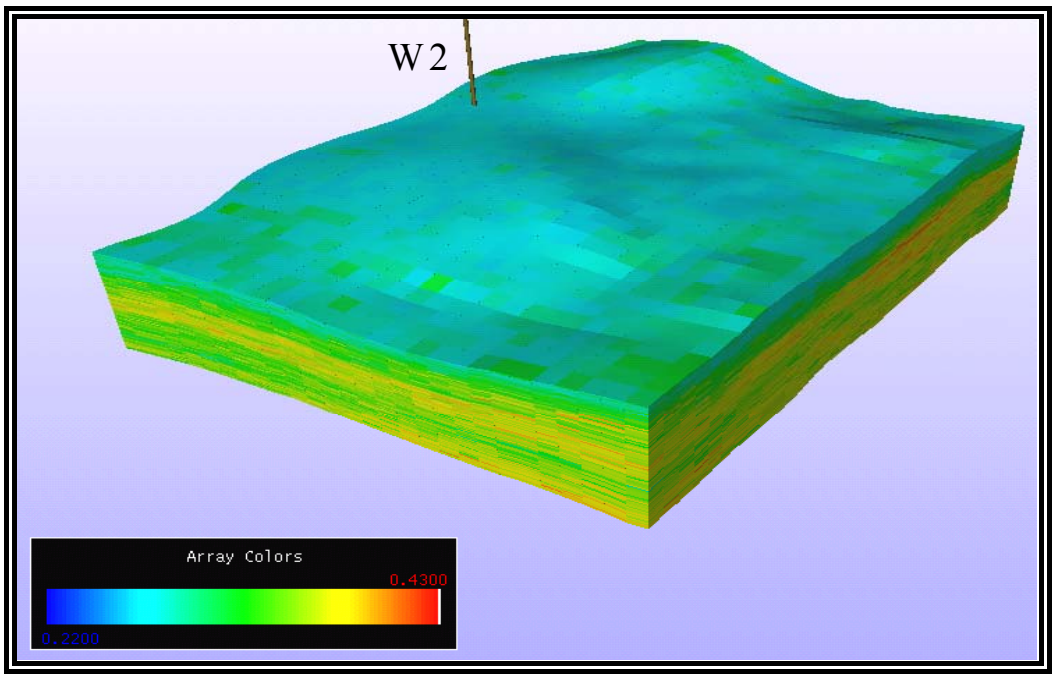

Figure 3-1 Porosity model of a fine scale for model A

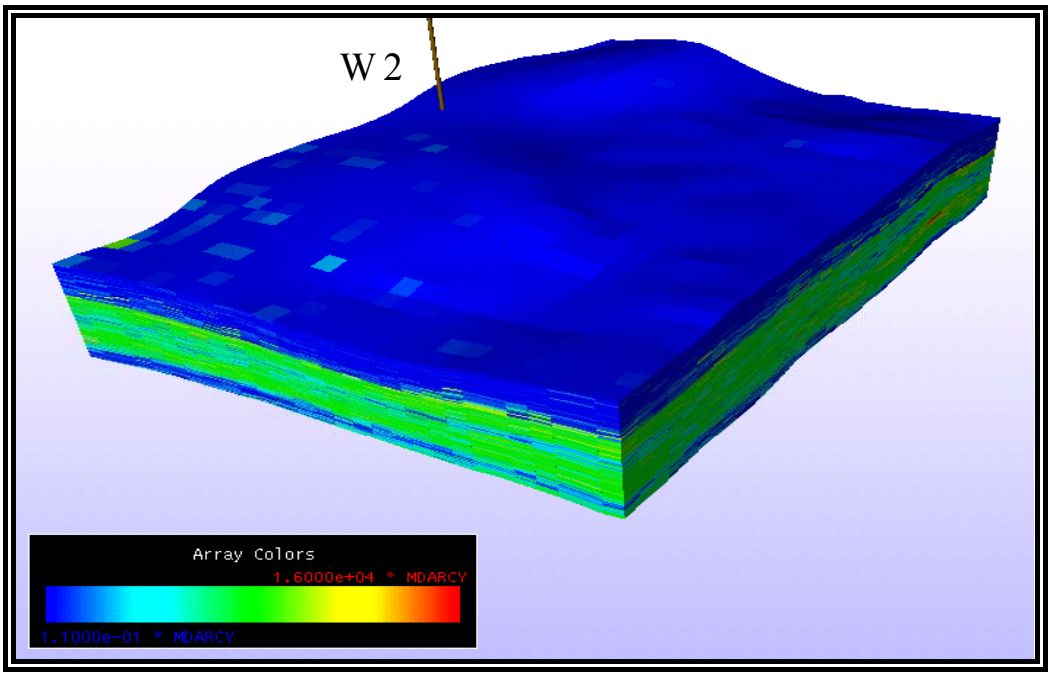

Figure 3-2 Permeability model of a fine scale for model A

The following relative permeability based on various permeability classes as shown in Table 3-1 are used to assigned in the Model A.

Table 3-1 Relative Permeability with Various Permeability Classes Assigned for Model A

Rock Type	1	2	3	4	5	6
Kair Range (Darcy)	**> 7.5**	**5 – 7.5**	**2.5 – 5**	**1– 2.5**	**0.5 – 1**	**<0.5**
Initial Water Saturation	0.079	0.158	0.241	0.332	0.440	0.760
Oil Relative Permeability (oil-water) Parameters						
Corey Coefficient for oil, Now	1.1	1.1	1.1	1.1	1.1	1.1
Krow end-point	0.8	0.8	0.8	0.8	0.8	0.8
Residual oil saturation for water displacement, Sorw	0.116	0.150	0.230	0.230	0.230	0.200
Water Relative Permeability (oil-water)						
Corey Coefficient for water, Nw	3.7	3.7	3.7	3.7	3.7	3.7
Krw end-point	0.3	0.3	0.3	0.3	0.3	0.3
Gas Relative Permeability (gas-oil)						
Corey Coefficient for gas, Ng	2.741	2.741	2.741	2.741	2.741	2.741
Krg end-point	0.8	0.8	0.8	0.8	0.8	0.8
Corey Coefficient for oil, Nog	1.1	1.1	1.1	1.1	1.1	1.1
Krog end-point	0.8	0.8	0.8	0.8	0.8	0.8
Residual oil saturation for gas displacement, Sorg	0.116	0.150	0.230	0.230	0.230	0.200
Critical gas saturation, Sgc	0.02	0.02	0.02	0.02	0.02	0.02

3.1.1. Coarse grid model

In this research, Model A will be coarsened from 28 x 36 x 90 cells (90,720 cells) to 14 x 18 x 9 cells (2,268 cells).

Model A (fine): 28 x 36 x 90 (90,720 cells)
Model A (coarse): 14 x 18 x 9 (2,268 cells)

Upscaling Ratio: 2: 2: 10 (1 coarse cell = 400 fine cells)

In this model, the lateral resolution is not as important as the vertical resolution, as it is quite homogeneous laterally and heterogeneous vertically. However, a sufficient amount of grid blocks are required to capture the spacing distance between wells laterally. In this upscaling comparison, the extreme vertical coarsening is used to test the limit of the upscaling method in representing the effective properties on the coarsened scale.

The relative permeability as shown in Table 3-1, is assigned the same way for this coarse scale Model A. The upscaled permeability parameter can become critical to the breakthrough timing and cumulative production, if the saturation tables assigned on the coarsened scale does not represent the average properties. Therefore, these assigning relative permeability tables could also influence the outcome of accuracy of upscaling.

3.1.2. Comparison results

The results of Model A are summarised in the following figures.

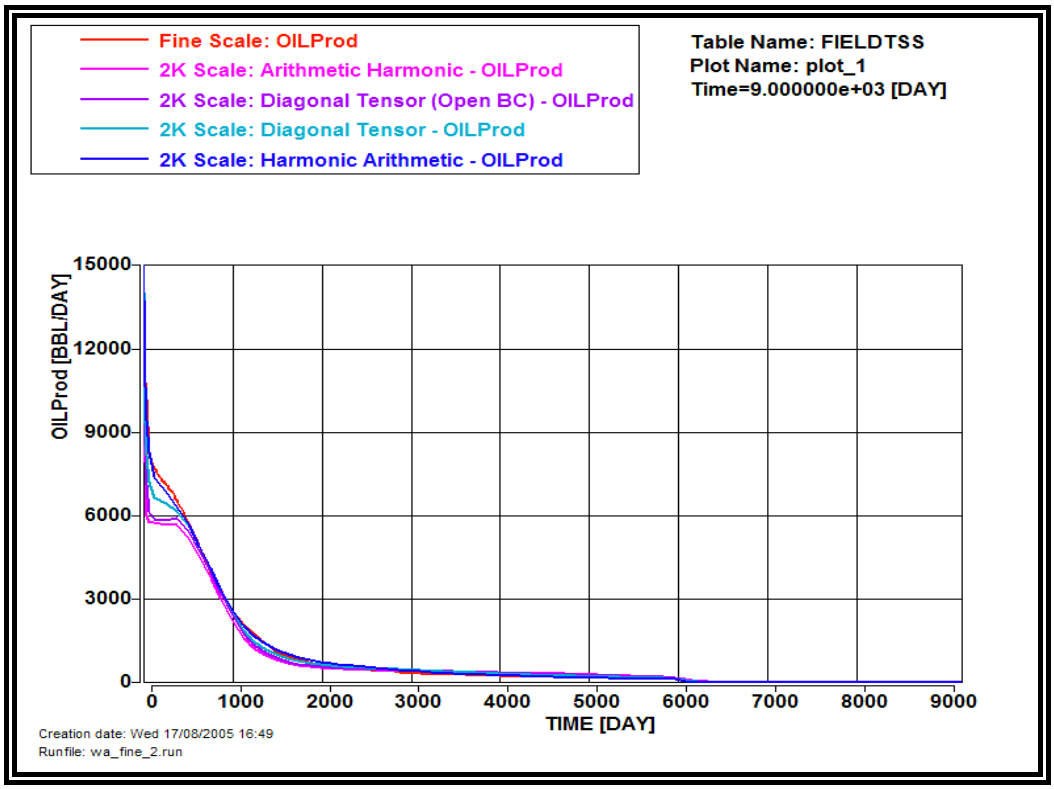

Figure 3-3 Comparison plot of oil production rate for Model A

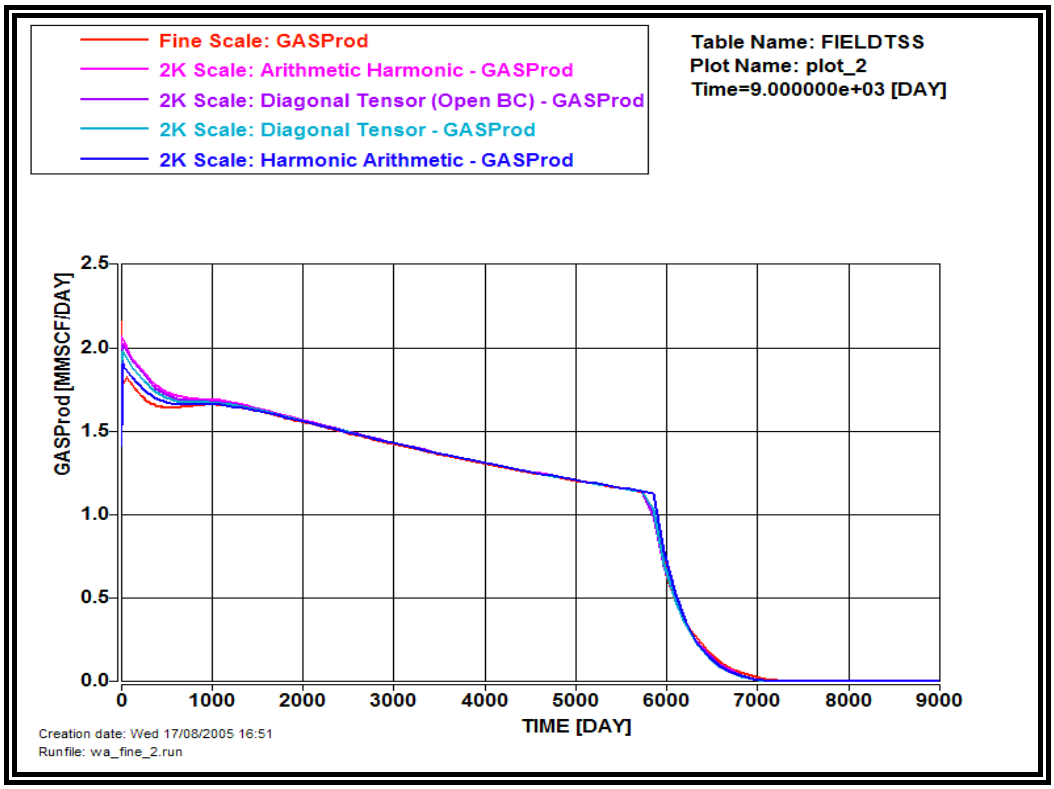

Figure 3-4 Comparison plot of gas production rate for Model A

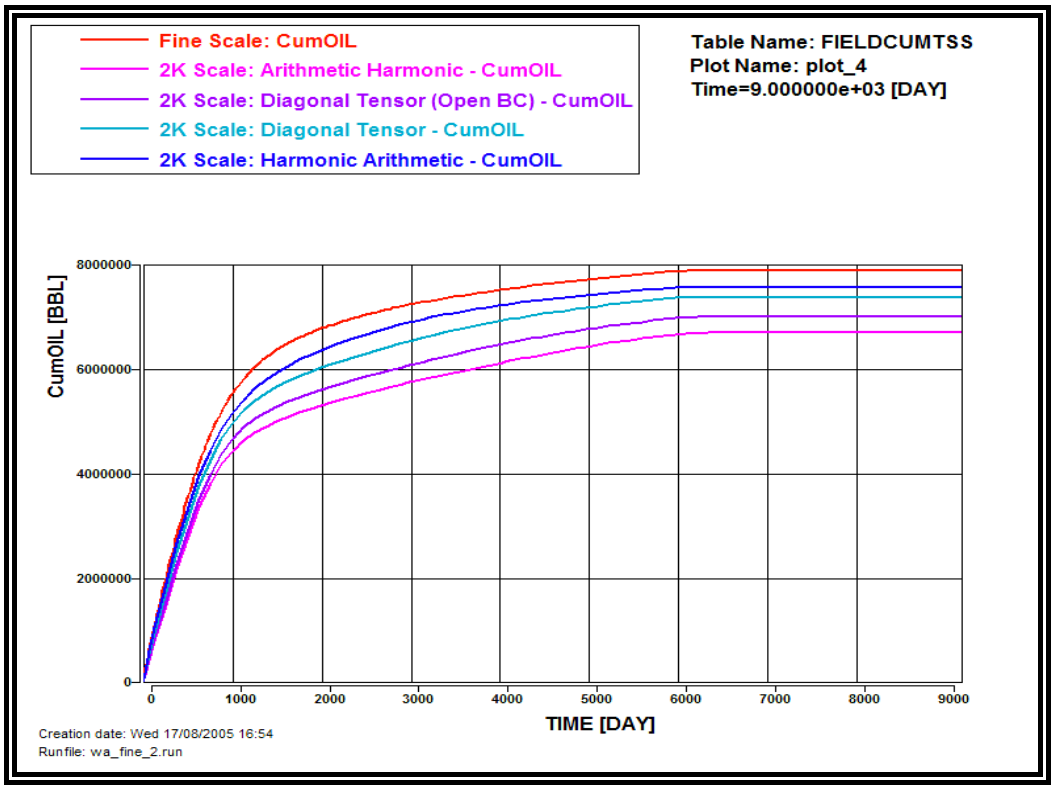

Figure 3-5 Comparison plot of cumulative oil production for Model A

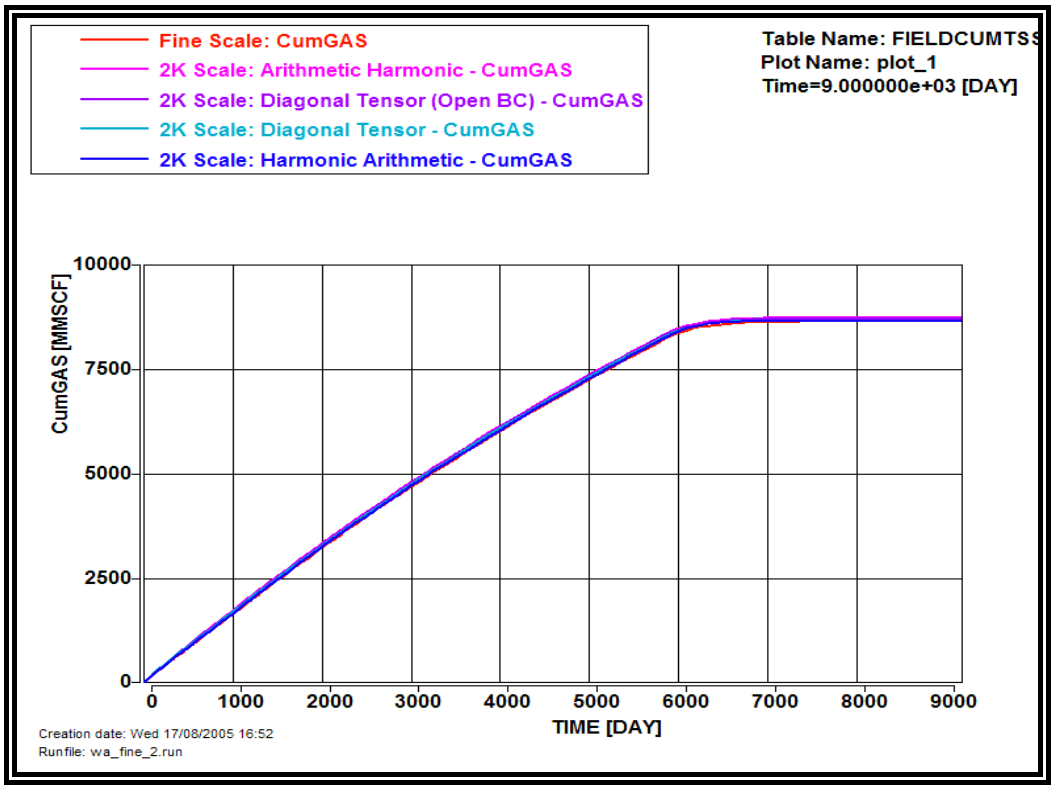

Figure 3-6 Comparison plot of cumulative gas production for Model A

Figure 3-3 to Figure 3-6, indicate clearly that the possible algorithms that could be used to represent the fine scale fluid flow behaviour are arithmetic-harmonic, harmonic-arithmetic and diagonal tensor. However, it seems that the predictions at the coarse scale level underestimated the recovery of the oil produced in the reservoir. As mentioned above, the assigning of relative permeability to the specific permeability class could be the influencing factor to the cumulative production of the oil and hence the recovery of the oil produced in the reservoirs. Further investigation on factors affecting oil production recovery will be discussed in detail in Chapter 4 and Chapter 5.

3.2. MODEL B

Model B is the 2D reservoir model (vertical cross sectional flow model with 2000 cells (100 x 1 x 20 cells)) of an oil reservoir, which is taken from the first case of the *Tenth SPE Comparative Solution Project: A Comparison of Upscaling Techniques* (SPE 72469) (Christie *et al.*, 2001, p. 308-316). The model is a heterogeneous reservoir, as shown in Figure 3-7. The permeability is correlated and distributed geo-statistically over a small correlation length with the extensive size of shale strips acting as barriers in the model. The gas injection is used in this model to enhance the ultimate recovery of the oil produced.

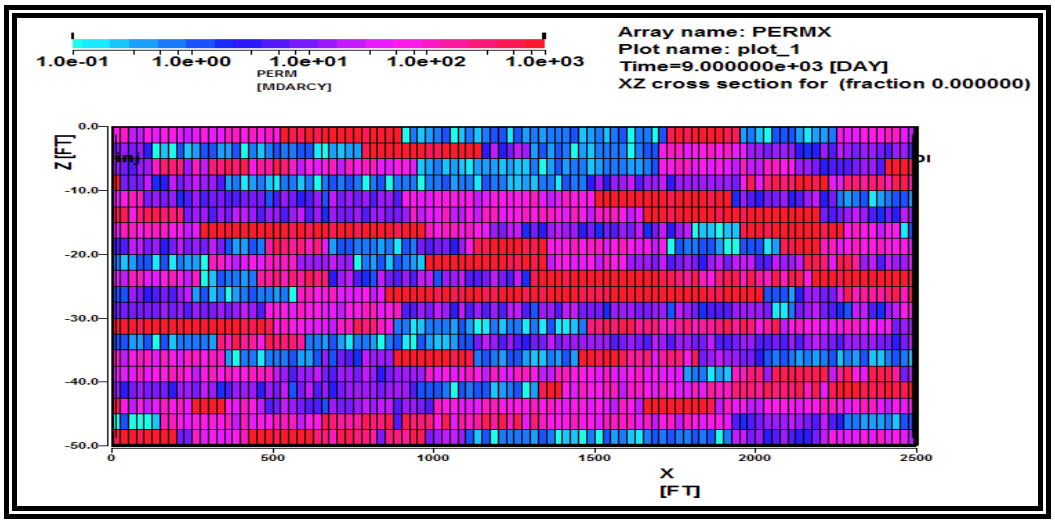

Figure 3-7 Permeability model at a fine scale for Model B

A single relative permeability as shown in the following figure is assigned for the entire model.

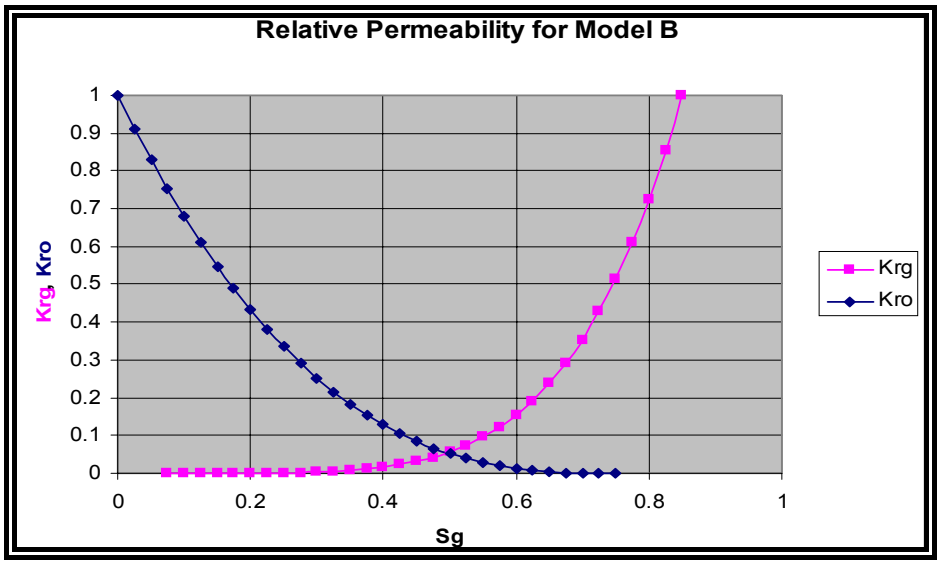

Figure 3-8 Relative Permeability for Model B

Throughout the research, this model will be referred to as Model B.

3.2.1. Coarse Grid Model B

In this research, Model B will be coarsened from 100 x 1 x 20 cells (2,000 cells) to 5 x 1 x 5 cells (25 cells).

Model B (fine): 100 x 1 x 20 (2,000 cells)
Model B (coarse): 5 x 1 x 5 (25 cells)
Upscaling Ratio: 20: 1: 4 (1 coarse cell = 80 fine cells)

In this model, both lateral and vertical variability of the permeability are quite heterogeneous. For the upscaling comparison, the effective properties at any coarser scale will be required. Thus, in this research, model B is scaled to represent 80 fine cells with 1 coarse cell.

3.2.2. Comparison results

The results of Model B using different upscaling algorithms are summarised below.

The results from Figure 3-9 to Figure 3-13, indicate clearly that the possible algorithms that could be used to represent the fine scale fluid flow behaviour could be arithmetic-harmonic and diagonal tensor. However, the predictions at the coarse scale level had a higher recovery of the oil produced in the reservoir. Further investigation on factors affecting the oil production recovery will be discussed in detail in Chapter 4 and Chapter 5.

The harmonic-arithmetic algorithm seemed to underestimate the gas breakthrough and fluid flow performance at the coarse scale level.

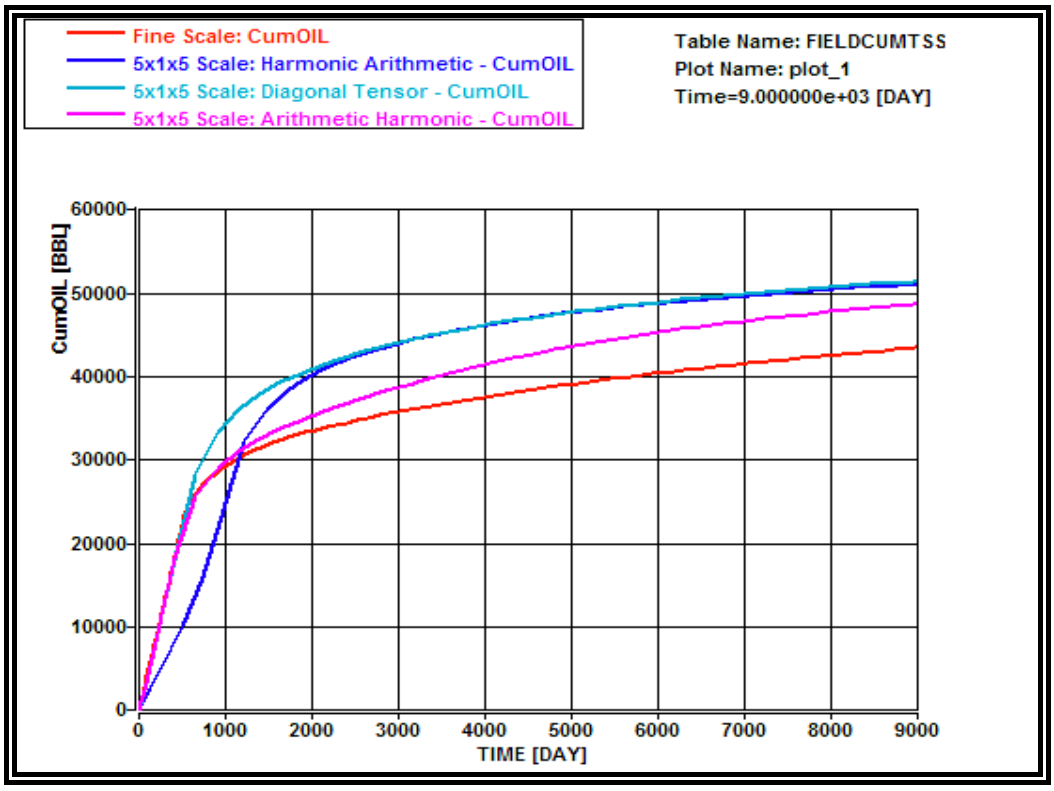

Figure 3-9 Comparison plot of cumulative oil production for Model B

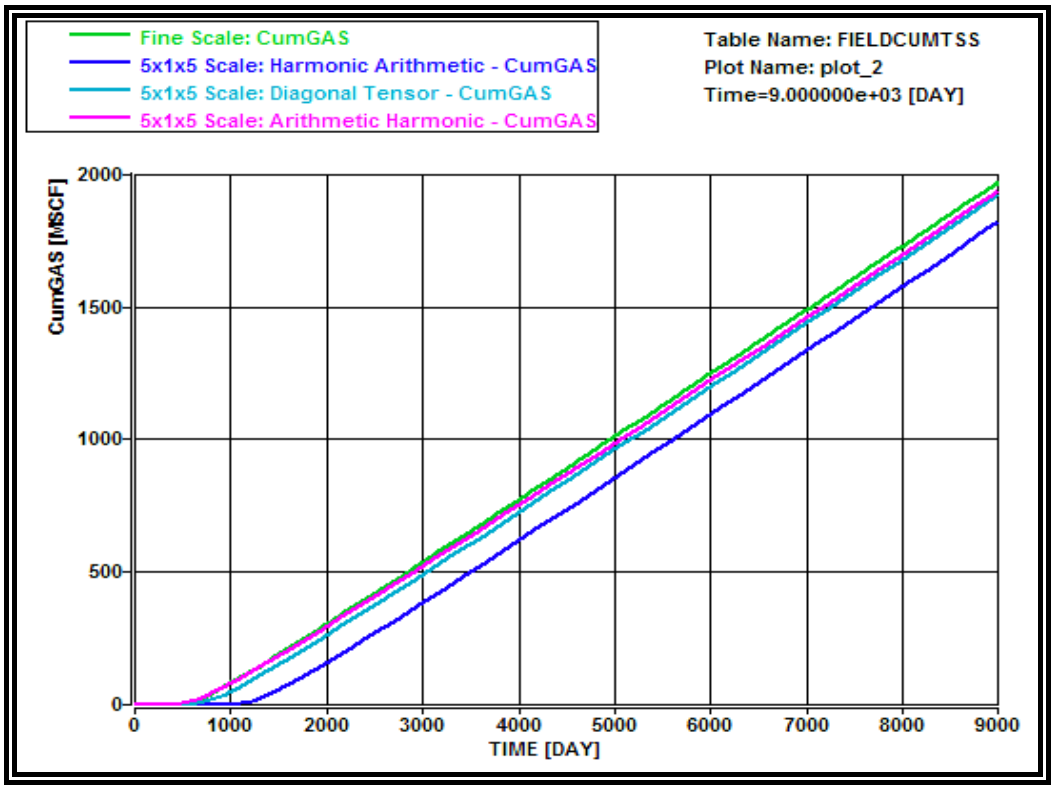

Figure 3-10 Comparison plot of cumulative gas production for Model B

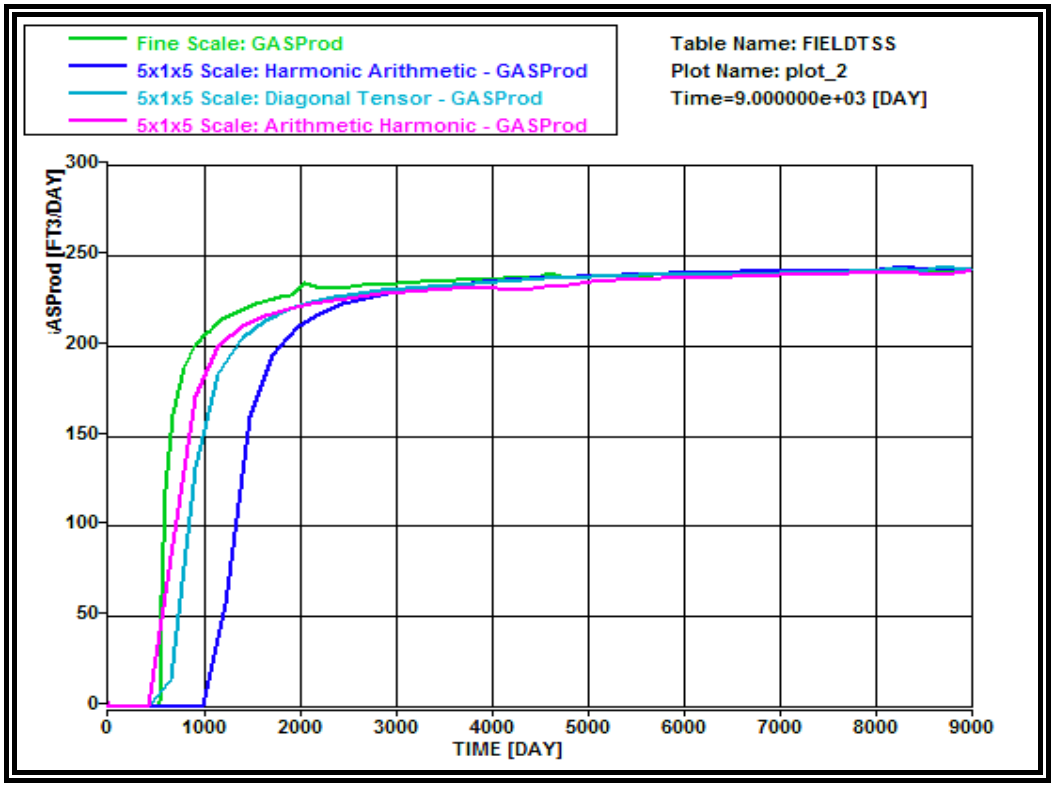

Figure 3-11 Comparison plot of gas production rate for Model B

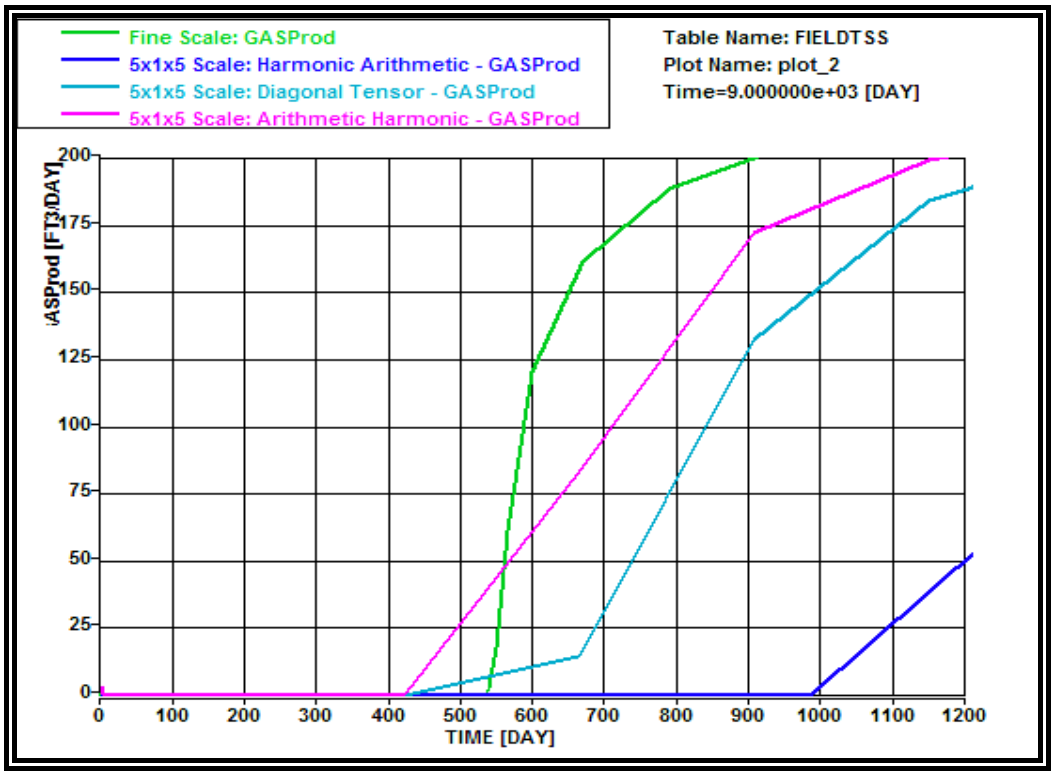

Figure 3-12 Comparison plot of the breakthrough timing with respect to gas production rate for Model B

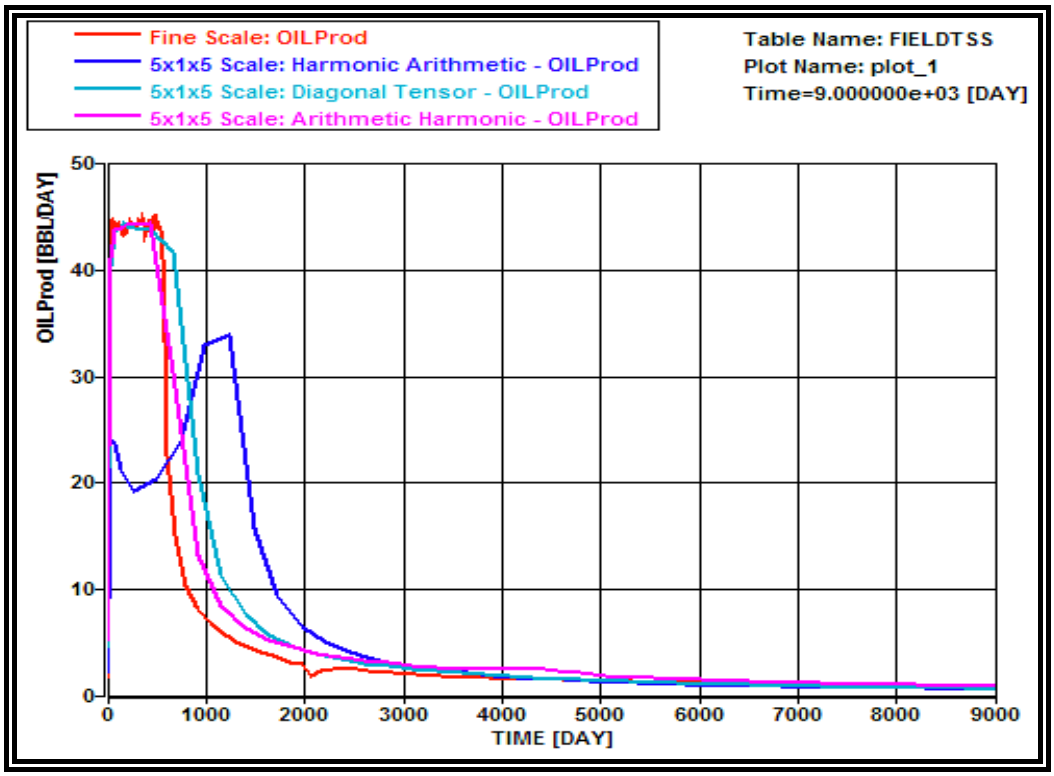

Figure 3-13 Comparison plot of oil production rate for Model B

3.3. MODEL C

Model C is the 3D water-flood reservoir model with 1.1 million cells geo-statistical model (60 x 220 x 85 cells), taken from the second case of the *Tenth SPE Comparative Solution Project: A Comparison of Upscaling Techniques* (SPE 72469) (Christie *et al.,* 2001, p. 308-316). The model is a heterogeneous reservoir, as shown in Figure 3-14 for its porosity model. Throughout the research, this model will be referred to as Model C.

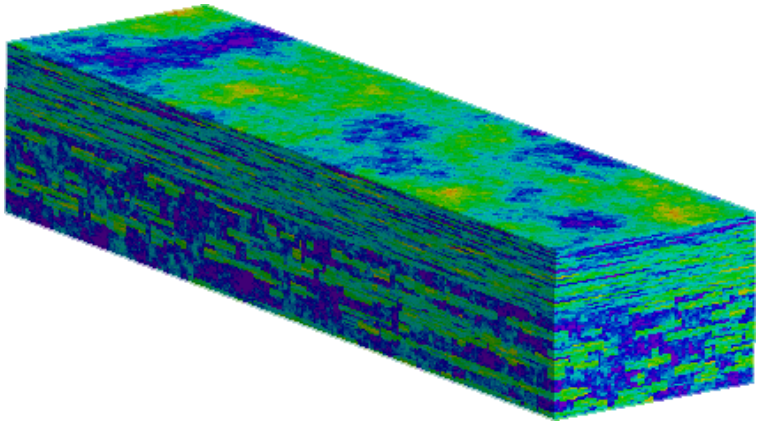

Figure 3-14 Porosity model at a fine scale for Model C (Christie *et al.,* 2001, p. 309)

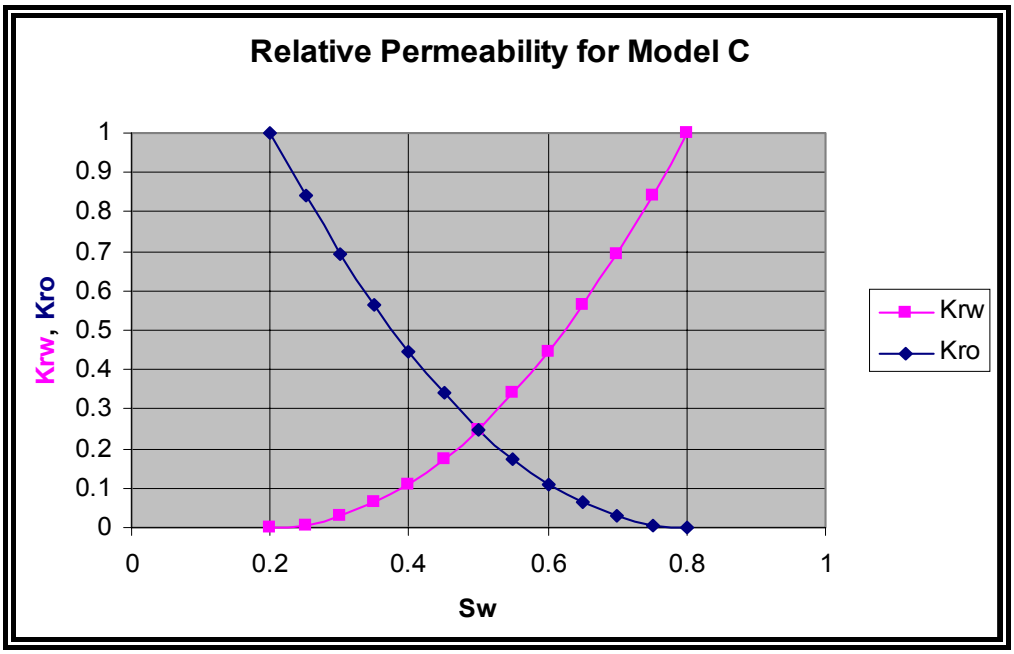

Figure 3-15 Relative Permeability for Model C

A single relative permeability as shown in Figure 3-15 is assigned for the entire model.

3.3.1. Coarse Grid Model C

In this research, Model C will be coarsened from 220 x 60 x 85 (1,122,000 cells) to 15 x 55 x 17 (14,025 cells).

Model C (fine): 60 x 220 x 85 (1,122,000 cells)
Model C (coarse): 15 x 55 x 17 (14,025 cells)
Upscaling Ratio: 4: 4: 5 (1 coarse cell = 80 fine cells)

Similar to Model B, this model has a large variability in permeability, both vertically and horizontally. Both vertical and horizontal permeability are important for this model to represent the connected volume within the reservoir. Thus, a proportional upscaling factor is used for coarsening both the vertical and horizontal directions. A scaling factor of 80 fine cells representing one coarse cell is used for the upscaling comparison of this model.

3.3.2. Comparison results

For comparison purposes, the sector model of Model C has been used in running the reservoir simulation due to limited computer resources for running such a large number of fine gridded cells on the full field scale of the geological model. The entire Model C fluid performance will then be compared against the published results at the fine scale level (Christie *et al.,* 2001, p. 308-316).

3.3.2.1. Sub Model C

The results of testing Sub-Model C using different upscaling algorithms are summarised below.

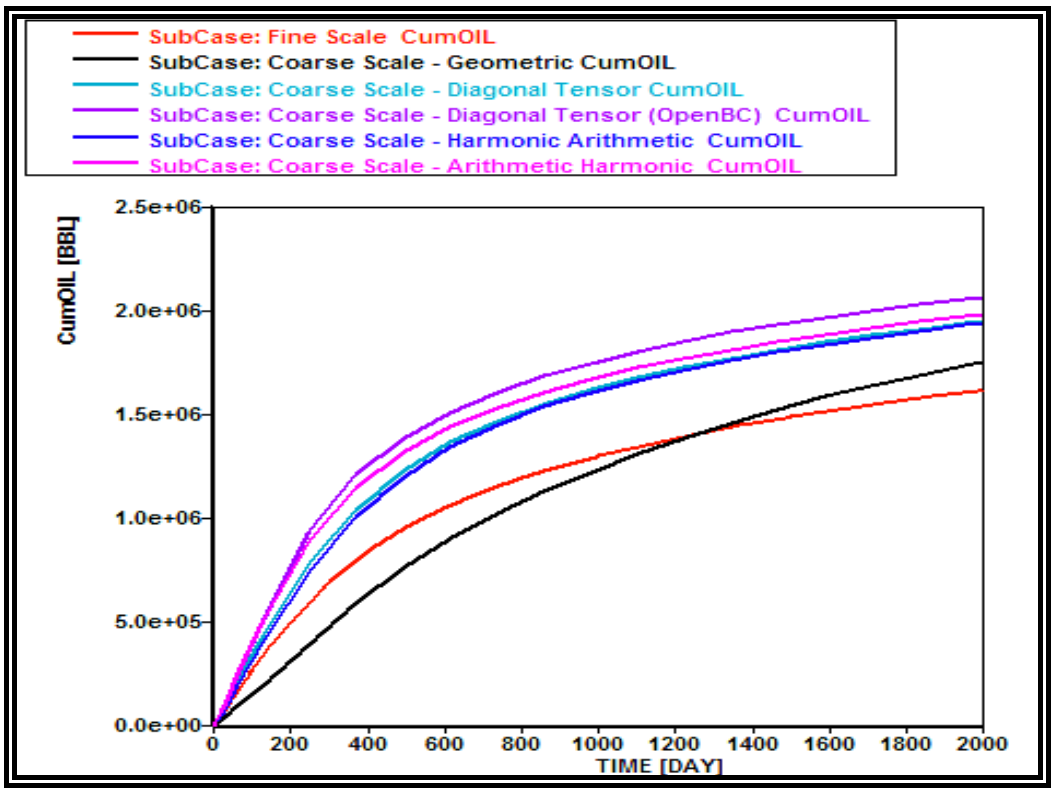

Figure 3-16 Comparison plot of cumulative oil produced for Sub-Model C

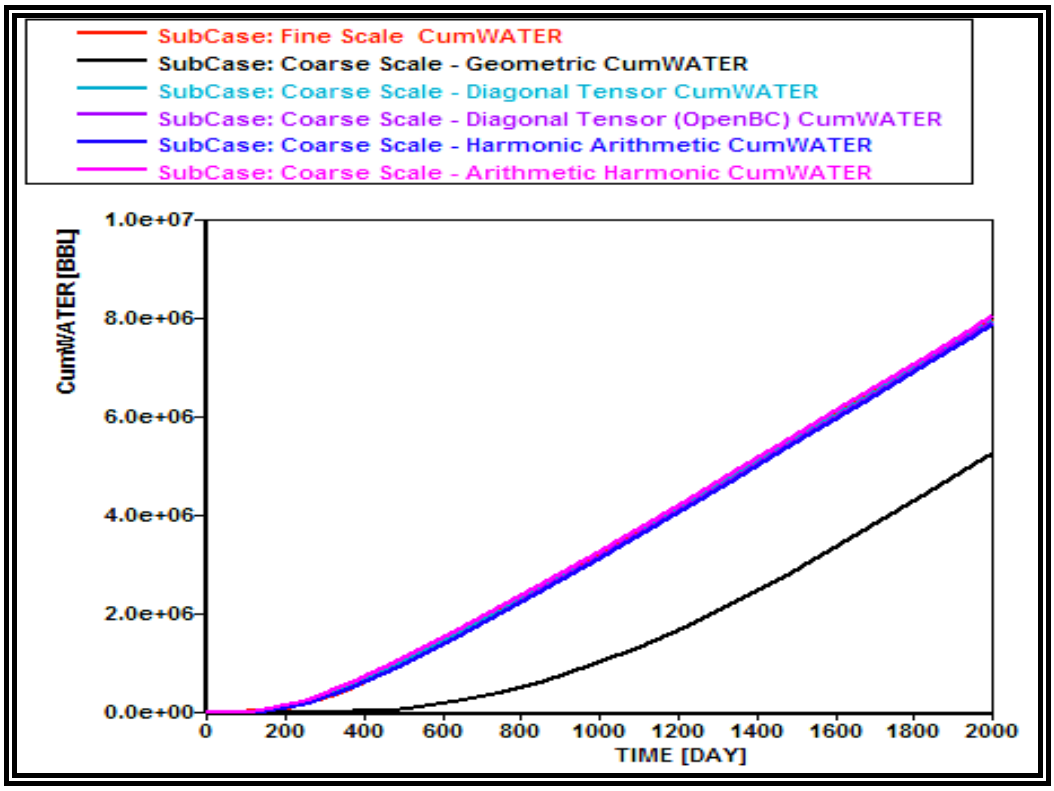

Figure 3-17 Comparison plot of cumulative water produced for Sub-Model C

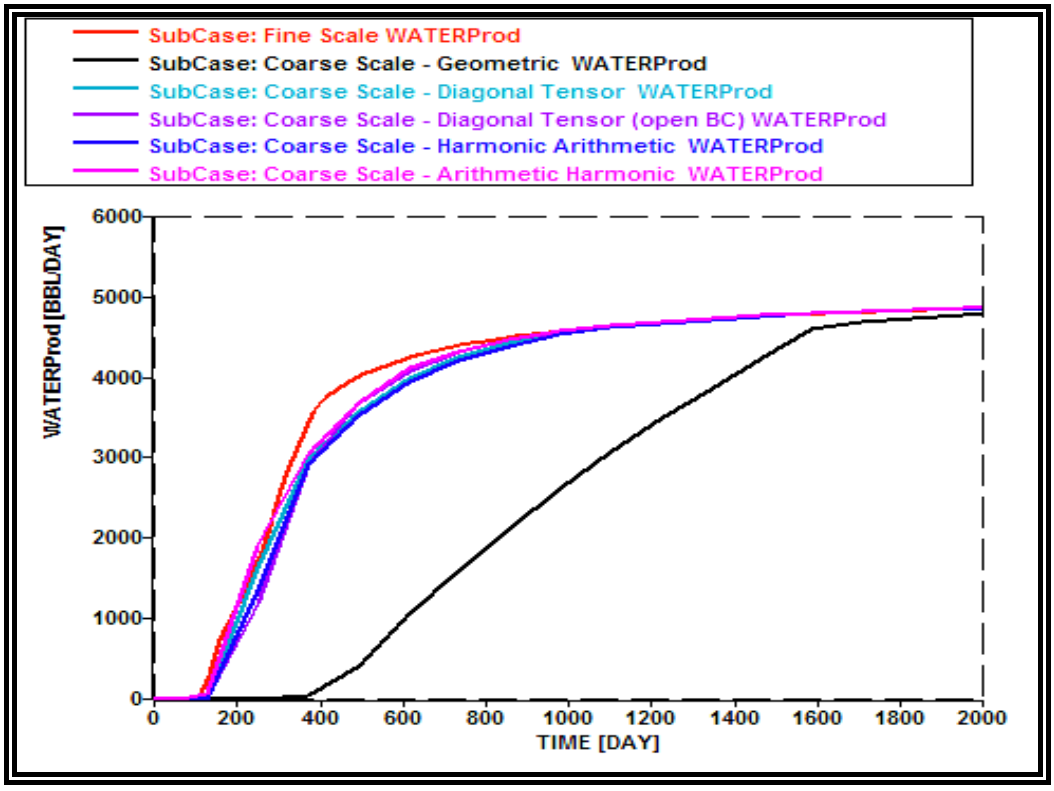

Figure 3-18 Comparison plot of water production rate for Sub-Model C

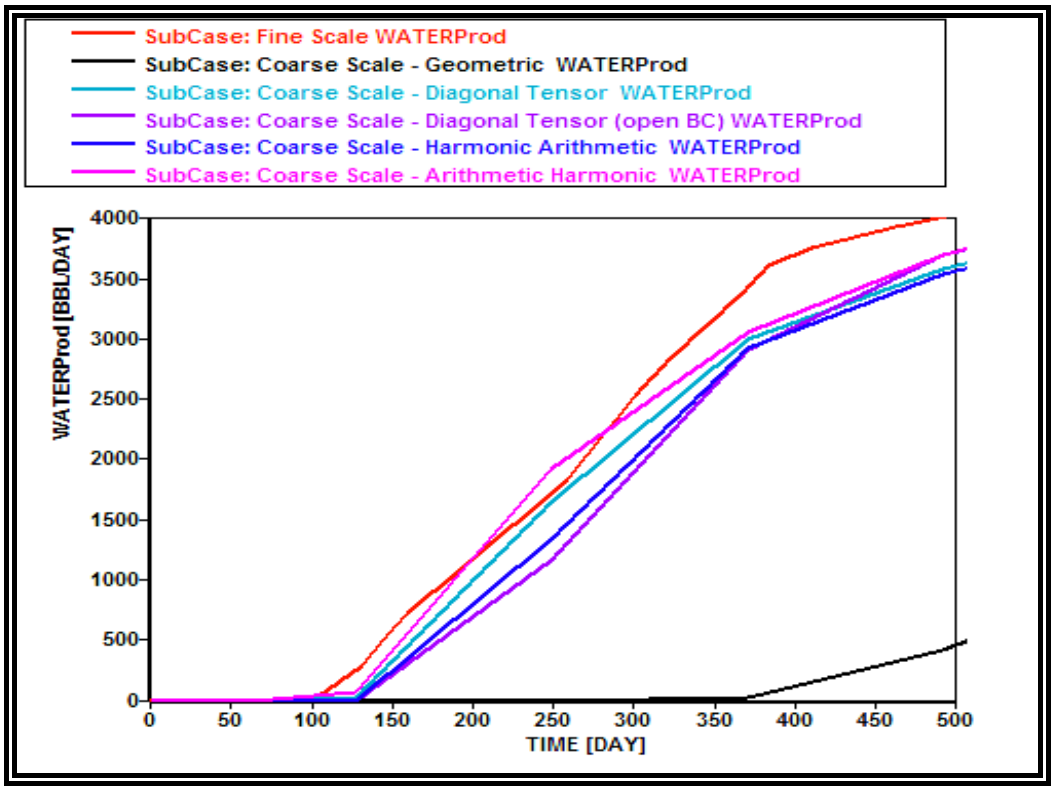

Figure 3-19 Comparison plot of the breakthrough timing with respect to water production rate for Sub-Model C

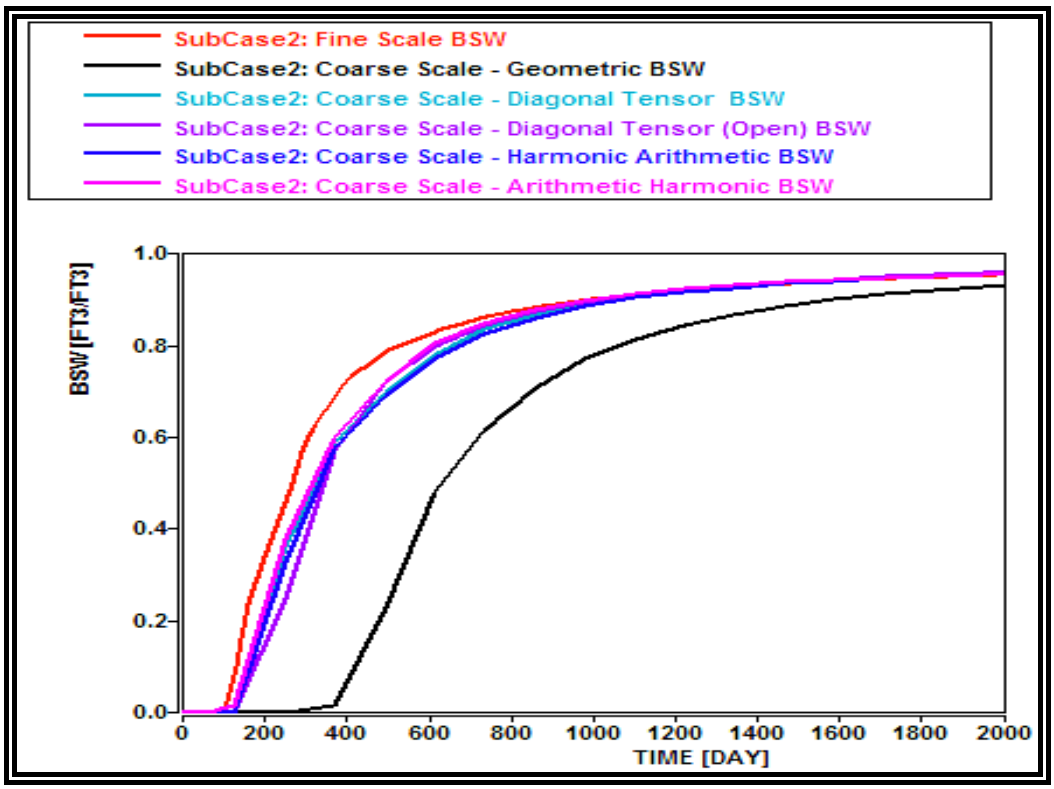

Figure 3-20 Comparison plot of water cut ratio for Sub-Model C

Figure 3-20 indicates clearly that the possible algorithms that could be used to represent the fine scale fluid flow behavior could be arithmetic, arithmetic-harmonic, harmonic-arithmetic and diagonal tensor. However, similarly to Model B, it seems that the predictions at the coarse scale level have a higher recovery of the oil produced in the reservoir. Further investigation on factors affecting the oil production recovery will be discussed in detail in Chapters 4 and 5.

The geometric and harmonic algorithms seem to underestimate the water breakthrough and fluid flow performance at the coarse scale level.

3.3.2.2. Entire Model C

The results of testing Model C using different upscaling algorithms are summarised below with the comparison against the published SPE results at the fine scale simulation (Christie *et al.,* 2001, p. 308-316).

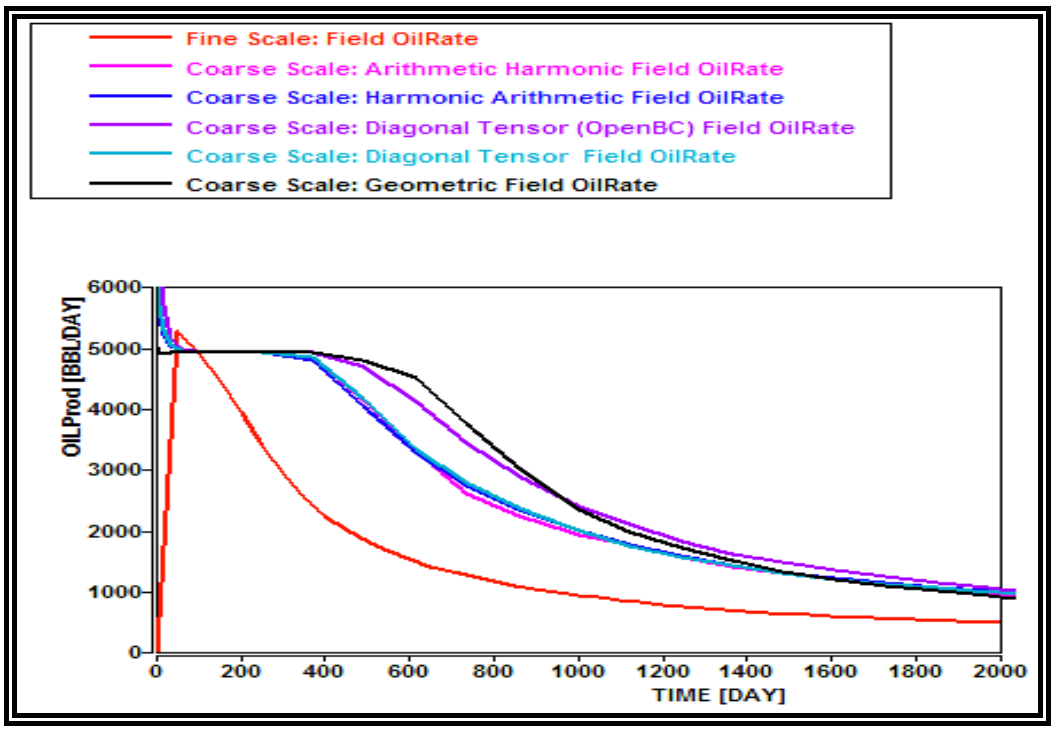

Figure 3-21 Comparison plot of field production rate using various existing algorithms for Model C with published results

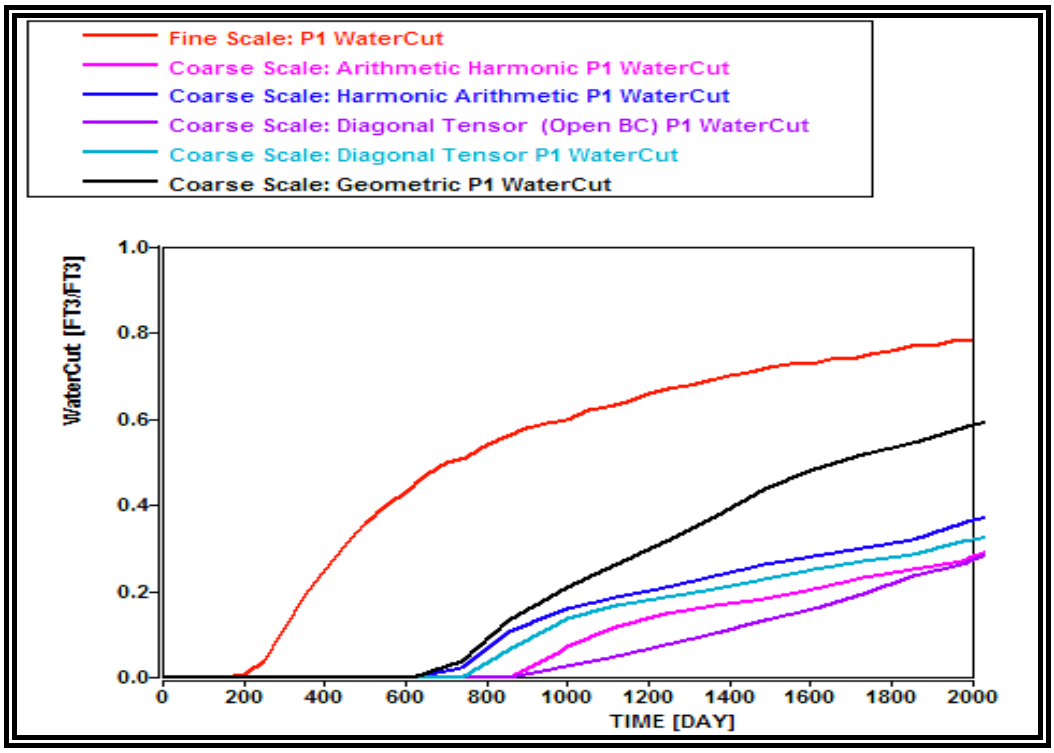

Figure 3-22 Comparison plot of producer-1 water cut ratio using various existing algorithms for Model C with published results

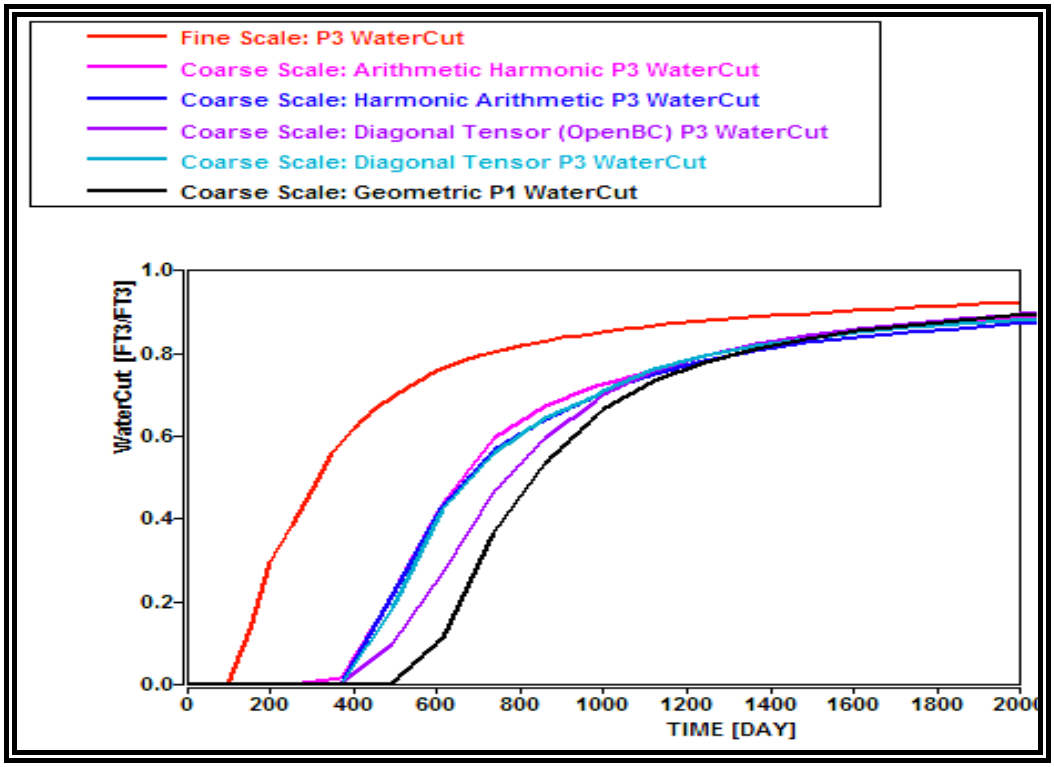

Figure 3-23 Comparison plot of producer-3 water cut ratio using various existing algorithms for Model C with published results

Figure 3-21, Figure 3-22 and Figure 3-23 have shown similar behavior as indicated by the sub-model C. Fluid flow behaviors predicted by using various upscaling algorithms (arithmetic, arithmetic-harmonic, harmonic-arithmetic and diagonal tensor) were significantly different from the behavior at the fine scale. The field production rate seemed to be predicted at the higher rate, which implied higher recovery of the oil produced in the reservoir. The water breakthrough was also predicted to come later than the prediction at the fine scale. Thus, further investigation on factors affecting the oil production recovery and water breakthrough will be discussed in detail in Chapter 4 and Chapter 5.

3.4. CONCLUSION FROM EXISTING ALGORITHMS

Based on the observations above, the use of different existing algorithms resulted in different overall field performances for various depositional environments. From simple heterogeneity like Model A, to more complex heterogeneity such as Model C, a comparison has been made between the existing algorithms and how they behave differently compared to their coarse scale and fine scaled models.

Prior to any upscaling procedure, the most important thing is the design and generation of the simulation coarse grid. If possible, the fine grid and the coarse grid should be aligned to the primary flow directions to minimise the deviation in principal permeability directions. For transmissibility in different directions to be approximately the same, the ratio between thickness and length of a coarse grid should ideally be equal to the inverse of a square root of ratio between the vertical and horizontal permeability. This is not always the case, as most of the geological models are based on a single directional permeability log to represent the geological permeability field in a model. If this is the case, engineering judgment will be required to decide the best design for the coarse grid model geometry depending on the anisotropy and variance of the permeability field and also taking the flow conditions for the reservoir into consideration.

For a simple case of heterogeneous formation made up of parallel beds of uniform permeability, a simple analytical solution of the Darcy's flow equation yields effective permeability. For flow, which is parallel to the bedding plane, the arithmetic algorithm can be used to determine the effective property of permeability. On the other hand, for flow that is perpendicular to the bedding plane, the harmonic mean can be used as the upscaling algorithm for effective permeability. Refer to Appendix A for more detail on the derivation of arithmetic and harmonic means based on an analytical solution of Darcy's flow equation.

For a general case of heterogeneous formation with arbitrary spatial arrangement of permeability, the effective permeability lies in between the arithmetic mean and harmonic mean. This observation is consistent with previous research findings as summarised and discussed in Chapter 2. For deterministic geological models similar to Model A, where the spatial distribution of permeability is assumed to be known at given scale of heterogeneity, a simple analytical solution can be used to obtain the effective permeability for arbitrary conditions and may not necessarily require the full tensor treatment. It uses the assumptions of single phase, steady state flow and continuity equation with the combination of Darcy law to arrive at a pressure solution. An exact solution can also be obtained only if there is a simple heterogeneity and anisotropy.

For the case of purely random permeability distribution, the effective permeability is statistically best represented by the geometric mean, but this is not always the case for every random permeability reservoir model. The combined averaging techniques such as geometric-arithmetic mean (first take the geometric mean then take the arithmetic mean of the geometric mean), harmonic-arithmetic mean, and arithmetic-harmonic mean can also be used for the effective permeability determination. However, the proper method of averaging should depend on the nature of heterogeneity in the primary flow direction.

For complex cases with high permeability anisotropy and heterogeneity, full-tensor may be necessary. A combination of simple analytical averaging can also be used,

but the accuracy of using this simple analytical method will depend on the flow path tortuosity, as it will increase due to the presence of shales. When there are fine scale barriers at the length scales of the coarse grids, care should be taken in using diagonal tensor, full tensor or re-normalisation methods, because unrealistically low effective permeability may be produced due to the applied boundary conditions. In such cases, it is probably best to use diagonal or full tensors with skin added to each coarse grid.

As shown in the comparison of the fine to coarse scale model behaviours on the above models, upscaling of only the absolute permeability under the assumption of single-phase flow may not ensure a satisfactory agreement between fine and coarse-grid multiphase flow simulation results. Due to this, relative permeability and capillary pressure upscaling should also be considered.

Further complex upscaling, such as using the pseudo upscaling for generating the pseudo properties of the upscaled model, is sometimes not really effective. The reason being is that it would require the reservoir simulation with the fine grid cells in order to get the dynamic properties (i.e. average reservoir pressure, average fluid saturation, average fluid relative permeability and equivalent average permeability at time step intervals to the end of the simulation run) of the reservoir model. Therefore, for models with a small number of grid cells, running the dynamic simulation would be the most feasible. However, as the number of fine grid cells increases in the model, more extensive computer power would be required. Furthermore, in some cases, this could become a limitation to running the pseudo upscaling, and thus, this upscaling method could become infeasible.

In summary, the selection of the upscaling method should be consistent with the degree of the geologic complexity of reservoir. Also, the average technique should be consistent with the reservoir geology determined by the original depositional environment and second alternations of the reservoir rocks. The permeability heterogeneity and anisotropy are controlled by the texture and structure of litho facies and litho facies architecture. Thus, for optimal upscaling and minimising the

uncertainty error in upscaling processes, a consistency between the fine scaled geological model and its coarse scaled dynamic simulation model is required.

The turn around time will also be the critical judgement in deciding the best possible upscaling solution, as some upscaling algorithms will take longer to run for better accuracy in providing the effective properties of the upscaled model. A simple summary chart is shown in Figure 3-24 for the comparison of speed versus accuracy for various existing upscaling algorithms. The accuracy here was defined as the way the effective permeability of the upscaled model was being determined. Also, the greater the permeability variability used within a coarse cell for averaging, the greater the uncertainty will be of the upscaled permeability. Degrees of upscaling should then be chosen such that an optimum balance is achieved between the flow simulation time on the coarse grid and the preservation of important geologic features in the fine grid model.

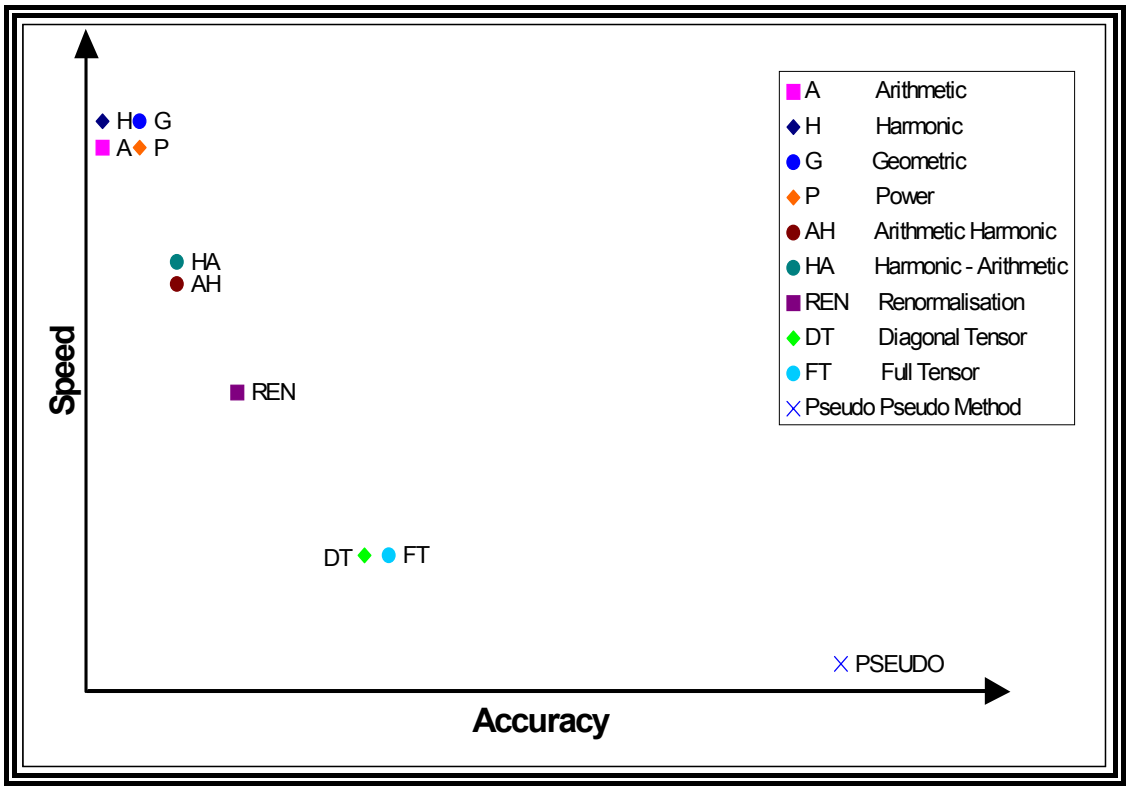

Figure 3-24 Comparison of speed vs. accuracy for various existing upscaling algorithms

Chapter 4.
THE NEW UPSCALING ALGORITHM

The main purpose of upscaling is to find the most representative of the effective homogeneous grid cells that produce the same fluid flow characteristics under the same boundary conditions of the heterogeneous cells at a finer scale. Based on the observations in Chapter 3, different upscaling algorithms for permeability may have several advantages and disadvantages in predicting the similarity of the fluid flow performance at the coarser scale to the fine scale level. However, there is no specific algorithm that can be generally understood and used for various heterogeneity applications. Furthermore, a common observation for all three various upscaling cases indicated optimistic results in the cumulative fluid being recovered.

In this section, the derivation of the new algorithm will be proposed. The accuracy of the new estimation of the effective properties as applied to flow in the porous media will then be judged by how well the fluid flow predictions made at the coarser (macro scale) level mimic the predictions made at the finer (micro scale) level. Further detailed discussions regarding the theories and practicality for the new upscaling algorithm will feature in Chapters 4 and 5 respectively.

4.1. DERIVATION OF NEW ALGORITHM

In the development of the new upscaling algorithm, the most important concept in upscaling is being able to find the most representative of the effective grid cell values at larger reservoir simulation modelling scales. The upscaling of permeability will be the main focus, with additional enhancing treatments for supporting higher levels of accuracy, as this is the most complex property in upscaling, as discussed in previous chapters.

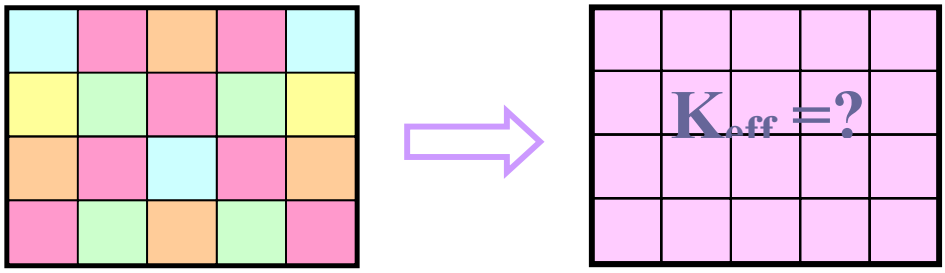

Figure 4-1 Problem statement for the new upscaling algorithm

Following is a summary of observations as has been discussed in previous chapters. All of these factors will be main considerations in the development of the new upscaling algorithm.

- There should not be a direct application for solutions at the fine scale to estimate the flow behaviour at the coarser scale, as this violates the main purpose of upscaling, which is to avoid conducting time-consuming flow simulations.
- An unrestricted number of grid blocks to be upscaled should not be a constraint in any upscaling algorithm.
- Designing and generating the simulation coarse grid should be, as much as possible, aligned with the primary flow direction to minimise the deviation in principal permeability directions. This implies similar methodology in designing the geological fine grid model.
- Generating a single averaged property at a coarse grid level is typically obtained by solving flow problems of original multiphase systems within a coarse grid under local boundary conditions.
- A general algorithm should not be deviated from the upscaling principal theory/observation (i.e. a simple case with parallel bedding can be represented by using the arithmetic mean, while a case with directional flow perpendicular to the bedding can be represented by using the harmonic mean). Also the effective average permeability should be within the following bounds:

$$K_A > K_{AH} > K_{eff} > K_{HA} > K_H$$

Based on previous experiments using the existing algorithm, several algorithms, such as diagonal tensor, arithmetic-harmonic, harmonic-arithmetic and renormalisation, are believed to be the most representative of the upscaling for permeability from the fine scale to its coarser scale. In this research, the new algorithm is based on a combination principal theory of diagonal tensor, renormalisation and arithmetic-harmonic/harmonic-arithmetic algorithms, which are proven to be valid upscaling algorithms, and will be proposed and tested further.

The following upscaling concept is proposed for the new algorithm as shown below.

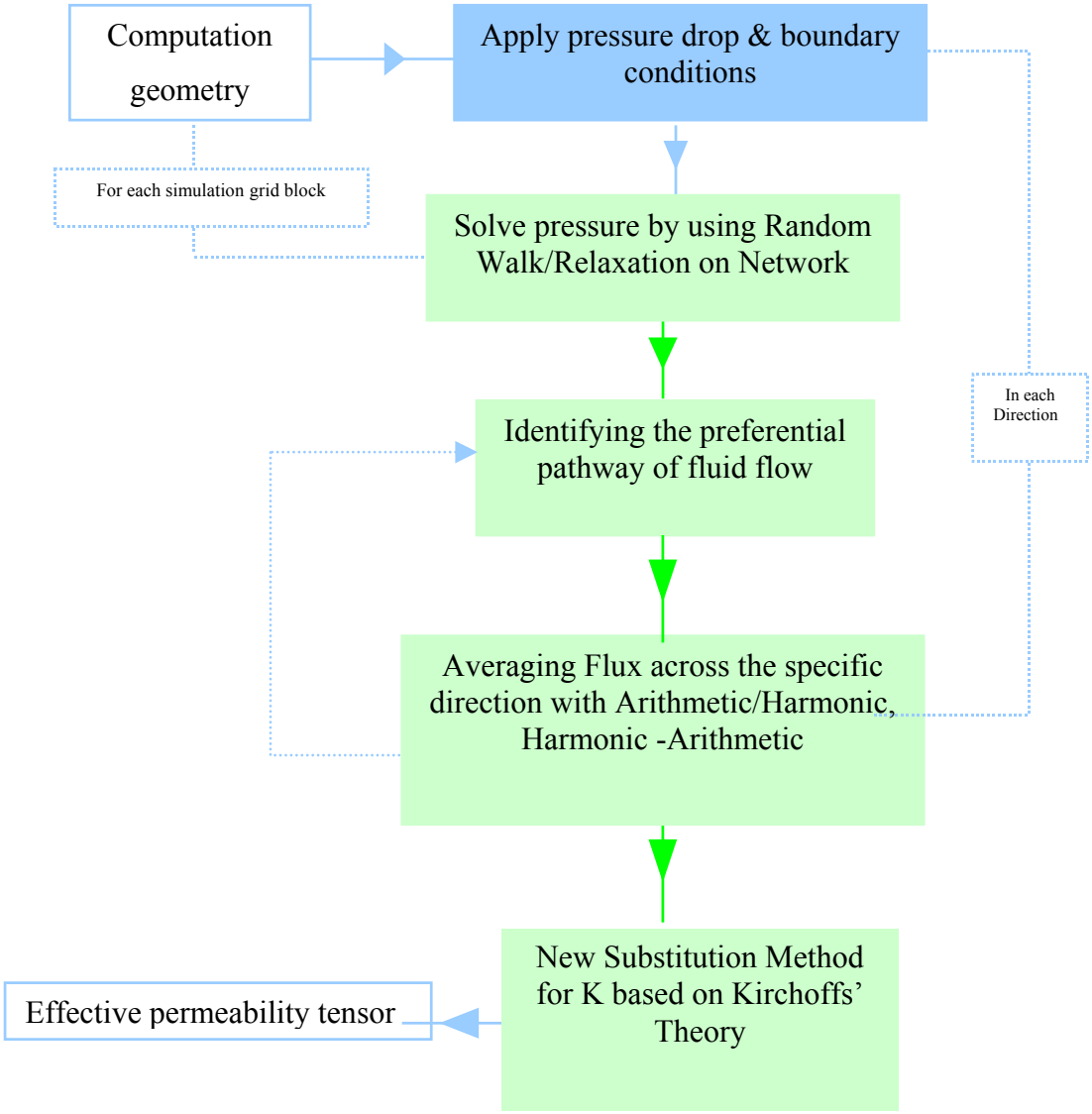

Figure 4-2 Process flowchart on the new upscaling algorithm

The steps procedures will be discussed in detail in the following sections.

4.1.1. Periodic boundary conditions

The initial step in the upscaling concept is conducted by defining the pressure boundary for the area of interest. The pressure boundary is defined similarly to the diagonal tensor or full tensor's principal, by applying arbitrary pressure equal to one and zero at the inlet and outlet respectively. The law of nature indicates that any fluid flow or particle will always move from a high potential to a low potential. By

defining the pressure boundary, the fluid flow can be forced to flow in a specific direction and can be expressed as shown in Figure 4-3. A periodic boundary for different directions can then be applied according to a similar principal.

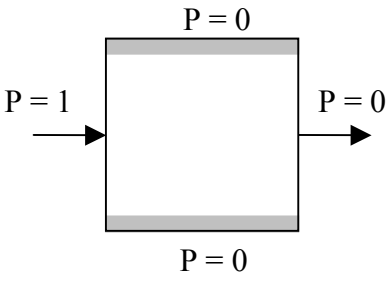

Figure 4-3 Pressure boundary conditions on new upscaling algorithm

4.1.2. Pressure solution with random walk/relaxation method on network

To be able to solve the fluid flow equation in a numerical performance, a similar method to the renormalisation method could possibly be used, by utilising the equivalent resistors of the electrical network. In this section, similarity between the fluid flow equation and the electrical network solution will be discussed further. The pressure solution, with a combination of the random walk and relaxation method on network, will be described in detail.

4.1.2.1. Equivalent expression of Darcy's law (fluid flow) with Ohm's law (electrical network)

The rate of the fluid flow in the porous media may be expressed using Darcy's law and is defined as follows:

$$Q = -\frac{KA}{\mu}\frac{\Delta P}{\Delta X}$$

Equation 4-1 Darcy's law of fluid flow in porous media

By referring to the above equation and the renormalisation theory, Darcy's equation may possibly be expressed similarly to the simple Ohm's law for the electrical network principal.

$$\text{Darcy's law} \qquad Q = -\frac{KA}{\mu}\frac{\Delta P}{\Delta X}$$

$$\text{Ohm's law} \qquad V = IR$$

Equation 4-2 Comparison of Darcy's law of fluid flow in porous media and Ohm's law of electrical network

Both equations use the law of nature theory, meaning the fluid or charge particle will move if there are any potential differences and will flow from its high potential to its low potential. In this case, the Voltage (V) for the electrical theory expressed the potential difference for the electrical charge to move, while on the other hand, in the fluid flow theory, the pressure drop $\frac{\Delta P}{\Delta X}$ expression indicates the potential difference for the movement of fluid to flow in the porous media. The current (I) flow through the electrical network is equivalent to the amount of fluid flow through the media (Q). Also, the resistivity can be expressed for both the electrical and porous media with the equivalent of electrical resistance (R) and the inverse of permeability (1/K) respectively.

Therefore, both equations can be expressed according to the following equivalent expression:

- Voltage [V] is equivalent to pressure drop $\frac{\partial P}{\partial X}$ or in mathematical expression $\left[V \propto \frac{\partial P}{\partial X}\right]$
- Current [I] is equivalent to fluid flow rate [Q], or in mathematical expression $[I \propto Q]$

- Resistance [R] is equivalent to its inversely proportional of permeability [K], or in mathematical expression $\left[R \propto \frac{1}{K} \right]$

4.1.2.2. Equivalent resistor network for permeability parameter model

To be able to provide the pressure solution of the fluid flow in the numerical simulation, the equivalent resistor is required to be defined for the representation of the permeability parameter in the numerical simulation model. The equivalent resistor of each fine cell is $\frac{1}{K}$. Thus, the permeability at the centre of the fine cell can be represented using the equivalent to two resistors in the series, which is $\frac{1}{2K}$. In general, permeability is defined with the directional dependent in x, y and z directions. Therefore, each block can be replaced with a cross of resistors as shown in Figure 4-4 in a two-dimensional illustration. For isotropic media, the resistors will be the same in either direction as the permeability in x and y directions are the same.

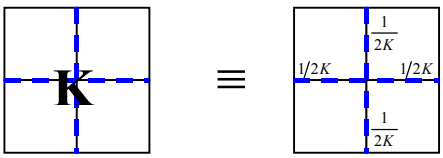

Figure 4-4 Equivalent resistor for isotropic permeability parameter ($K_x = K_y$) in a two-dimensional model

The equivalent resistors of permeability parameters at each coarse grid cell can then be illustrated in the following diagram:

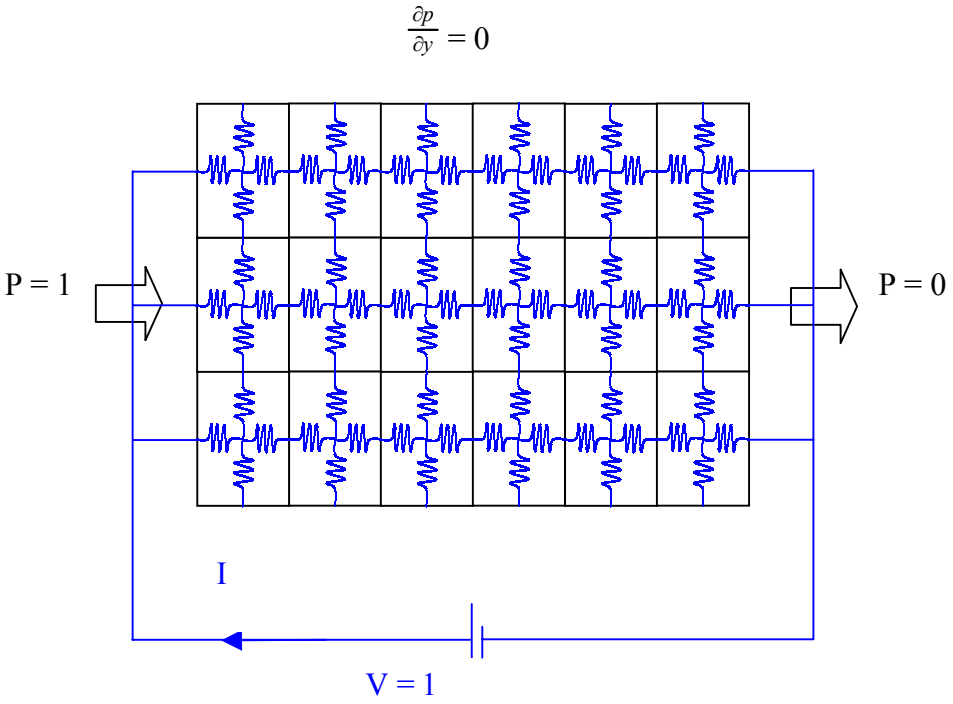

Figure 4-5 Equivalent resistors for permeability parameter at each coarse cell in a two-dimensional model

As mentioned above, in determining the effective permeability at one direction, the pressure boundaries are set such that the fluid will flow to a specific direction with the inlet and outlet uniform pressures of one and zero respectively, with no flow across to the other sides of the coarse grid block ($\delta P/\delta y=0$, $\delta P/\delta z = 0$). Here, the fluid flow is only considered in one direction. By referring to Figure 4-5, there are several dead-end edges at the other directions. Therefore, for a better representation for calculating the effective permeability, these dead-end branches are eliminated and simplified in the following equivalent resistor network.

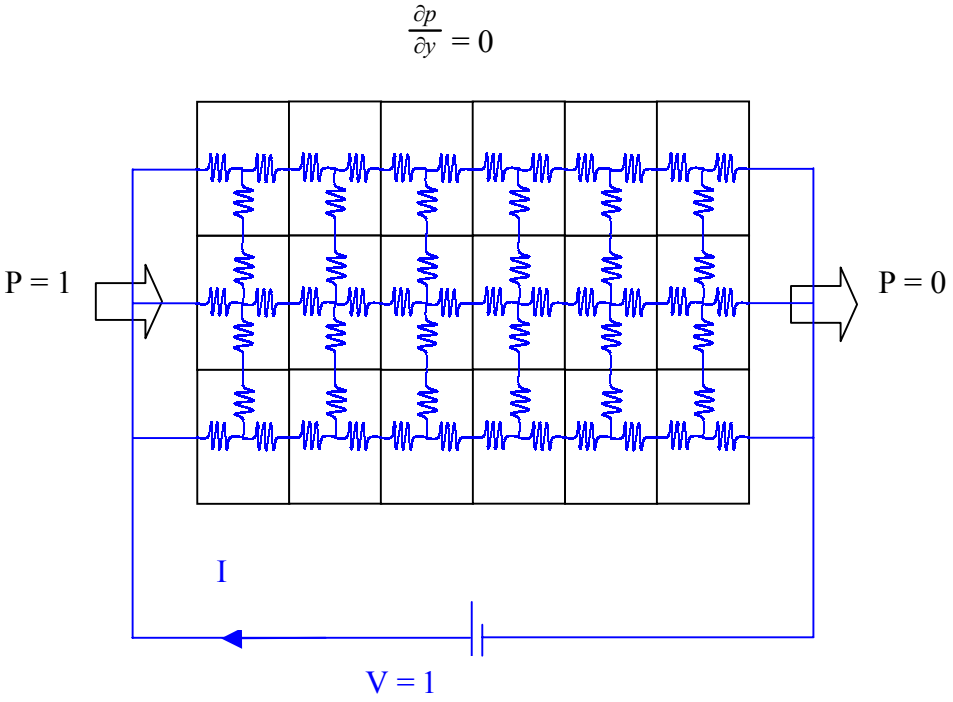

Figure 4-6 Simplified equivalent resistors for permeability parameter at each coarse cell in a two-dimensional model

This network is then used to provide the pressure solution within the coarse grid cell.

4.1.2.3. Pressure solution with random walk and method of relaxation

To be able to solve the pressure solution in fluid flow, or the equivalent current solution in the electrical network as illustrated in Figure 4-6, the 'random walk' and 'method of relaxation' are proposed to be used with a combination of Kirchhoff's theories.

4.1.2.3.1 Random walk and method of relaxation

The method of relaxation was introduced for providing the approximate solutions to the discrete Dirichlet problem. The method uses the function that has the specific boundary values, for the value at which the interior points is the average of the

values of its neighbours. This is similar to the problem that must be solved, as there are boundary conditions and each cross flow/resistor is dependent on the values of its neighbours.

The way the method of relaxation works is that initially, all the interior points are set to zero and the boundary points are fixed with the constant values of one and zero. It begins with an interior point, and the value is then adjusted with the average of values at its neighbours. Random walk with any potential alternate pathways, as shown in Figure 4-7, to the next interior point is then approximated with a similar averaging method of the neighbours' values. This process is then repeated for the rest of the interior points. (Doyle *et al.,* 1984, p.22-25)

After adjusting all the interior points, the results will not be harmonic anymore as most of the time the values are adjusted at a point to be the average value of its neighbours and those neighbours' values are also adjusted in the next process. In other words, readjusting those neighbours' values has destroyed the harmony in this specific problem boundary. However, the values are more nearly in harmony, if not in harmony, than the initial function we started with. Thus, by repeating the above procedure, a better approximation closer to the solution can be obtained.

The method of relaxation is summarised in Figure 4-8.

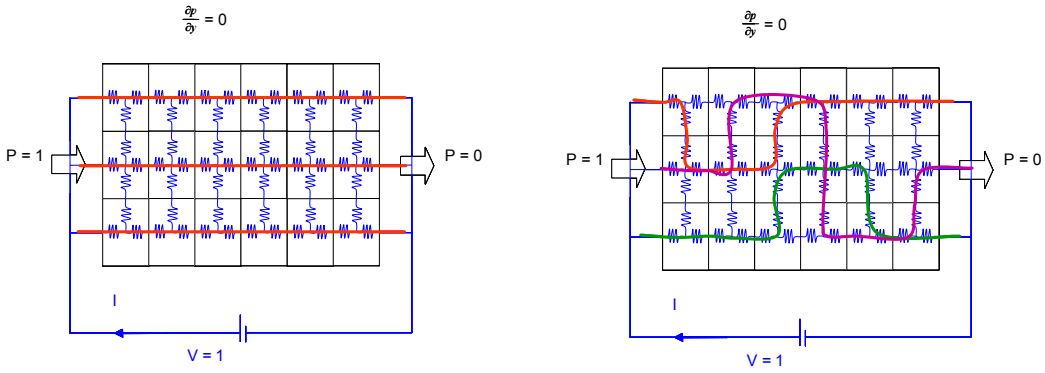

Figure 4-7 Few Possible Alterate Path Ways (indicated by lines) in solving the Simplified Network where Random Walks can be applied

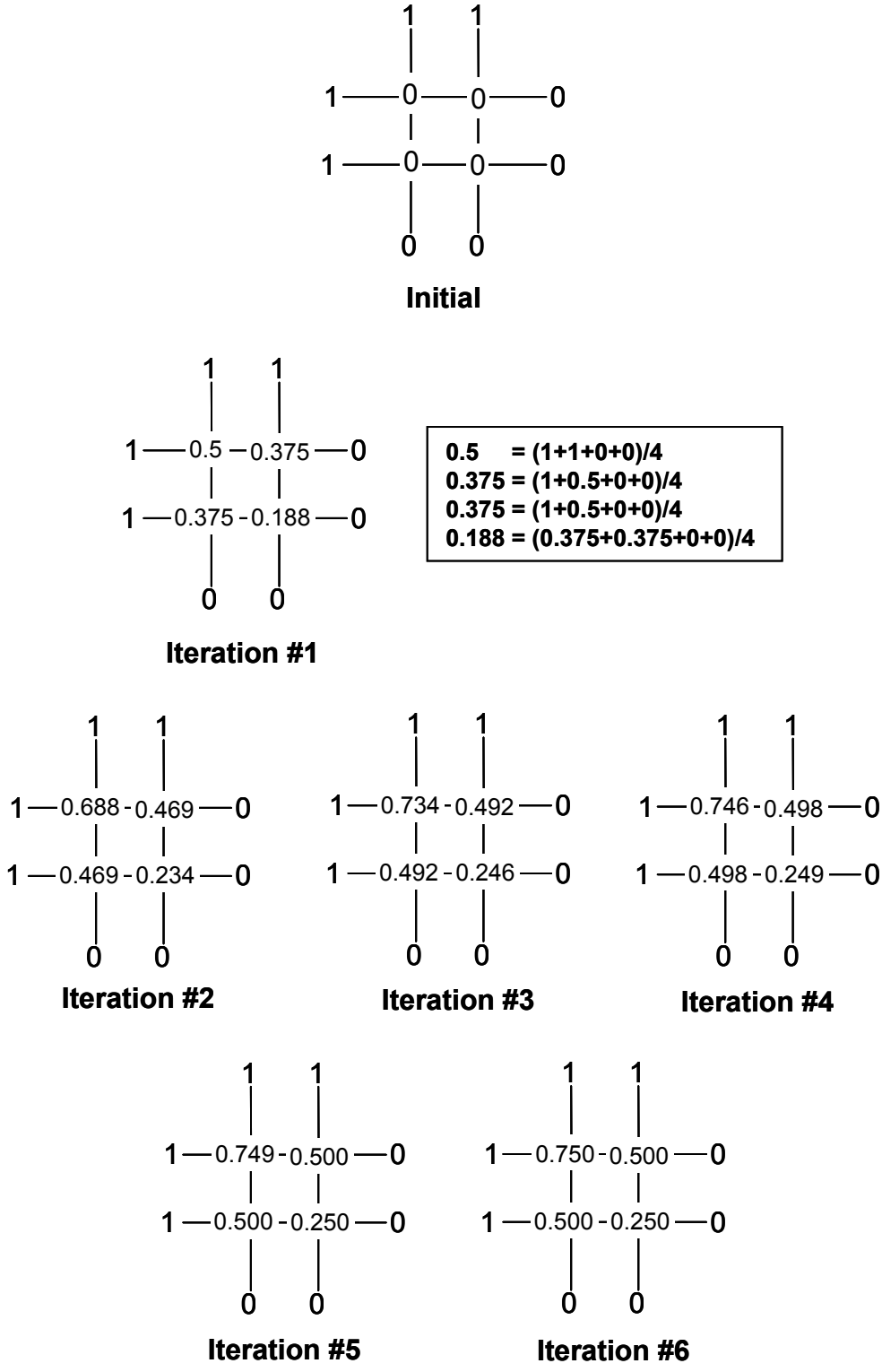

Figure 4-8 the Relaxation Method

So, how can the method of relaxation be related to our problem?

4.1.2.3.2 Kirchhoff's theories and method of relaxation

As stated in Section 4.1.2.1, Darcy's law of equation, which governs the fluid flow equation, can be expressed with an equivalent equation as Ohm's law equation for the electrical network. The voltage [V] in the electrical network is equivalent to the pressure drop $\frac{\partial P}{\partial X}$ and the flowing current [I] is equivalent to the fluid flow rate [Q]. The permeability, which is the property of fluid flow in porous media, can be expressed with the equivalent terms of inverse value of resistance [R].

In the electrical network's principal, the current and voltage at any nodes can be solved by using Kirchhoff's laws. They are:

- Kirchhoff's current law
- Kirchhoff's voltage law

Kirchhoff's current law states that the sum of the currents entering or leaving a junction point at any instant is equal to zero (Del Toro, 1986, p. 15-17).

$$\sum_{j=1}^{k} I_j = 0$$

Equation 4-3 Kirchhoff's current law, where k denotes the number of circuit elements connected to the node in question

Kirchhoff's current law holds the principle of conservation of charge. The number of electrons passing per second must be the same for all points in the circuit. Thus, this principle of conservation of charge is also equivalent to the conservation of mass within the porous media under a steady state condition, as the fluid flow rate at any time into the reservoir should be equal to the fluid flow out from it. An illustration of Kirchhoff's current law is shown in Figure 4-9.

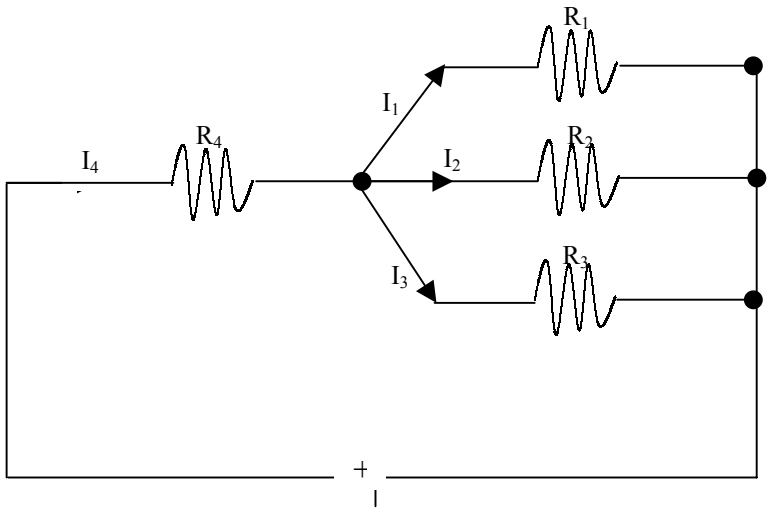

Figure 4-9 Illustrating diagram of Kirchhoff's current law

By referring to Figure 4-9, Kirchhoff's current law can be expressed as:

$$I_4 = I_1 + I_2 + I_3$$
$$I_4 - I_1 - I_2 - I_3 = 0$$

Kirchhoff's voltage law states that at any time instant, the sum of voltages in a closed circuit is zero (Del Toro, 1986, p. 15-17). This voltage law holds the principle of conservation of energy, which is also required in the fluid flow description. The mathematical expression for illustrating Kirchhoff's voltage law is:

$$E = V_1 + V_2 + \ldots + V_n$$

Equation 4-4 Kirchhoff's voltage law

The following diagram illustrates the above Kirchhoff's voltage law.

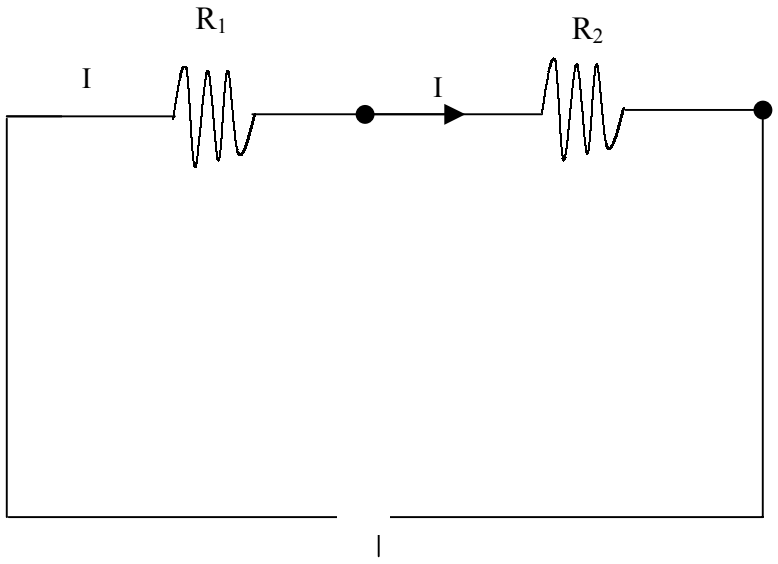

Figure 4-10 Illustrating diagram of Kirchhoff's voltage law

Therefore, for the following network as illustrated in Figure 4-11, the above-mentioned Kirchhoff's voltage and current laws can be recombined to obtain the voltage (V) at the centre of the nodes.

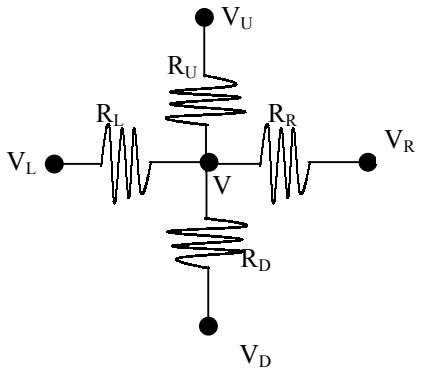

Figure 4-11 A cell network diagram for solving permeability fine scale network (Figure 4-6)

By using Kirchhoff's current law, the network as illustrated in Figure 4-10 can then be solved as follows:

$$I_L = I_R + I_U + I_D$$

Substituting it with Ohm's law as V = IR, then:

$$\frac{V_L - V}{R_L} = \frac{V - V_R}{R_R} + \frac{V - V_U}{R_U} + \frac{V - V_D}{R_D}$$

Rearranging the above one, then:

$$\frac{V_L}{R_L} - \frac{V}{R_L} = \frac{V}{R_R} - \frac{V_R}{R_R} + \frac{V}{R_U} - \frac{V_u}{R_U} + \frac{V}{R_D} - \frac{V_D}{R_D}$$

$$\frac{V_L}{R_L} + \frac{V_R}{R_R} + \frac{V_u}{R_U} + \frac{V_D}{R_D} = V\left(\frac{1}{R_R} + \frac{1}{R_L} + \frac{1}{R_U} + \frac{1}{R_D}\right)$$

$$V = \frac{\frac{V_L}{R_L} + \frac{V_R}{R_R} + \frac{V_u}{R_U} + \frac{V_D}{R_D}}{\left(\frac{1}{R_R} + \frac{1}{R_L} + \frac{1}{R_U} + \frac{1}{R_D}\right)}$$

Equation 4-5 Solving Voltage (V) at the centre of the node as illustrated with Figure 4-11

From the simplified Equation 4-5, the voltage at any centre of the nodes can be solved by taking the inverse resistor (1/R) weighted average of the voltages in the neighbouring points. For the fluid flow in porous media, the pressure value (equivalent to voltage in electrical network) can then be approximated with the permeability weighted arithmetic average with the pressures at its surrounding cells. This averaging method is what the methods of relaxation use in the way of approximating the value at the centre points with its neighbouring points.

By taking the methods of relaxation and a simplified Equation 4-5, the bigger network with any unlimited number of cells as illustrated in Figure 4-6 can then be solved.

4.1.3. Averaging for new effective permeability

The next step, post solving the pressure solution within the network, is to identify the preferential pathways and to provide the single cell value for representing the average value of the effective permeability at the coarse scale model.

Once again, according to the law of nature, the particle will always move from the greater to the lower potential. This is the same principal with fluid flow in the reservoir. The greater the pressure drop across the cell is, the greater tendency of the fluid to flow from one point to another. Thus, once the pressure solution is obtained for the network as illustrated in Figure 4-6, the preferential path of fluid flow within the coarse grid system in the specific direction may be determined. These preferential paths should be used as the basis for the effective properties' determination, as this will govern the main prefential flow direction from the inlet to the outlet within the coarse cell.

By determining the preferential paths of the fluid to flow within the coarse grid cell, it was found that some dominant flow paths especially with high permeability streaks could be more preferable compared to other ones. In this upscaling method, a variation of the fluid flow paths captured within the cell would be beneficial, as in reality these various paths would represent the various break-through of fluid flows from one end to another end.

Therefore, what should the representation of a single value for the effective permeability within this coarse cell be?

Prior to averaging, the equivalent flow rate or current for the electrical term must be determined. By referring to Ohm's law equation (Equation 4-2), the potential difference (voltage or pressure drop) across one node to the neighbour nodes and the current (or fluid flow rate) may be determined by knowing the resistance (or permeability) between the two nodes. For an illustration of this, please refer to Figure 4-13.

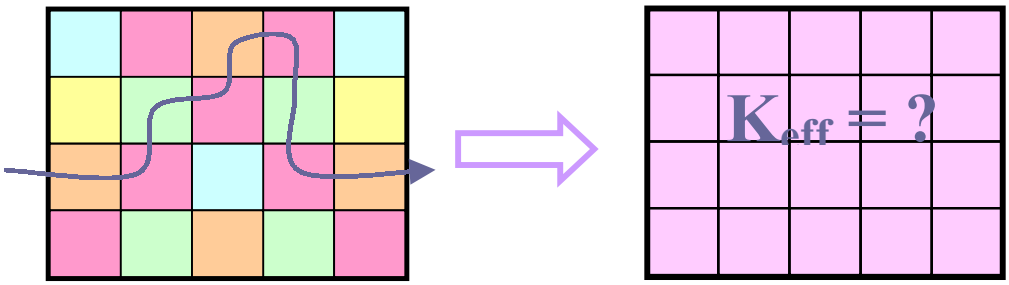

Figure 4-12 Illustrating preferential path within coarse grid cell

In order to obtain the effective value of permeability for the coarse cell, the estimation of the overall resistance must be determined. Within the coarse grid cell in the specific direction, the pressure difference (or the electrical potential/voltage difference) is known to be equal to one due to our definition for the pressure boundary. If the current flowing (or fluid flow rate) through this coarse cell is known, the resultant equivalent resistance (or permeability) may be determined.

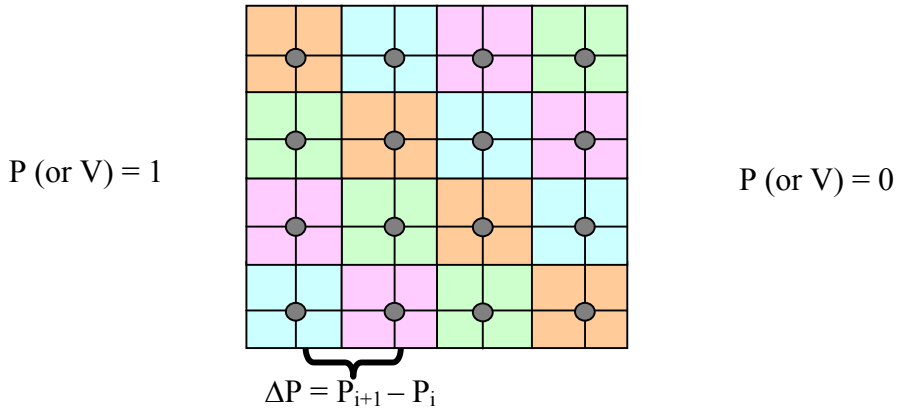

$V = IR$ (Electrical)

$\Delta P = Q.(1/K)$ ($\approx$ fluid flow equation)

Combining 2 equations:

$I_i = \Delta P_i * K_i$

Figure 4-13 Illustrating Voltage (or Pressure Difference), Current (or Fluid Flow Rate) within a coarse grid cell

Kirchhoff's law stated that the sum of current flowing into the network would be the same as the sum of current flowing out from the network. In this way, the current flowing through the coarse grid cell can be known. Thus, the effective permeability can be defined as follows:

$$V = IR$$
$$R = \frac{V}{I}$$
$$V = 1 \quad \text{and} \quad I = \sum I_{inlet} = \sum I_{outlet}$$
$$R = \frac{1}{\sum I_{inlet}} = \frac{1}{\sum I_{outlet}}$$
$$R = 1/K$$
$$K = \frac{1}{R} = \sum I_{inlet} = \sum I_{outlet}$$

Equation 4-6 Derivation for effective permeability

Permeability is an intensive property while resistance is an extensive one. Thus, the changes of dimensions are required for consideration when determining the effective permeability. In order to determine the average effective properties and convert the intensive properties of the permeability from the extensive parameters of the resistance, modification to Equation 4-6 is required. This can be expressed in a similar way to the arithmetic-harmonic method.

Steps on the modification of the effective permeability determination are summarised below:

1. The current on each fine cellblock is calculated by taking the product of the pressure difference with the permeability on that stream.
2. The sum of the current on each row is then determined. For the electrical network, the total current flowing through each row will be the same as between the inlet and outlet current. Thus, the effective permeability as an extensive property becomes the total current as shown in Equation 4-6. However, the final modification on the effective permeability to become an

intensive property must then be multiplied by the block dimension on that direction. For each row, the effective permeability is then determined using the following equation:

For each row :

$$K_{extensive} = \frac{1}{R} = I_{inlet} = I_{outlet}$$

$$K_{eff} = K_{extensive} * (nx / nz) \approx \sum I_{each\_row}$$

$nx =$ no of cells in direction x within a coarse cell

$nz = 1$ for each row

3. Similar to step 2, the final step must take the average current of all rows within the coarse cell. For the electrical network, the total current will be the sum of currents on each row. Thus, the effective permeability as an extensive property becomes the total current as shown in Equation 4-6. Similar to step 2, dimensional changes must be incorporated for the intensive property, such as permeability. Therefore, the final modification for the effective permeability as an intensive property must be divided by the total number of rows within the coarse cell. Thus, the effective permeability is then simply the average of the total currents on each row.

For sum of rows :

$$K_{extensive} = \frac{1}{R} = \sum I_{inlet} = \sum I_{outlet}$$

$$K_{eff} = K_{extensive} * (nx / nz) \approx \frac{(\sum I_{each\_row})}{nz}$$

$nx = 1$

$nz =$ no of cells perpendicular to direction x within a coarse cell

The summary of the steps in determining the effective permeability in direction x is shown in Figure 4-14.

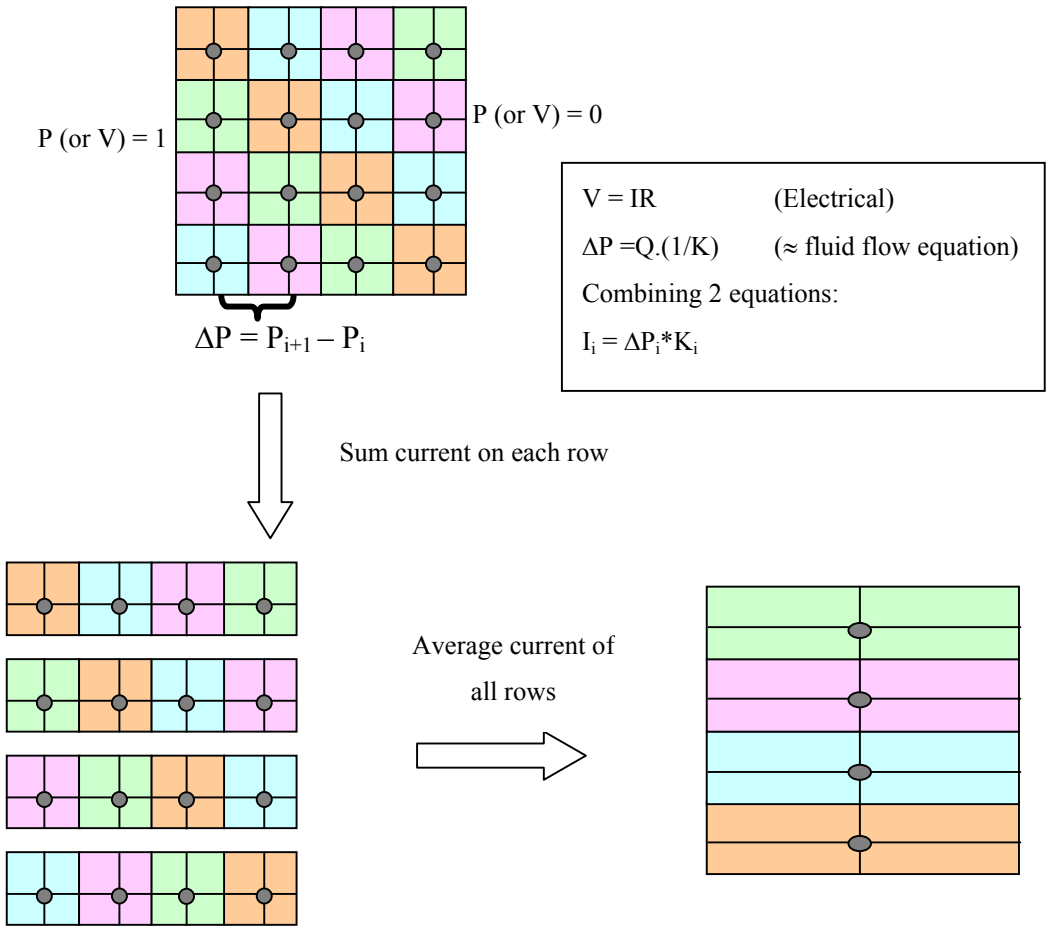

Figure 4-14 Modification for determining the effective permeability

4.2. OTHER PARAMETERS IN THE NEW UPSCALING

In the previous section, the derivation of the new algorithm only concentrated on finding the effective permeability. The effective permeability only signifies the tendency of fluid flow from one cell to another one within the coarse scale model. However, this does not give an indication on how the upscaled model will perform as though it were at the fine scale level. In this section, several enhanced treatments for supporting the accuracy of upscaling will also be discussed. They are:

- Treatment for incorporating unswept area in low permeability rock
- Well inflow performances.

4.2.1. Treatment for incorporating unswept area in low permeability rock

In any reservoir simulation study, the relative permeability (which describes the fraction of permeability that is available for one fluid in the presence of the other fluid flowing simultaneously through a porous media) is often defined by a single set of data to be used for any scaled model. This is not always true, as the fluid behaviour of gas, oil and/or water is affected by permeability, porosity and fluid saturation. This can be seen clearly from Darcy's law of fluid flow, which states that the fluid flow rate is proportional to the permeability. Therefore, the greater the permeability, the greater the fluid flow rate will be. As a consequence of this, fluid within low permeability rock has a tendency to be stationary or become the least preferential fluid to flow.

$$Q = -\frac{KA}{\mu}\frac{\Delta P}{\Delta X}$$

Equation 4-7 Darcy's law of fluid flow in porous media

In the upscaled coarse scale model however, the fluid in the low permeability rock, which most likely becomes stationary and remains in the reservoir, will be treated differently. With upscaling, the expected permeability values and its variance have in general decreased. Thus, the high and low permeability streaks become more or less closer to the average expected value. Due to this reason, fluid trapped in the low permeability rock which is supposed to be stationary, becomes movable under the upscaled coarse scale model. This could be the reason why the fluid recovery was optimistic in most cases, as described in Chapter 3.

Due to the reason described above, the appropriate value to describe the immobile fluid must be determined. Permeability, which is the measure of the pore connectivity for the fluid flow in the porous media, is the highest contributing factor in the remaining fluid saturation. The fluid remaining in the system will normally be

in the shale area where it has the least preferential fluid flow path in the system and the permeability and porosity properties are very low. Shale permeability is found in the range up to 0.5 mDarcy. Due to this, the following arbitrary permeability cut-off is used for describing the unswept area or a non-net area where the major residual fluid is still remaining in the system and will not be drained by any depletion scenarios.

Reservoir Fluid	Permeability Cut-off (mDarcy)
Gas	0.10
Oil	1.00

Table 4-1 Permeability cut-off for residual fluid remaining in the reservoir

The arbitaray permeability cut offs as shown in Table 4-1 are based on the traditionally adopted rules of thumb for cutoffs used by the Western petroleum industries. (Deakin *et al.*, 1998, Balbinski *et al.*, 2002, Cordell *et al.*, 1965, Worthington *et al.*, 2005)

For incorporating the remaining fluid, the relative permeability, which describes the residual fluid saturation component in the reservoir, can then be altered. This is normally described in Corey's equation as follows:

$$K_{rw} = K^*_{rw}\left(\frac{S_w - S_{wc}}{1 - S_{wc} - S_{orw}}\right)^{Nw}$$

$$K_{row} = K^*_{row}\left(\frac{1 - S_w - S_{orw}}{1 - S_{wc} - S_{orw}}\right)^{Now}$$

Equation 4-8 Corey equations for oil-water system

$$K_{rg} = K^*_{rg}\left(\frac{S_g - S_{gc}}{1 - S_{gc} - S_{org}}\right)^{Ng}$$

$$K_{rog} = K^*_{rog}\left(\frac{1 - S_g - S_{org}}{1 - S_{gc} - S_{org}}\right)^{Nog}$$

Equation 4-9 Corey equations for oil-gas system

By treating the pore volume with low permeability as the additional residual fluid remaining in the system, the total residual fluid saturation within the coarse grid cell can then be recalculated and included in the relative permeability description. The new set of relative permeability with the modified residual fluid saturation for each grid cell can then be used in the reservoir simulation at the upscaled model.

Similar treatment can also be applied for incorporating the unpenetrated fluid from the current production wells and/or the unswept remaining reservoir fluid due to reservoir discontinuity (i.e. isolated sand due to shale barriers). Streamline simulations may be used to give an indication of the remaining fluid in the reservoir.

4.2.1.1. Verification of incorporating unswept area in low permeability rock

For verification, Model B has been used at the fine scale level for rectifying the correct implementation of saturation modification and also the permeability cut-off used. The comparison simulation results are shown below and indicate a good agreement between the cases with and without the saturation modification. Therefore, this will not alter any simulation results, but will help to implement a correct representation of the unswept fluid at the low permeability rock within the coarse scale model.

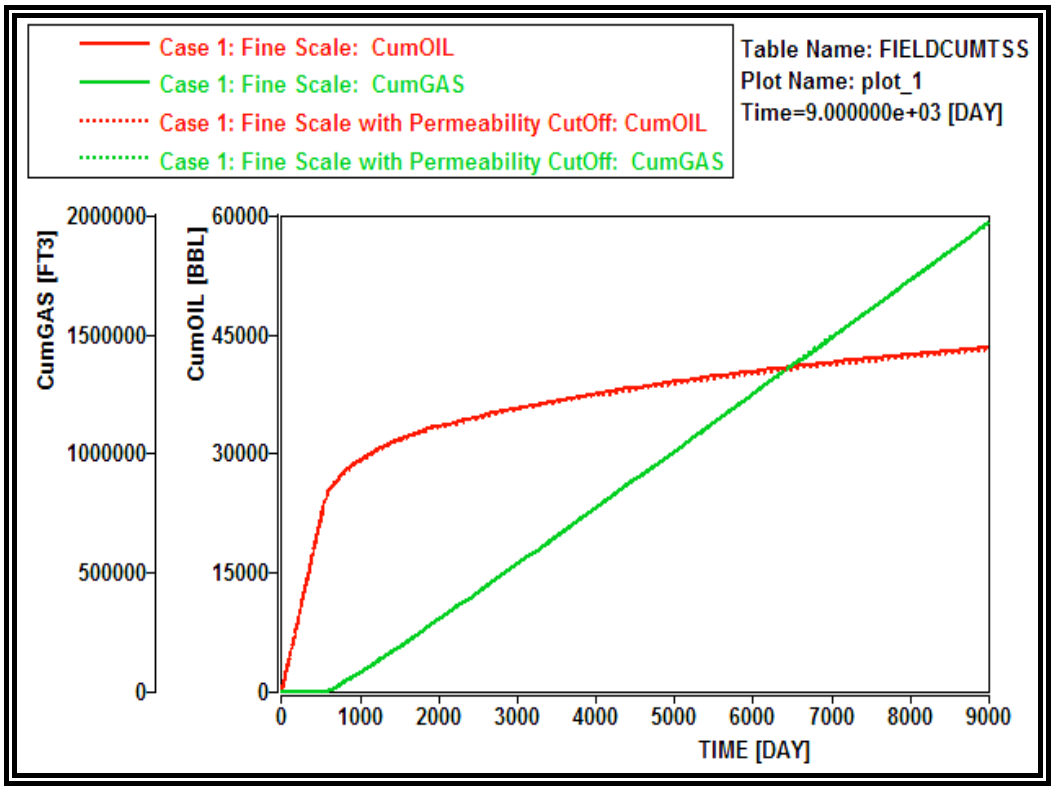

Figure 4-15 Comparison plot of gas and oil production rate for Model B with and without saturation modification

Further verification of the concept for improving the predictions at the coarse model is discussed in Chapter 5.

4.2.2. Well inflow parameter

Another important parameter to be considered in the reservoir simulation is the treatment of wells for the well performances. The material balance of the fluid flow equations for the reservoir provides the grid block pressures and material fluid accumulations. Another model, known as the well model, is also required to relate flow in the grid area surrounding the well to the well bore flow and to define the relationship between the grid block pressures and down-hole well bore pressures. This model will allow the simulation of realistic physical conditions at wells under specific reservoir conditions and their properties. (Dake, 1978, p.136-147)

The well inflow equation is usually described with an analytical method known as the Peaceman inflow model. This model treats the well as the line source, in which relates the grid block conditions (pressure and fluid composition), the well bore pressure and the well flow in the reservoir as the strength of the source.

For a steady state, the Peaceman equation can be outlined as follows:

$$\overline{p} - p_{wf} = \frac{q\mu}{2\pi kh}\left(\ln\frac{r_e}{r_w}\right)$$

For a semi-steady state, the Peaceman equation can be outlined as follows:

$$\overline{p} - p_{wf} = \frac{q\mu}{2\pi kh}\left(\ln\frac{r_e}{r_w} - \frac{3}{4}\right)$$

For a vertical well, the interval permeability height product is given by the block thickness (Δz) times the geometric average of the horizontal permeability. This parameter is related to the physical properties of the model within the well perforation intervals. This is subject to change due to the upscaled parameters of permeability at the coarser scaled cells compared to its fine scaled cells within the well perforation intervals. A solution for treating this parameter at the coarser scale will be discussed later.

$$KH = \sqrt{K_x K_y}\,\Delta z$$

Another parameter used in Peaceman's prescription is the equivalent well block radius. It is calculated by using the following equation:

$$r_E = G\sqrt{\Delta x^2\sqrt{\frac{K_x}{K_y}} + \Delta y^2\sqrt{\frac{K_x}{K_y}}}\Big/\left(\sqrt[4]{\frac{K_x}{K_y}} + \sqrt[4]{\frac{K_y}{K_x}}\right)$$

This parameter depends on the x and y dimensions of the intersected grid block (Δx and Δy) and on the local permeability in the horizontal plane. G is a mathematical constant, which can be expressed using the Euler constant, γ .

$$G = e^{-\gamma} / 2 \approx 0.2807298$$

For the isotropic horizontal permeability ($K_x = K_y$), the equation to calculate the equivalent radius simply becomes the following equation:

$$r_E = 0.1403649\sqrt{\Delta x^2 + \Delta y^2}$$

Based on the simplified equation, the equivalent radius will only depend on the dimensions of the intersected grid block. With upscaling, the cell block dimensions seen at the well intervals at the coarser scaled model are sure to be much larger compared to the cell block dimension at its finer scaled model. The change in dimension on a different scaled model will contribute to the changes of equivalent well radius.

Other parameters used in Peaceman's equation are well rates and the pressure difference at the reservoir and at the well bore, which are the result of a material balance in the reservoir model. Therefore, in order to have the same well performance at the coarse scale compared to its fine-scaled model, these two parameters must be kept the same. Thus, treatments for parameters like permeability height product and equivalent radius, which affect the well performance calculation, are required such that the well performance within the fine grid cells is preserved in the coarse grid.

Therefore, the well inflow performance parameter at the coarse grid can be defined as follows:

$$(KH)_{coarse} = \sum (KH)_{fine}$$

$$(KH)_{coarse} = \left(\sum \left(\sqrt{K_x K_y} . \Delta z \right)_{fine} \right)$$

The above modification can become significant, since in most field simulation studies, the well bore radius is only a very small fraction of the grid cell's dimension and the volume contained in the well bore is much smaller than that present in an average grid block. Thus, incorporating a consistency well performance within the coarse grid model to its fine grid model will be required. This will result in forcing the reservoir simulator to take the time steps needed to accurately represent the well inflow performance and its interaction with well variables like pressures and flow rates.

Chapter 5.
NEW UPSCALING ALGORITHM – ANALYSIS AND DISCUSSION

The three different reservoir models described in Chapter 3 are used to investigate the accuracy of the new upscaling algorithm. The improvements made to the new algorithm can then be quantified by how well the reservoir predictions made at the coarser scale mimic its' fine scale prediction. The prediction will also be compared with the existing upscaling algorithms' predictions.

The upscaling procedure shown in Figure 4-2 will be used to upscale the permeability parameter. The enhancement treatments for co-operating the unswept remaining fluid, due to low permeability in reservoir and well treatment, will also be included. Similar coarsening of the fine grid model to its coarse model, and other upscaling parameters such as porosity, capillary pressure, initial fluid distribution, and fluid PVT properties will be treated in the same way as described in Chapter 3.

Insights drawn from the comparison of the new upscaling algorithm will also be discussed in detail in this chapter.

5.1. MODEL A

Model A, which represents a quite homogeneous reservoir, can be represented by any upscaling algorithm to describe its coarser grid parameters. However, as identified earlier, the predictions at the coarse scale level seemed to underestimate the recovery of the oil produced in the reservoir. In this case, the new upscaling algorithm will be compared to how well the new results fit within the previous results using the existing algorithms, and also how well it will correct the oil production recovery rate at its coarse scale predictions. The results illustrating the flow performance with the new upscaling algorithm are shown in Figure 5-3 to

Figure 5-6. The upscaled permeability model for Model A (Figure 5-2) is comparable to the fine scale model shown in Figure 5-1.

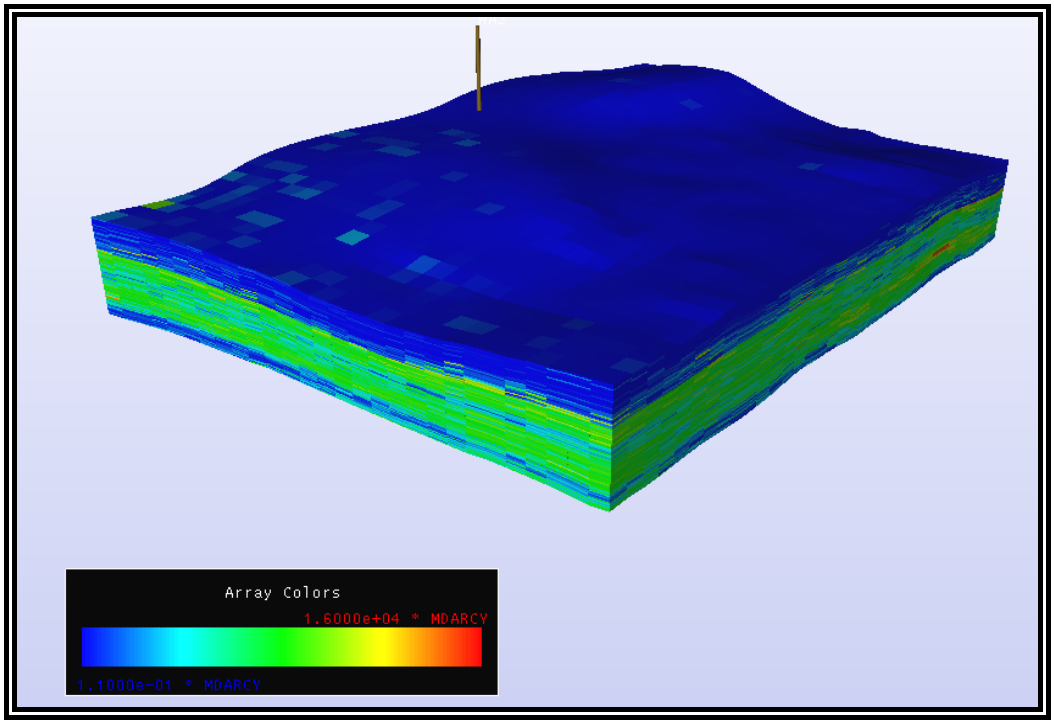

Figure 5-1 Permeability model at fine scale for Model A

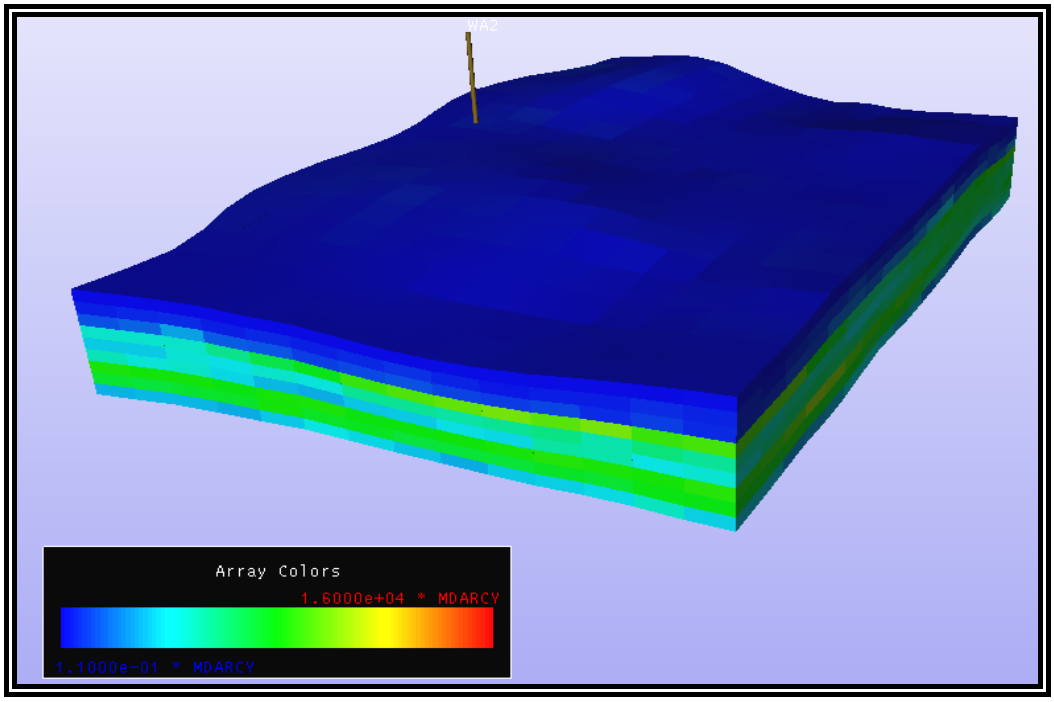

Figure 5-2 Permeability model at coarse scale for Model A

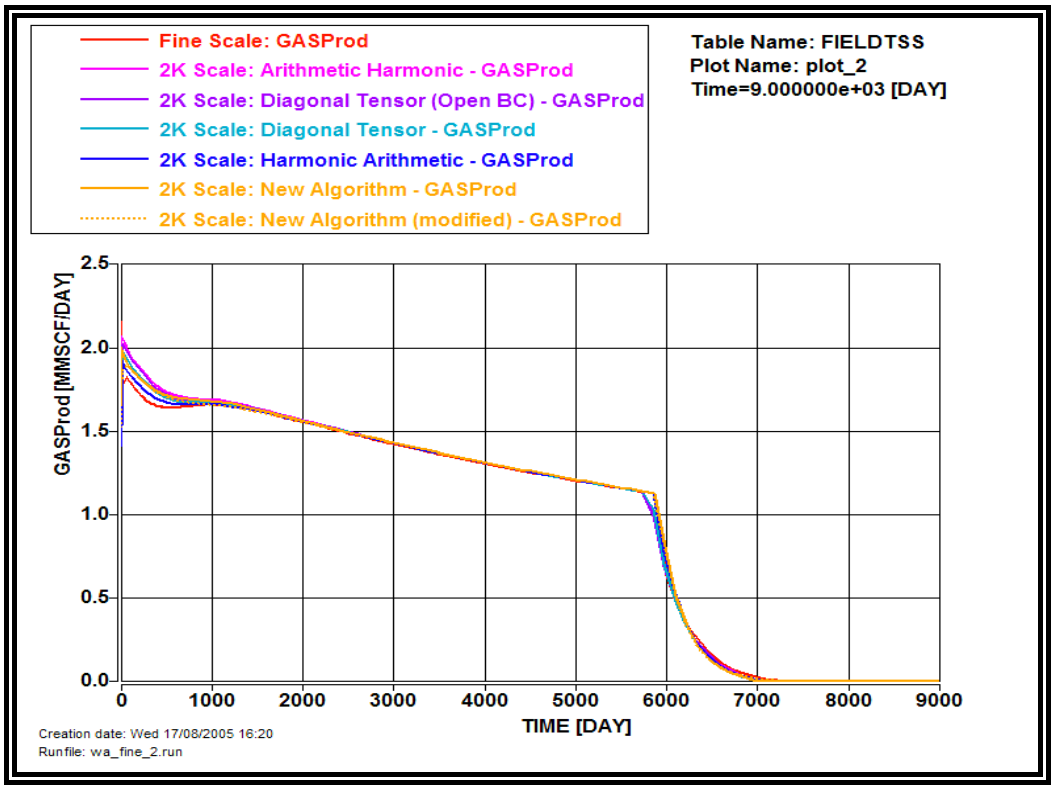

Figure 5-3 Comparison plot of gas production rate for Model A

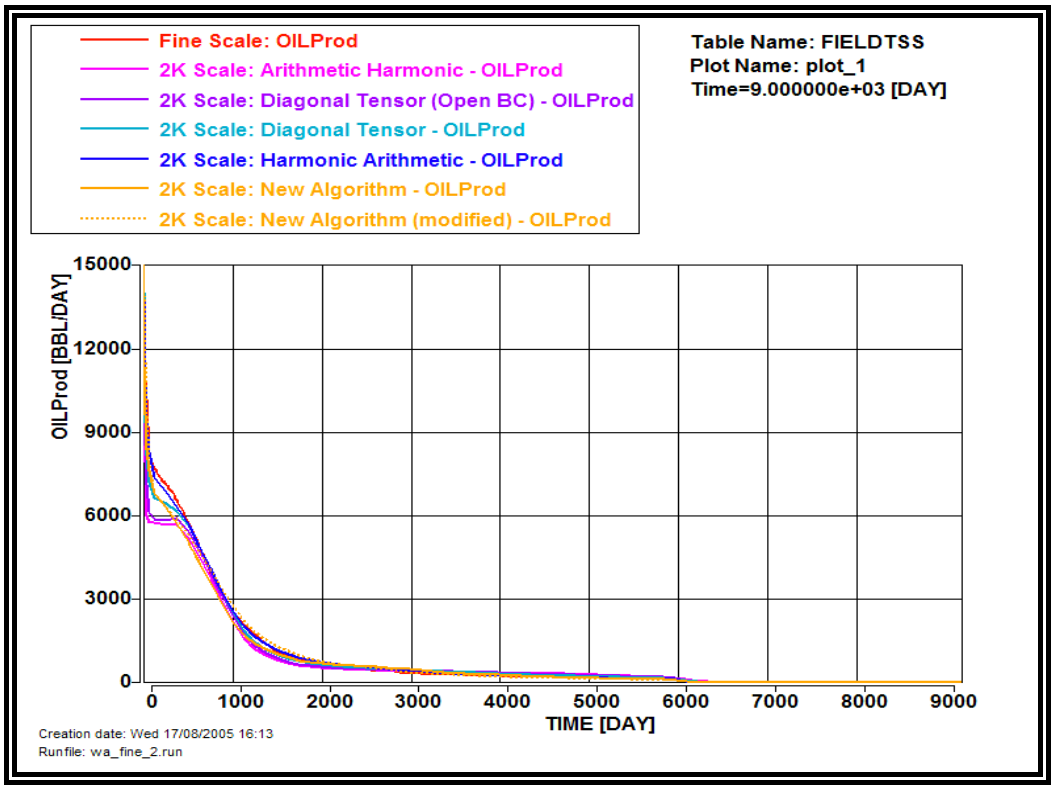

Figure 5-4 Comparison plot of oil production rate for Model A

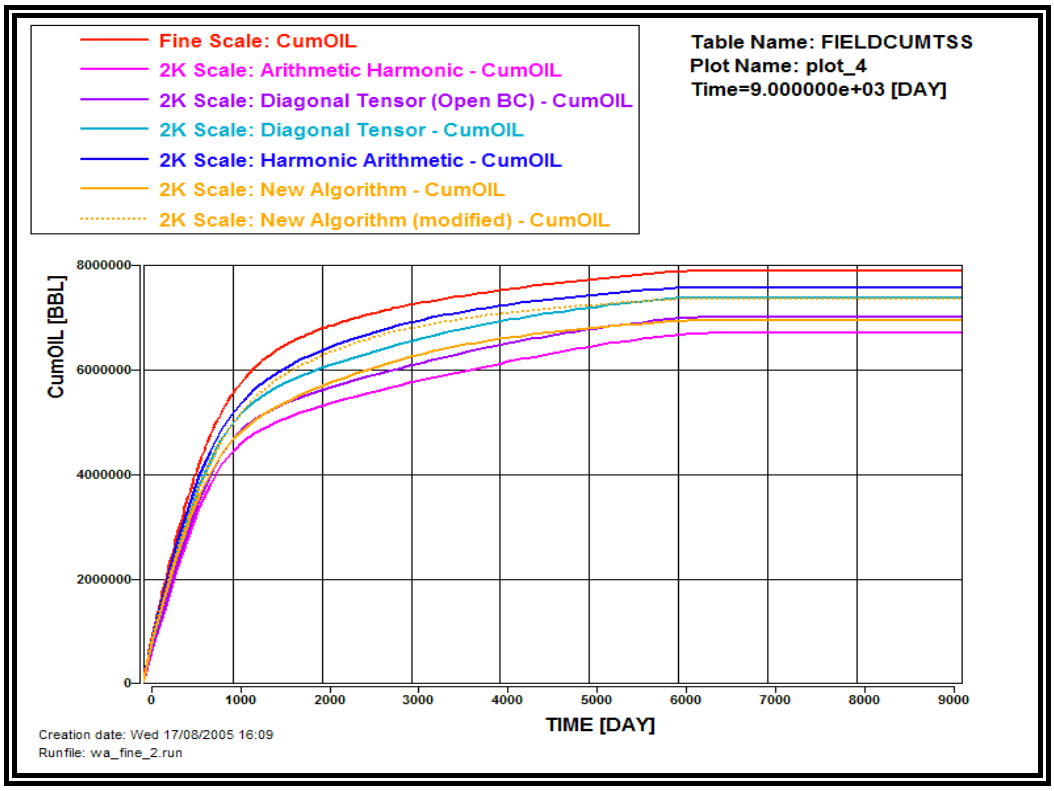

Figure 5-5 Comparison plot of cumulative oil production for Model A

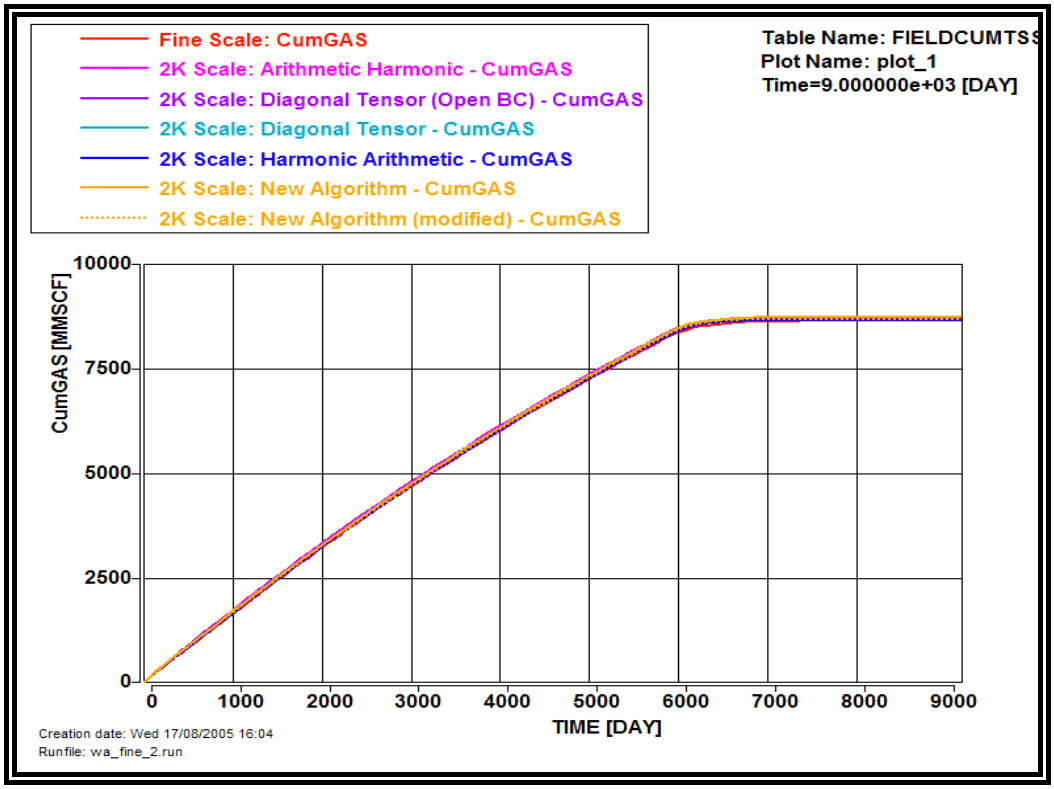

Figure 5-6 Comparison plot of cumulative gas production for Model A

Table 5-1 Comparison table for oil and gas ultimate recovery for Model A

Statistic (2K scale to Fine Scale)
End 9000 days simulation

Algorithm	Remaining OIP (MMBBL)	Remaining GIP (BSCF)	UR (Condensate)	UR (Gas)
Fine Scale	216.14	14.553	3.53 %	37.3 %
Arithmetic Harmonic	217.33 (0.55 %)	14.458 (-0.65%)	3.00 % (-15.0 %)	37.7 % (1.1 %)
Harmonic Arithmetic	216.46 (0.15%)	14.521 (-0.22%)	3.39 % (-4.0 %)	37.4 % (0.3%)
Diagonal Tensor	216.65 (0.23%)	14.517 (-0.25%)	3.30 % (-6.5%)	37.4 % (0.3%)
Diagonal Tensor (Open BC)	217.03 (0.41%)	14.483 (-0.48%)	3.13 % (-11.3 %)	37.6 % (0.8%)
New Algorithm	217.01 (0.40%)	14.466 (-0.60%)	3.14 % (-11.0 %)	37.7 % (1.1 %)
New Algorithm (Modified SW)	216.68 (0.25%)	14.502 (-0.35%)	3.29 % (-6.8 %)	37.5 % (0.5%)
Original Fluid In Place	224.05	23.206	-	-

* Values in bracket indicate the error difference between fine scale simulation to the coarse scale with appropriate algorithm.

The comparison plots indicate clearly that the results obtained using the new upscaling algorithm fits with the results of the existing algorithms for Model A as expected. It predicts similar behaviour to the numerical approaches of upscaling (such as the diagonal tensor method with closed and open boundary approaches) and also the analytical upscaling algorithms like arithmetic-harmonic and harmonic-arithmetic methods.

With the further treatment in incorporating the remaining unswept area within the model, the prediction for the oil produced recovery in the reservoir at a coarser scale model can be improved without altering any fluid flow communications (or transmissibility) in between grid cells. This modification can be used with any upscaling algorithms.

As a general conclusion, any upscaling algorithm can be used to describe the upscaled permeability parameter and to obtain similar flow behaviours at its coarser

scale, for reservoirs with quite homogeneous distributions. Therefore, use of the analytical method is recommended, as it is faster in the upscaling process and yet has a similar accuracy compared to any of the other numerical algorithms, including the new upscaling algorithm. However, careful consideration is still required as the degree of homogeneity/heterogeneity is often judged by each individual.

5.2. MODEL B

Model B is the 2D reservoir model, which has a heterogeneous characteristic both vertically and horizontally with the extensive shale strips acting as barriers within the reservoir. The gas injection is used for the enhancement of the ultimate recovery of the oil produced. Similar to Model A, the predictions at the coarse scale level had a higher recovery of oil produced in the reservoir compared to its prediction at the fine scale model. Also, not all existing upscaling algorithms can be used to represent the upscaled permeability parameter at the coarser scale. The new upscaling algorithm results of Model B are summarised below in Figure 5-9 to Figure 5-12. The upscaled permeability of Model B (Figure 5-8) is comparable to the fine scale permeability shown in Figure 5-7.

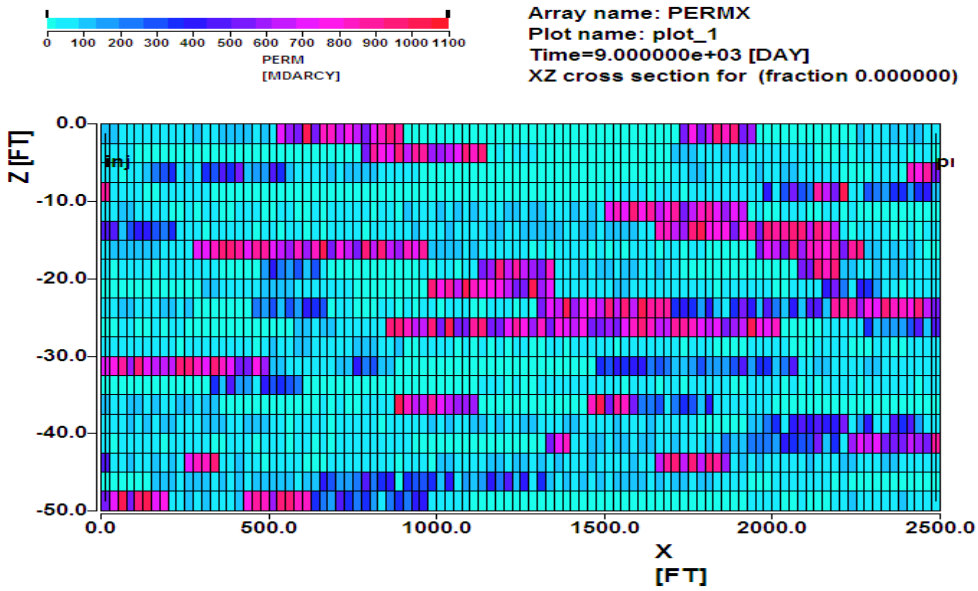

Figure 5-7 Permeability model at fine scale of Model B

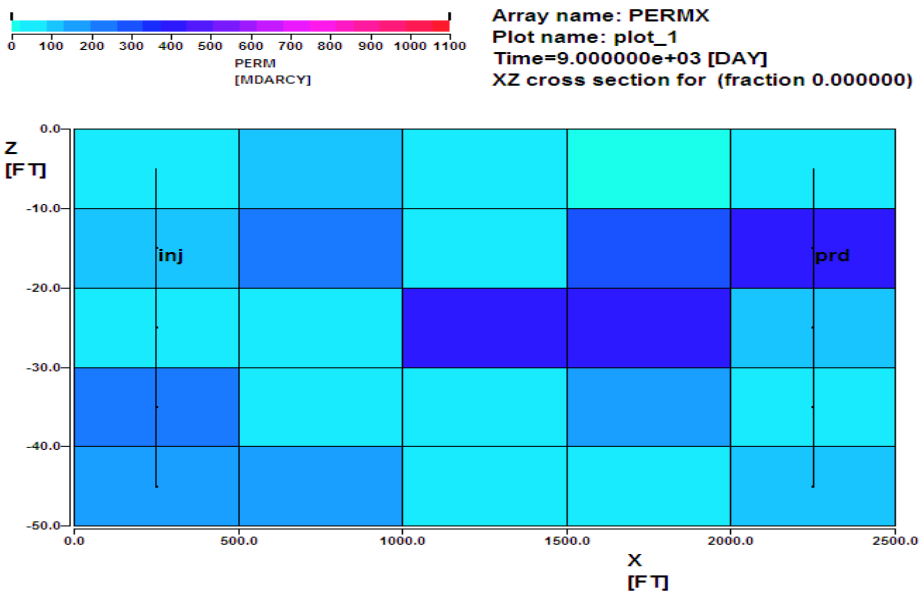

Figure 5-8 Permeability model at coarse scale of Model B

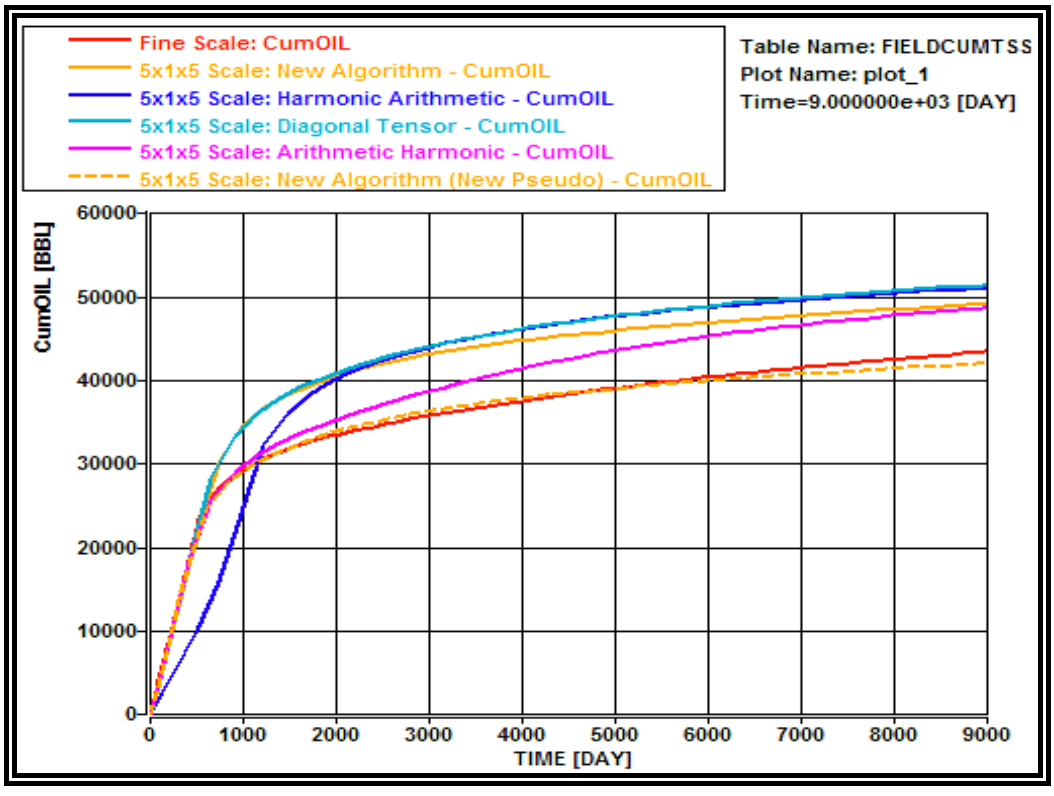

Figure 5-9 Comparison plot of cumulative oil production for Model B

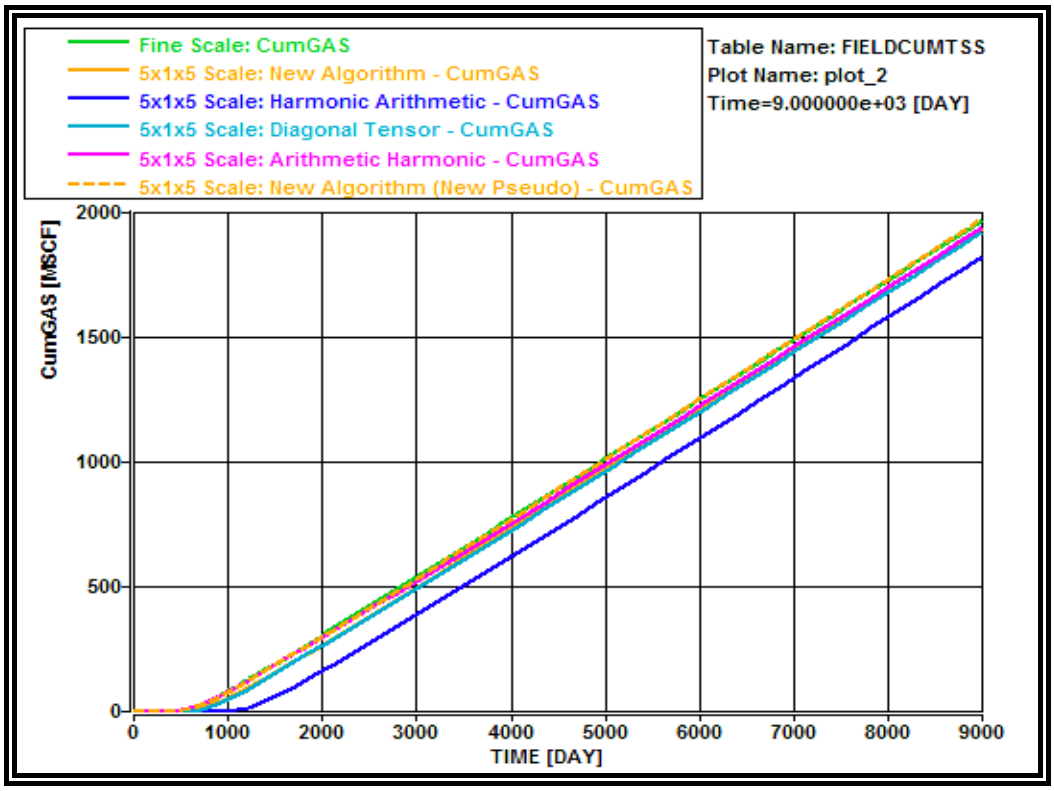

Figure 5-10 Comparison plot of cumulative gas production for Model B

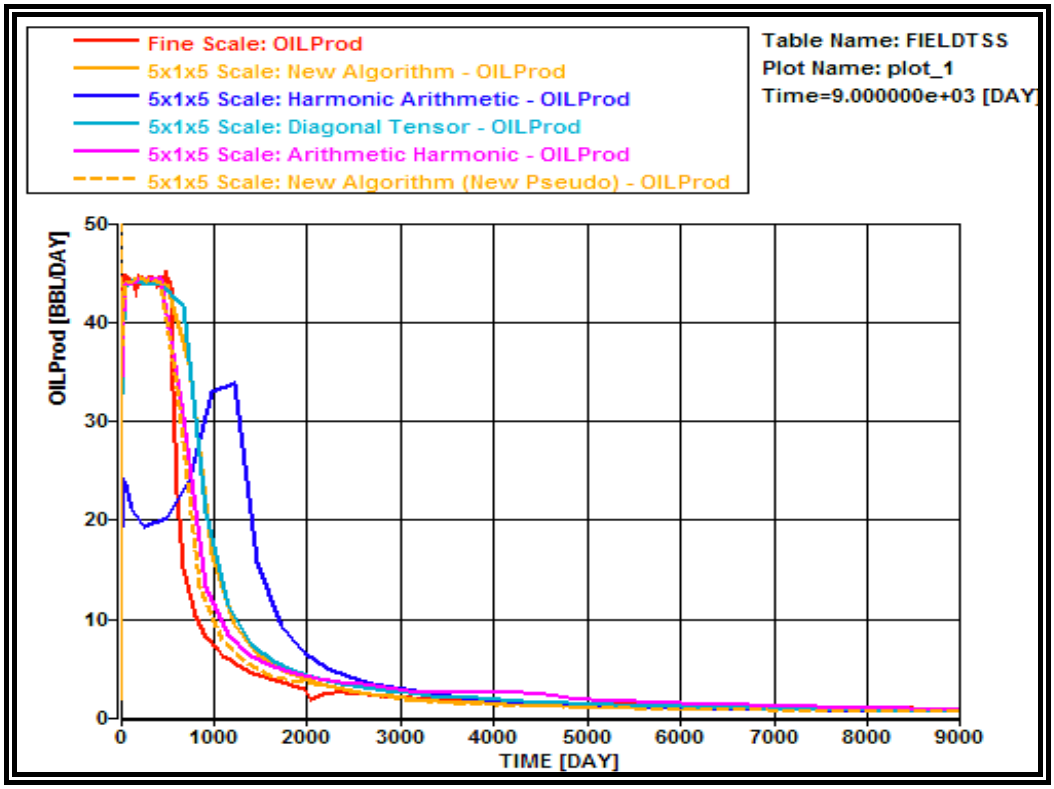

Figure 5-11 Comparison plot of oil production rate for Model B

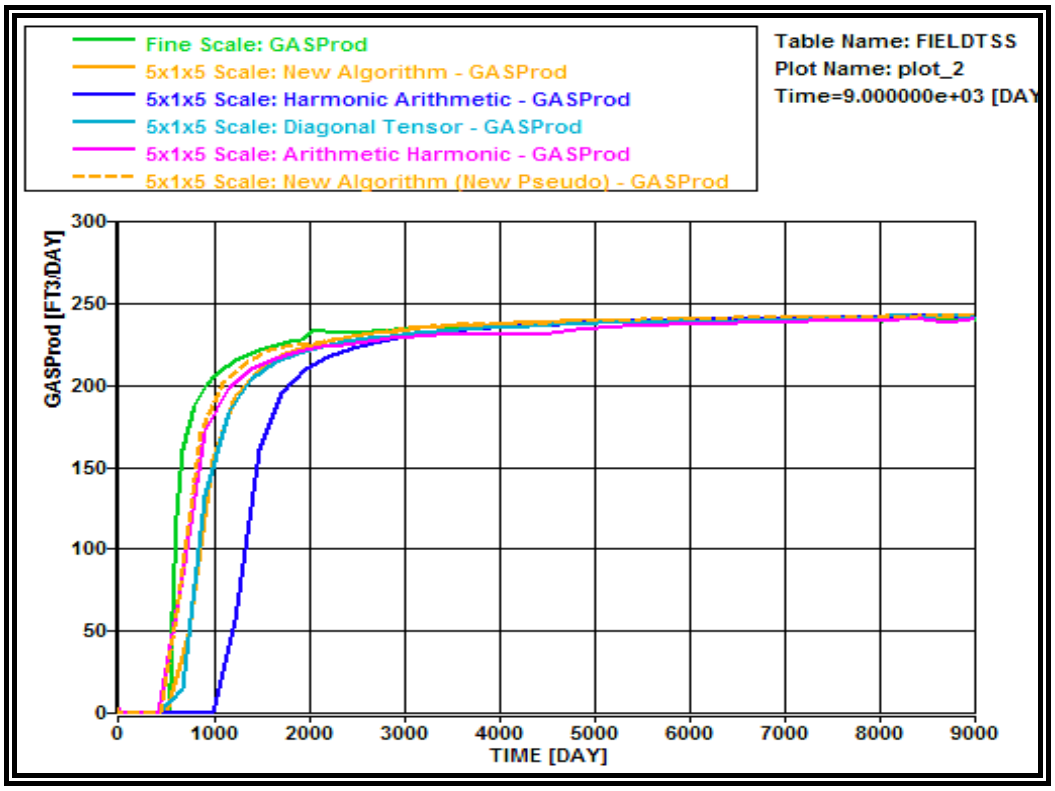

Figure 5-12 Comparison plot of gas production rate for Model B

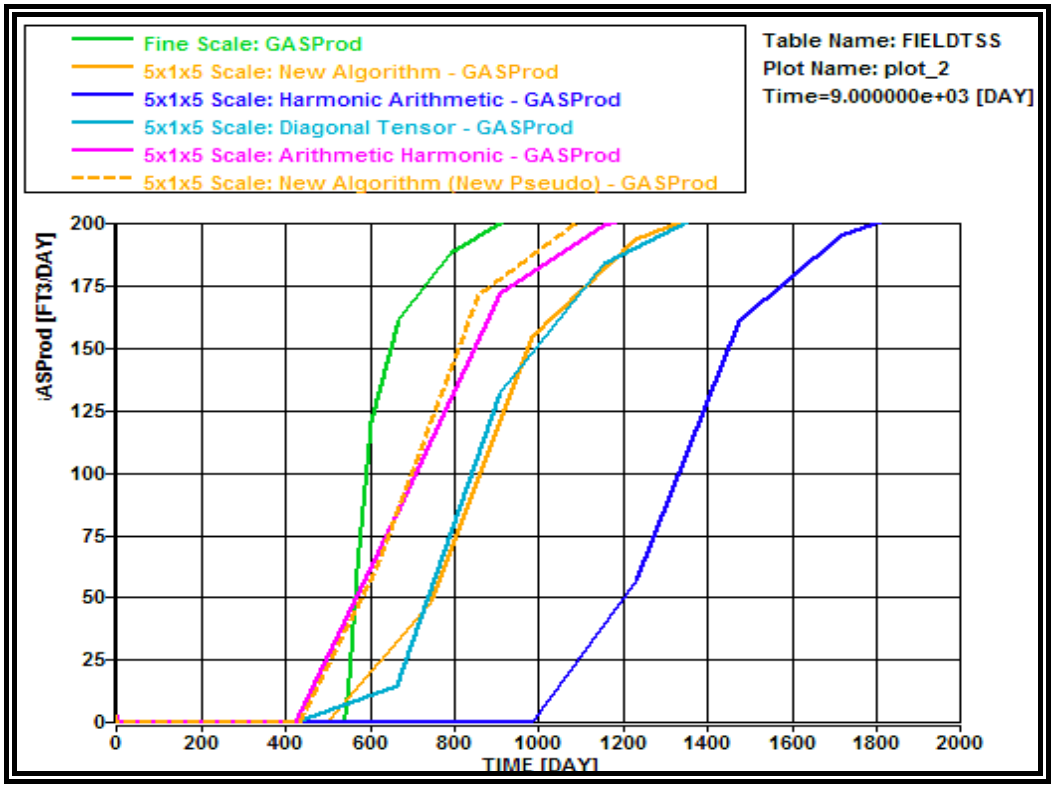

Figure 5-13 Comparison plot of the breakthrough timing with respect to gas production rate for Model B

From the comparison plots above, the results obtained with the new algorithm have been able to better predict the fluid flow behaviour compared to other existing upscaling algorithms. The breakthrough of the gas being injected can be closely predicted using the new algorithm as the upscaling method for the permeability parameter. An alternative upscaling method that could be used is the diagonal tensor method, where the breakthrough timing is predicted to be around 30 days earlier compared to the prediction using the new algorithm.

The new upscaling algorithm, with its modifications, has not only better predicted the fluid flow behaviour at the coarse scale level, but has also improved the prediction of the oil recovery. The arithmetic-harmonic algorithm can be used as an alternative method to predict the oil recovery; however there is dissimilarity in terms of the fluid flow behaviour by using this algorithm as shown in Figure 5-9. The prediction of the cumulative oil produced using the arithmetic-harmonic method has a very small difference at the beginning of the gas breakthrough, but it deviates further with further production.

The oil saturation predicted at the end of the simulation is also compared in the simulations at the fine scale and coarse scale with the new algorithm, as shown in Figure 5-14 and Figure 5-15 respectively. They are quite similar in predicting the fluid movement within the models.

For a heterogeneous characteristic reservoir model with the extensive size of shale strips acting as barriers within the reservoir, the reservoir description at the coarse scale is especially important. The parameter needs to represent the heterogeneity as much as possible at its coarse scale level, so that the reservoir performance can mimic it as if it was at its fine scale level. From the above upscaling investigation, the new algorithm can be concluded to be the most representative algorithm in this case.

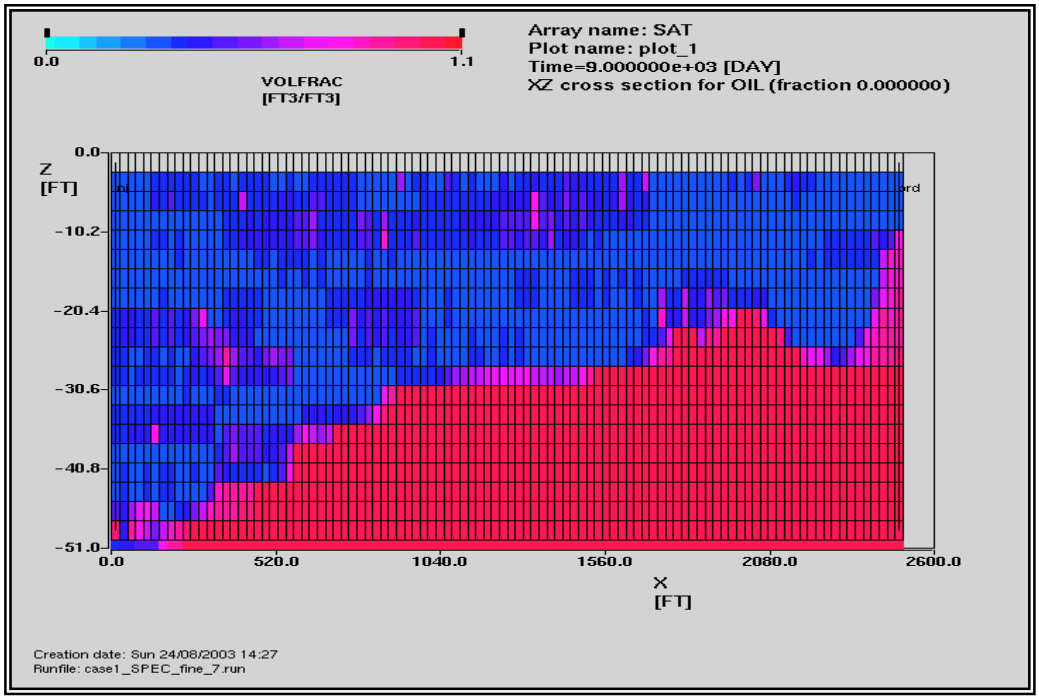

Figure 5-14 Fluid saturation plot at fine scale for Model B

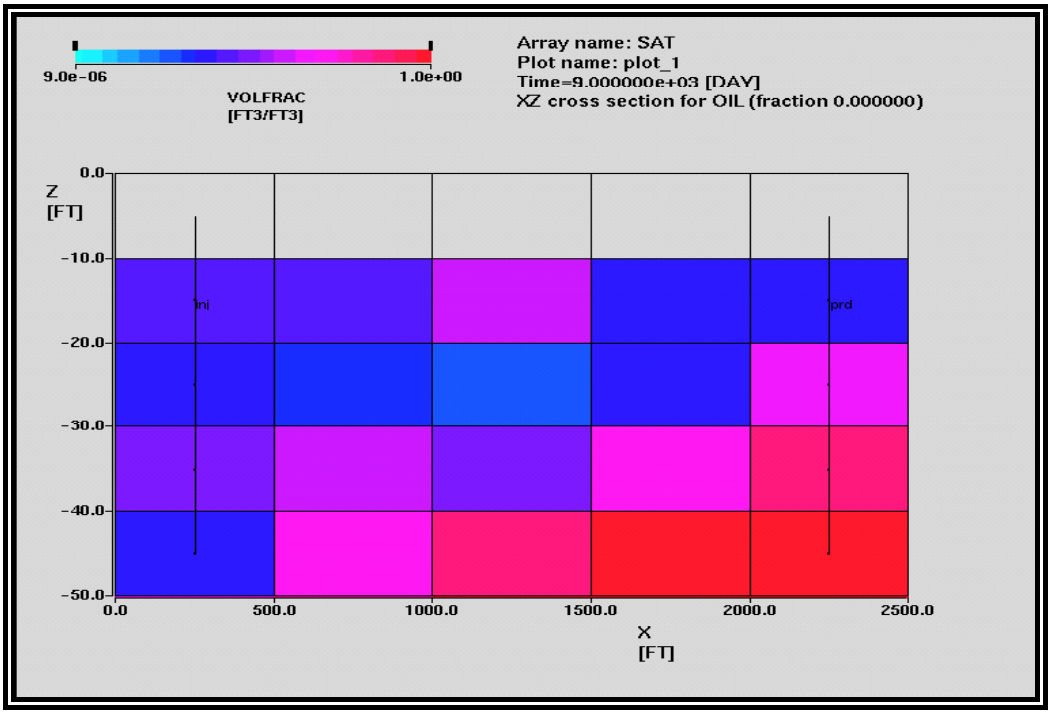

Figure 5-15 Fluid saturation plot at coarse scale (5x1x5 cells) for Model B

5.2.1. Comparison of New Algorithm to Pseudo Upscaling (Kyte and Berry)

The results using the new upscaling algorithm are also compared with the prediction using pseudo upscaling approaches like the Kyte and Berry method, since the fine scale model is small enough to be run in the dynamic simulation model. The comparison results are shown in Figure 5-16 and Figure 5-17.

The breakthrough timing of the gas being injected is predicted very similarly to each other. However, the remaining oil within the reservoir is better predicted using the new algorithm, rather than the pseudo upscaling method. Furthermore, the new upscaling algorithm involves only a single time-step calculation at the fine scale level, compared to multiple time-step calculations to the end of the simulation period used by the pseudo upscaling method. In this way, the new upscaling method not only provides better predictions at the coarse scale level, but also speeds up the turn-around time for the upscaling process and simulation.

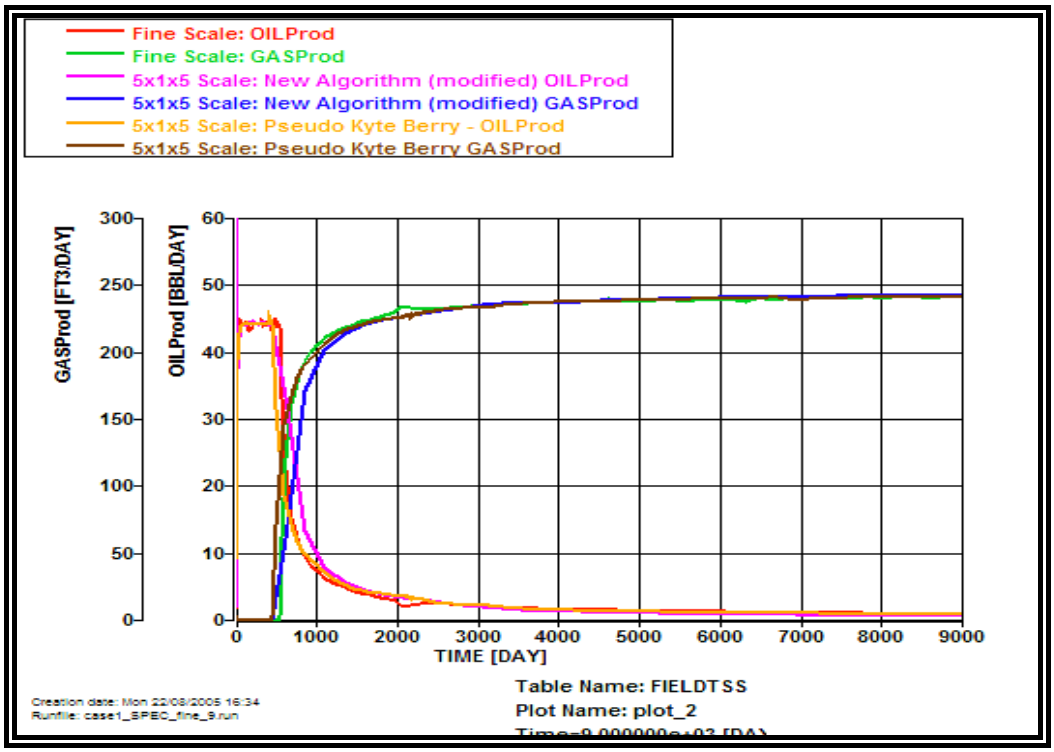

Figure 5-16 Comparison plot of oil and gas production rates for Model B with pseudo upscaling (Kyte and Berry)

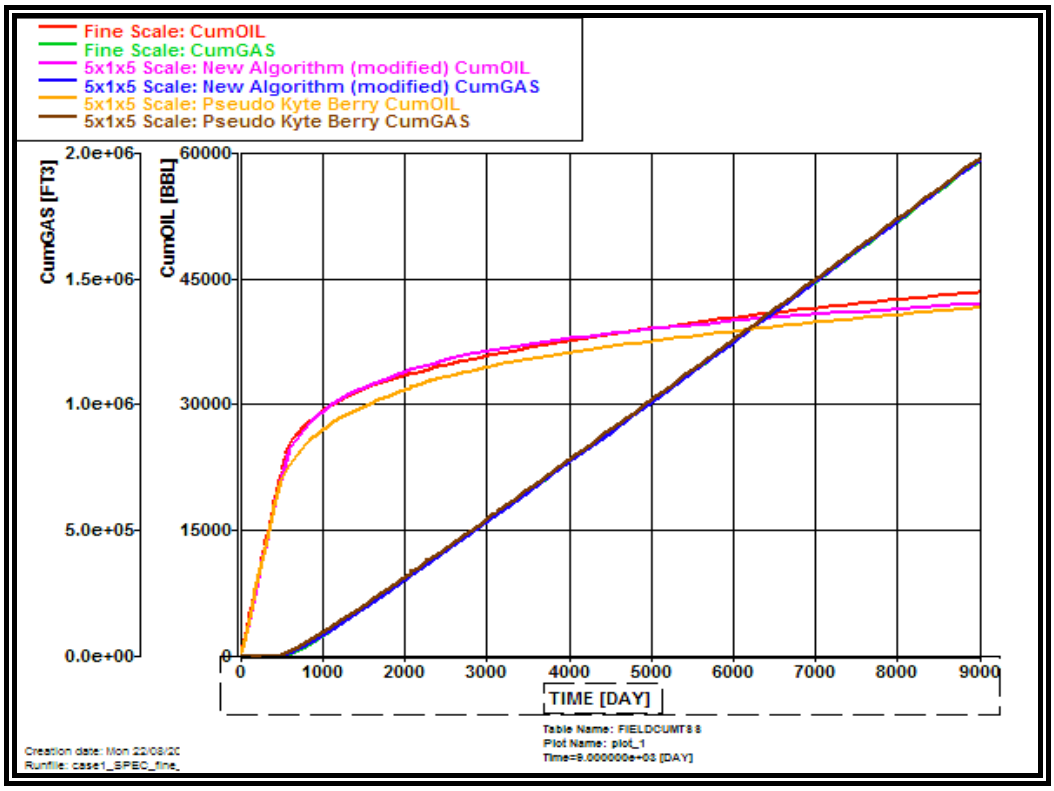

Figure 5-17 Comparison plot of cumulative oil and gas produced for Model B with pseudo upscaling (Kyte and Berry)

5.2.2. Quality check on Model B at different scale of 10 x 1 x 5 coarse cells

For the quality checking of the new upscaling algorithm, Model B at the fine scale is also upscaled to 10 x 1 x 5 (50 cells) with the upscaling ratio of 10:1:4 (1 coarse cell = 40 fine cells). The dynamic simulation results are shown in Figure 5-18 to Figure 5-21. The findings with different coarsening grids are consistent with the earlier findings for the 5 x 1 x 5 coarse scale Model B. The breakthrough timing and the ultimate oil recovery using the new algorithm with modifications are found to be consistent with the behaviour at the fine scale level.

In this particular coarsening model, where the amount of fine scale cells to be represented by a single coarse cell is little and the differences in the outcome of the

upscaled parameter using different upscaling algorithms are small, it is found that the new algorithm can predict more accurately compared to other existing algorithms. The statistics summarising the difference in the reservoir performances with various upscaling algorithms are shown in Table 5-2.

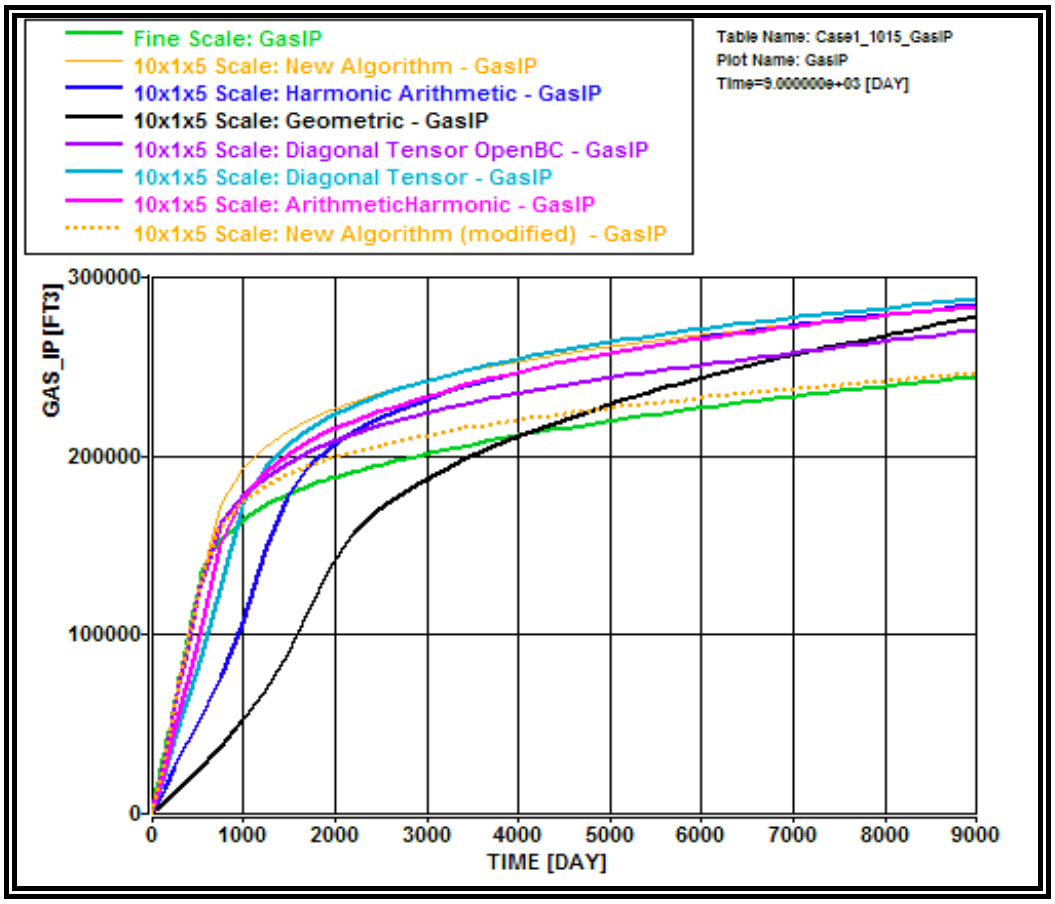

Figure 5-18 Comparison plot of gas in place for Model B with 10 x 1 x 5 coarse cells

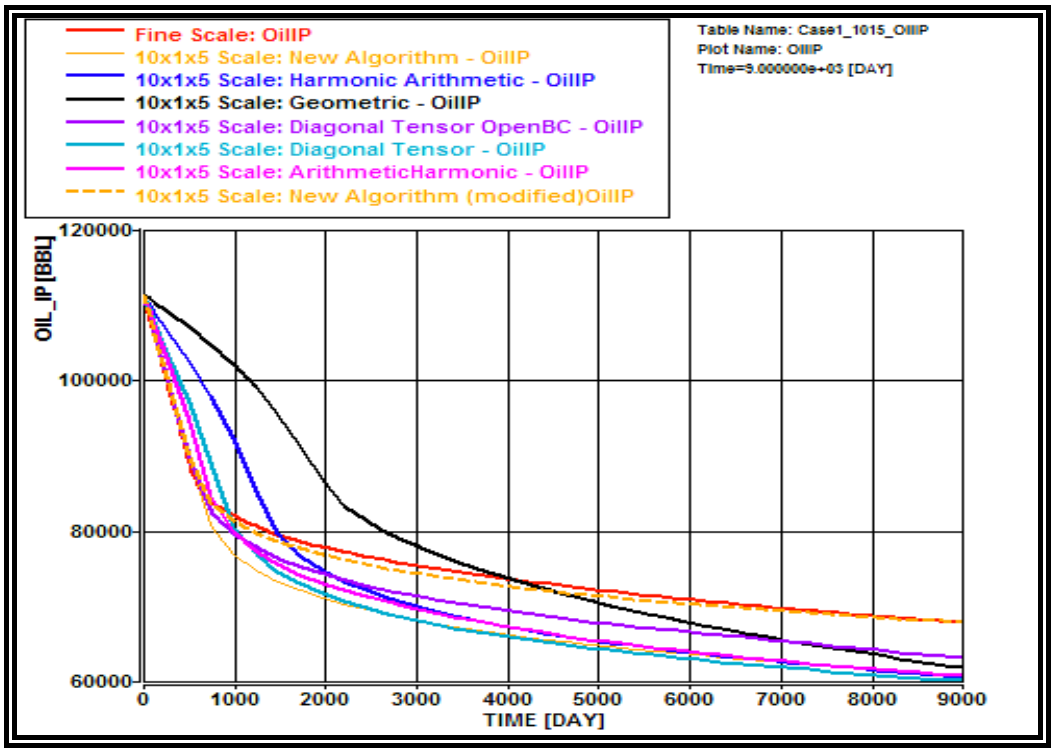

Figure 5-19 Comparison plot of remaining oil in Place for Model B – 10 x 1 x 5 coarse cells

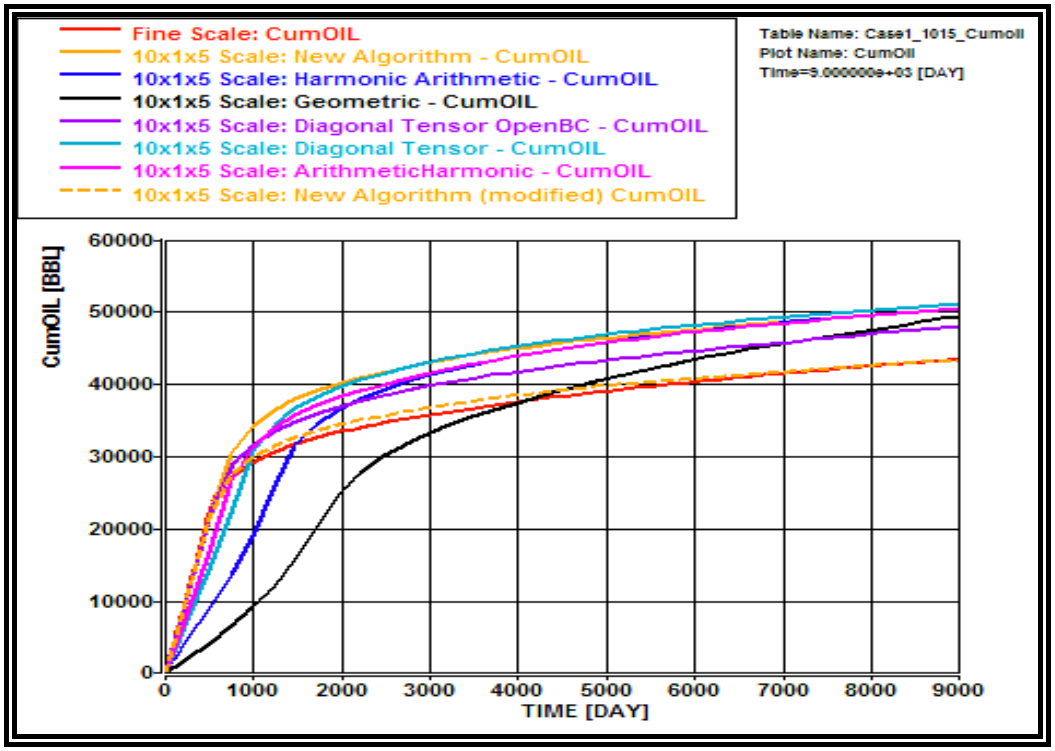

Figure 5-20 Comparison plot of cumulative oil produced for Model B with 10 x 1 x 5 coarse cells

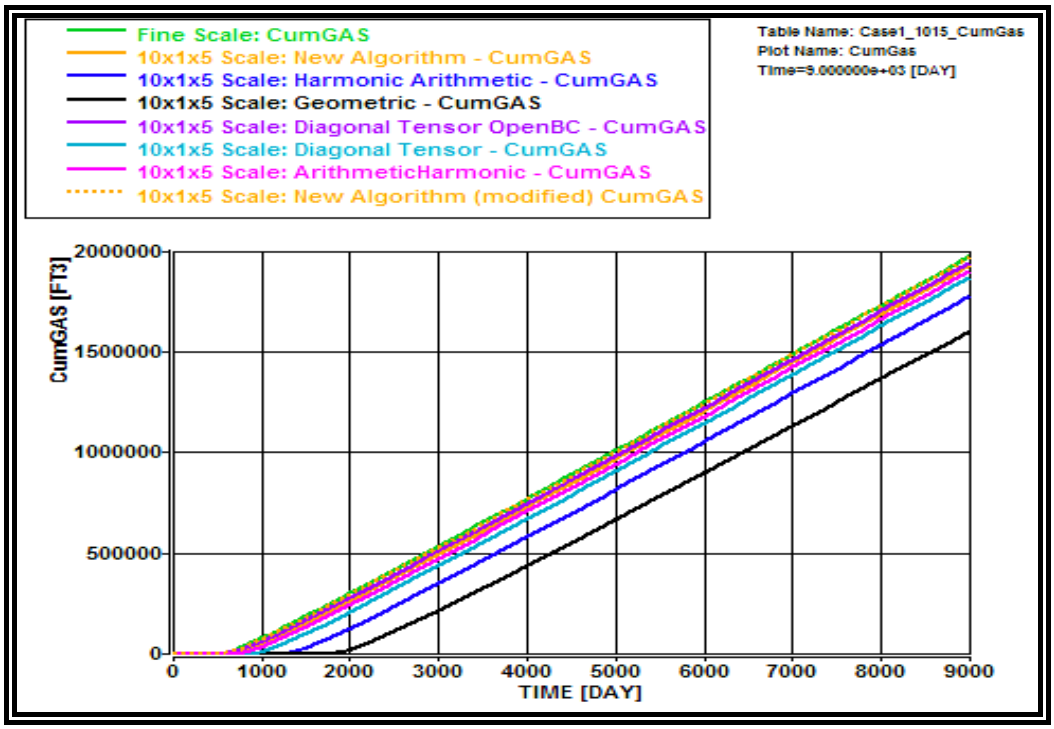

Figure 5-21 Comparison plot of cumulative gas produced for Model B with 10 x 1 x 5 coarse cells

Table 5-2 Comparison table for oil and gas ultimate recovery for Model B – 10 x 1 x 5 coarse cell

Model B – 10x1x5	**Remaining GasIP MMSCF**	**Remaining OilIP BBL**	**CumGas MMSCF**	**CumOil BBL**	**CumGasInj MMSCF**
Fine Scale	**0.244**	**67893**	**1.97**	**43434**	**2.22**
Arithmetic Harmonic	0.284 (+16.3%)	60791 (-10.5%)	1.90 (-3.5%)	50534 (+16.3%)	2.19 (-1.3%)
Harmonic Arithmetic	0.284 (+16.5%)	60742 (-10.5%)	1.78 (-9.9%)	50578 (+16.4%)	2.06 (-6.98%)
Diagonal Tensor	0.287 (+17.8%)	60157 (-11.4%)	1.87 (-5.1%)	51166 (+17.8%)	2.16 (-2.6%)
Geometric	0.278 (+13.9%)	61857 (-8.9%)	1.61 (-18.5%)	49468 (+13.9%)	1.89 (-14.9%)
New Algorithm	0.283 (+16.0%)	60923 (-10.3%)	1.9308 (-2.1%)	50399 (+16.0%)	2.22 (0.0%)
New Algorithm (Pseudo & Modified)	0.244 (0.0%)	67903 (0.0%)	1.97 (0.0%)	43419 (0.0%)	2.22 (0.0%)

5.3. MODEL C

The new upscaling algorithm is also tested using Model C. As in Chapter 3, a sector model of Model C has been used for comparison against the fine scale reservoir simulation predictions, due to limited computer resources for running such a large number of fine gridded cells. The entire Model C fluid performance will then be compared against the published results at the fine scale level.

5.3.1. Sub Model C

A sector model of Model C, which is taken from the first 20 layers of Model C, is a heterogeneous model with low reservoir connectivity. The upscaled permeability as shown in Figure 5-23 is comparable with the fine scale model (Figure 5-22). The comparison results of the sector Model C with the new upscaling algorithm to the different existing upscaling algorithms are shown in Figure 5-24 to Figure 5-28.

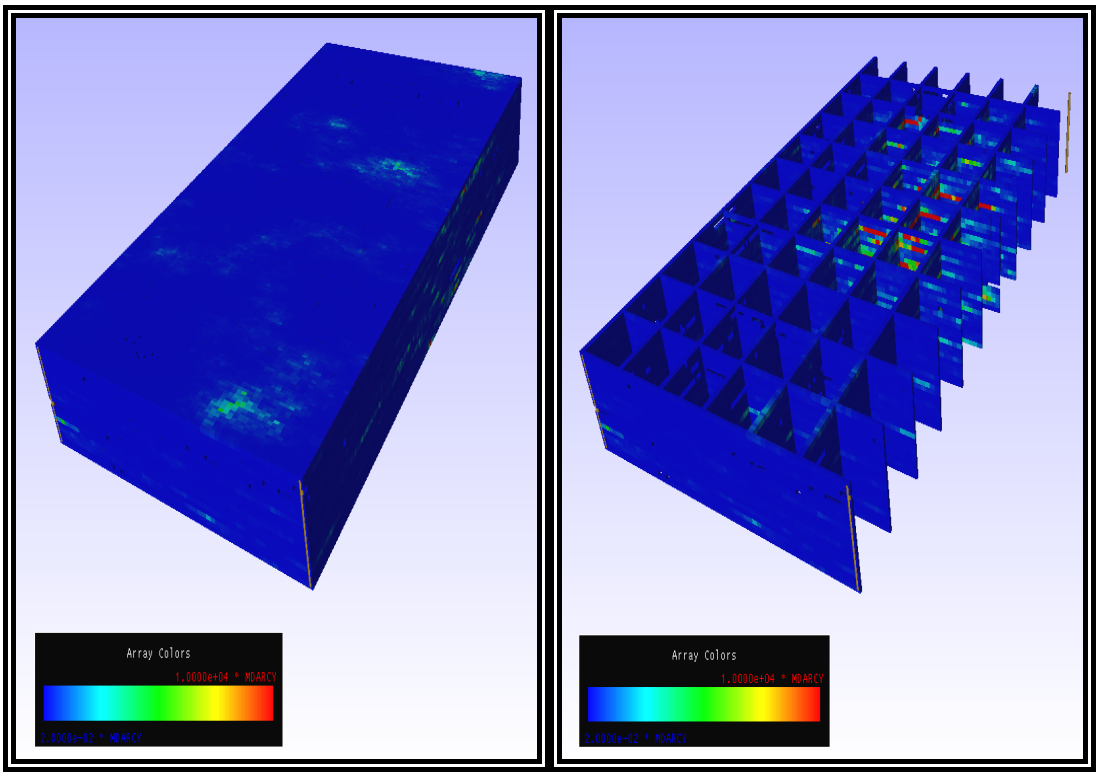

Figure 5-22 Permeability model with its cross sectional view of Sub-Model C at fine scale

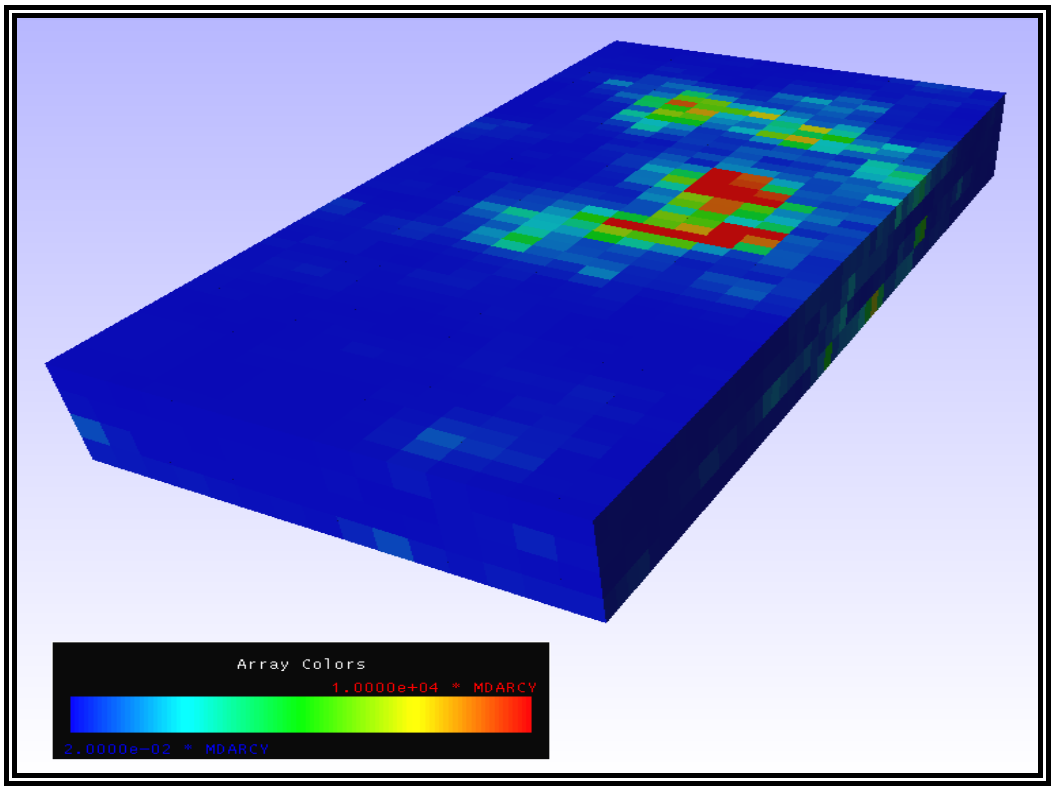

Figure 5-23 Permeability model at the coarse scale of Sub-Model C with the new upscaling algorithm

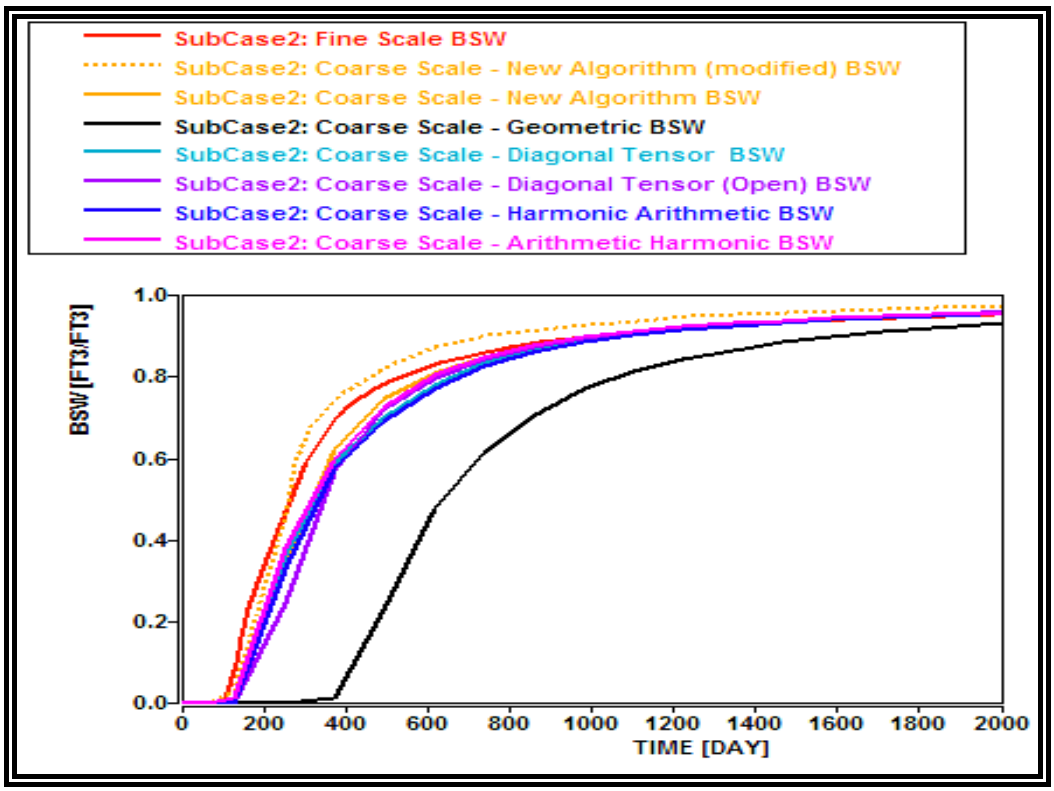

Figure 5-24 Comparison plot of water cut ratio for Sub-Model C

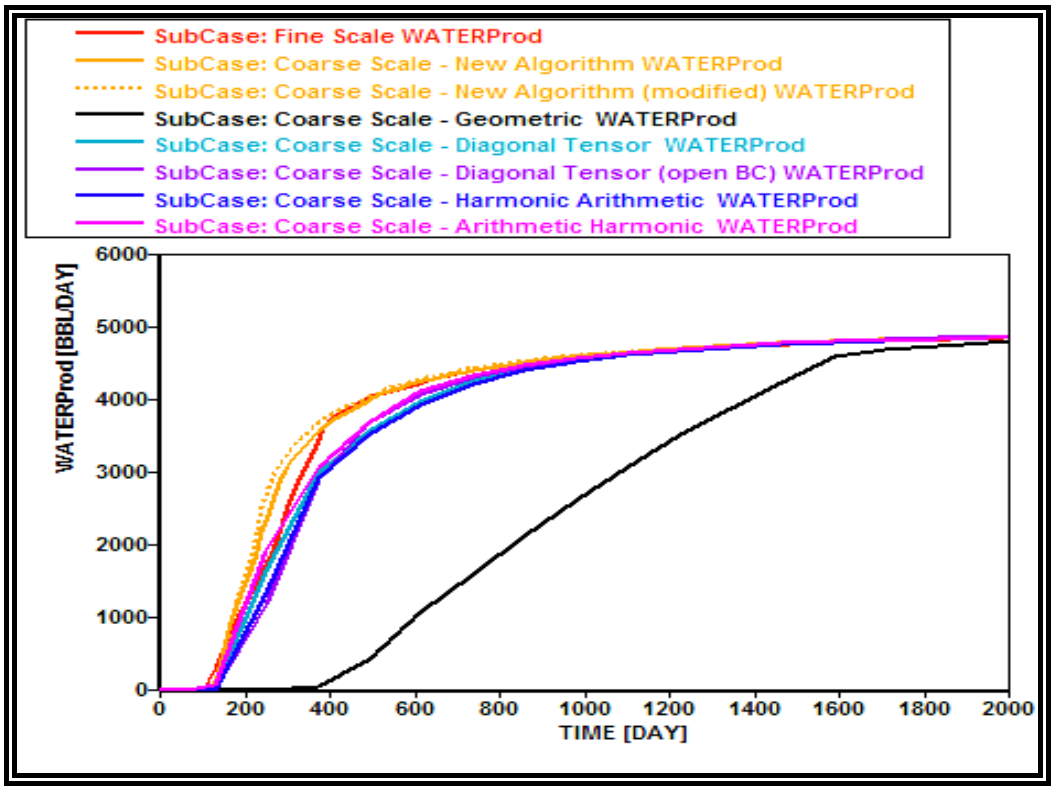

Figure 5-25 Comparison plot of water production rate for Sub-Model C

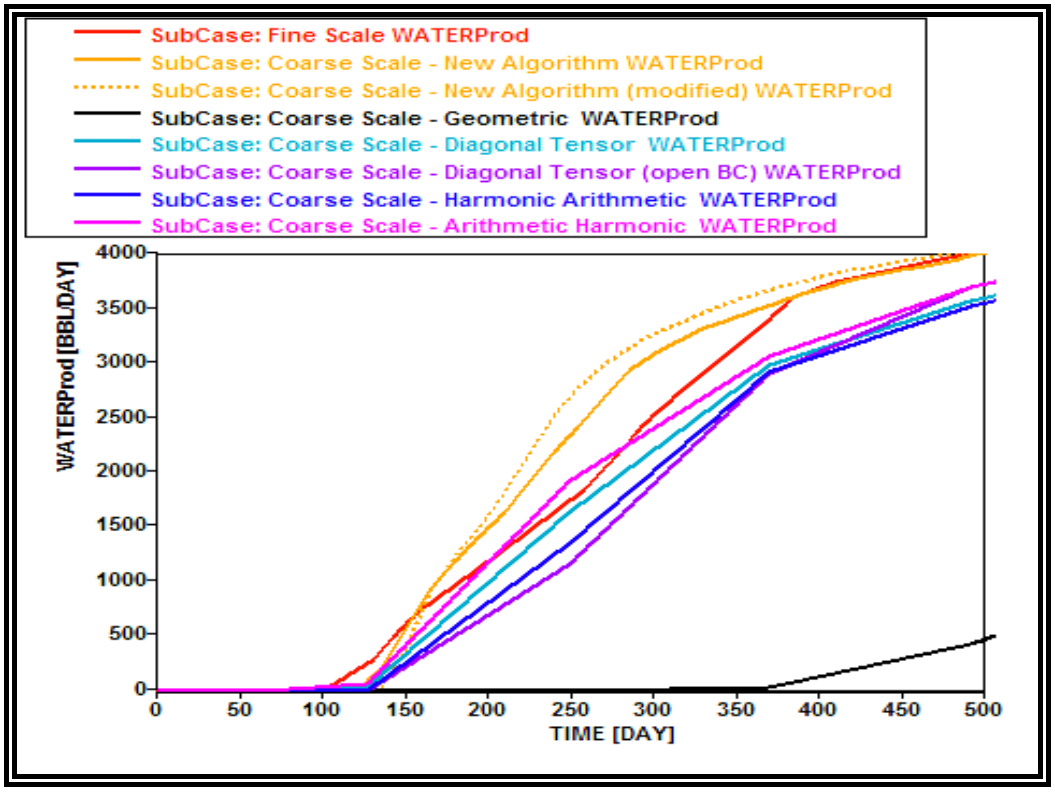

Figure 5-26 Comparison plot of the breakthrough timing with respect to water production rate for Sub-Model C

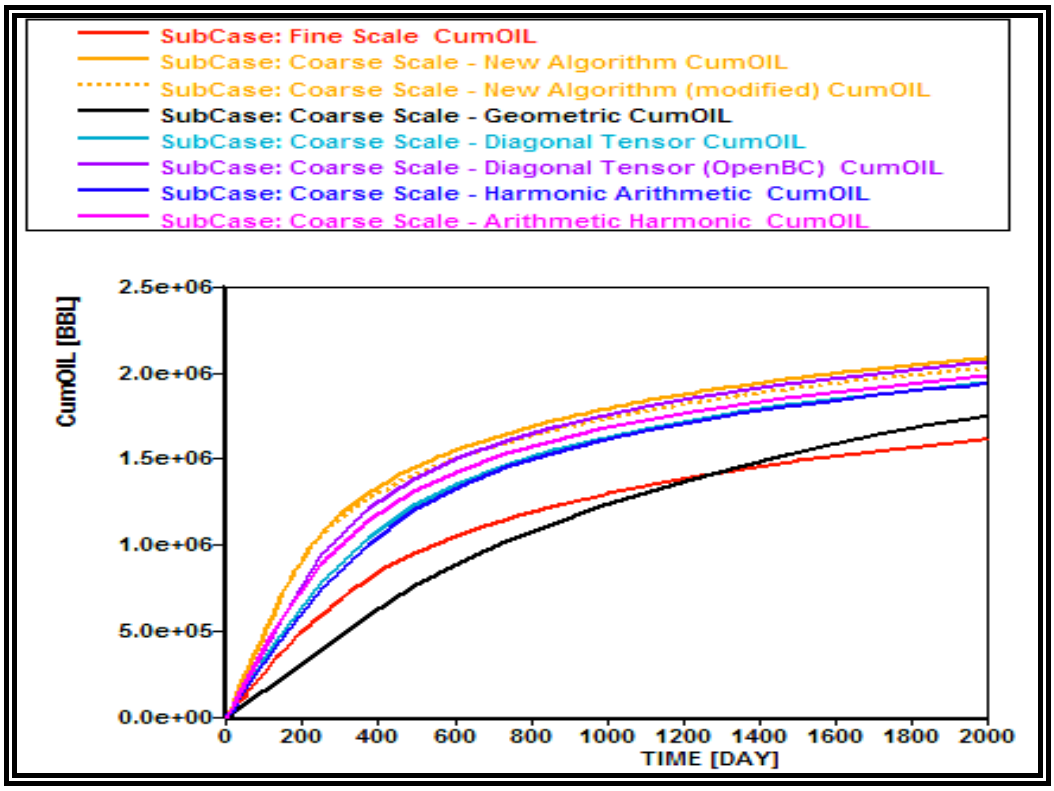

Figure 5-27 Comparison plot of cumulative oil produced for Sub-Model C

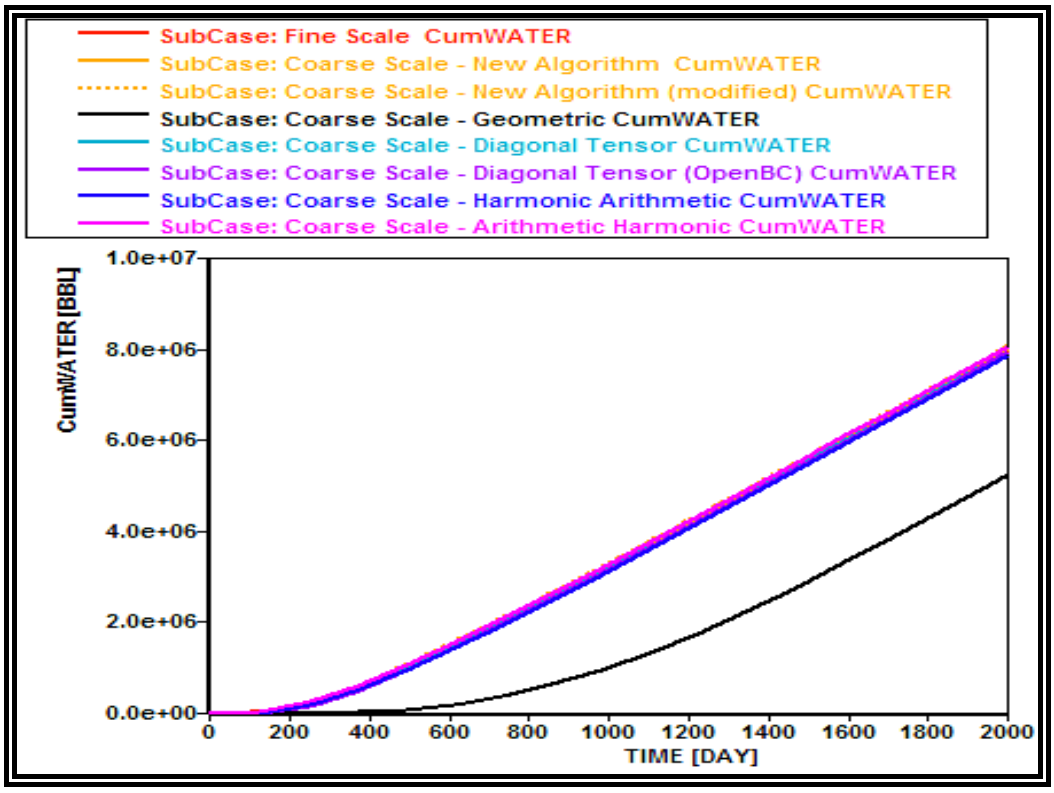

Figure 5-28 Comparison plot of cumulative water produced for Sub-Model C

Table 5-3 Comparison table for oil and gas ultimate recovery for Sub-Model C

Model C – Sub Case	**Estimated Water Break through (Day)**	**Remaining Oil In Place (mmbbl)**	**CumOil 10^6 BBL**	**CumWater Injected Mmbbl**
Fine Scale	**89.8**	**1.98**	**1.62**	**9.67**
Arithmetic	63.0	1.62	1.01	10.18
Arithmetic Harmonic	63.0	1.62	1.98	10.10
Harmonic Arithmetic	127.0	1.66	1.94	9.89
Harmonic	1101.0	2.53	1.07	1.49
Diagonal Tensor (seal)	63.0	1.65	1.95	9.97
Diagonal Tensor (open)	127.0	1.54	2.06	10.07
Geometric	248.8	1.85	1.75	7.08
New Algorithm	63.0	1.53	2.07	10.15
New Algorithm (modified)	63.0	2.02	1.57	10.06

From the above comparison plots (Figure 5-24, Figure 5-25 and Figure 5-26), the ratio of water cut and the corresponding water production rates are reasonably accurately predicted using the new upscaling algorithm. The cumulative oil and water produced shown in Figure 5-27 and Figure 5-28 have also indicated good agreement between the predictions at the fine scale and the coarse scale with the new upscaling algorithm.

5.3.2. Entire Model C

The results for Model C with the new upscaling algorithm are shown in Figure 5-30 to Figure 5-32 with the comparison against the published SPE results at the fine scale simulation.

The upscaled permeability with the new upscaling algorithm is shown in Figure 5-29.

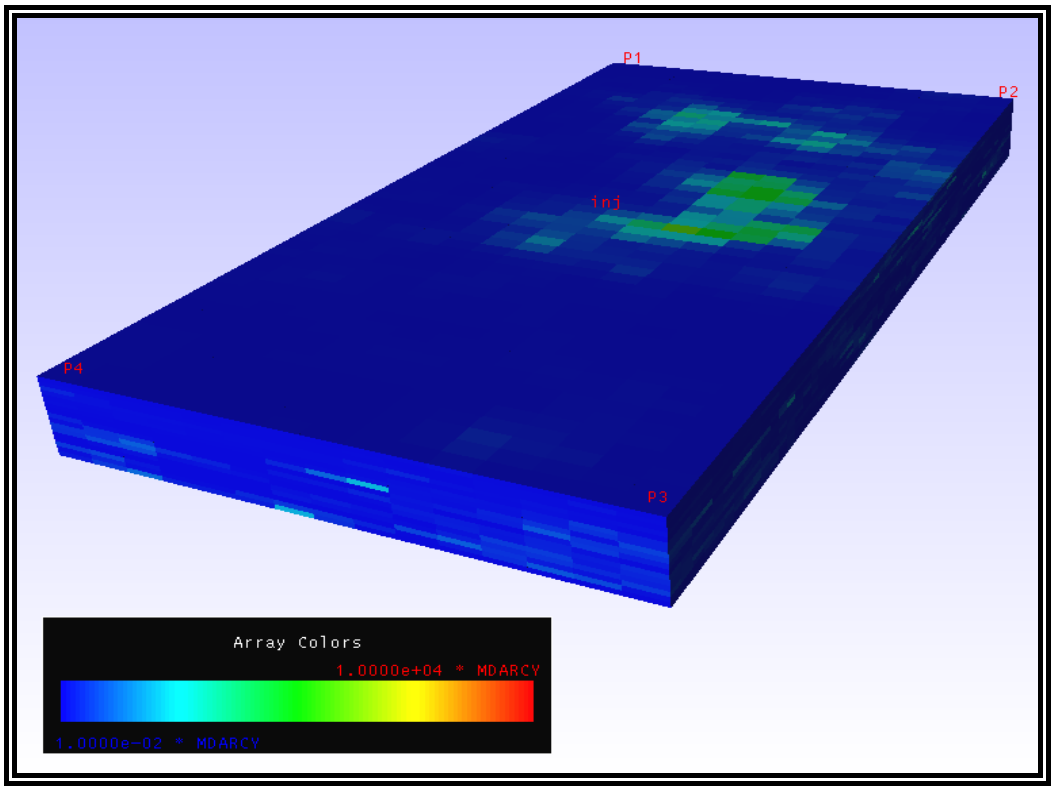

Figure 5-29 Permeability model at the coarse scale of Model C with new upscaling algorithm

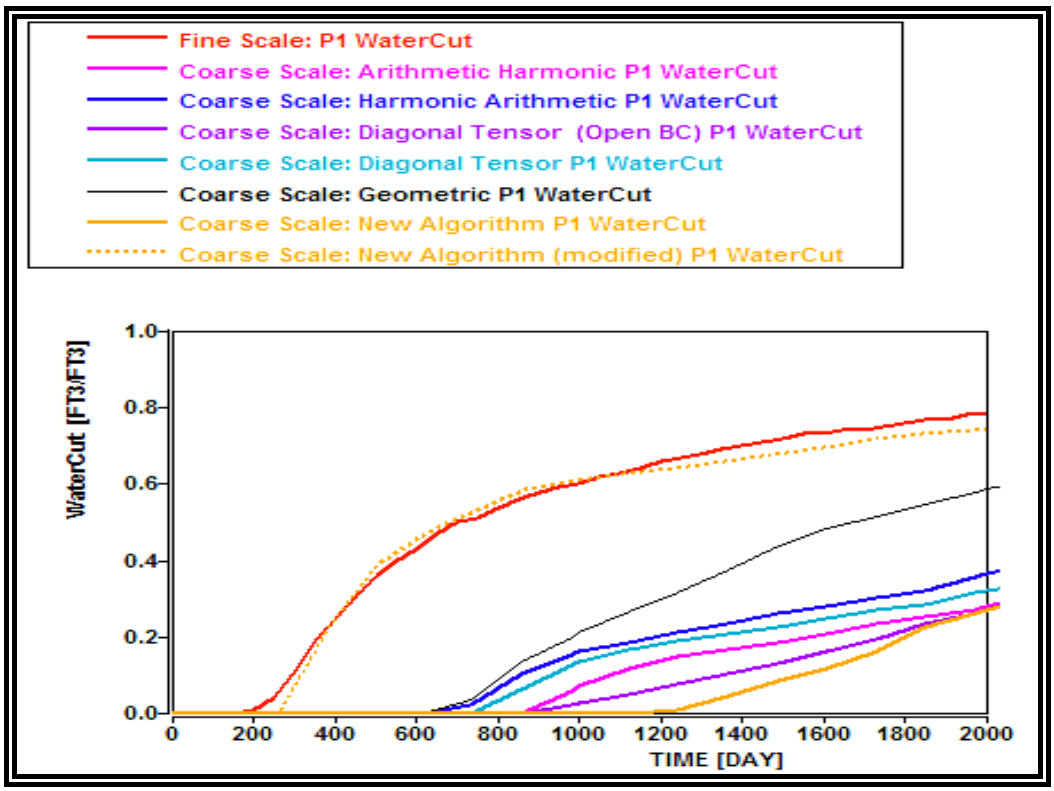

Figure 5-30 Comparison plot of producer P1 water cut for Model C

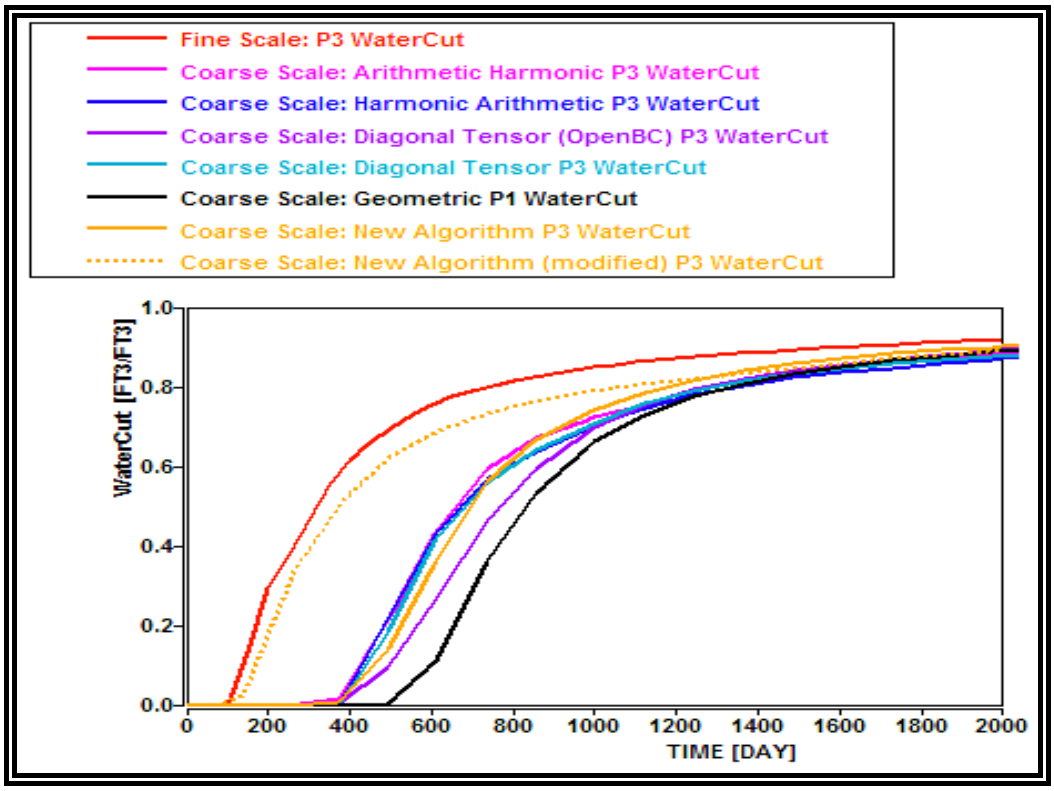

Figure 5-31 Comparison plot of producer P3 water cut for Model C

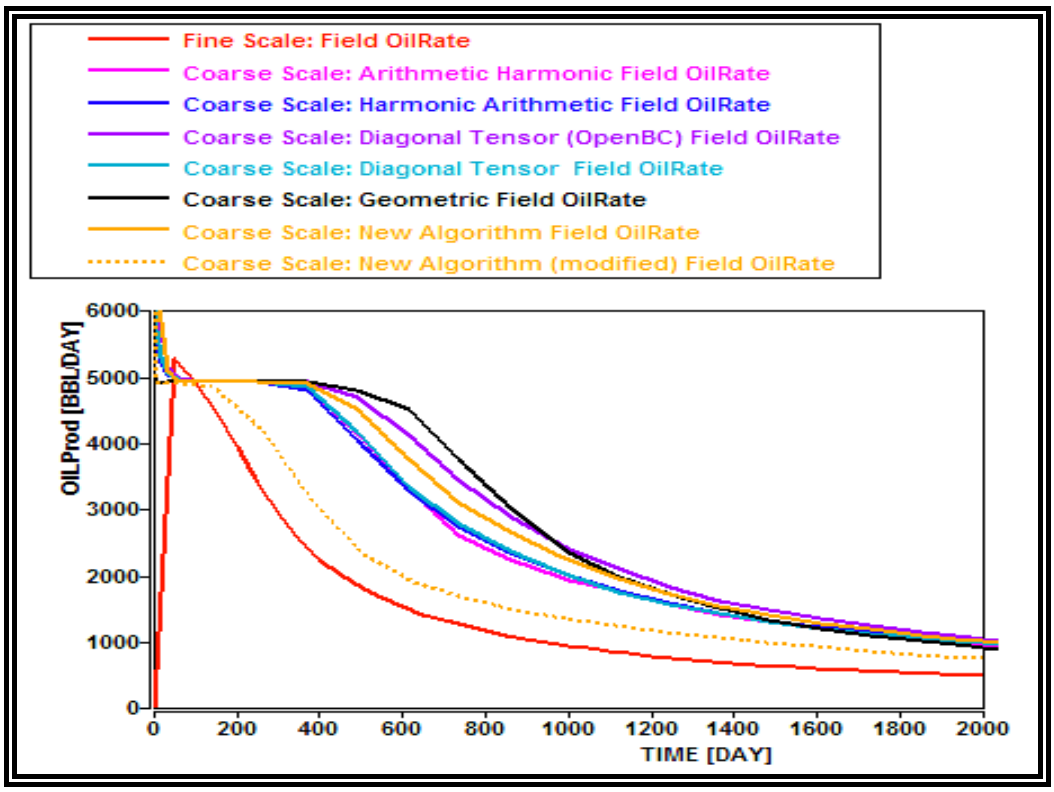

Figure 5-32 Comparison plot of total field oil production rate for Model C

In this model, preserving the connectivity (or transmissibility) between grid cells to be represented at the coarser scale is also important, as well as upscaling the permeability parameter. There are lots of micro high connectivity (shown in Figure 5-33) within the coarse grid cells, which may influence the fluid flow pathways between the injector and the producers and hence later, breakthrough of the water being injected. The upscaled permeability using the new algorithm only represents the average intra-connectivity within a coarse grid cell and not the inter-connectivity between coarse grid cells. Therefore, to be able to match the fine scale behaviours, the micro-connectivity at the fine scale levels were studied using the single-phase streamline simulation. Further modification to incorporate the micro-connectivity was also implemented as part of the upscaling process and the history matching of this model to its fine scale field performance.

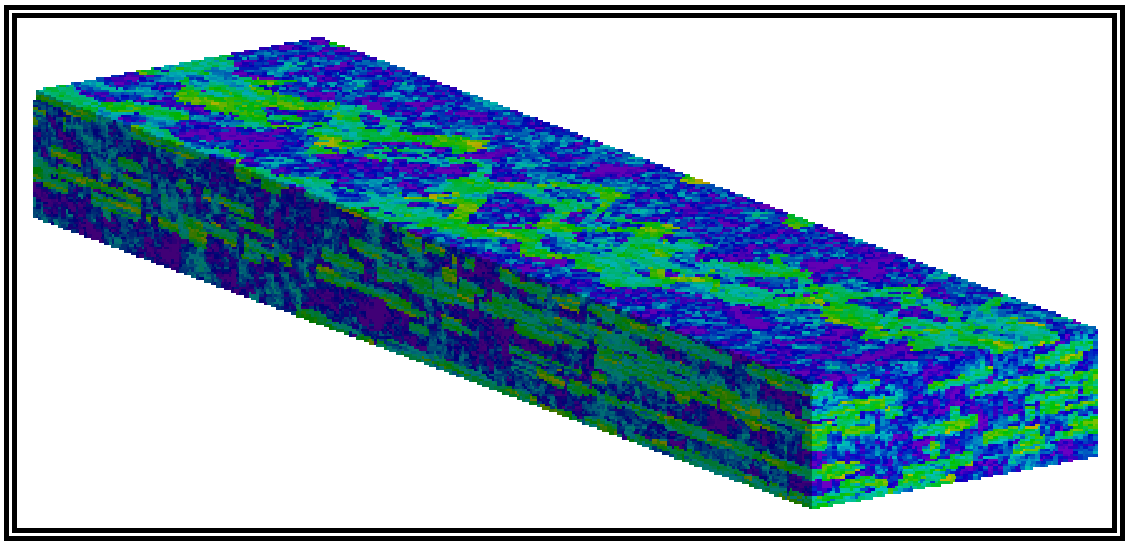

Figure 5-33 Porosity model (lower part on last 50 layers) of Model C (Christie *et al.,* 2001, p. 309)

The modification has not only helped in improving the match of the reservoir performance at the coarse scale, but also improves the breakthrough time of the water being injected at the producers.

A further refinement on matching the field performances between the fine scale and the coarse scale model can possibly be performed by redefining the well inflow

performance representation in the coarse scale model. A mathematical representation for the well inflow performance, which is used as part of the new upscaling algorithm, is typically represented using the isotropic permeability assumption (i.e. the permeability values are assigned to be the same for all x, y and z directions). Model C has an anisotropic permeability with a kv/kh of 0.3 in the channels and a kv/kh of 10^{-3} in background reservoir. Due to the limited scope of this research, the well inflow performance at the coarse scale level may not be represented as precisely as the well inflow performance at its fine-scale level. As a consequence, there are still slight discrepancies predicted with each individual producers/injector production/injection rate, as outlined in Figure 5-32.

5.4. SUMMARY OF NEW UPSCALING RESULTS

Based on the comparisons above, the new upscaling algorithm can be used to improve the overall field performance predictions for various depositional environments. The predictions made at the coarse scale level using the new upscaling algorithm are comparable to fine scale performances from the homogeneous model (similar to Model A), to mostly heterogeneous models (such as Model B and C). The new algorithm not only better predicts the fluid flow behaviour, but it also improves the fluid injected breakthrough time and gives better predictions of the ultimate fluid recovery based on the coarse scale model.

Chapter 6.
DISCUSSION

In any of the oil and gas industries, a prediction of reservoir performance is normally carried out by reservoir simulation. In the full field reservoir model, the geological representation of the reservoir is often modeled at a scale of 50m x 50m x 1m by using the average values of the core/log scale data at a scale of 10cm x 10cm x 10cm. This fine scale geological model often has around one to 100 million grid cells, which cannot be carried out in a reservoir simulation due to limited computer power for the implicit and iterative procedures in the dynamic calculation. Due to this, a coarsening of the fine geological model is required with the appropriate average representation of the effective properties at the coarse scale. The rock properties that need to be upscaled are typically porosity, absolute and relative permeability and capillary pressure.

In any reservoir prediction, a realistic description of the reservoir behavior under any depletion scheme is probably the most important factor. Permeability, which describes the ability of fluid to flow through the connectivity of the pores of the rock in the porous media, is the major parameter that affects the reservoir behaviour. In upscaling, unlike other parameters such as porosity and saturation which can be represented by weighted arithmetic averaging techniques, permeability is really the most complicated matter, since it is not an additive variable (i.e. the equivalent permeability in the reservoir scale cannot be calculated by arithmetic means). The expected permeability values have, in general, decreased and permeability variance has also decreased in reservoir simulation scales compared to much finer scales such as geological or core scales. Consequently, reducing the number of cells in any scale results in reducing the accuracy of the parameter model and also smooths the ability to describe the heterogeneity flow behaviour in the reservoir model. Therefore, a balance is required between the loss of accuracy due to the smoothing (averaging) process and the gain in computer speed due to fewer numbers of grids.

Various upscaling algorithms for representing the effective properties at the coarse scales are commercially available. They are based on various approaches from the simplest analytical form to more complex numerical forms of upscaling methods. The pseudo method based on the averaging of fine scale dynamic results is also being derived.

The simplest analytical forms of upscaling such as arithmetic, harmonic and geometric averages are the most easy, fast and simple compared to other available upscaling algorithms. However, these algorithms, in general, may not all be used for any reservoir models. The reason is that upscaled permeability parameters can only be described as single directional properties. In reality, this is not necessarily the case, as permeability is a tensor property, which has the variability in a three-dimensional space to go from one direction to another. These algorithms are best suited for the simplest homogeneous rock arrangements in either parallel or perpendicular to the bedding for arithmetic and harmonic averages respectively. In theory, these algorithms can represent the upper and lower bounds of the effective properties. For a random rock arrangement, the geometric average could be used, but high uncertainties in upscaled parameters will result.

With any uniform flow, upscaling algorithms such as arithmetic-harmonic and harmonic-arithmetic are considered to be the most effective and efficient methods to use. These algorithms are quite economical in terms of processing time for upscaling processes and in determining the directional effective properties of the permeability. Furthermore, the effective properties may not always lead to accurate results, but they are generally honoured in the detailed reservoir descriptions (Lozano *et al.,* 1996, p. 328-338). Theoretically, these directionally dependant arithmetic-harmonic and harmonic-arithmetic averages are believed to represent the upper and lower bounds of the effective permeability respectively. For shaly geological environments, where barriers or shales are described within reservoirs as having a low permeability, careful consideration for using these directional dependant algorithms is required. Biased upscaled properties to the lower permeability values may form as a result, which would not represent true reservoir properties.

A common limitation to most of the analytical methods is the presence of the nil value(s), which is often defined for non-flow or barriers (i.e. shale or undefined/non-active cells) in the system. Any undefined values will limit the validity range to the effective permeability as a result.

With these analytical upscaling methods, several theoretical bounds are also commercially available, and the average of the theoretical bounds is often used in determining the effective permeability. They are normally easy to implement within the upscaling process and tend to be very fast in terms of computational speed. However, the disadvantages as described for each analytical algorithm are still valid and the effective permeability is only the approximated average value within the bound.

Other better forms of upscaling algorithms are the diagonal tensor and full tensor methods, which are based on the Darcy's law of flow equation and the law of mass conservation. In general, they will give a better representation for the effective upscaled permeability, since they represent the solution of the fluid flow and yield the diagonal tensor of permeability in nature. Periodic boundary to the appropriate direction is used to obtain the diagonal tensor permeability (k_{xx}, k_{yy}, k_{zz}).

For the full tensor, a direct method for finding the effective permeability on the principal diagonal directions (k_{xy}, k_{xz}, k_{yx}, k_{yz}, k_{zx}, k_{zy}) can only be used since it is only required to provide three-dimensional solutions. Certain ill-conditioned full tensor permeability can, however, give significant errors in the procedure. Furthermore, these principal directions of effective permeabilities are generally neglected by the reservoir simulators, as there are no available simulators to handle principal directional permeabilites.

These tensor methods are also more expensive than other methods, since these methods are often time consuming and slow in speed for upscaling processes.

Other methods like renormalisation are also available and are based on the analogy of the electrical network and a successful star triangle transformation. The effective permeability can be estimated by using a successive averaging over small regions (i.e. 2 x 2 x 2 of the fine scale block) to form a new 'average permeability' distribution with lower variance (i.e. reducing the variance) than the original scale. A further reduction in variance at the intermediate scale is then carried out before ending up with the coarse block size. Each step is upscaled using an appropriate method such as single-phase flow simulation with the effective medium conductivity calculation. This method is also good for taking large problems and breaking them down into a hierarchy of manageable problems, as has been proven successfully in theoretical physics areas. However, this upscaling method can only be used as a local upscaling procedure. It is poor for highly anisotropy media and probably unreliable due to unrealistic boundary condition effects.

Another extensive computer upscaling method is the pseudo method. It involves running the reservoir simulation at the fine scale. The pseudo properties are then averaged out at different time steps, such that the reservoir properties change with time and will always have the same properties at the coarse scale to its fine scale. The set of pseudo properties generated for the coarse scale, however, is only problem specific. Thus, for any other new requirement of the coarse scale, or at different coarse scales, the whole procedure needs to be repeated to obtain the necessary information.

This method also tends to be time consuming and requires extensive computer power for solving the dynamic simulation at the fine scale and generating the pseudo properties. With dynamic reservoir simulations, which involve iterative procedures for obtaining dynamic properties like pressure, flow and fluid changes within the reservoir, a limited number of fine grid cells will be a constraint of using this method due to limited available computer memory and hardware resources. Furthermore, with the new technology of using geo-statistical methods, many geologists tend to generate much finer geological models for capturing finer heterogeneity of the

geological properties. Thus, these pseudo methods will be limited in use due to computer limitations in running such a large number of fine geological cells.

Various models with different degrees of geological heterogeneity are used for investigating the available upscaling algorithms. Based on the experiments described in detail in Chapter 3, various available upscaling algorithms to describe the coarse scale effective properties have resulted in different fluid flow behaviours in comparison to their fine scale's overall field performances for various different depositional environments.

For a model with quite homogeneous depositional environments similar to Model A, any upscaling algorithm could be used to represent its coarse scale permeability parameter. The simplest analytical algorithm would be the best selection in this specific case, since this would give a reasonable representation of the permeability parameter, and would also be significantly faster in the upscaling process turn around time.

For a more complex heterogeneous environment, however, a heavy numerical upscaling algorithm (e.g. the diagonal tensor method) should be considered, since a realistic representation of the fine scale fluid flow behaviour must be mimicked at the coarse scale level. Simple algorithms such as arithmetic-harmonic or harmonic-arithmetic may possibly be used, but the accuracy needed to mimic the fine scale behaviour will depend highly on the flow path tortuosity with the presence of shales. When there are fine scale barriers at the length scales of the coarse grids, care should be taken in using numerical methods such as diagonal/full tensor or renormalisation methods, because unrealistically low effective permeability may be produced due to the applied boundary conditions.

Further treatments such as upscaling the relative permeability and/or capillary pressure, or even using pseudo upscaling, are sometimes required to ensure a satisfactory agreement between fine and coarse grid flow simulation results.

The selection for choosing the appropriate upscaling algorithm is normally based on the geological depositional environment, rock fabric and fluid flow direction. This is sometimes cumbersome as it often depends on human judgement for its degree of geological complexity. In reality, it is more complex than this, as the geological model is more heterogeneous than what can be described even within the core scale level. Furthermore, with a lack of upscaling understanding, a simple upscaling algorithm such as arithmetic or harmonic average is often used. Inappropriateness in the use of any upscaling algorithm can result in different reservoir behaviours at its coarse scale level. Thus, the history matching at the coarse scale level can become a lengthy exercise, since the coarse scale behaviour can become significantly different to its fine scale behaviour due to the geological representation at the coarse scale level.

Based on the above observations of using different available upscaling algorithms, a new upscaling algorithm has been developed for various depositional geological environments. The aim of this algorithm is to find the best representation of the effective homogeneous grid cell that produces same fluid flow characteristics under the same boundary conditions of the heterogeneous cells at its fine scale level. It is based on the combination principal theory of diagonal tensor, renormalisation and arithmetic-harmonic/harmonic-arithmetic algorithms. The upscaling concept is summarised in the following process diagram (Figure 6-1).

A periodic boundary condition similar to diagonal tensor or full tensor's principal theory is defined by applying arbitrary pressure equal to one and zero at the inlet and outlet respectively. By defining the pressure boundary, the fluid flow can be forced to flow in a specific direction, and thus, the effective properties representing the specified direction can then be obtained.

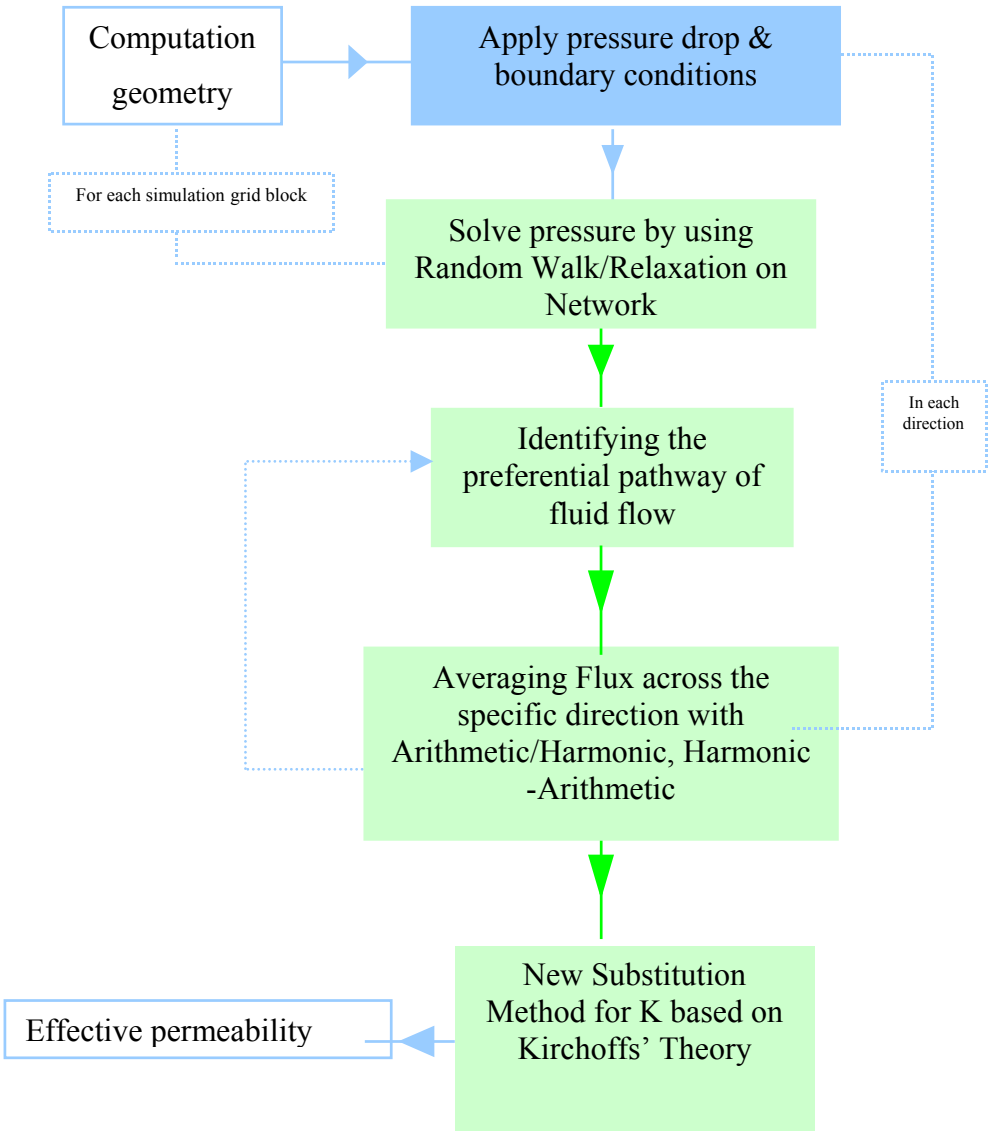

Figure 6-1 Process flowchart on new upscaling algorithm

The pressure solution within a coarse scale cell can be solved by using a combination of the random walk and relaxation methods. Prior to providing the pressure solution of the fluid flow in the numerical simulation, an equivalent resistor network to represent the fine-scale permeability parameter model is constructed similarly to the approach used for the re-normalisation method. Both Kirchhoff's electrical network theory and Darcy's fluid flow equations use the same principal in preserving the conservation of charge and mass respectively. By using Kirchoff's electrical network theory and obtaining the equivalent electrical parameters to the fluid flow

parameters, the pressure solution can then be obtained via the random walk and relaxation methods.

With the law of nature, particles will move from the greater to the lower potential. This is the same principal for fluid flow in the reservoir. The greater the pressure drop is across the cell to the neighboring cell, the greater the tendency of the fluid to flow from one point to another. The preferential paths of the fluid flow within the coarse grid cell in the specific direction can then be determined. These preferential paths are used as the basis for the effective properties' determination, as this will govern the main preferential flow direction from the inlet to the outlet within the coarse scale cell. With upscaling, these preferential pathways need to be captured, as in reality, these various paths will represent the various breakthrough point of the fluid flow from one end to the other end.

A single cell value, representing the average value of the effective permeability at the coarse scale model, can then be obtained by capturing the various flow potential within the coarse scale cell. An averaging method similar to the arithmetic-harmonic and harmonic-arithmetic algorithms is used on the derivation basis of conservation of mass and charge for Darcy's fluid flow equation and Kirchhoff's electrical network laws respectively.

The derivation of the new algorithm as described above only concentrated on representing the effective properties at the coarse scale level from the fluid flow aspects in reservoir. However, this does not give an indication of how these upscaled properties may influence other parameters. Enhancement treatments for incorporating the unswept volume due to low rock permeability and representing the fine scale well inflow performances at the coarse scale level are also integrated.

In general, the new upscaling algorithm has been successfully developed to represent the effective properties for various geological depositional environments. It can be used for various reservoir models from quite homogeneous reservoirs, like Model A, to the most heterogeneous model with flow barriers similar to Models B and C. A

better representation of the geological fine scale permeability at the coarse scale level can be obtained. The reservoir fluid flow performance at the coarse scale level quite closely mimics its fine scale level via the upscaling with the new algorithm. For a model with gas injection as the Enhancing Oil Recovery (EOR) process, the breakthrough timing for the fluid being injected is very important. With the new algorithm, it not only better predicts the fluid flow behaviour, but it also improves the fluid injected breakthrough time and results in better predictions of the ultimate fluid recovery based on the coarse scale model.

The most important element to be considered in any upscaling is the grid design for the coarse scale model. The grid orientation should be aligned as much as possible to the main fluid flow direction. Where possible, this orientation should also be consistent between the geological and coarse scaled dynamic simulation models. This will give a better upscaling representation at the coarse grid level and will also reduce the uncertainty due to grid orientation. In this way, the assumption made for the new upscaling algorithm with regards to the fluid boundary will also be honored and the optimal upscaling can be achieved.

A mathematical representation for the well inflow performance is typically represented using the isotropic permeability assumption (i.e. the same permeability values are assigned for all x, y and z directions). Due to the limited scope of this research, for the model with an anisotropic permeability representation similar to Model C, the well inflow performance at the coarse scale level may not be represented as precisely as at its fine scale level. The consequence of this is incorrect representation of the well inflow performance at the coarse scale level which may influence the process for matching the well rates and pressure drawdown (i.e. pressure decline rates). This will also impact the slowing down and limit the process for the success of the overall upscaling procedure.

Therefore, in accessing the accuracy of the new upscaling algorithm, the well performance matching of each individual well for Model C was performed by modifying the well inflow properties. This modification did not impact the fluid

flow aspect and its connectivity in reservoir, but modified the well off-take rates and pressure drawdown which could be constrained by minimum bottom-hole pressure or specified tubing head pressure.

The future improvement to representing a better well inflow performance for the upscaled model will also be recommended.

Finding the most effective and efficient upscaling algorithm to represent the reservoir heterogeneity from the geological model scale to the reservoir simulation scale is the main focus in this research. Thus, this research is based on the available data from geologists (the geological reservoir model with its petrophysical parameters), the laboratory data (PVT, capillary pressure and also, the relative permeability curves) and also the study of the flow characteristics of the reservoir. Any potential impact due to the change in scale of the reservoir model to any of the parameters stated above is not going to be analysed, as the impact will not affect the heterogeneity representation of the fluid flow in the reservoir.

Furthermore, in reality, the representation of the well inflow performance and data used, such as geological models, PVT, capillary pressure and relative permeability, are often uncertain. Further refining with additional reservoir information from the pressure and production data monitoring are often carried out as part of the reservoir management process for reducing any uncertainty.

Chapter 7.
CONCLUSIONS

Upscaling, which lies in determining the effective properties representing the heterogeneous parts of reservoir descriptions, is perhaps the most complex mathematical problem. With new development technologies, geological models tend to be built in a very fine resolution, such that the degree of heterogeneity in the reservoir is captured within the model. This large number of fine grid resolution cells is not able to be carried out in reservoir simulations. Thus, the average of these heterogeneities will always be required in the form of upscaling to represent the effective properties within the coarse scale for dynamic reservoir simulations.

For additive rock properties, such as porosity and saturation, a simple averaging algorithm such as the 'volume weighted arithmetic average' could be considered as the best estimator in determining the effective porosity and initial saturation of the coarser grid. This is because the rock pore volume and the fluid pore volume at the initial reservoir condition, which governs the fluid in place within the reservoir, can be preserved between the fine scale and coarse scale models.

For permeability, which describes the ability of fluid to flow through the connectivity of the rock pores in the porous media and influence the dynamic reservoir behaviour, simple averaging algorithms (such as arithmetic and harmonic averages), in general do not always work in representing the effective properties at the coarse scale model. Therefore, selection of the appropriate upscaling algorithm needs to be carried out prior to upscaling. Factors such as geological depositional environment, degree of heterogeneity, and also the variability of permeability in the finer scale model are often the main criteria for selecting the appropriate upscaling algorithms.

A new upscaling algorithm based on the combination principal theory of diagonal tensor, renormalisation and a combination of analytical algorithms has been successfully developed for generating the effective properties at various different

geological environments. The average effective heterogeneity properties of the reservoir model can generally be used to more accurately represent the fluid flow behaviours at the coarse scale level as if it were at the fine scale level. The enhanced recovery by fluid injection, the breakthrough time of the fluid being injected and the ultimate fluid recovery, are all better predicted by using the new algorithm in comparison to any other upscaling algorithms available. The consequence of using this new upscaling algorithm is a slower turn-around time due to a longer upscaling process. However, more accurate representations of the effective properties can be achieved in dynamic simulation predictions.

There are several other available upscaling algorithms, which may result in a quicker upscaling process than the extensive numerical approach, and may also possibly be used to represent the effective properties of the upscaled parameters. However, careful consideration in selecting the appropriate upscaling algorithm will be required. Inappropriate usage of any upscaling algorithm can result in different reservoir behaviours at the coarse scale level. Thus, the history matching process can become a lengthy exercise resulting in a slower turn around time for the entire process of reservoir predictions, since the coarse scale behaviour can become significantly different to its fine scale behaviour due to geological representations at the coarse scale level.

The successful answer to solving the upscaling process lies in the turn around time available for the upscaling and dynamic simulation processes to be carried out in day-to-day business. This is often where the critical judgement lies in finding the best possible upscaling solution, as more accurate upscaling algorithms take longer to run for better accuracy in providing the effective properties for the upscaled model. The greater the heterogeneity or variability of the fine scale properties to be upscaled (as a single coarse cell by averaging), the greater the uncertainty will be of the upscaled permeability. The extensive numerical upscaling algorithm is therefore required for consideration in these instances as the appropriate upscaling algorithm. By using the extensive numerical upscaling process, an optimum balance of accuracy

can then be achieved between flow simulation time on the coarse grid and the upscaling process in preserving important geological features in fine grid models.

REFERENCES

1. Aasum, Y., Kasap, E. & Kelkar, M. 1993, 'Analytical Upscaling of Small – Scale Permeability Using a Full Tensor', paper SPE 25913, Society of Petroleum Engineer, Denver, p. 679-692.
2. Abtahi, M. & Torsaeter, O. 1998, 'Experimental and Numerical Upscaling of Two-Phase Flow in Homogeneous and Heterogeneous Porous Media', paper SPE 50572, Society of Petroleum Engineers Inc., Texas, p. 45-55.
3. Almeida, J. A., Soares, A. & Pereira, M. J. 1996, 'Upscaling of Permeability: Implementation of a Conditional Approach to Improve the Performance in Flow Simulation', paper SPE 35490, Society of Petroleum Engineers Inc., Texas, p. 97-108.
4. Azoug, Y and Tiab, D. 2003, 'The Performance of Pseudo Functions in the Upscaling Process', paper SPE 80910, Society of Petroleum Engineers Inc., Texas, p. 1-19.
5. Balbinski, E.F., Masters, J. & Makin, J. 2002, 'A New Flow-Based CutOff Criterion for Permeability in Dry Gas Reservoirs', *Trans*., SPWLA European Symposium on Reservoir Characterisation, London, p. 1-8.
6. Barker, J. W. & Thibeau, S. 1997, 'A Critical Review of the Use of Pseudo Relative Permeabilities for Upscaling', paper SPE 35491, *SPE Reservoir Engineering Journal*, May edn., Society of Petroleum Engineers Inc., Texas, p. 138-143.
7. Beggs, Kay, A., Gustason, E. R. & Angert, P. F. 1993, 'Characterising and managing the dynamic reservoir – a multi disciplinary approach: Characterisation of a complex fluvial – deltaic reservoir for simulation', at the 4th Annual Archie Conference, Texas, p. 143-148.
8. Binder, K & Heermann, D.W. 1988, *Springer series in solid-state sciences 80 – monte carlo simulation in statistical physics*, Springer-Verlag, Berlin.
9. Blumenfeld, R. 1988, 'Probabilistic densities of homogeneous functions: explicit approximation and applications to percolation networks', *Journal of Physical A. Mathematical and General*, vol. 21, p. 815-825.

10. Blunt, M. J., King, P. R. & Goshawk, J. A. 1992, *Mathematics in oil recovery – simulations of viscous fingering in a random network*, Clarendon Press, Oxford, p. 243-262.
11. Catchpole, J. P. & Fulford, G. 1966, 'Dimensionless groups', *Industrial and Engineering Chemistry*, vol. 58, no. 3, p. 46-60.
12. Chardaire, G., Chavent, J. J. & Liu, J. 1992, *Mathematics in oil recovery – relative permeabilities and capillary pressure estimation through least square fitting*, Clarendon Press, Oxford, p. 721-734.
13. Christie, M. A. 1988, *Mathematics in oil production – application of high resolution simulation to modelling fluid instabilities*, Clarendon Press, Oxford, p. 269-284.
14. Christie, M. A. 1997, 'A Fast Procedure for Upscaling In Compositional Simulation', paper SPE 37986, Society of Petroleum Engineers Inc., Texas, p. 105-113.
15. Christie, M. A. 1997, 'Upscaling for Reservoir Simulation', paper SPE 37324, *Journal of Petroleum Technology*, Society of Petroleum Engineers Inc., Texas, p. 1004-1010.
16. Christie, M. A. and Blunt, M. A 2001, 'Tenth SPE Comparative Solution Project: A Comparison of Upscaling Techniques', paper SPE 72469, *SPE Reservoir Evaluation & Engineering*, Society of Petroleum Engineers Inc., Texas, August, p. 308-316
17. Christie, M.A., Mansfield, M., King, P.R., Barker, J.W. 1995, 'A Renormalisation Based Upscaling Techniques for WAG Floods in Heterogeneous Reservoirs', paper SPE 29127, Society of Petroleum Engineers Inc., Texas, p. 353-361.
18. Coats, K. H. 1969, 'Use and Misuse of Reservoir Simulation Models', paper SPE 2367, Society of Petroleum Engineers Inc., Texas, p. 183-190.
19. Cordell, J.C & Ebert, C.K. 1965, 'A Case History – Comparison of Predicted and Actual Performance of a Reservoir Producing Volatile Crude Oil', *JPT*, November edn., p. 1291.
20. Crotti, M. A. and Cobenas, R. H. 2001, 'Scaling Up of Laboratory Relative Permeability Curves. An Advantageous Approach Based on Realistic Average

Water Saturations', paper SPE 69394, Society of Petroleum Engineers Inc., Texas, p. 1-7

21. Dake, L. P. 1978, *Fundamentals of reservoir engineering*, Elsevier Scientific Publishing Co., Amsterdam.
22. Dale, M. 1992, *Mathematics in oil recovery – averaging relative permeability in composite cores*, Clarendon Press, Oxford, p. 649-682.
23. Deakin, M. & Manan, W. 1998, 'The Integration of Petrophysical Data for the Evaluation of Low Contrast Pay', paper 39761, Society of Petroleum Engineers Inc., Texas.
24. Del Toro, V. 1986, *Electrical engineering fundamentals*, Prentice-Hall, Englewood Cliffs.
25. Demirmen, F. 1998, *Reserves uncertainty: some historical trends and wider implications*, EAGE, London, p. 143-149.
26. Derrida, B. & Vannimenus, J. 1982, 'A transfer matrix approach to random resistor networks', *Journal of Physical A. Mathematical and General*, vol. 15, p. 557-564.
27. Doyle, P.G & Snell, J.L. 1984, *The carus mathematical monographs number twenty two – random walks and electrical networks*, The Mathematical Association of America, Washington.
28. Durlofsky, L. J. 1997, 'Use of Higher Moments for the Descriptions of Upscaled, Process Independent Relative Permeabilities', paper SPE 37987, Society of Petroleum Engineers Inc., Texas.
29. Durlofsky, L. J., Behrens, R. A., Jones, R. C. & Bernath, A. 1995, 'Scale Up of Heterogeneous Three Dimensional Reservoir Descriptions', paper SPE 30709, Society of Petroleum Engineers Inc., Texas, p. 53-66.
30. Durlofsky, L.J., Jones, R.C. & Milliken, W. J. 1997, 'Non-uniform coarsening approach for the scale up of displacement processes in heterogeneous porous media', *Advance Water Resources*, vol. 20, no. 335.
31. Durrett, R & Kesten, H 1991, *Random walks, brownian motion and interacting particle systems*, Birkhäuser, Boston.

32. Ekrann, S. & Dale, M. 1992, *Mathematics in oil recovery – averaging of relative permeability in heterogeneous reservoirs*, Clarendon Press, Oxford, p. 173-198.
33. Fanchi, J.R 2000, *Integrated flow modelling – development in petroleum science 49*, Elsevier, Amsterdam.
34. Farmer, C. L. 1988, *Mathematics in oil production – the generation of stochastic field of reservoir parameters with specified geostatistical distributions*, Clarendon Press, Oxford, p. 235-252.
35. Fayers, F. J. 1988, *Mathematics in oil production – an introduction to some of the mathematical and physical problems of modelling oil displacement in porous media*, Clarendon Press, Oxford, p. 1-52.
36. Fayers, F. J., Barker, J. W. & Newley, T. M. J. 1992, *Mathematics in oil recovery – effects of heterogeneities on phase behaviour in enhanced oil recovery*, Clarendon Press, Oxford, p. 115-150.
37. Floris, F. J. T. and Peersman, M. R. H. E. 1998, *Petroleum geoscience – uncertainty estimation in volumetrics for supporting hydrocarbon exploration and production decision – making*, EAGE/Geological Society, London, p. 33-40.
38. Hagoort, J., Brinkhorst, J. W. & van der Kleyn, P H. 1998, 'Development of An Offshore Gas – Condensate Reservoir by Nitrogen Injection vs. Pressure Depletion', *Journal of petroleum technology,* Society of Petroleum Engineers Inc., Texas, p. 463-469.
39. Hastings, J. J., Muggeridge, A. H. and Blunt, M. J. 2001, 'A New Streamline Method for Evaluating Uncertainty in Small Scale, Two Phase Flow Properties', paper SPE 66349, Society of Petroleum Engineers Inc., Texas, p. 1-9.
40. Holden, L. & Nielsen, B. F. 1999, *Global upscaling of permeability*, Norwegian Computing Centre, Oslo.
41. Holden, L. & Nielsen, B. F. 1998, *Global upscaling of permeability in heterogeneous reservoirs: the output least square (OLS) method*, Norwegian Computing Centre, Oslo.

42. Holden, L., Soleng H. H. & Syversveen A. R. 1998, *History matching with uncertainty quantification*, Norwegian Computing Centre, Oslo.
43. Hove, K., Olsen, G., Nilsson, S. & Tonnesen, M. 1992, 'From Stochastic Geological Description to Production Forecasting in Heterogeneous Layered Reservoirs', paper SPE 24890, Society of Petroleum Engineers Inc., Texas, p. 311-325.
44. *IRAP RMS User Manual*, 1999, Smedvig Technologies, p. 331-348.
45. *IRAP RMS IPL Manual*, Roxar Ltd.
46. Kempers, L. J. T. M. 1992, *Mathematics in oil recovery – effects of fluid properties on convective dispersion: comparison of analytical model with numerical simulations*, Clarendon Press, Oxford, p. 775-784.
47. Killough, J. & Fang, Y. P. 1992, *Mathematics in oil recovery – viscous/gravity scaling of pseudo relative permeabilities for the simulation of moderately heterogeneous reservoirs*, Clarendon Press, Oxford, p. 471-494.
48. King, P.R & Edwards, Sir S. 1988, *Mathematics in oil production - effective values in averaging*, Clarendon Press, Oxford, p.217-234.
49. Koehler, K. R. 1996, *The nature of fluids*, http://www.rwc.uc.edu/koehler/biophys/3b.html.
50. Kumar, A. & Farmer, C. L. 1997, 'Efficient Upscaling from Cores to Simulation Models', paper SPE 38744, Society of Petroleum Engineers Inc., Texas, p. 257-272
51. Kyte, J. R. & Berry, D.W. 1975, 'New Pseudo Functions to Control Numerical Dispersion', paper SPE 5105, *Society of Petroleum Engineers Journal*, August edn., p. 269-276
52. Lawler, G. F. & Coyle, L. N. 1999, *Lectures on contemporary probability, american mathematical society institute for advanced study*, Rhode Island.
53. Lee, J., Kasap, E. & Kelkar, M. G. 1995, 'Development and Application of a New Upscaling Techniques', paper SPE 30712, Society of Petroleum Engineers Inc., Texas, p. 89 –101.
54. Lemouzy, P.M., Romeu, R.K. 1993, 'A New Scaling Up Method to Computer Relative Permeability and Capillary Pressure for Simulation of Heterogeneous

Reservoir', paper SPE 26660, Society of Petroleum Engineers Inc., Texas, p. 1-8

55. Lozano, J. A., Costa, L. P., Alves, F. B, & Silva, A. C. 1996, 'Upscaling of Stochastic Models for Reservoir Simulation – An Integrated Approach', paper SPE 36205, Society of Petroleum Engineers Inc., Texas, p. 328-338.
56. Lyon, W. C. 1996, *Standard handbook of petroleum & natural gas engineering*, Vol. 2, Gulf Professional Publishing, Houston.
57. Mansoori, J. 1992, *Review of basic upscaling procedures: advantages and disadvantages*, Amoco Production Company, Tulsa, p.65-74.
58. Mardras, N. 2000, *Field institute communications – monte carlo method*, American Mathematical Society, Rhode Island.
59. Milliken, W. J and Emanuel, A.S. 2001, 'Application of 3D Streamline Simulation to Assist History Matching', paper SPE 74712, Society of Petroleum Engineers Inc., Texas.
60. Muggeridge, A. H. 1992, *Mathematics in oil recovery – modelling flow through heterogeneous porous media using effective relative permeabilities generated from detailed simulations*, Clarendon Press, Oxford, p. 449-470.
61. Narayanan, K., Lake, L. W. & Willis, B. J. 1999, 'Response Surface Methods for Upscaling Heterogeneous Geologic Models', paper SPE 51923, Society of Petroleum Engineers Inc., Texas.
62. Nomura, M. 2002, 'Fast Computation of Effective Properties for Two Phase Flow Problems', paper SPE 77570, Society of Petroleum Engineers Inc., Texas.
63. Odeh, A. S. 1969, 'Reservoir Simulation … What is It?', *Journal of petroleum technology,* Society of Petroleum Engineers Inc., Texas, p. 1383-1388.
64. Panfilov, M. 1998, *Recent advances in problems of flow & transport in porous media, upscaling two phase flow in double porosity media: nonuniform homogenisation*, Kluwer Academic Publisher, Netherlands, p. 195-215.
65. Pavone, D. 1992, *Mathematics in oil recovery – equations for two-phase flow in porous media derived from space averaging*, Clarendon Press, Oxford, p. 199-210.

66. Pallister, I. C. & Ponting, D. K. 2000, 'Asset Optimisation Using Multiple Realizations and Streamline Simulation', paper SPE 59460, Society of Petroleum Engineers Inc., Texas, p. 1-11.
67. Peaceman, D.W. 1997, 'Effective Transmissibilities of a Gridblock by Upscaling – Comparison of Direct Methods with Renormalisation', *SPE Journal*, Society of Petroleum Engineers, Inc., Texas, vol. 2, September edn., p. 338-349
68. Poulisse, H. N. J. 1992, *Mathematics in oil recovery – effective absolute permeability in the presence of sub-grid heterogeneities: an analytical approach*, Clarendon Press, Oxford, p. 699-720.
69. Ponting, D. K. 1998, 'Hybrid Streamline Methods', paper SPE 39756, Society of Petroleum Engineers, Texas.
70. Ponting, D. K. 1992, *The mathematics of oil recovery – corner point geometry in reservoir simulation*, Clarendon Press, Oxford, p. 45-66
71. Quintard, M., Bertin, H. & Whitaker, S. 1992, *Mathematics in oil recovery – two-phase flow in heterogeneous porous media: large scale capillary pressure and permeability determination*, Clarendon Press, Oxford, p. 751-766.
72. Renard, Ph. & de Marsily, G. 1997, 'Calculating equivalent permeability; a review', *Advances in Water Resources*, vol. 20, no. 5-6, p. 253-278.
73. Saad, N., Cullick, A. S. & Honarpour, M. N. 1995 'Effective Relative Permeability in Scale up and Simulation', paper SPE 29592, Society of Petroleum Engineers Inc., Texas, p. 451-464.
74. Scatter, A. & Thakur, G. 1994, *Integrated petroleum reservoir management*, Pennwell Publishing Co., Tulsa, p. 268-289.
75. Sun, H.D., Liu, L., Zhou, F. & Gao, C. 2003, 'Exact Solution of Two Layer Reservoir with Cross flow under Constant Pressure Conditions', SPE 81043, Society of Petroleum Engineers Inc., Texas, p. 1–6.
76. Tang, Z., Gaquerel, G. & Gawith, D. E. 1993, 'Characterising and Managing the Dynamic Reservoir – A multi disciplinary approach', Integrating Geoscience and Engineering for Improved Field Management and Appraisal at the 4th Annual Archie Conference, Texas, p. 29-41.

77. Tchelep, H. A., Durlofsky, L. J., Chen, W. H., Bernath, A. & Chien, M. C. H. 1997, 'Practice Use of Scale Up and Parallel Reservoir Simulation Technologies in Field Studies, paper SPE 38886, Society of Petroleum Engineers Inc., Texas, p. 1-15.

78. Tchelep, H. A., Durlofsky, L. J., Chen, W. H., Bernath, A. & Chien, M. C. H. 1999, 'Practice Use of Scale Up and Parallel Reservoir Simulation Technologies in Field Studies', paper SPE 57475, *SPE Reservoir Evaluation and Engineering*, Society of Petroleum Engineers Inc., Texas, p. 368-376.

79. Telleria, M. S., Virues, C. J. J & Crotti, M. A. 1999 'Pseudo Relative Permeability Functions. Limitations in the Use of the Frontal Advance Theory for 2-Dimensional Systems', paper SPE 54004, Society of Petroleum Engineers Inc., Texas, p. 1-7.

80. Thomas, G. W. 1995, *Reservoir simulation: principles and strategies*, G. W. Thomas & Associates Ltd, Kelowna, Canada.

81. Tidwell, V. C. & Wilson, J.L. 2000, 'Heterogeneity, Permeability Patterns, and Permeability Upscaling: Physical Characterisation of a Block of Massillon Sandstone Exhibiting Nested Scales of Heterogeneity', paper SPE 65282, *SPE Reservoir Evaluation and Engineering*, vol 3, no. 4, Society of Petroleum Engineers Inc., Texas, p. 283-291.

82. Timmerman, E. H 1982, *Practical reservoir engineering, Part 1 – method for improving accuracy or input into equations and computer programs*, PennWell Publishing Co., Tulsa.

83. Thibeau, S. & Barker, J. W. 1995, 'Dynamic Upscaling Techniques Applied to Compositional Flows', paper SPE 29128, Society of Petroleum Engineers Inc., Texas, p. 363-373.

84. Van Wunnik, J. N. M & Wit, K. 1992, *Mathematics in oil recovery – a simple analytical model of the growth of viscous fingers in heterogeneous porous media*, Clarendon Press, Oxford, p. 263-280.

85. Versteeg, H. K. & Malalasekera. W. 1995, *An introduction to computational fluid dynamics – the finite volume method*, Prentice Hall, Harlow, England.

86. Wardren, D. 1988, *Mathematics in oil production – discretisation techniques for multiphase flow*, Clarendon Press, Oxford, p. 285-294.

87. Wilkinson, D. 1988, *Mathematics in oil production – fluid dynamics at pore scale*, Clarendon Press, Oxford, p. 343-362.
88. Williams, J.K. 1992, *Mathematics in oil recovery – simple renormalisation schemes for calculating effective properties of heterogeneous reservoirs*, Clarendon Press, Oxford, p. 281-298.
89. Worthington, P. F. & Cosentino, L. 2005, 'The Role of Cutoffs in Integrated Reservoir Studies', *SPE Reservoir Evaluation & Engineering*, August 2005 edn., vol. 8, no. 4, p. 276-290.
90. Zeng, X.C., Bergman, D. J., & Stoud, D. 1988 'Numerical study of transport properties in continuum percolation', *Journal of Physical A. Mathematical and General*, vol. 21, p. 949-953.
91. Zhang, H. R. & Sorbie, K.S. 1995, 'The Upscaling of Miscible and Immiscible Displacement Processes in Porous Media', paper SPE 29931, Society of Petroleum Engineers, Inc., Texas, p. 427-440.

APPENDICES

APPENDIX A DERIVATION OF SOME EXISTING ALGORITHMS

APPENDIX B RELATED PUBLISHED PAPERS & PRESENTATIONS

APPENDIX C NEW UPSCALING ALGORITHM IN IRAP RMS IPL SCRIPT

Appendix A
Derivation of Some Existing Algorithms

Darcy's law

The equation which governs most upscaling algorithms' principal is the basic fluid flow equation in the porous media known as Darcy's law. Darcy's law states that the fluid flow rate is proportional to the cross sectional area and the pressure difference ΔP across a length of Δx, and inversely proportional to the viscosity of the fluid. The proportionality constant is referred to as the 'permeability'. Therefore, for a single flow, it is defined as:

$$Q = -\frac{KA}{\mu}\frac{\Delta P}{\Delta x}$$

Equation A- 1 Darcy's law

Permeability is a physical property of a large number of pores which influence the tendency of the fluid to flow from one place to another. It is a micro scale property which is also by the grain size distribution and its shapes. The permeability usually decreases as grain size decreases. This is normally used to distinguish the rock type classification depending upon its geological rock depositional and its properties. For example, the clean and unconsolidated sands may have permeability as high as five to 10 Darcies, while the compacted and cemented sandstone rocks tend to have a lower permeability. Productive sandstone reservoirs usually have permeability in the range of 10 to 1000 mD. Furthermore, the presence of clay, which may swell on contact fresh water, can also affect permeability resulting in the reduction of rock's permeability by several orders of magnitude.

Permeability does not only act upon one direction. The flow in porous media often occurs in three principle directions, horizontally on x and y directions and also

vertically on the z direction. Therefore, by regarding the potential gravitational effects, the three directional flows can be defined as:

$$\begin{bmatrix} Q_x \\ Q_y \\ Q_z \end{bmatrix} = -\frac{A}{\mu} \begin{bmatrix} K_{xx} & K_{xy} & K_{xz} \\ K_{yx} & K_{yy} & K_{yz} \\ K_{zx} & K_{zy} & K_{zz} \end{bmatrix} \begin{bmatrix} \partial\phi/\partial x \\ \partial\phi/\partial y \\ \partial\phi/\partial z \end{bmatrix}$$

Equation A- 2 Darcy's law in 3-directional flow

Effective Reservoir Properties

In the reservoir modelling, the reservoir properties, which include porosity, permeability and fluid saturation, are typically assigned with the average value representation on each individual grid cells. The average cell value is normally called 'the effective properties' of a heterogeneous block.

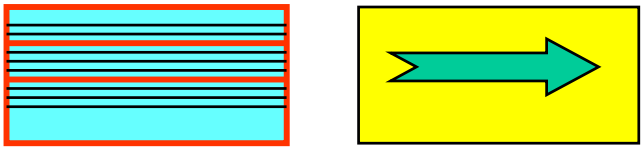

Figure A- 1 Graphical representation of effective properties

Porosity and Initial Fluid Saturation

For the porosity or initial fluid saturation, the effective properties can easily be defined as these properties serve a function of preserving the total pore volume and the pore volume occupied by the fluid for porosity and water saturation respectively. By definition, the pore volume is basically the combination of the grid block porosity with the volume of the block, while the fluid pore volume is the combination of pore volume and the percentage of fluid saturation within the pore volume.

Porosity

The definition of the effective porosity can then be derived with the following equations.

$$\text{Pore Volume at coarse scale} = \text{Total Pore Volume at fine scale}$$

$$PV_{coarse} = \sum PV_{i,fine}$$

$$V_{bulk,coarse} \cdot \bar{\phi} = \sum V_{bulk,i,fine} \cdot \phi_{i,fine}$$

$$\bar{\phi} = \frac{\sum V_{bulk,i,fine} \cdot \phi_{i,fine}}{V_{bulk,coarse}}$$

Equation A- 3 Derivation of effective porosity

Therefore, from the derivation shown above, the effective porosity can be defined by using the bulk volume weighted arithmetic average.

Initial Fluid Saturation

Similar to porosity, the initial fluid saturation will affect the total pore volume occupied by the fluid within the medium. In the reservoir modelling, the initial fluid saturation is normally assigned by using the water saturation, while the remaining pore volume will be the pore volume occupied by the hydrocarbon. As mentioned earlier, preserving the hydrocarbon pore volume between the two different scales will be the main objective in creating the effective fluid saturation.

Hydrocarbon PV at coarse scale = Total Hydrocarbon PV at fine scale

$$HCPV_{coarse} = \sum HCPV_{i,fine}$$

$$V_{bulk,coarse}.\bar{\phi}(1-\bar{S}_w) = \sum V_{bulk,i,fine}.\phi_{i,fine}.(1-S_w)$$

$$PV_{coarse}.(1-\bar{S}_w) = \sum PV_{i,fine}.(1-S_{w,i})$$

$$(1-\bar{S}_w) = \frac{\sum PV_{i,fine}.(1-S_{w,i})}{PV_{coarse}}$$

$$\bar{S}_w = 1 - \frac{\sum PV_{i,fine}.(1-S_{w,i})}{PV_{coarse}}$$

Equation A- 4 Derivation of effective initial water saturation

From the derivation shown above, the effective water saturation can then be defined by using the pore volume weighted arithmetic average.

Permeability

For the permeability, which depends on the boundary conditions, the derivation is not as straight forward as the effective porosity or effective initial fluid saturation. The effective permeability is defined as the permeability of the homogeneous block, which will produce the same fluid-flow under the same boundary conditions. It is not an instinsic property of rock, since it is influenced by the boundary conditions, the geological depositional beddings and also the fluid flow within the system.

Therefore, for simplicity, here are the following two derivations for determining the upper and lower bounds of the effective permeability by using the arithmetic and harmonic upscaling algorithms respectively.

Arithmetic Upscaling Algorithm Derived based on Parallel Bed (Linear Flow)

The arithmetic algorithm uses the assumption that the fluid flow in the linear manner, which can be described as the fluid flow in the parallel bed having a different permeability for each layer.

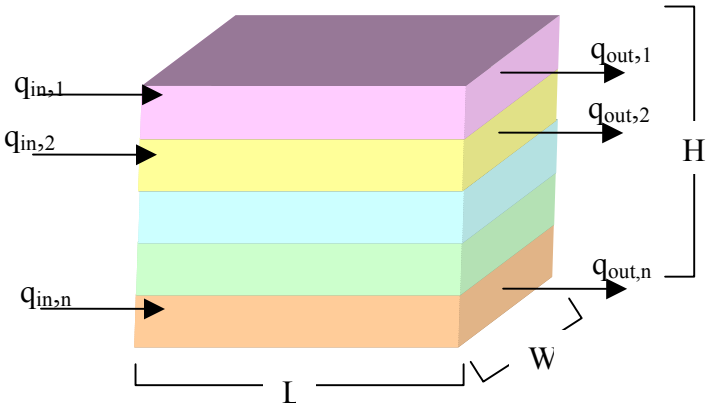

Fine Scale

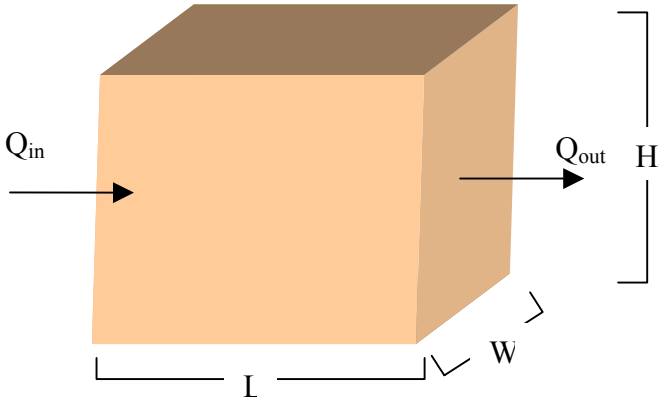

Coarse Scale

Figure A- 2 Graphical representation of linear Flow in parallel bed for arithmetic upscaling algorithm derivation

For a fluid flow in the same boundary conditions, the pressure is assumed to be constant at each end of the flow system. The total flow rate can then be representated as the sum of the rates q_i in each layer.

$$Q_T = \sum_i q_i$$

By applying Darcy's law of equation, the above equation can then be determined as the following equation:

$$\frac{K_{ave} H_T W (P_{in} - P_{out})}{\mu L} = \sum_i \frac{K_i h_i W (P_{in} - P_{out})}{\mu L}$$

For the same block dimensions, the fluid viscosity and the pressure boundary conditions for both fine and coarse scale blocks, the common terms can then be cancelled on both sides of the equation. The equation then becomes the following:

$$K_{ave} H_T = \sum_i K_i h_i$$

The average (effective) permeability can then be obtained by rearranging the above equation as shown in Equation A- 5.

$$K_{ave} = \frac{\sum_i K_i h_i}{H_T}$$

Equation A- 5 The derivation of effective permeability with arithmetic average on parallel bed

The above equation indicates that the average permeability is the height weighted arithmetic average of the individual layered permeability.

Harmonic Upscaling Algorithm Derived based on Serial Bed

The fluid flow in the series of beds can be illustrated with the following picture.

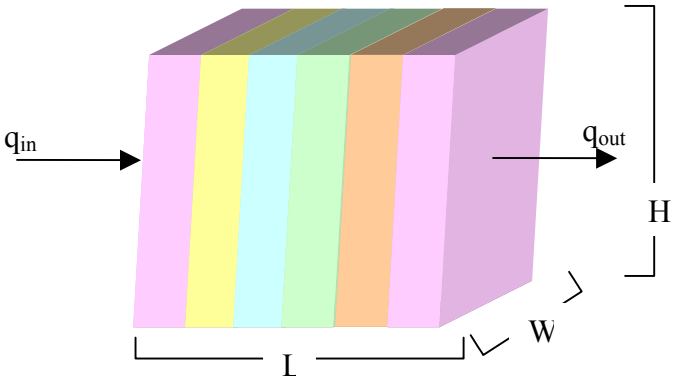

Fine Scale

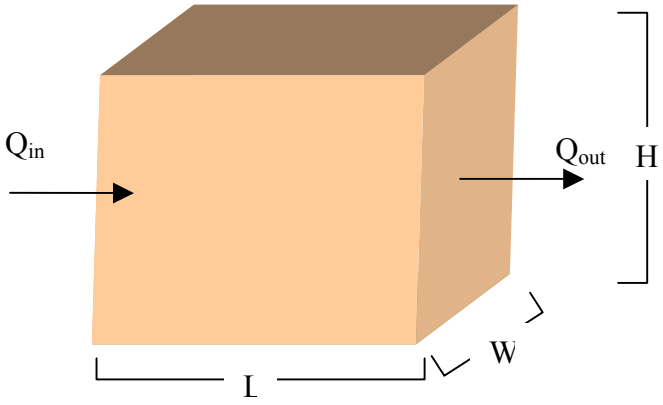

Coarse Scale

Figure A- 3 Graphical representation of fluid flow in serial bed for harmonic upscaling algorithm derivation

With the law of mass conservation, the fluid flow into the block will be equal to the sum of the accumulation of the fluid flow within the blocks and the flow rate out from the block. Under the steady state at the equilibrium condition, the accumulation of fluid within the blocks will be negligible. Thus, the fluid will flow at the same

flow rate across each bed. For the same flow rate across each bed, the pressure difference will then be proportional to the length of the bed, i. The fluid flow can be illustrated by applying Darcy's law of equation as the following equation:

$$\frac{K_{ave}H_T W(p_{in}-p_{out})}{\mu L}=\frac{K_1 H_T W(p_{in}-p_{1,out})}{\mu L_1}+\frac{K_2 H_T W(p_{2,in}-p_{2,out})}{\mu L_2}+\ldots+\frac{K_n H_T W(p_{n,in}-p_{out})}{\mu L_n}$$

For the same block dimensions and the fluid viscosity, the common terms can then be cancelled on both sides of the equation. The equation is then as follows:

$$\frac{K_{ave}(p_{in}-p_{out})}{L}=\frac{K_1(p_{in}-p_{1,out})}{L_1}+\frac{K_2(p_{2,in}-p_{2,out})}{L_2}+\ldots+\frac{K_n(p_{n,in}-p_{out})}{L_n}$$

From the equation above and the Darcy's fluid flow equation, the pressure differences between the blocks will serve as a function of the block permeability over the length i. Therefore, by assuming a proportion of pressure difference on each block over the total pressure differences with the ratio of block permeability over the length i, the average permeability can then be obtained as follows:

$$\frac{K_{ave}(p_{in}-p_{out})}{L}=\frac{K_1}{L_1}\frac{L_1}{K_1}\sum\frac{Ki}{L_i}(p_{in}-p_{out})+\frac{K_2}{L_2}\frac{L_2}{K2}\sum\frac{Ki}{L_i}(p_{in}-p_{out})+\ldots+\frac{K_n}{L_n}\frac{Ln}{Kn}\sum\frac{Ki}{L_i}(p_{in}-p_{out})$$

Canceling some of the sum of the pressure differences and rearranging the above equation, the average permeability for the serial beds can then be obtained as the following equation:

$$K_{ave}=\frac{L}{\sum_i L_i/K_i}$$

Equation A- 6 The derivation of effective permeability with harmonic average on serial bed

The above equation indicates that the average permeability on the serial bed can be defined with the length weighted harmonic average of each serial bed permeability.

Appendix B

Related Published Papers & Presentations

1. **Paper on "Different Scales & Integrated of Data in Reservoir Simulation" submitted for the Upscaling Downunder Conference in Melbourne – Australia on 7th February 2000.**

2. **Presentation on "Different Scales & Integrated of Data in Reservoir Simulation" held at AAPG Conference in Bali – Indonesia on 18th October 2000.**

3. **Paper on "New Upscaling Technique by Integration of Data in Reservoir Simulation" submitted for the Journal of Petroleum Science and Engineering in Perth - Australia on 7th February 2004**

Paper on "Different Scales & Integrated of Data in Reservoir Simulation" submitted for the Upscaling Downunder Conference in Melbourne – Australia on 7th February 2000.

DIFFERENT SCALES AND INTEGRATION OF DATA IN RESERVOIR SIMULATION

Lina Hartanto, Robert Amin & Raj Rajeswaran
Curtin University of Technology
Kent Street, Bentley WA 6012, Australia

Abstract

The term upscaling and determination of pseudo-curves or effective parameters used on a coarse scale simulation grid are related to the complex and extensive problems associated with the reservoir studies. The primary strategy is mainly focused on the good physical and practical understanding of the particular processes in questions, and an appreciation of reservoir model sensitivities. Thus, the building of reservoir simulation models can be optimally determined.

By concentrating on modeling and upscaling gas injection for Enhanced Oil Recovery (EOR) process, which included Interfacial Tension (IFT) and amicability effect, a new effective and efficient algorithm of upscaling will be investigated and determined by using several upscaled parameters. The sensitivities of these determined coarse scale parameters, i.e. porosity, absolute & relative permeabilities and capillary pressure, will also be studied through history matching of the existing field.

Introduction

Prediction of reservoir performance is normally carried out by reservoir simulation. A numerical reservoir simulator solves approximately the equations of fluid flow in the reservoir, based on partitioning of the reservoir into a set of numerical grid blocks. Each grid block is assumed to be homogeneous. In full field reservoir simulations, grid blocks are typically in the region of 10-m times 100-m times 5-m. Consequently, there is a need to "average" the laboratory data before using them in simulators. The typical 3D geological models is usually with the resolution of 25m by 25 m by 1 m or through the scale of available data such as logs, cores, or outcrops which may contain up to more than 10 million block. However, the available black oil simulator can only handle no more than 300,000 grid cells due to computer memory and speed limitation in numerical simulation. Thus, this is the upscaling problem. The rock properties that need to be upscaled are porosity, absolute and relative permeabilities, and capillary pressure, which each simulation grid block should represent the heterogeneous parts of the reservoir.

Except in the case of truly homogeneous reservoirs, upscaling must always be carried out, although present day practice is not always recognized as such. For instance, plotting measured relative permeabilities as a function of

normalized saturation, and choosing some average curve as representative, is a form of upscaling. Such a procedure does not take into account the spatial arrangement of the different rock types, and will therefore be unreliable. In media where the ratio between horizontal and vertical correlation lengths is large, for example, the proper upscaled relative permeabilities may be significantly different from their rock counterparts, even if all participating rock types have identical relative permeability curves.

In history matching reservoir performance, relative permeabilities are perhaps the first parameter to be adjusted. Somewhat simplistically, this process should be interpreted as posteriors upscaling. The willingness to sacrifice relative permeabilities signals a perceived unreliability of the a priori upscaling originally carried out.

Upscaling is a broad term, also encompassing techniques to increase numerical accuracy at the passage of sharp saturation fronts. Our main interest is more specific: If heterogeneities are small relative to the distance between wells, one can define "effective" properties of the heterogeneous medium, i.e. effective absolute and relative permeabilities and capillary pressure. Effective properties are physical parameters valid on the larger scale, and capture the average effect of small-scale heterogeneity. Hence, coarsening the fine scale geological description by using the appropriate upscaling algorithm is important to maintain the integrity of the model for the fluid flow modeling purposes (i.e. maintain agreement in flow results between fine and coarse models).

Several algorithms are commercially available for upscaling by using either analytical or numerical approaches. From the simple methods such as arithmetic, geometric and harmonic averages to the complicated tensor methods, such as Diagonal and Full tensor methods have been developed and existed commercially. However, there are several advantages and disadvantages associated with each upscaling algorithm.

The simple upscaling method is the sampling. It is basically sample the permeability at the center of the grid block. It is simple but is inaccurate in preserving the heterogeneity of the reservoir. [Ref. 7, 9]

The analytical methods such as Arithmetic, Geometric, Harmonic and Power averages, have been regarded as the fast and simple intuitively methods for upscaling. Some of these methods, i.e. harmonic, power and geometric methods would be disadvantageous with null values, as these zeros would create an undefined heterogeneity of the reservoir. Thus, limited range for validity is as a result. In additional to these limitations, for determining the effective permeability, these methods can only solve the simple 1D or 2D reservoir model. This is not the case in the real life. It requires more complex calculations than that, which is the three-dimensional approach. Furthermore, it suffers from some limitations in applicability. [Ref. 4, 5, 7, 8, 9]

Directional averages, i.e. Arithmetic-Harmonic and Harmonic – Arithmetic methods, have been developed in order to simplify the determination of effective properties in 3-dimensional model. The computation cost is low. However, these directional methods

would still not represent the effective permeability. The harmonic - arithmetic average is a finer lower bound to the effective permeability than the harmonic method. On the other hand, the arithmetic - harmonic method is the finer upper bound to the effective permeability than the arithmetic method (refer to Cardwell & Parsons' bounds). Furthermore, null value will still be the problem in these methods. [Ref. 7, 8, 9]

In additional to this, renormalisation method has been implemented and used for many reservoir studies. They regard this method as the fast way of estimating effective properties by carrying out successive upscaling to obtain properties at the required scale. It is more accurate than averaging methods in cases. It is also good for taking the large problems and breaking it down into a hierarchy of manageable problems as it is proven successfully in theoretical physics areas. However, this upscaling method is only a local upscaling procedure. It is poor for highly anisotropic media and probably unreliable due to unrealistic boundary condition effects. [Ref. 2, 3, 4, 7, 9, 10]

Numerical methods, i.e. Diagonal and full tensor methods are also available based on the Darcy's Law and the mass conservation on each volume represented by a coarse grid block. By applying the relevant boundary conditions for the calculations, the directional effective permeability, i.e. x, y and z directions, can be determined. Null values can also be delimited by using these methods. Diagonal tensor can only determine the x-x, y-y and z-z directions of effective permeability. The effective permeabilities on the principle directions, i.e. x-y, x-z, y-x, y-z, z-x, and z-y, have been neglected. These effective permeabilities on the principal directions can be determined by using the Full Tensor. However, these principal direction effective permeabilities will be neglected by the reservoir simulators, as there is no available simulator to handle these principal direction permeabilities. Also, as these numerical methods were based on applying the relevant boundary conditions, can these boundary conditions approximate the true reservoir conditions? [Ref. 1, 4, 6, 7]

Overly, the main limitation of upscaling is that does not usually give indication on the validation of assumption made. There is limited attempt in analyzing the upscaling process, as there is no good theory exists to state whether the upscaled values are good or bad approximation. Only validation in the fundamental of inequality of the effective equivalent permeability has been published in several papers.

Wiener's bound states that the effective permeability is lied between Harmonic mean and Arithmetic mean. Several authors, such as Wiener, Cardwell & Parsons, Matheron and other authors have demonstrated this bound theory. [Ref. 7, 9]

Haskin & Shtrikman bounds is determined by using the method of self - consistent media and calculated on the based of the model of the medium built of composite sphere. The maximum permeability is obtained by assuming that the spheres are the low permeability and the shells are the high permeability, on the contrary, the inverse situation will be for the lower bound of the permeability determination. This result is found to be similar to Wiener bounds. [Ref. 9]

Cardwell & Parsons bounds are used an electric analogy. The arithmetic mean of the harmonic mean of the point permeability, calculated on each cell line parallel to the given direction, indicates the lower bound of the effective permeability. On the other hand, the upper bound of the effective permeability is obtained from the harmonic mean of the arithmetic means of the point permeability calculated over each slice of a cell perpendicular to the given direction. [Ref. 7, 9]

How reliable are these bounds in the real field study of the reservoir?

For sure, in some situations, such as composite materials with the effective properties, which can be measured directly, the simple analytical upscaling method will be sufficient. The effective permeability may lie between the fundamental inequality of the effective permeability by using one of the "inequality" theories. However, we are not as fortunate in our business, since measurements can only practically be made on the cm scale in the laboratory and some reservoirs can only be represented with the heterogeneous models. Thus, the determination of effective properties is in practice a mathematical problem.

Objectives

The first stage objectives of the research are:

- Finding the effective homogeneous physical properties that yield the same flow response as the heterogeneous one (rock type, porosity and permeability) for each grid cell
- To focus on the good physical and practical understanding of particular process in questions and an appreciation of reservoir model sensitivities. Thus, optimal building of the reservoir simulation model can be built.

This program provides upscaling tools to easily coarsen very large reservoir models to sizes acceptable to commercial fluid reservoir simulator. Using IRAP RMS, these large models can be manipulated quite easily. However, the variety of algorithms for determining the upscaled grid and calculating the upscaled reservoir properties gives the user the flexibility to create models are upscaled optimally for the given situation.

Furthermore, through personal experiences dealing with geologists and engineers from several different companies, the understanding of upscaling method is very limited. Simple analytical methods (i.e. Harmonic method used for upscaling the permeability and arithmetic method for porosity) are normally used without knowing the availability of different algorithms and pros & cons of each individual algorithm. In this way, through the understanding of existing upscaling algorithms will lead to the development of the new algorithm which is efficient and better understood by our petroleum or oil & gas industries.

The work will focus in particular on modeling and upscaling gas injection processes. In the coarse of the research program, a new algorithm for upscaling of relative permeability and capillary pressure based on a fine grid compositional or black oil simulation

will be developed. The algorithm will be implemented in a - computer program, which will be tied to our in-house compositional simulator, black oil simulator MORE/Smedvig.

As several exiting upscaling algorithm based on the simulation grid, careful determination of gridding the simulation grid (i.e. coarse grid) is designed initially for the full field reservoir study. It is initially based on the single well models around the well. These single well models are used to understand a single well performance (i.e. history match of each individual well in the reasonable coverage reservoir area). Also, the uncertainties involved in the reservoir characterization in the geological way are investigated. By examining these single well models, similar characteristics of the geological model may be group into sector model. It is used to investigate further on the influence of reservoir characteristics of the particular field and studying the fluid movement of the particular reservoir units. This study is then carried out for a further building of the full field model. Each of these models is gridded and filled with petrophysical properties by using the appropriate upscaling algorithms. [Ref. 10]

The upscaling algorithm is based on mass conservation, i.e. the determination of the coarse scale relative permeabilities and capillary pressures that minimize the error in the mass (mole number) of each component in all grid blocks at the end of a coarse scale time step. The algorithm differs from other approaches in three main respects:

- Time steps may be different (longer) in the coarse scale simulation than in the fine scale simulation. This reflects the true situation, and tends to smooth out noise in the generated pseudo.
- The optimization is performed on the whole coarse scale model, i.e. in all grid blocks simultaneously and not on individual grid block walls.
- Compositional information is utilized. This opens for the possibility of simultaneously upscaling of phase behavior and relative permeability. This possibility has not yet been fully implemented in the code. The necessary additions may, however, easily be implemented.

The selection of the effective and efficient algorithms will be mainly based on the conservation of the reservoir heterogeneities (i.e. reducing the uncertainties of reservoir throughout the reservoir geological model & laboratory data) and also the capability of the upscaled parameter data used to match the history of the productions. Furthermore, the accuracy of such effective properties as applied to flow through porous media will be judged by how well the fluid-flow prediction made at the coarser (macro-scale) level mimic predictions made at the finer (micro-scale) level. Thus, the research will be based on the data analysis of the available data from the geologists (reservoir model with its petrophysical parameters), the rock laboratory data (PVT, capillary pressure and also the relative permeability curves) and also the study of the flow characteristic of the reservoir.

Results/Discussion

The reservoir model which is used throughout the research has the heterogeneous characteristics as indicated by the porosity and permeability 3D - parameters as shown in Figure 1 and 2 respectively. This geological model has 600,000 grid cells.

In order to build the geological reservoir model, the geological log data is usually used as the hard data. This can be shown in Figure 3 the comparison in scale between the log curve data and the blocked well in the geological size of the reservoir model. This is one of the upscaling stages in the reservoir characterization.

For any reservoir simulator, however, coarser grid is required, as mentioned previously.

Apart from the grid cell, data required for the simulation are: rock properties (permeability, porosity, relative permeability & capillary pressure), reservoir geometry (the grid size, thickness & well location), initial fluid distribution ((initial fluid saturation); fluid properties (PVT data) and well production data (production schedule & productivity index or skin factor).

The grid resolution sensitivities were initially studied before validating the upscaling algorithms. Three different models are used, they are:

- Model 1: 65*80*30 (160,000 cells)
- Model 2: 32*40*30 (38,000 cells)
- Model 3: 32*40*15 (19,000 cells)

Several scaling up algorithms were used in studying the fluid flow with the grid sensitivities in the coarser grid. For porosity, volumetric weighted arithmetic average was selected as preserving the pore volume was the main consideration. For the permeability, however, several algorithms such as Arithmetic-Harmonic average, Harmonic – Arithmetic average and diagonal tensor methods were selected and studied.

General comparison on the algorithms based on the permeability 3D parameters theoritically were found as follows:

Arithmetic – Harmonic & Harmonic – Arithmetic Averages

- It is directional dependent; however, they suffer due to null values of the fine parameter values.
- The effective permeability was found to be bounded between Arithmetic – Harmonic and Harmonic – Arithmetic averages.

Diagonal Tensor

- It represents the solution of flow equations and yields the diagonal tensor.
- Relevant boundary conditions are required to be applied with this method.

Results on the upscaled parameter values were shown in Figures 9 and 10 for the porosity and permeability in the x direction with diagonal tensor for Model 2, respectively.

In order to illustrate the sensitivities in the grid resolution, Streamlines Technology was used. This is also used for the validation of the upscaled parameters by comparing it with the fine simulation result. Various permeability upscaling methods were studied.

Data for testing the streamlines were using 5 OPEN well producers with the initial condition of 300 bar as the

reference pressure at 3000 m, with 80% net to gross.

Streamlines for fine geological model, Model 1, 2 and 3 simulations grids were shown in Figures 4, 5, 6 and 7 respectively. It was found that the fluid flow drainage patterns on the plane view for simulation models were similar to the fine resolution pattern. The drainage performances of each model were shown otherwise though. By coarsening it furthers in any directions, it reduced the drainage capabilities slightly for each well, as shown in Figure 8 for comparing Model 1 and 2 with the fine grid. This could be due to increasing the uncertainties both in the geological model and the However, in reducing further on the z direction, the result for Model 3 was found to be totally different from the other simulation model and the fine grid one.

Thus, fine grid can be reproduced on a coarser grid with the sensible upscaling. Simulation results confirm the predictions from the upscaled permeability. Hence, it is highly recommended to use the streamline technology as the tool for validation of simulation grid resolution sensitivities and should be studied initially in any individual field of studies.

From the streamline results, it can be concluded that Model 1 & 2 are acceptable in coarsening the fine geological grid. Model 3, however, is too coarse and does not show the preservation in the well performances. Thus, study of fluid flow for different upscaling algorithms for permeability and porosity will be mainly based on Model 2 due to proportionality of speed with respect to the number of grid cells.

As mentioned previously, volumetric weighted arithmetic average was used for scaling up the porosity parameter of the reservoir, while three (3) different algorithms (Arithmetic – Harmonic, Harmonic – Arithmetic and diagonal tensor methods) were used for scaling up the permeability parameter.

Conclusion & Recommendations

Streamlines technology has been expanding further in order to reduce the cost in time and concluded to be the fast validation of the grid sensitivities.

With any uniform flows, several algorithms in upscaling have been concluded to be the most effective and efficient methods to use. Volume weighted arithmetic average is concluded to be the good estimator for determining the effective porosity of the coarser grid. Arithmetic – Harmonic and Harmonic – Arithmetic algorithms are economical for determining the effective properties of the permeability. However, there is another algorithm, Diagonal Tensor which will give a better effective result on the upscaling of the permeability by considering the mass conservation and flow determination, but it is more expensive to use due to time and its speed.

The development of multi phase upscaling and study of fluid flow in details are highly recommended in reducing the uncertainties in upscaling algorithms, but it will be costly.

References:

1. Aasum, Y, Kasap, E and Kelkar, M. (1993) **SPE 25913 – Analytical Upscaling of Small – Scale Permeability Using a Full Tensor**, Society of Petroleum Engineer, Denver, pp. 679 –92.

2. Begg, Kay, A., Gustason, ER and Angert, P.F. (1993) **Characterization of a Complex Fluvial – Deltaic Reservoir for Simulation**, The 4th Annual Archie Conference "Characterizing and Managing the Dynamic Reservoir – A multi disciplinary approach", Texas, pp. 143-8.

3. Christie, MA, Mansfield, M, King, PR, Barker, J.W. (1995) **SPE 29127 – A Renormalisation Based Upscaling Technique for WAG Floods in Heterogeneous Reservoirs**, Society of Petroleum Engineers, Texas, pp. 353-61.

4. Christie, MA (1996) **Upscaling for Reservoir Simulation**, Journal of Petroleum Technology, Nov edn, London, pp. 1004-1010.

5. Durlofsky, L.J., Behrens, R.A., Jones, R.C., and Bernath, A. (1995) **SPE 30709 – Scale up of Heterogeneous Three Dimensional Reservoir Descriptions**, Society of Petroleum Engineers, Texas, pp. 53-66.

6. Hove, K., Olsen, G., Nilsson, S. and Tonnesen, M. (1992) **SPE 24890 - From Stochastic Geological Description to Production Forecasting in Heterogeneous Layered Reservoirs**, Society of Petroleum Engineers, Texas, pp. 311-325.

7. **IRAP RMS User Manual** (1999), Smedvig Technologies, pp. 331-48.

8. Lemouzy, P.M., Romeu, R.K (1993) **SPE 26660 – A New Scaling-Up Method to Compute Relative Permeability and Capillary Pressure for Simulation of Heterogenous Reservoir**, Society of Petroleum Engineers, Texas, pp. 1-8.

9. Renard, Ph & De Marsily, G., (1997) **Calculating equivalent permeability: a review,** Advanced in Water Resources, vol. 20, No. 5-6, pp. 253-278.

10. Tang, Z., Gaquerel, G. and Gawith, DE (1993) **Integrating Geoscience and Engineering for Improved Field Management and Appraisal**, The 4th Annual Archie Conference "Characterizing and Managing the Dynamic Reservoir – A multi disciplinary approach", Texas pp. 29 - 41.

11. Tchelep, H.A., Durlofsky, L.J., Chen, W.H. Bernath, A., and Chien, M.C.H. (1997) **SPE 38886 – Practice Use of Scale Up and Parallel Reservoir Simulation Technologies in field Studies**, Society of Petroleum Engineers, Texas, pp. 1-15.

APPENDICIES

APPENDIX I: Petrophysical Properties of Fine Geological Grid

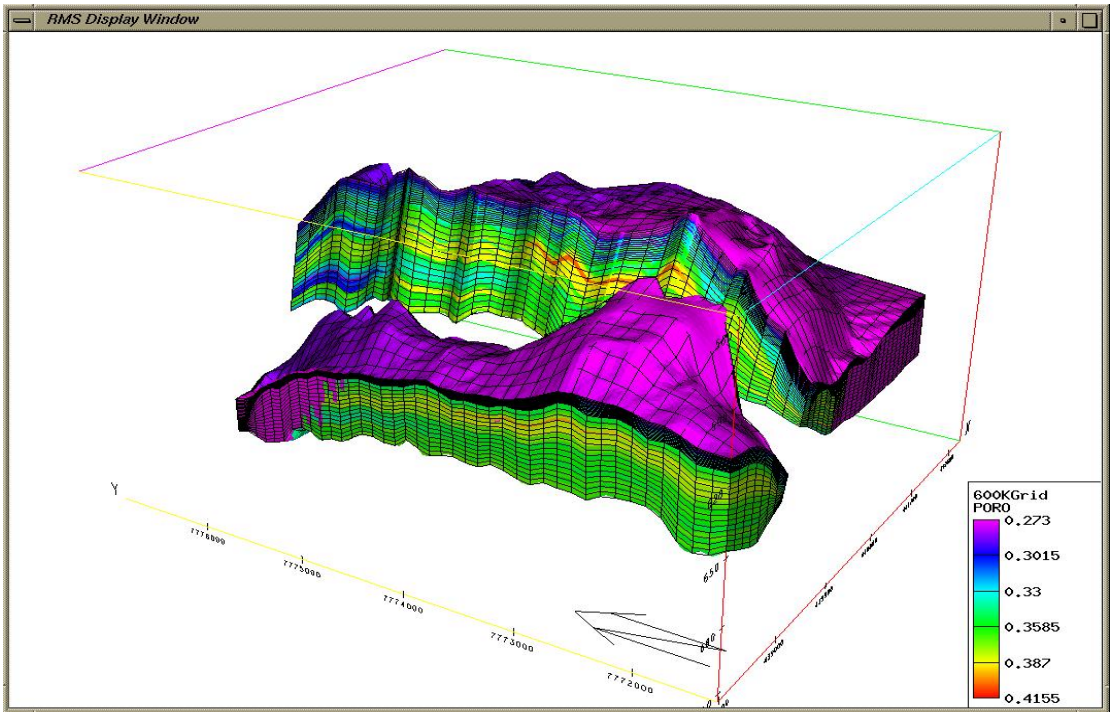

Figure 1. Porosity of the Fine Geological Grid with 600,000 grid cells

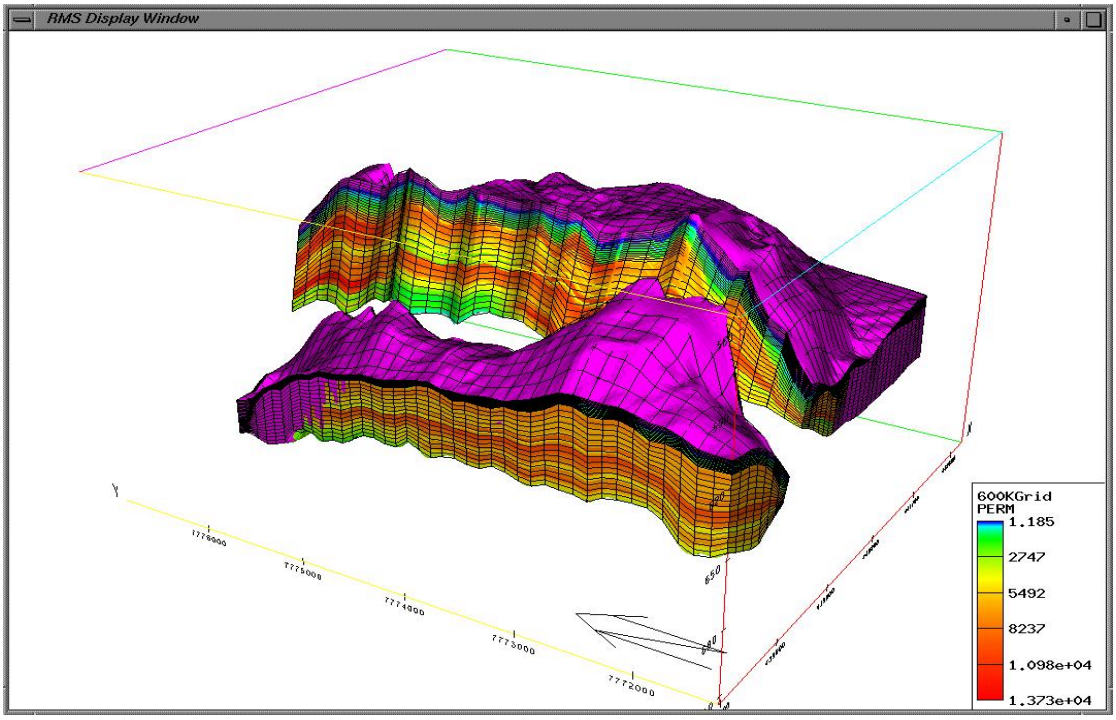

Figure 2. Permeability of the Fine Geological Grid with 600,000 grid cells

APPENDIX II: Changing Scales between Log and Geological Model Scales

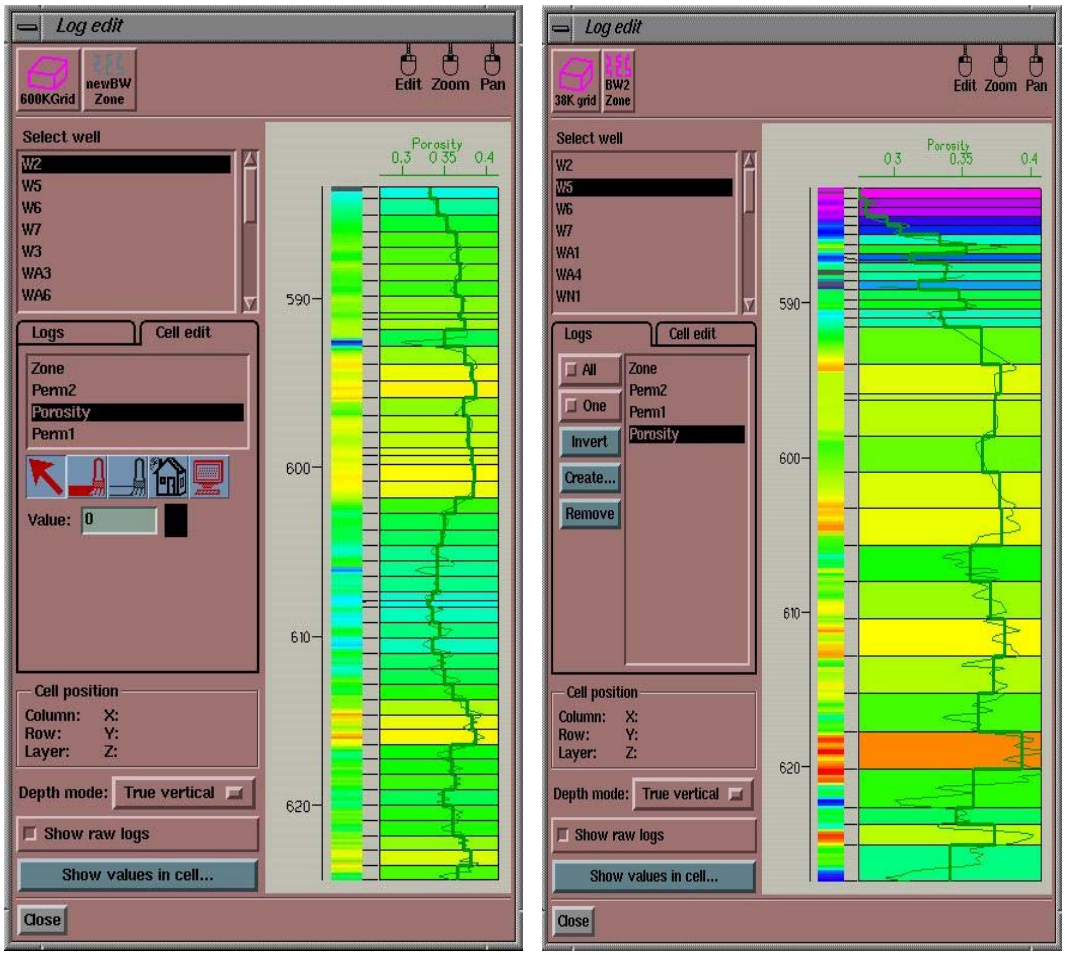

Figure 3. Comparison on Well-Blocking between Geological Grid and Simulation Grid II.

APPENDIX III: Streamlines for Model 1, 2 & 3 and fine geological grid model

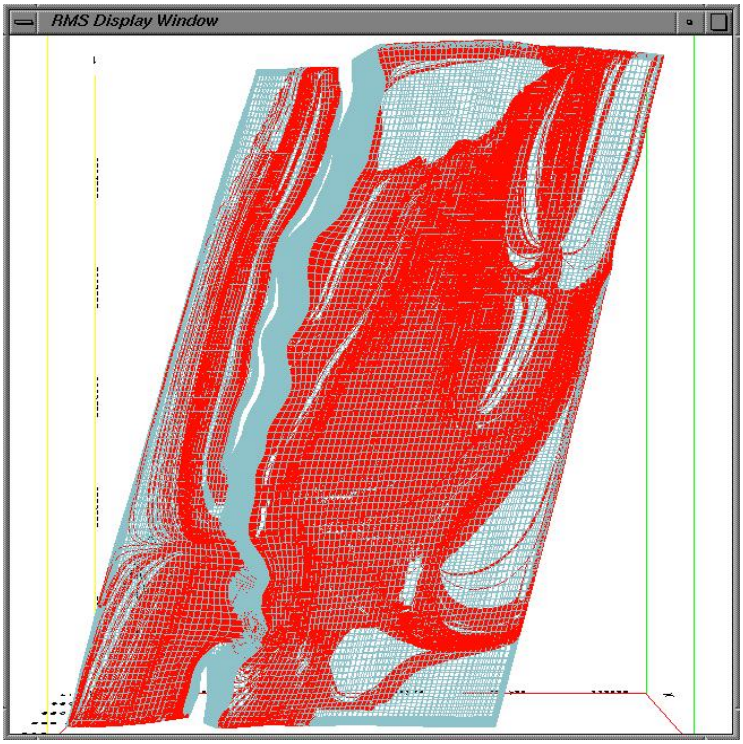

Figure 4. The streamlines of Fine Geological Grid with 600,000 grid cells

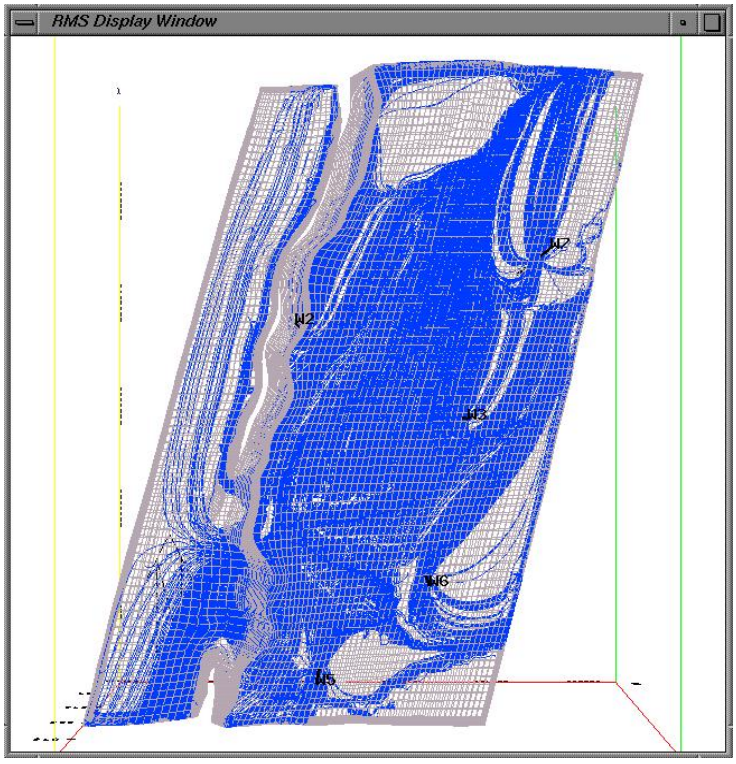

Figure 5. The streamlines of Simulation Grid I with 160,000 grid cell

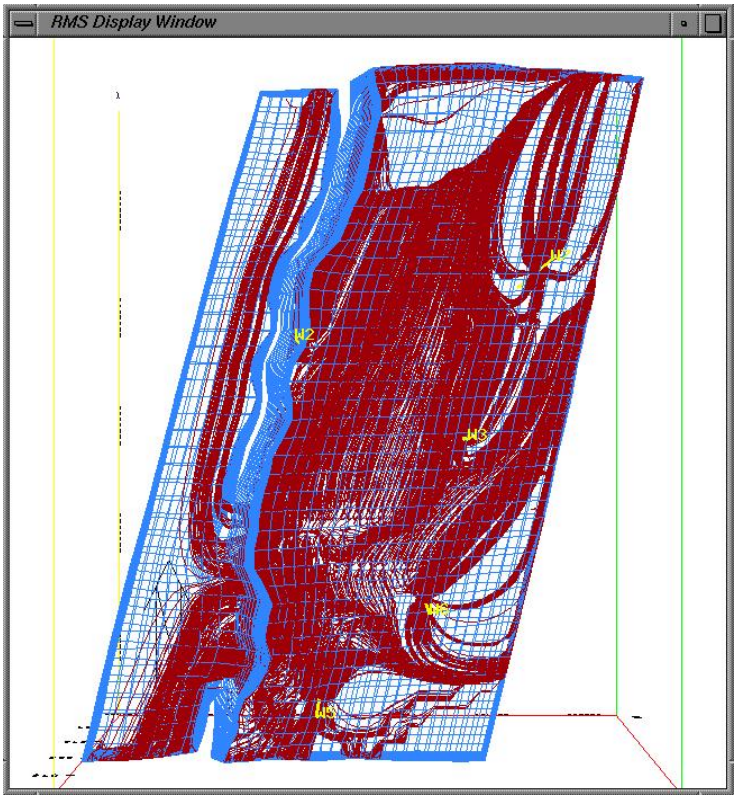

Figure 6. The streamlines of Simulation Grid II with 38,000 grid cells

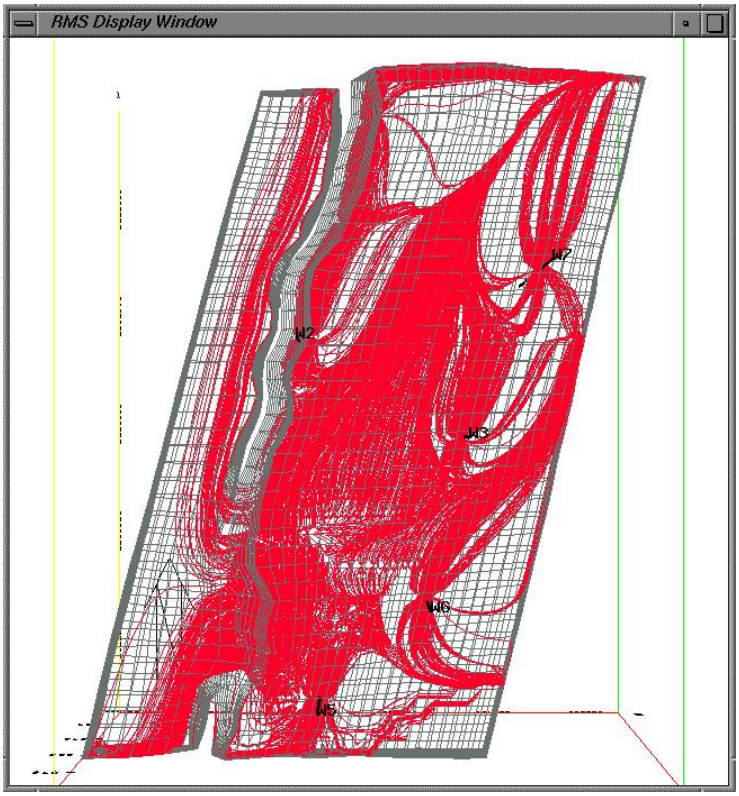

Figure 7. The streamlines of Simulation Grid III with 19,000 grid cells

APPENDIX IV: Drainage Profiles for Models 1, 2, 3 and Geological Grid

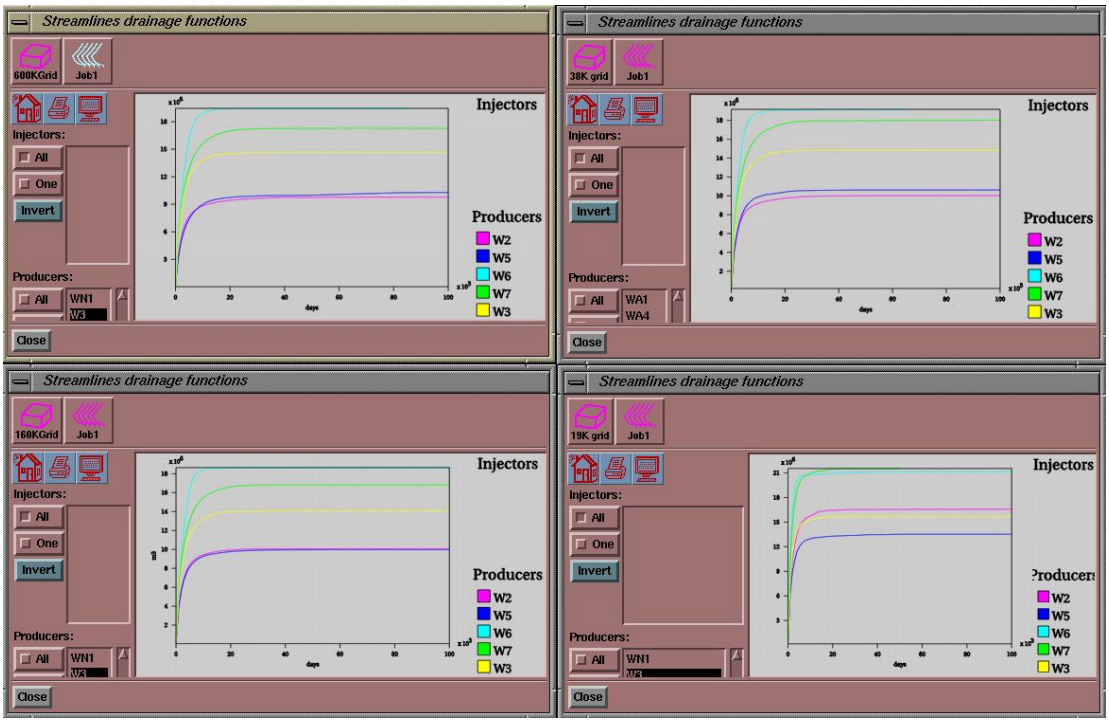

Figure 8. Drainage Profile of Different Simulation Grids

APPENDIX V: Simulation Results on Upscaled Porosity and Permeability for Model 2

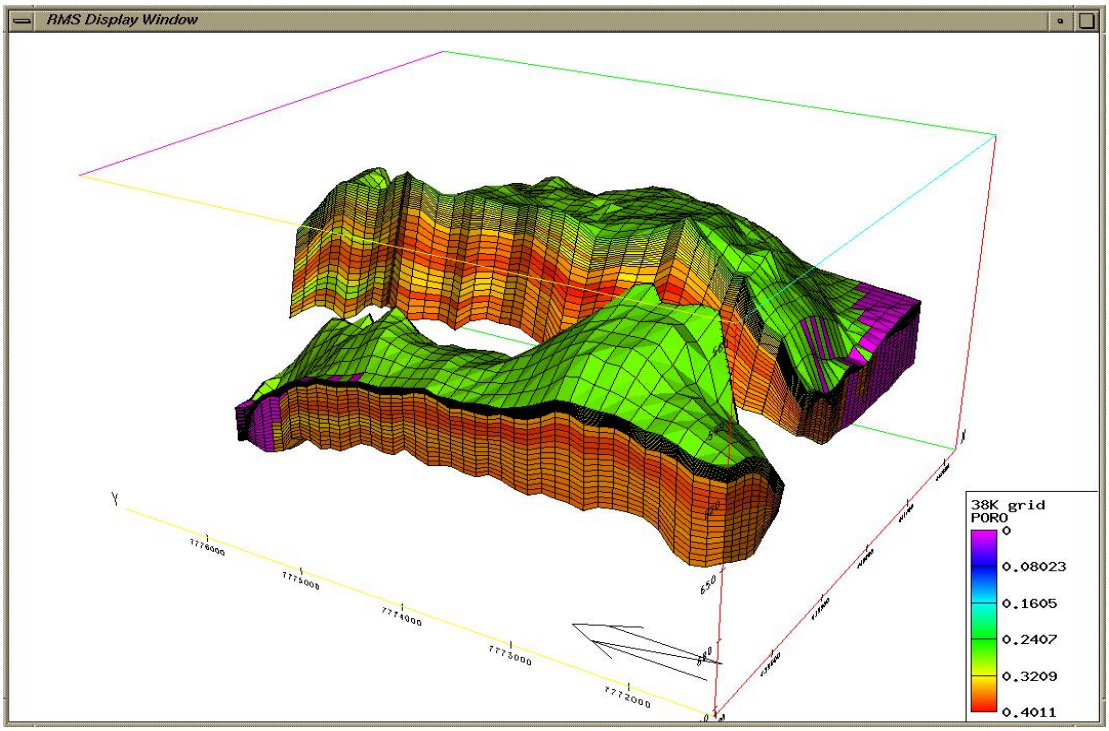

Figure 9. Scaled up Porosity Parameter for Simulation Grid II (38,000 grid cells)

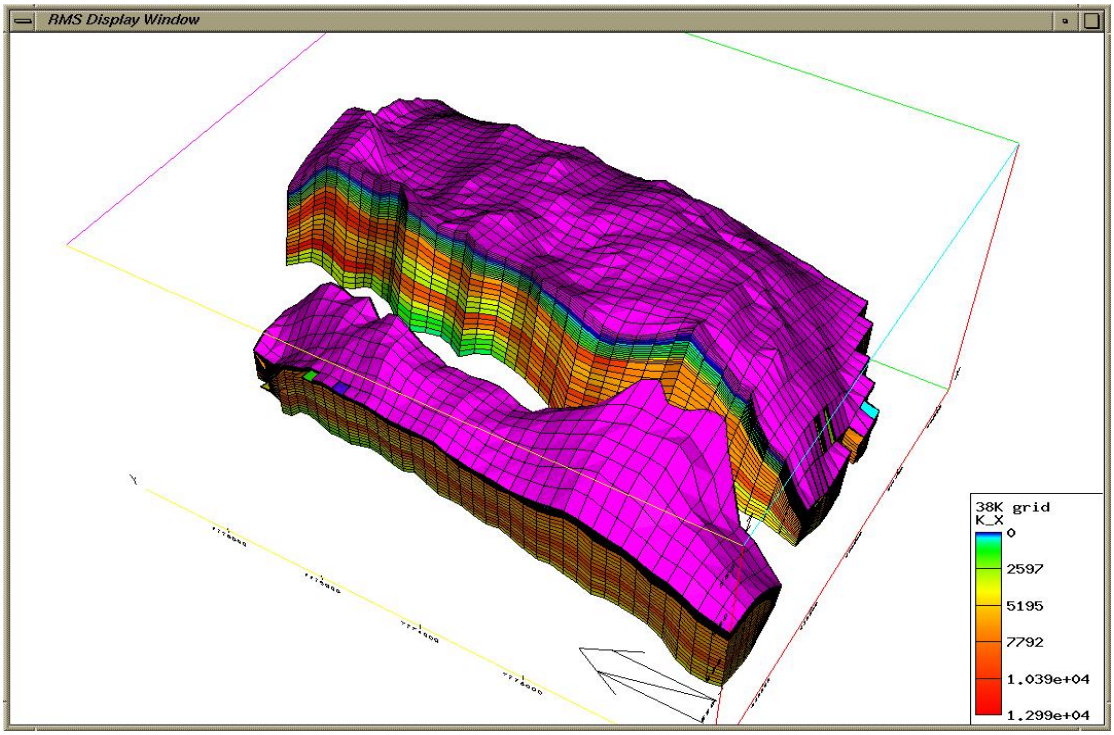

Figure 10. Scaled up Permeability (x direction) Parameter for Simulation Grid II (38,000 grid cells)

APPENDIX VI: Production Profiles for Comparing Different Upscaling Algorithms with Simulation Model 2

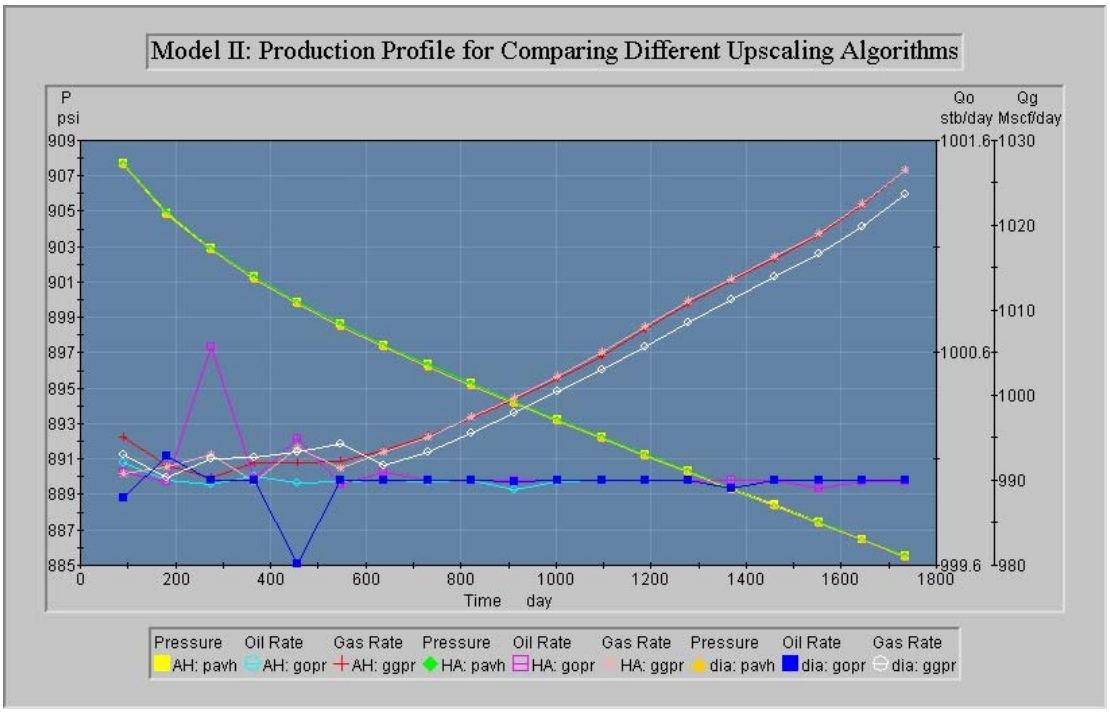

Figure 11. Comparison on Different Upscaling Methods on the Production Performances of Simulation Grid II.

APPENDIX VII: Statistical Comparison for Several Upscaling Algorithms for Model 2.

Core data:
- Porosity: range 0.271 – 0.433 Average: 0.355
- Permeability: range: 0.177 – 16390.8 Average: 5282.7

Fine Grid:
- Porosity: range 0.272 – 0.420 Average: 0.349
- Permeability: range: 0.185 – 13727.9 Average: 4826.04
- Volumetric: Gas: 21.35 x 10^6 m3 Oil: 137.2 x 10^6 m3

Model 2:
- Porosity: range 0.273 – 0.400 Average: 0.345
- Volumetric: Gas: 21.12 x 10^6 m3 Oil: 136.5 x 10^6 m3
- Arithmetic – Harmonic
  - Permeability: range: 1.706 – 12710.8 Average: 4335.6
- Harmonic – Arithmetic
  - Permeability: range: 1.706 – 12699.9 Average: 4293.9
- Diagonal Tensor:
  - Permeability: range: 1.712 – 12727.3 Average: 4312.6

Presentation on "Different Scales & Integrated of Data in Reservoir Simulation" held at AAPG Conference in Bali – Indonesia on 18th October 2000.

Different Scales & Integration of Data in Reservoir Simulation

AAPG,

18 October 2000

Bali - Indonesia

By: Lina Hartanto (Roxar/Curtin)
Prof. Robert Amin (Curtin)
Prof. Raj Rajeswaran (Curtin)

Presentation Outline

- Objectives
- Upscaling? Why?
- Grid Sensitivities
- Scaling Up Geological model with various algorithms
- Validation of Algorithms
- Results on Segmentation Simulations
- Summary & Conclusions

Objectives

- Find the effective homogeneous physical properties that yield same flow response as the heterogeneous one (rock type, porosity and permeability) for each grid cell

- to focus on particular process in questions & an appreciation of reservoir model sensitivities --> Optimal building of the reservoir simulation model

Upscaling? Why?

- General 3D geological models:
  - resolution of 50 x 50 x 1 m3 (or scale of available data: logs, cores, outcrops)
  - up to ~10 million blocks
- Available black oil simulator (unless parallel processing/simulator)
  - May only handle no more than 300,000 blocks (computational, computer memory & speed limitations)
- Each simulation grid block represents heterogeneous parts of the reservoir
- Fine scale heterogeneity affects displacement processes

Grid Comparisons

- Fine: 48*106*90 cells (460,000 grid cells)
- Simulation grid: (4 cases)
  - Model I: 48*106*45 cells (230,000 grid cells)
  - Model II: 24*53*90 cells (115,000 grid cells)
  - Model III: 24*53*45 cells (57,000 grid cells)
  - Model IV: 16*36*30 cells (17,000 grid cells)

Very Important: Simgrid design and orientation should be close as possible to the original geological fine grid.

Porosity (Fine Grid Model)

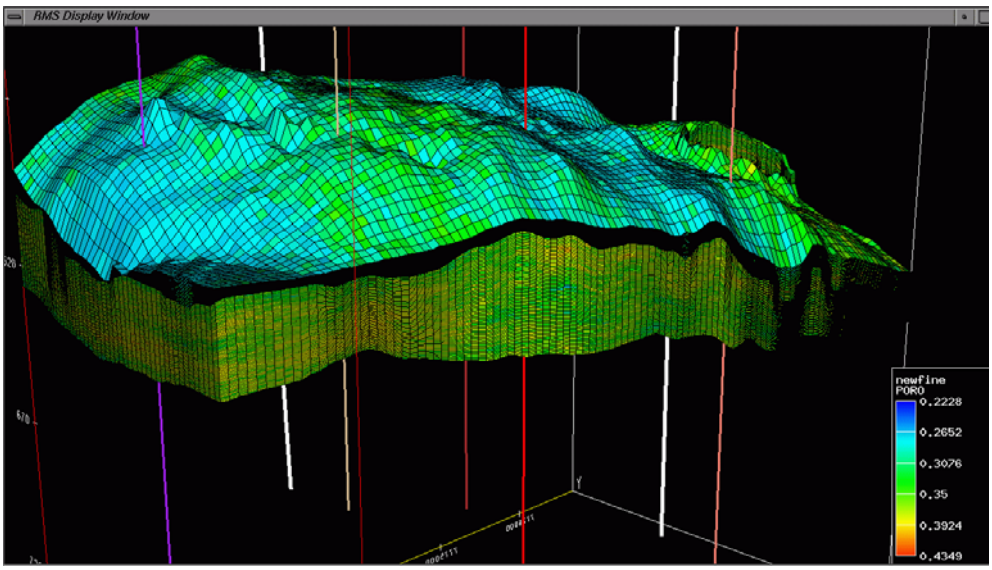

Permeability (Fine Grid Model)

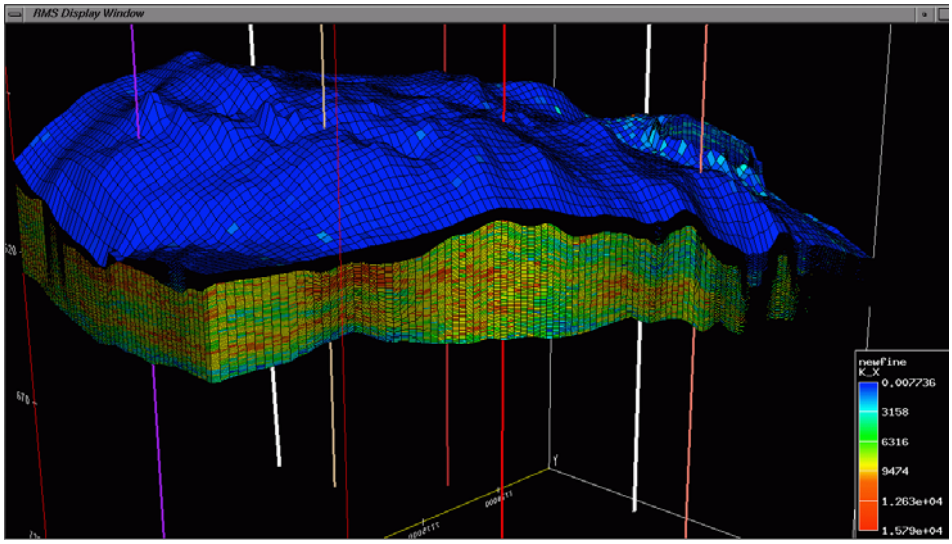

Various Available Upscaling Algorithms

Using RMSsimgrid from Roxar.

- Arithmetic
- Harmonic
- Geometric

} Simple Algorithms (1 direction)

- Arithmetic-Harmonic
- Harmonic - Arithmetic

} Mix Simple algorithms

- Diagonal Tensor
- Full Tensor

} Tensor algorithms

- Renormalisation

Scaling Up of Geological Model

- Porosity
  - Volumetric weighted arithmetic average
  - Preserving the pore volume locally and globally throughout reservoir
- Permeability - 4 algorithms
  - Arithmetic - Harmonic Average
  - Harmonic - Arithmetic Average
  - Diagonal tensor
  - Full Tensor

Algorithms comparison

- Arithmetic - Harmonic & Harmonic - Arithmetic Average
  - direction dependent
  - suffer null value
  - A(H(K)) < Keff < H(A(K))
- Diagonal tensor
  - represent the solution of flow equations
  - yield diagonal tensor
  - apply relevant boundary conditions

Validation of Algorithms

- Use streamlines:
  - Validate upscaled parameters by comparison with fine simulation result
  - Compare the results for various permeability upscaling methods ==> comparing tracer breakthrough
  - Illustrate sensitivity of grid resolution

Grid Sensitivities / Validation of Algorithms

- Streamline technology:
  - (In this study, it is using RMSstream from Roxar)
  - 7 wells: 4 OPEN well producers and 3 OPEN well injectors
  - Initial condition: reference pressure 900 psi at 600 m
  - Studied the dynamic response(s) from the geological reservoir model rapidly. ==> comparing tracer breakthrough
  - Calculating transmissibility when underlying transport properties (K, NTG) have a strong dependence on orientation not just on positions
  - Should be studied initially in any individual field study.

Grid Sensitivities (cont.…)

- Preference: flow direction within reservoir in simulation
  - representation of permeability as full tensor
  - should minimize the diagonal directions of permeability

Graph 1. Model III Breakthrough Time - Various Algorithms

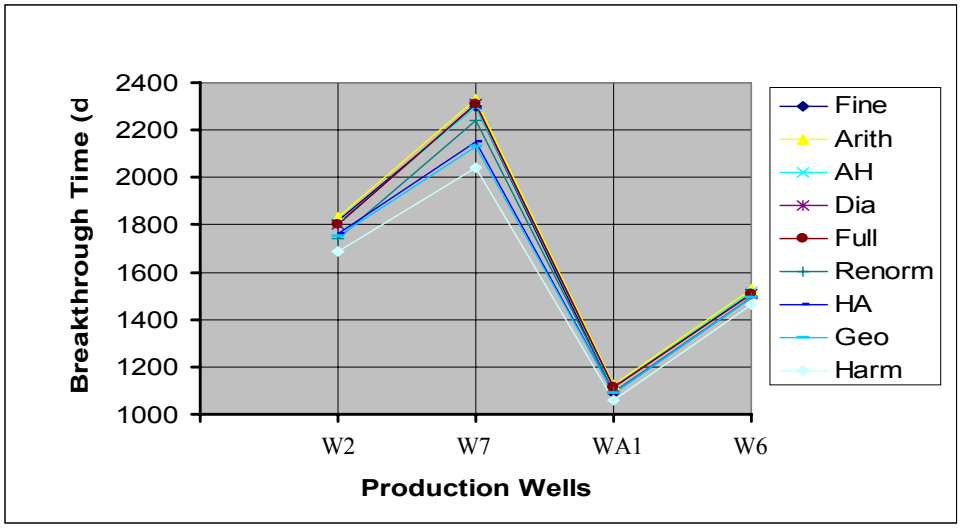

Graph 2. Model III - Difference in Breakthrough Time Various Algorithms

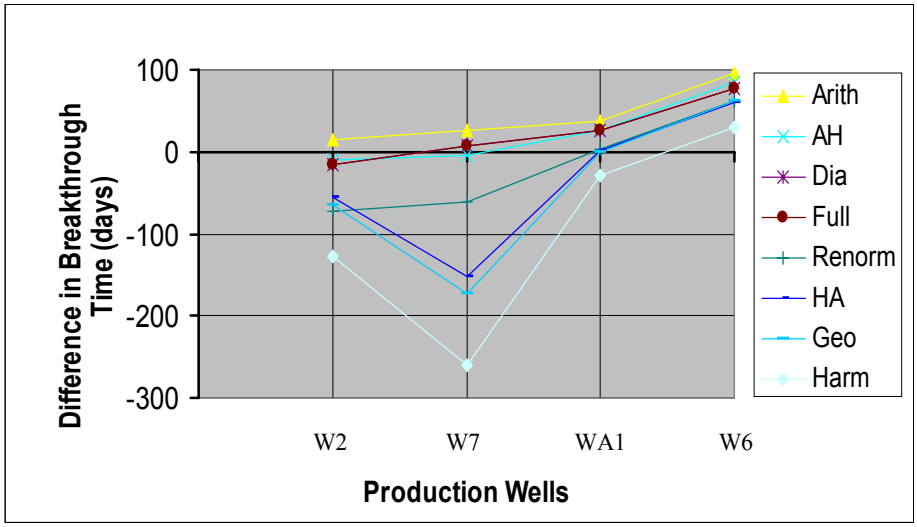

Graph 3. Model III - Difference in Breakthrough Time (AH & Diagonal Tensor)

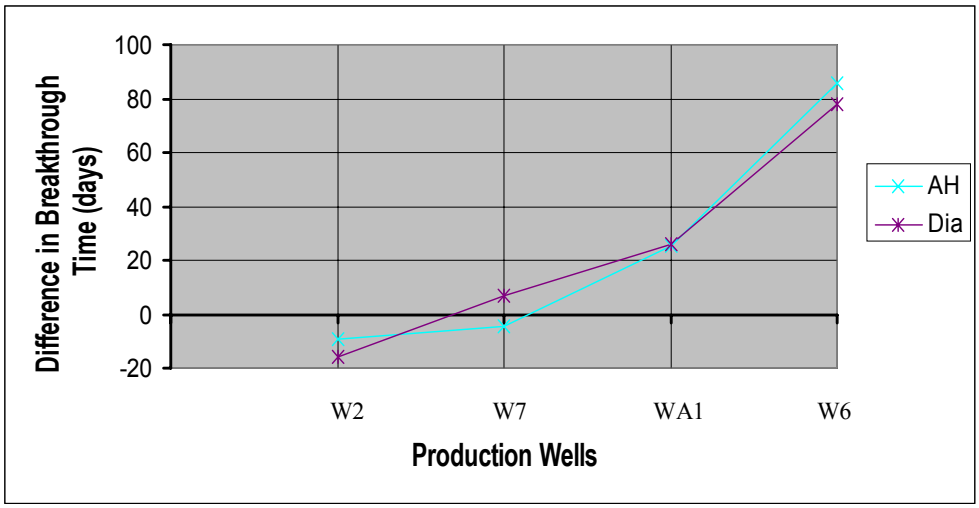

Validation on Various Upscaling Algorithms

- Upscaling algorithm for Permeability:

DIAGONAL TENSOR ALGORITHM

Model Selection

- Effective Permeability: Diagonal Tensor
- Single Well Simulation
  - Simulated grid segment: around 1000 m radius from Well W2.
  - Capillary Pressure, PVT analysis & Relative Permeability are the same for both Fine & Coarse Grids.

Graph 4. Various Models Breakthrough Time (Diagonal tensor)

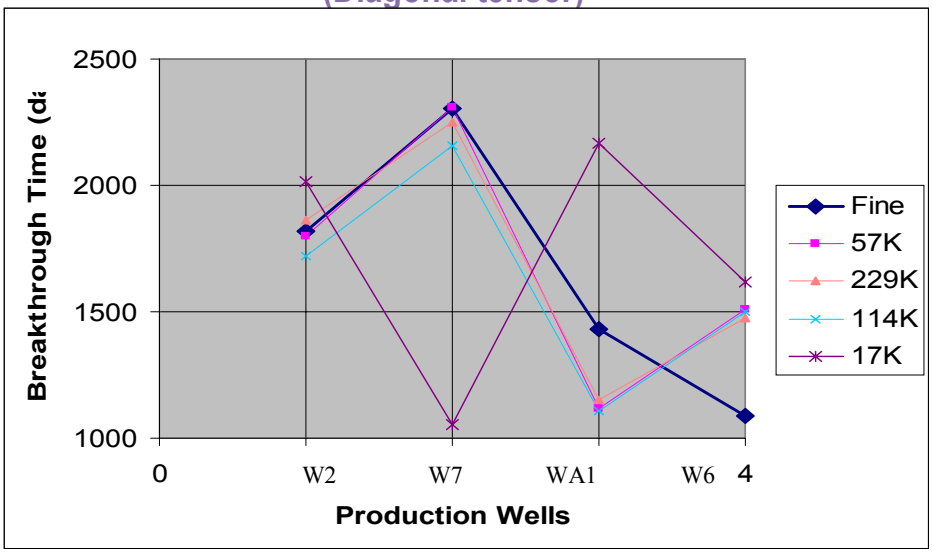

Simulated Fine Permeability Parameter

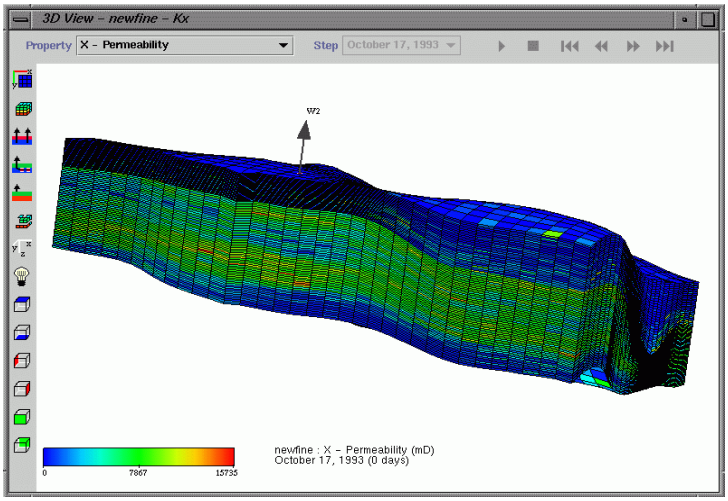

Graph 5. Oil Production Rate for Various Models (Diagonal Tensor)

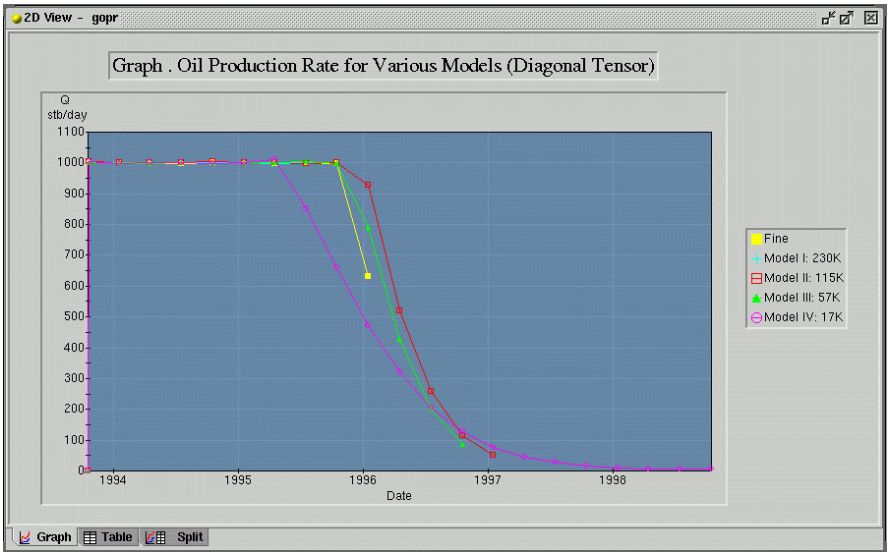

Graph 6. Gas Production Rate for Various Models (Diagonal Tensor)

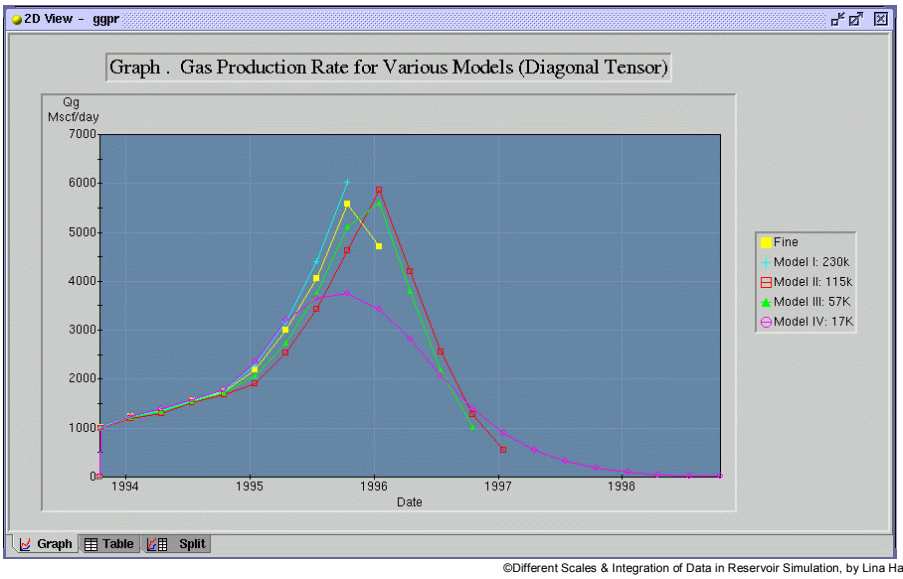

Graph 7. Cumulative Oil Production for Various Model (Diagonal Tensor)

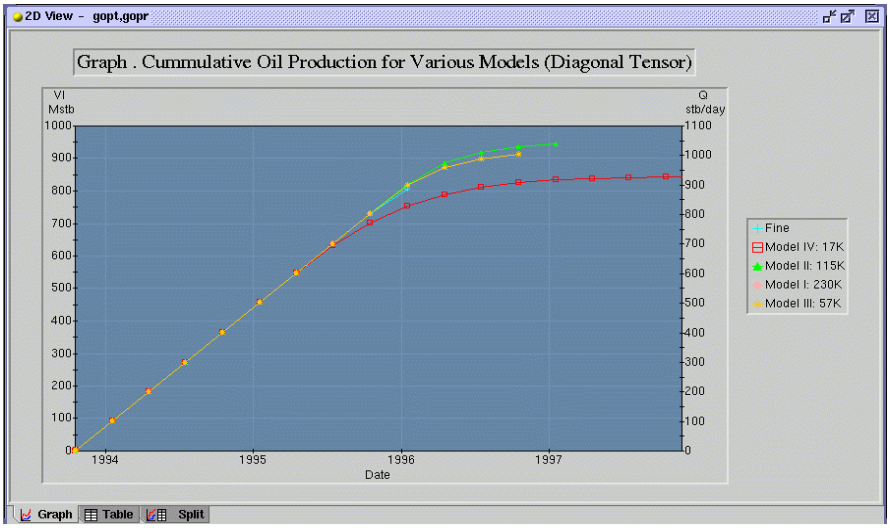

Graph 8. Cumulative Gas Production for Various Model (Diagonal Tensor)

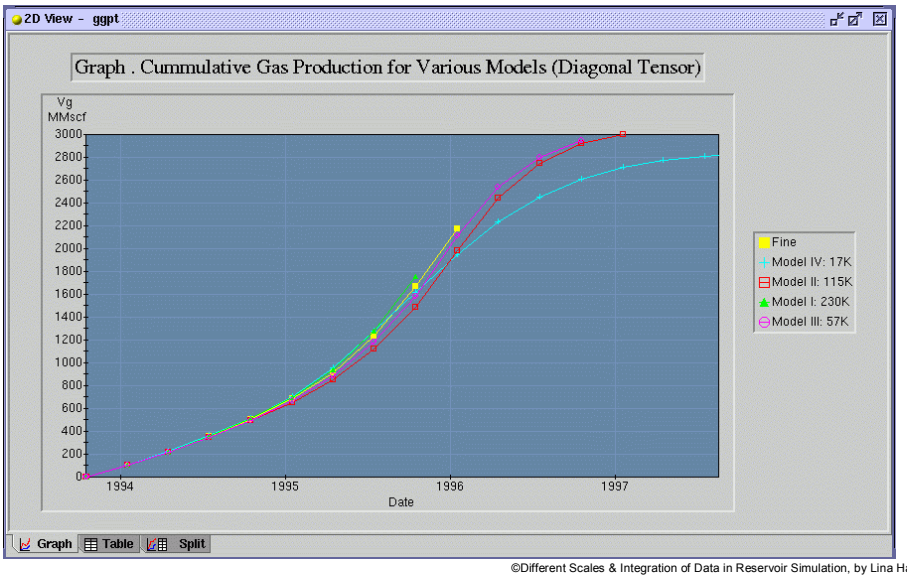

Summary/Conclusions

- Heterogeneous properties can be reproduced on a coarse grid with sensible upscaling procedures.
- Grid sensitivities & flow directions need to be studied FIRST
  - Via Streamlines
  - Increase model turnaround time
  - fast dynamic validation of grid resolution sensitivities
- Final Selection based on results:
  - Effective Porosity: Volume weighted arithmetic average
  - Effective Permeability: Diagonal Tensor (viscous effect of fluid flow)
  - Grid sensitivity limitation: Model III the best to proceed further for history matching, case study, well planning, etc.
- Future study should include the use of MULTIPHASE upscaling to validate models. (MAY BE!)

Acknowledgement

Special thanks to:

roxar

Curtin UNIVERSITY OF TECHNOLOGY

ExxonMobil

Paper on "New Upscaling Technique by Integration of Data in Reservoir Simulation" submitted for the Journal of Petroleum Science and Engineering in Perth - Australia on 7th February 2004.

NEW UPSCALING TECHNIQUE BY INTEGRATION OF DATA IN RESERVOIR SIMULATION

Lina Hartanto*, Prof. Robert Amin
Department of Petroleum Engineering, Curtin University of Technology
Dumas Road, Bentley WA 6012, Australia

Abstract

Upscaling and determination of effective parameters on a coarse scale simulation grid have remained related to complex and extensive problems associated with the reservoir studies. The primary strategy is mainly focused on the good physical and practical understanding of the particular processes in question, and an appreciation of reservoir model sensitivities. Thus, the building of the reservoir models can be optimally determined.

In this paper, by concentrating on modeling and upscaling gas injection of the Enhanced Oil Recovery (EOR) process, a new effective upscaling algorithm is derived and investigated for upscaling some required petrophysical parameters. The sensitivities of these determined coarse scale parameters, i.e. porosity, absolute and relative permeabilities would be studied through history matching by comparing on how well the reservoir performance at the coarse scale to its performance at the fine scale.

Keywords: Upscaling, Effective Parameters, Effective Permeability, Enhanced Oil Recovery, Upscaling Algorithm

1 Introduction

A numerical reservoir simulation is often used for the prediction of reservoir performance. It is based on solving the fluid flow of equations in the reservoir by partitioning the reservoir into a set of numerical grid blocks. Each grid block is assumed to be a homogeneous block in which its physical properties are represented by a single value. The solution for fluid flow equations in each block is then solved by implicit and iterative approaches for fine difference element within the fluid flow equations. This will require sufficient computational memory/power, which is highly dependent on the number of grid blocks used to solve. In full field reservoir studies, the grid blocks in the geological modelling are typically in the regions of 50-meter times 50-meter times 1-meter from the basis of scaling the available data such as logs, cores or outcrops which may contain up to more than a million grid blocks. However, this large number of geological grid blocks is not possible to be carried out in the numerical dynamic reservoir simulation due to computer memory and speed limitations. Consequently, there is a need to "average" the laboratory data/geological data in such a way that the data can be handled efficiently in the reservoir simulation modelling. The properties that are typically upscaled are porosity, absolute & relative permeability and capillary pressures, which each simulation grid block should represent the heterogeneous parts of the reservoir.

In any reservoir predictions, in the reservoir simulation scales, a realistic description of the reservoir behaviour under any depletion scheme is probably the main important factor. Permeability, which describes the ability of the fluid to flow through the connectivity of the pores of the rock in the porous media, is the major parameter that affects the reservoir

* Corresponding author. Tel/fax: +61 8 9313 3703
Email-address: lhartanto@ozemail.com.au (L.Hartanto)

behaviours. In upscaling, permeability is really the complicated matter, since it is not an additive variable, i.e. the equivalent permeability in the reservoir scale is not possible to be calculated by the arithmetic mean. The expected permeability values have in general decreased and the permeability variance has also decreased in the reservoir simulation scales compared to its finer scales like geological or core scales. Therefore, reducing the number of cells in the scales results in reducing the accuracy of the parameter model and also smoothing the ability to describe the heterogeneity flow behaviour in the reservoir model. A balance is required between loss of accuracy due to the smoothing (averaging) process and the gain in the computer speed due to fewer number of grid cells.

Except in the case of truly homogeneous reservoirs, upscaling must always be carried out, although present day practice is not always recognized as such. For instance, plotting measured relative permeabilities as a function of normalized saturation, and choosing some average curve as representative, is a form of upscaling. Such a procedure does not take into account the spatial arrangement of the different rock types, and will therefore be unreliable. In media where the ratio between horizontal and vertical correlation lengths is large, for example, the proper upscaled relative permeabilities may be significantly different from their rock counterparts, even if all participating rock types have identical relative permeability curves.

In history matching reservoir performance, relative permeabilities are perhaps the first parameter to be adjusted to balance the loss of permeability descriptions within the reservoir model. Somewhat simplistically, this process should be interpreted as posteriors upscaling. The willingness to sacrifice relative permeabilities signals a perceived unreliability of the a priori upscaling originally carried out.

Upscaling is a broad term, also encompassing techniques to increase numerical accuracy at the passage of sharp saturation fronts. Our main interest is more specific: If heterogeneities are small relative to the distance between wells, one can define "effective" properties of the heterogeneous medium, i.e. effective absolute and relative permeabilities and capillary pressure. Effective properties are physical parameters valid on the larger scale, and capture the average effect of small-scale heterogeneity. Hence, coarsening the fine scale geological description by using the appropriate upscaling algorithm is important to maintain the integrity of the model for the fluid flow modelling purposes (i.e. maintain agreement in flow results between fine and coarse models).

In this paper, by concentrating on modeling and upscaling gas injection of the Enhanced Oil Recovery (EOR) process, a new effective upscaling algorithm is derived and investigated for upscaling some required petrophysical parameters. The sensitivities of these determined coarse scale parameters, i.e. porosity, absolute and relative permeabilities would be studied through history matching by comparing on how well the reservoir performance at the coarse scale to its performance at the fine scale. Furthermore, comparison with the existing upscaling algorithms will also be performed to validate the improvement by using the new upscaling algorithm.

2 Background information / Existing Upscaling Algorithms

Several algorithms are commercially available for upscaling by using either analytical or numerical approaches. From the simple methods such as arithmetic, geometric and harmonic averages to the complicated tensor methods, such as diagonal and full tensor methods have been developed and existed commercially. Even a more complex method, referred as the multiphase upscaling or pseudo method, is also existed, in which it involves generating the solution of the reservoir simulation's properties by either estimating the properties statically or running the full field reservoir simulation at its finer scale to provide the "average" properties dynamically. However, there are several advantages and disadvantages associated with each upscaling algorithm.

The simple upscaling method is the sampling. It is basically sampling the permeability at the centre of the grid block. It is simple but is inaccurate in preserving the heterogeneity of the reservoir. [10,13]

The analytical methods such as arithmetic, geometric, harmonic and power averages, have been regarded as the fast and simple intuitively methods for upscaling. Some of these methods, i.e. harmonic, power and geometric methods would be disadvantageous with null values, as these zeros would create an undefined heterogeneity of the reservoir. Thus, limited range for validity is as a result. In additional to these limitations, for determining the effective permeability, these methods can only solve the simple 1D or 2D reservoir model. This is not the case in the real life. It requires more complex calculations than that, which is the three-dimensional approach. Furthermore, it suffers from some limitations in applicability. [4, 7, 10, 11, 13]

Directional averages, i.e. Arithmetic-Harmonic and Harmonic – Arithmetic methods, have been developed in order to simplify the determination of effective properties in 3-dimensional model. The computation cost is low. However, these directional methods would still not represent the effective permeability. The harmonic arithmetic average is a finer lower bound to the effective permeability than the harmonic method. On the other hand, the arithmetic harmonic method is the finer upper bound to the effective permeability than the arithmetic method (refer to Cardwell & Parsons' bounds). Furthermore, null value will still be the problem in these methods. [10, 11, 13]

In addition to this, renormalization method has been implemented and used for many reservoir studies. They regard this method as the fast way of estimating effective properties by carrying out successive upscaling to obtain properties at the required scale. It is more accurate than averaging methods in cases. It is also good for taking the large problems and breaking it down into a hierarchy of manageable problems as it has been proven successfully in theoretical physics areas. However, this upscaling method is only a local upscaling procedure. It is poor for highly anisotropic media and probably unreliable due to unrealistic boundary condition effects. [2, 3, 4, 10, 13, 14]

Numerical methods, i.e. Diagonal and full tensor methods are also available based on the Darcy's Law and the mass conservation on each volume represented by a coarse grid block. By applying the relevant boundary conditions for the calculations, the directional effective permeability, i.e. x, y and z directions, can be determined. Null values can also be delimited by using these methods. Diagonal tensor can only determine the x-x, y-y and z-z directions of effective permeability. The effective permeabilities on the principle directions, i.e. x-y, x-z, y-x, y-z, z-x, and z-y, have been neglected. These effective permeabilities on the principal directions can be determined by using the Full Tensor. However, these principal direction effective permeabilities will be neglected by the reservoir simulators, as there is no available simulator to handle these principal direction permeabilities. Also, as these numerical methods were based on applying the relevant boundary conditions, can these boundary conditions approximate the true reservoir conditions? [1, 7, 10, 12, 13]

The most complex upscaling method is the multi-phase upscaling or also known as the Pseudo method. It is relatively complicated compared to the numerical or analytical single phase upscaling as it involves more complex solution for non-linear with coupling between rock properties and fluid flow effects. The pseudo properties are normally generated for inputs to the reservoir simulation either from the basis of static estimation of the properties or from the “average” dynamic properties derived based on the reservoir simulation results at the finer scales. The result at a coarse grid with the average properties should give comparable results to the fine grid simulation, since the inputs are based on the fine scale’s result. However, this multiphase upscaling can become very time consuming, as it requires the generation of the fine grid cell simulation prior to obtaining information required at the coarse scale. Due to its involvement with much finer scale and huge number of grid block cells; this will also require an extensive computer power to solve the simulation at the fine scale. Furthermore, the set of pseudo functions generated for the coarse scale is problem specific. Thus, for a new requirement of the coarse scale, the whole procedure is required to be repeated to obtain the necessary information. Also, this is not easy to generate for any other flow geometries. The widely used pseudo methods are Coats, Hearn, Stiles, Dykstra/Parson and Kyte/Berry methods.

Overly, the main limitation of upscaling is that it does not usually give indication on the validation of assumption made. There is limited attempt in analysing the upscaling process, as there is no logical theory existing to state whether the upscaled values are good or bad approximation. Only validation in the fundamental of inequality of the effective equivalent permeability has been published in several papers.

Wiener's bound states that the effective permeability is laid between Harmonic mean and Arithmetic mean. Several authors, such as Wiener, Cardwell & Parsons, Matheron and other authors have demonstrated this bound theory. [12, 13]

Haskin & Shtrikman bounds is determined by using the method of self - consistent media and calculated on the based of the model of the medium built of composite sphere. The maximum permeability is obtained by assuming that the spheres are the low permeability and the shells are the high permeability, on the contrary, the inverse situation will be for the lower bound of the permeability determination. This result is found to be similar to Wiener bounds. [13]

Cardwell & Parsons bounds used an electric analogy. The arithmetic mean of the harmonic mean of the point permeability, calculated on each cell line parallel to the given direction, indicates the lower bound of the effective permeability. On the other hand, the upper bound of the effective permeability is obtained from the harmonic mean of the arithmetic means of the point permeability calculated over each slice of a cell perpendicular to the given direction. [13, 14]

How reliable are these upscaling algorithms and upscaling bounds in the real field study of the reservoir? Comparison studies with various upscaling algorithms will be discussed further in detail in Results/Discussion section.

For sure, in some situations, such as composite materials with the effective properties, which can be measured directly, the simple analytical upscaling method will be sufficient. The effective permeability may lie between the fundamental inequalities of the effective permeability by using one of the "inequality" theories. However, we are not as fortunate in our business, since measurements can only practically be made on the cm scale in the laboratory and some reservoirs can only be represented with the heterogeneous models. Thus, the determination of effective properties is in the practice of a mathematical problem.

3 New Upscaling Methodology

In this new upscaling algorithm's development, the important concept in upscaling is finding the most representative of the effective grid cell values at larger reservoir simulation modelling scale such that the effective homogeneous grid cell produces the same fluid flow behaviour under the same boundary conditions of the heterogeneous cells at its finer scales. The effective properties of the permeability will be the main focus in this new upscaling algorithm with the additional enhancing treatments for supporting the accuracy of upscaling. The new estimation of the effective properties as applied to flow in the porous media will then be judged by how well the fluid flow predictions made at the coarser (macro scale) level mimic compared to the predictions made at the finer (micro scale) level.

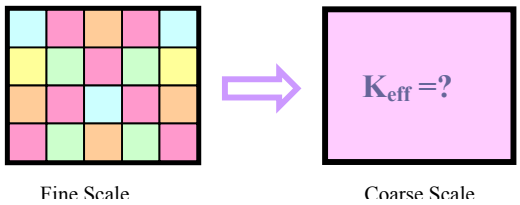

Figure 1 Problem Statement for the New Upscaling Algorithm

Several assumptions used prior to the upscaling development are summarized as follows:

- No direct application for solution at fine scale to estimate the flow behaviour at the coarser scale, as it is violating the main purpose of upscaling which is to avoid conducting such time-consuming flow simulation.
- No restriction on the number of grid blocks to be upscaled.
- Selection of flexible gridding algorithm to better represents variation in reservoir heterogeneity & treatment of permeability, as full tensor is among many methods

developed to reduce the inherent errors associated with approximation.

- Replacing original multiphase system with one in which averaged props at coarse grid is obtained by solving flow problem within coarse grid using local boundary conditions (sensitive to choice of boundary conditions & average flow simulation results.
- Replace multiphase system with a single phase, steady state flow field in which local boundary assumptions is applied to upscale absolute permeability or block interface transmissibility.

The following upscaling concept is proposed for the new algorithm. (Refer to Figure 3 for the process flow diagram). It is based on the combination principal theories of several existed algorithms, which are believed to be the most representation of the upscaling for permeability from its fine scale to its coarser scale. They are diagonal tensor, renormalization and arithmetic harmonic / harmonic arithmetic algorithms. Each process step for the proposed methodology will be discussed in detail.

1. Define the periodic boundary as Diagonal tensor/Full Tensor by assuming only fluid flow in the specific direction from one side to the other side, and no flow across to the other 2 directions.

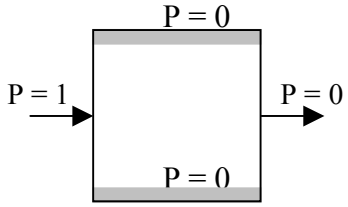

Figure 2 Pressure Boundary Conditions on New Upscaling Algorithm

2. Solve the pressure by using Random Walk/Relaxation method on network with the combination of the electrical network principal similar to the renormalization theory.
3. Identifying the preferential path of the fluid flow within the single coarse cell by identifying the larger pressure differences across the grid block and the preferential connection for this large pressure drop of a solved pressure solution.
4. Determine the single representation of the fluid flow across the coarse grid by using the average flow rate/flux on each cell across the specific direction and sum of flux for the flow across the other 2 directions. I.e. arithmetic harmonic mean for horizontal permeability and harmonic-arithmetic mean for the vertical permeability.

3.1 Periodic Boundary Conditions

The initial step of the upscaling concept is defining the pressure boundary for the area of interest. The pressure boundary is defined similar to Diagonal Tensor or Full tensor principal, by applying arbitrary pressure equal to 1 and 0 at the inlet and outlet respectively. From the law of nature, it indicates that any fluid flow or particle will move from high potential to the low potential. By defining the pressure boundary, the fluid flow can be forced to flow in a specific direction and can be expressed as shown in Figure 2.

3.2 Pressure Solution with Random Walk/Relaxation Method on Network

To be able to solve the fluid flow equation in the numerical performance, similar method like the renormalization method can possibly be used to solve by using the equivalent resistors of the electrical network. In this section, the similarity of the fluid flow equation and the electrical network solution will be discussed further. Pressure solution with the combination of the random walk and relaxation method on network will be described in detail.

Equivalent Expression of Darcy's law (Fluid Flow) with Ohm's law (Electrical Network)

The rate of the fluid flow in the porous media may be expressed with Darcy's Law and is defined as follows:

$$Q = -\frac{KA}{\mu}\frac{\Delta P}{\Delta X}$$

Equation 1 Darcy's Law of Fluid flow in porous media

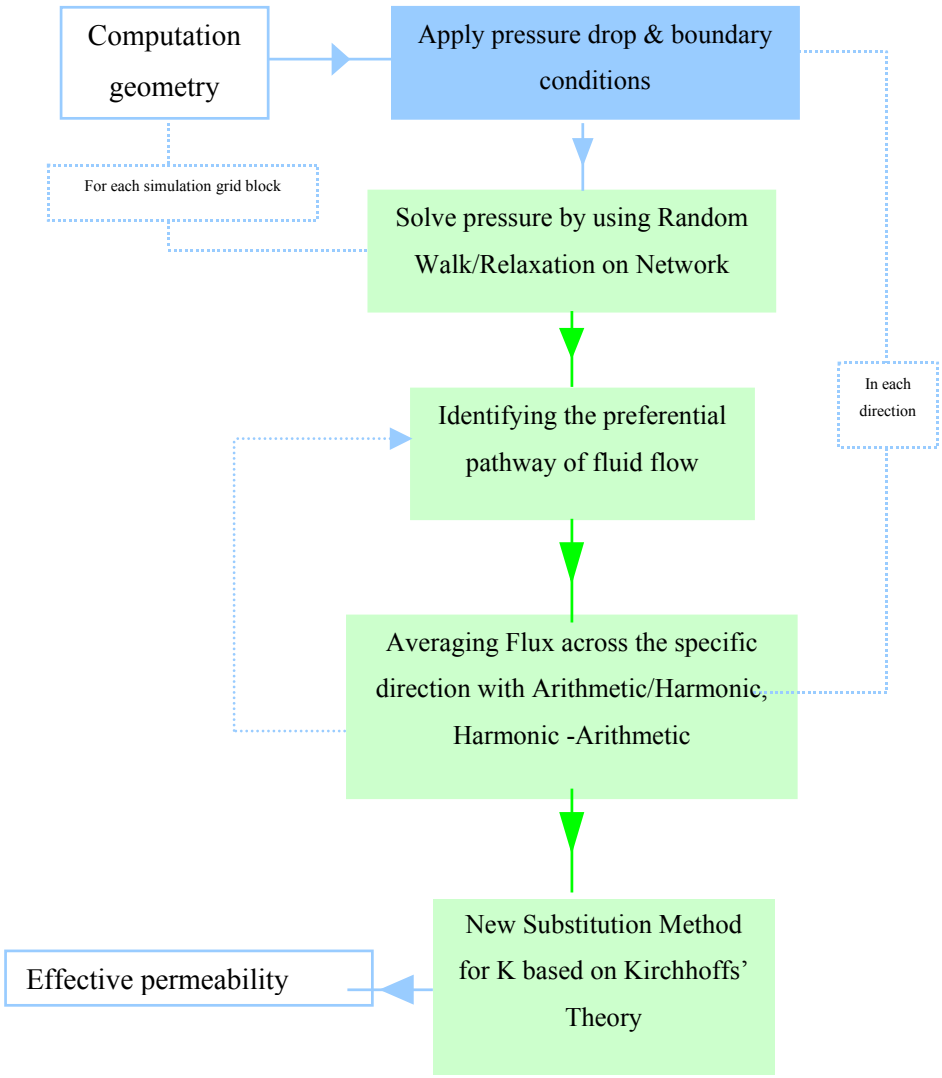

Figure 3 Process Flowcharts on New Upscaling Algorithm

By referring to the above equation and renormalization theory, the Darcy's equation may possibly be expressed similar to the simple Ohm's law for the electrical network principal.

Darcy's law $$Q = -\frac{KA}{\mu}\frac{\Delta P}{\Delta X}$$

Ohm's law $$V = IR$$

Equation 2 Comparison of Darcy's Law of Fluid flow in porous media and Ohm's law of Electrical Network

Both equations are using the law of nature theory in which the fluid or charge particle will move if there are any potential differences and will flow from high potential to its low potential. For this case, the Voltage (V) for the electrical theory expressed the potential difference for the electrical charge to move, while on the other hand, in the fluid flow, the pressure drop $\frac{\Delta P}{\Delta X}$ expression indicates the potential difference for the movement of fluid to flow in the porous media. The current (I) flow through the electrical network is equivalent to the amount of fluid flow through the media (Q). Also, the resistivity can be expressed for both electrical and porous media with the equivalent of electrical resistance (R)

and the inverse of permeability (1/K) respectively.

Therefore by rearranging both equations, it can be expressed as the following equivalent expression:

- Voltage [V] is equivalent to pressure drop $\frac{\Delta P}{\Delta X}$ or in mathematical expression $\left[V \propto \frac{\Delta P}{\Delta X}\right]$
- Current [I] is equivalent to fluid flow rate [Q] or in mathematical expression $[I \propto Q]$
- Resistance [R] is equivalent to its inversely proportional of permeability [K] or in mathematical expression $\left[R \propto \frac{1}{K}\right]$

Equivalent Resistor Network for Permeability Parameter Model

To be able to provide the pressure solution of the fluid flow in the numerical simulation, the equivalent resistor is required to be defined for the representation of permeability parameter in the numerical simulation model. The equivalent resistor of each fine cell is $\frac{1}{K}$. Thus, the representation of permeability at the centre of the fine cell is equivalent to two resistors in series, which is $\frac{1}{2K}$. In general, permeability is defined with the directional dependent in x, y and z directions. Therefore, each block can be replaced with a cross of resistors as shown in Figure 4 for two-dimensional illustration. For isotropic media, the resistors will be the same in either direction as the permeability in x and y directions are the same.

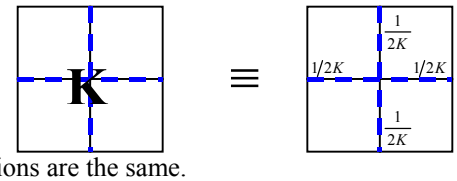

Figure 4 Equivalent Resistor for Permeability Parameter in 2-dimensional model

The equivalent resistors of permeability parameter at each coarse grid cell can then be illustrated with the following diagram.

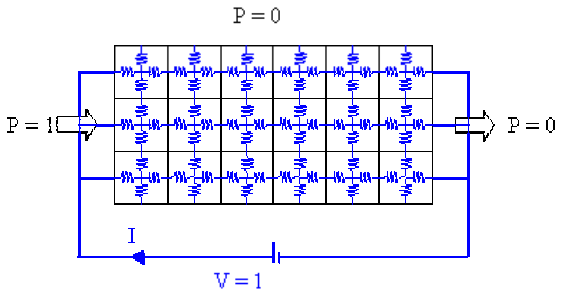

Figure 5 Equivalent Resistor for Permeability Parameter at each coarse cell in 2-dimensional model

As mentioned above, for determining the effective permeability at one direction, the pressure boundaries are set such that the fluid will flow to a specific direction with the inlet and outlet uniform pressures of 1 and 0 respectively and no flow across to the other sides of the coarse grid block (P=0). Here, we are only considering the fluid flow in one direction. By referring to Figure 5, we have several dead end edges at the other directions in which the fluid will never be flown to these end edges. Therefore, for the better representation of calculating the effective permeability, these dead-end branches are eliminated and simplified as the following equivalent resistor network.

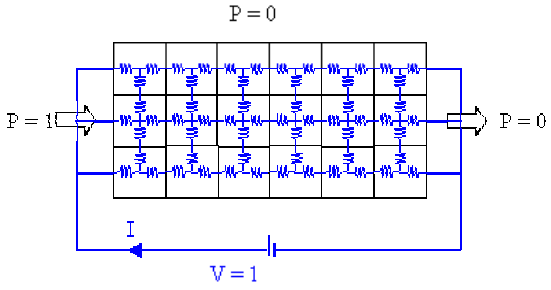

Figure 6 Simplified Equivalent Resistor for Permeability Parameter at each coarse cell in 2-dimensional model

This network is then used to provide the pressure solution within the coarse grid cell.

Pressure Solution with Random Walk and Method of Relaxation

To be able to solve the pressure solution in fluid flow or the equivalent current solution in the electrical network as illustrated in Figure 6, the random walk and method of relaxation are used with the combination of Kirchhoff's theories.

Random Walk and Method of Relaxation

The method of relaxation was introduced for providing the approximate solutions to the discrete Dirichlet problem. The method is using the function that has the specific boundary values, for which the value at the interior points is the average of the values of its neighbours. This is similar to the problem that is required to be solved as there are the boundary conditions and each cross flow/resistor is dependent on the values of its neighbours. [6, 8]

The way the method of relaxation works is that initially, all the interior points are set to be 0 and the boundary points are fixed with the constant values of 1 and 0. It begins with an interior point, which the value is then adjusted with the average of values at its neighbours. Random walk to the next interior point is then approximated with the similar averaging method of the neighbours' values. This process is then repeated for the rest of the interior points. [6, 8]

After adjusting all the interior points, the results will not be harmonic anymore as most of the time we are adjusting the value at a point to be the average value of its neighbours and also adjusting those neighbours' values in the next process. In other word, readjusting those neighbours' values has destroyed the harmony in this specific problem boundary. However, the values are more nearly harmony, if not harmony, than the initial function we started with. Thus, by repeating the above procedure, a better approximation more closely to the solution can be obtained. [6, 8]

So, how can the method of relaxation be related to our problem?

Kirchhoff's Theories and Method of Relaxation

As stated above, the Darcy's law of equation, which governs the fluid flow equation, can be expressed with the equivalent equation as Ohm's law equation for the electrical network. The voltage [V] in the electrical network is equivalent to the pressure drop $\frac{\Delta P}{\Delta X}$ and the flowing current [I] is equivalent to the fluid flow rate [Q]. The permeability, which is the property of fluid flow in porous media, can be expressed with the equivalent terms of inverse value of resistance [R].

In the electrical network's principal, the current and voltage at any nodes can be solved by using the Kirchhoff's laws. They are :

- Kirchhoff's current law
- Kirchhoff's voltage law

Kirchhoff's current law states that the sum of the currents entering or leaving a junction point at any instant is equal to zero. [Ref. 5]

$$\sum_{j=1}^{k} I_j = 0$$

Equation 3 Kirchhoff's Current Law, where k denotes the number of circuit elements connected to the node in question.

The Kirchhoff's current law holds the principle of conservation of charge. The number of electrons passing per second must be the same for all point in the circuit. Thus, this principle of conservation of charge is also equivalent to the conservation of mass within the porous media, as the fluid flow rate at any time into the reservoir should be equal to the fluid flow out from it. The illustration of the Kirchhoff's current law is as shown in Figure 7.

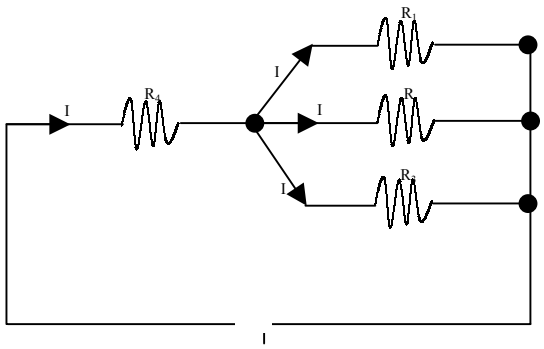

Figure 7 Illustrating Diagram of Kirchhoff's current law

By referring to Figure 7, the Kirchhoff's current law can be expressed as:

$$I_4 = I_1 + I_2 + I_3$$
$$I_4 - I_1 - I_2 - I_3 = 0$$

Kirchhoff's voltage law states that at any time instant the sum of voltages in a closed circuit is zero [Ref.5]. This voltage law holds the principle of conservation of energy, which is also required in the fluid flow description. The mathematical expression for illustrating this Kirchhoff's voltage law is:

$$E = V_1 + V_2 + ... + V_n$$

Equation 4 Kirchhoff's Voltage Law

The following diagram illustrates the above Kirchhoff's voltage law.

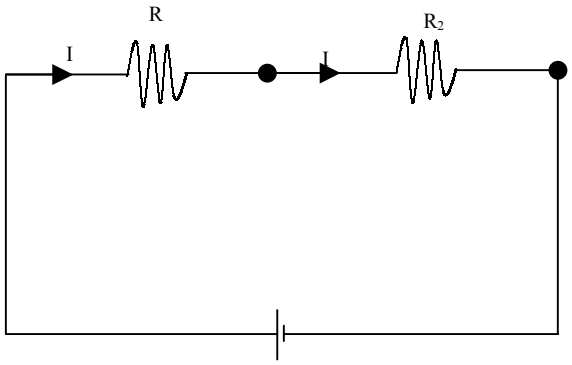

Figure 8 Illustrating Diagram of Kirchhoff's Voltage Law

Therefore, for the following network as illustrated in Figure 9, the above-mentioned Kirchhoff's Voltage and Current Laws can be recombined to obtain the voltage (V) at the centre of the nodes.

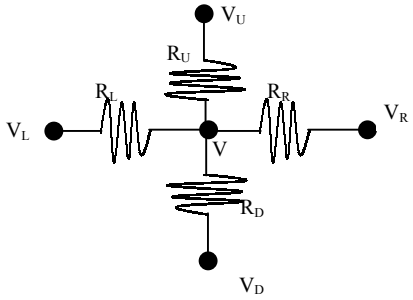

Figure 9 A Cell Network Diagram for Solving Permeability Fine Scale Network (Figure 4-6)

By using the Kirchhoff's current law, the network as illustrated in Figure 4-10 can then be solved as follows:

$$I_L = I_R + I_U + I_D$$

Substituting it with Ohm's law as V = IR, then:

$$\frac{V_L - V}{R_L} = \frac{V - V_R}{R_R} + \frac{V - V_U}{R_U} + \frac{V - V_D}{R_D}$$

Rearranging the above one, then:

$$\frac{V_L}{R_L} - \frac{V}{R_L} = \frac{V}{R_R} - \frac{V_R}{R_R} + \frac{V}{R_U} - \frac{V_u}{R_U} + \frac{V}{R_D} - \frac{V_D}{R_D}$$
$$\frac{V_L}{R_L} + \frac{V_R}{R_R} + \frac{V_u}{R_U} + \frac{V_D}{R_D} = V\left(\frac{1}{R_R} + \frac{1}{R_L} + \frac{1}{R_U} + \frac{1}{R_D}\right)$$
$$V = \frac{\frac{V_L}{R_L} + \frac{V_R}{R_R} + \frac{V_u}{R_U} + \frac{V_D}{R_D}}{\left(\frac{1}{R_R} + \frac{1}{R_L} + \frac{1}{R_U} + \frac{1}{R_D}\right)}$$

Equation 5 Solving Voltage (V) at the centre of the node as illustrated with Figure 4-11

From the simplified Equation 5, the voltage at any centre of the nodes can be solved by taking the inverse resistor (1/R) weighted average of the voltages in the neighbouring points. For the fluid flow in porous media, the pressure value (equivalent to voltage in electrical network) can then be approximated with the permeability weighted arithmetic average with the pressures at its surrounding cells. This averaging method is what the methods of relaxation used in the way of

approximating the value at the centre points with its neighbouring points.

By taking the methods of relaxation and simplified Equation 5, the bigger network with any unlimited number of cells as illustrated in Figure 4-6 can then be solved.

3.3 Averaging for New Effective Permeability

The next step post solving the pressure solution within the network is to identifying the preferential pathways and to provide the single cell value for representing the "average" value of the effective permeability at the coarse scale model.

With the law of nature, the particle will move from the greater to the lower potential. This is the same principal with fluid flow in the reservoir. The greater the pressure drop across the cell will have the greater tendency of the fluid to flow from one point to another one. Thus, once the pressure solution is obtained for the network as illustrated in Figure 4-6, the preferential path of fluid flow within the coarse grid system in the specific direction may be determined. These preferential paths will cause the differences in flow rates from one to another one within the coarse cell. Therefore, what should the representation of a single value for the effective permeability within this coarse cell be?

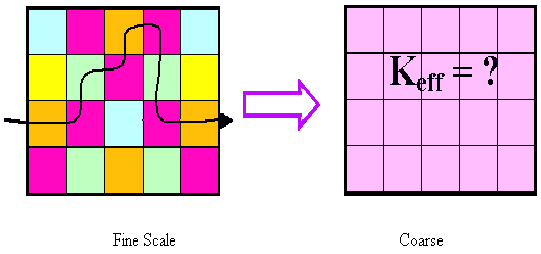

Figure 10 Illustrating Preferential Paths within a Coarse Grid Cell

Prior to averaging, the equivalent flow rate or current for the electrical term is required to be determined. By referring to Ohm's law equation (Equation 2), the potential difference (voltage or pressure drop) across one node to the neighbour nodes and the current (or fluid flow rate) may be determined by knowing the resistance (or permeability) between the two (2) nodes. For illustration, please refer to Figure 11.

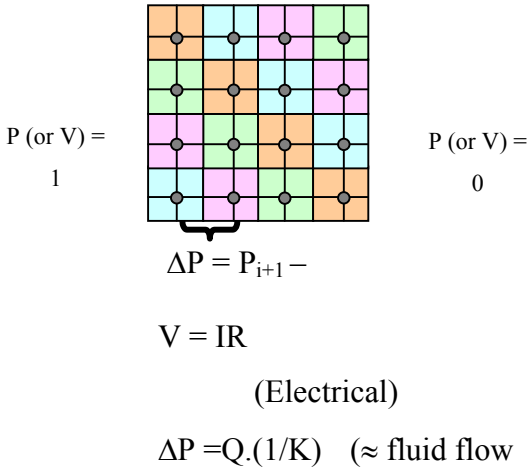

Figure 11 Illustrating Voltage (or Pressure Difference), Current (or Fluid Flow Rate) within a Coarse Grid Cell

In order to obtain the effective value of permeability for the coarse cell, the estimation of the overall resistance is required to be determined. Within the coarse grid cell in the specific direction, the pressure difference (or the electrical potential/voltage difference) is known to be equal to 1 due to our definition for pressure boundary. If the current flowing (or fluid flow rate) through this coarse cell is known, the resultant of equivalent resistance (or permeability) may be determined.

From the Kirchhoff's current law, it stated that the sum of current flowing into the network would be the same as the sum of current flowing out from the network. In this way, the current flowing through the coarse grid cell can be known. Thus, the effective permeability can be defined as follows:

$$V = IR$$
$$R = \frac{V}{I}$$
$$V = 1 \quad \text{and} \quad I = \sum I_{inlet} = \sum I_{outlet}$$
$$R = \frac{1}{\sum I_{inlet}} = \frac{1}{\sum I_{outlet}}$$
$$R = 1/K$$
$$K = \frac{1}{R} = \sum I_{inlet} = \sum I_{outlet}$$

Equation 6 Derivation for Effective Permeability

From determining the preferential paths of the fluid to flow within the coarse grid cell, it was found that some paths might be more preferable compared to the other one. In this upscaling method, variation of the fluid flow paths within the cell will be beneficial to be captured as in reality as these various paths will be representing the various breakthrough of fluid flows from one end to another end. Furthermore, permeability is an intensive property while the resistance is an extensive one. Thus, the changes of dimensions is required to be considered within the determination of the effective permeability. In order to capture the variability in fluid flow paths and the intensive properties of the permeability, modification on Equation 4-6 is required and similar averaging method to Arithmetic-Harmonic will be used.

Steps on the modification of the effective permeability determination are summarized below:

1. The current on each fine cellblock is calculated by taking product of the pressure difference with the permeability on that stream.
2. The sum of current on each row is then determined. For the electrical network, the total current flowing through each row will be the same between the inlet and outlet current. Thus, the effective permeability as an extensive property becomes the inverse of the total current as shown in Equation 4-6. However, the final modification on the effective permeability to become an intensive property is then required to be multiplied by the block dimension on that direction. For each row, the effective permeability is then determined as the following equation.

   For each row :

   $$K_{extensive} = \frac{1}{R} = I_{inlet} = I_{outlet}$$

   $$K_{eff} = K_{extensive} * (nx / nz) \approx \sum I_{each\_row}$$

   nx = no of cells in direction x within a coarse cell

   $nz = 1$ for each row

3. Similar to step 2, the final step is taking the average current of all rows within the coarse cell. For the electrical network, the total current will be the sum of current on each row. Thus, the effective permeability as an extensive property becomes the inverse of the total current as shown in Equation 4-6. Similar to step 2, dimensional changes are required to be incorporated for the intensive property such as permeability. Therefore, the final modification for the effective permeability as an intensive property is required to be divided by the total number of rows within the coarse cell. Thus, the effective permeability is then simply the average current of each row.

   For sum of rows :

   $$K_{extensive} = \frac{1}{R} = \sum I_{inlet} = \sum I_{outlet}$$

   $$K_{eff} = K_{extensive} * (nx / nz) \approx \frac{(\sum I_{each\_row})}{nz}$$

   $nx = 1$

   nz = no of cells perpendicular to direction x within a coarse cell

The summary of the steps in determining the effective permeability in direction X is shown in Figure 12.

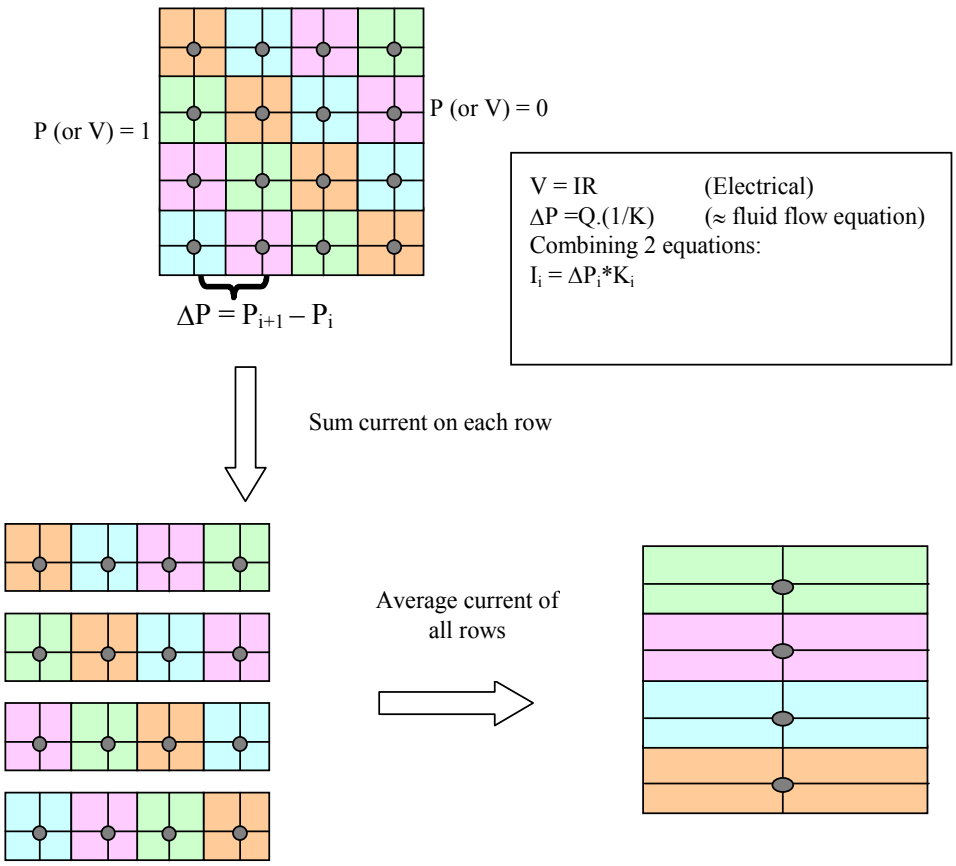

Figure 12 Modification for determining the Effective Permeability

Treatment for Incorporating Unswept Area by modifying Saturation

With any reservoir simulation studies, the relative permeability, which describes the fraction of permeability that is available for one fluid, in the presence of the other fluid flowing simultaneously through a porous media, is often defined by a single set of data at a constant porosity as Model B. This is not always true as the fluid behaviour of gas, oil and/or water is affected by the permeability, porosity and the initial water saturation. This can be seen clearly from the Timur's equation, which is often used to predict the relationship between porosity, permeability and the initial water saturation.

$$k = 0.136(\phi^{4.4} / S_{Wi}^{2})$$

Equation 7 Timur's equation

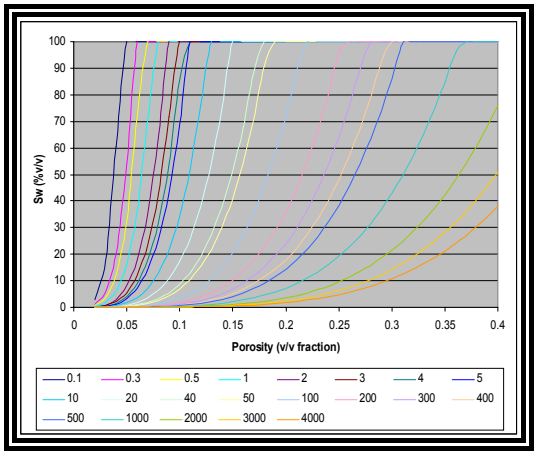

Figure 13 Variability of Permeability, Porosity and Water Saturation according to Timur's equation

Furthermore, fluid behaviour between two phases is often described with the Capillary number and Bond number. The bond number, which describes the fundamental behaviour of the system with the buoyancy forces, is fixed for a particular fluid pair. The magnitude of

the buoyant forces determines the maximum residual saturation and the threshold Capillary number for mobilization. The magnitude of the Capillary number, which is describing the capillarity of the fluid forces acting on the rock, then determines the corresponding residual saturation by determining the total force acting on residual. It is thus clear that the relationship between residual saturation and the capillary number derives from the geometry of the porous medium.

$$N_{Ca} = \frac{\mu_{Wetting} q_{Wetting}}{\sigma_{Wetting,nonWetting}}$$

Equation 8 Capillary Number (Catchpole and Fulford, 1966)

The Bond Number (N_{BO}) was used to quantify the contribution of buoyant forces, which arise from difference in density between the two fluids.

$$N_{BO} = \frac{(\rho_{Wetting} - \rho_{NonWetting}) g R^2}{\sigma_{Wetting,NonWetting}}$$

Equation 9 Bond Number

The "total effects" number (N_{Te}) is the total acting on residual.

$$N_{Te} = N_{Ca} + M.N_{BO}$$

Equation 10 "Total Effects" number

Due to this as described above, the modification in the relative permeability is required to co-operate the residual fluid remaining in the fine scale system. Permeability, which is the measure of the pore connectivity for the fluid flow in the porous media, is the most contributing factor in the remaining fluid saturation. The residual fluid remaining in the system will be mainly in the shale area where it is the least preferential fluid flow path in the system and the permeability & porosity are very low. Shale permeability is found in the range up to 0.5 mDarcy. Due to this, the following permeability cut-off is used for describing the unswept area where the major residual fluid is still remaining in the system and will not be drained by any depletion scenarios.

Initial Reservoir Fluid	Permeability Cut-off (mDarcy)
Oil Phase	0.100
Gas Phase	0.001

Table 1 Permeability cut-off for residual fluid remaining in the reservoir

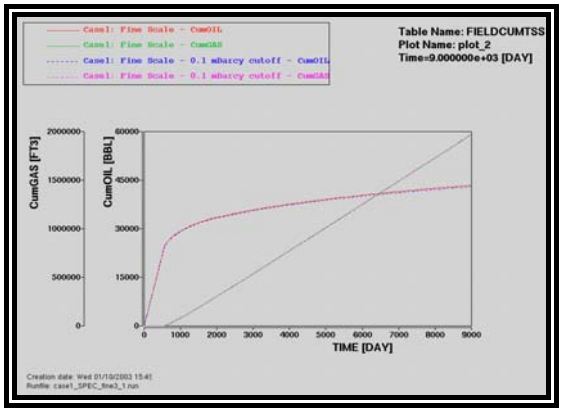

Figure 14 Comparison Plot of Gas & Oil Production Rate With and Without Saturation Modification

The relative permeability is normally described by the Corey's equation as the following equation.

$$K_{rw} = K^*_{rw}\left(\frac{S_w - S_{wc}}{1 - S_{wc} - S_{orw}}\right)^{Nw}$$

$$K_{row} = K^*_{row}\left(\frac{1 - S_w - S_{orw}}{1 - S_{wc} - S_{orw}}\right)^{Now}$$

Equation 11 Corey Equations for Oil-Water System

$$K_{rg} = K^*_{rg}\left(\frac{S_g - S_{gc}}{1 - S_{gc} - S_{org}}\right)^{Ng}$$

$$K_{rog} = K^*_{rog}\left(\frac{1 - S_g - S_{org}}{1 - S_{gc} - S_{org}}\right)^{Nog}$$

Equation 12 Corey Equations for Oil-Gas System

It is then altered for co-operating the modified residual fluid saturation for the coarse grid scale with the Corey equation as described above.

This is true for most of the cases. Under steady state for the immiscible flow, the displacement in the system will be closed to incompressible and will prevail in the reservoir condition with the reservoir pressure

at any point remaining constant. There must, of course, be a pressure differential between injection and production wells but the variation in the pressure dependent variables, viscosities and densities, resulting in this differential is ignored. In this displacement situation, the rate of the fluid being injected will result to be the same as the rate of fluid being produced.

4 Results/Discussion

Model description

The model used is the 2D reservoir model (i.e. vertical cross sectional flow model with 2000 cells (100x1x20 cells)) of an oil reservoir, which is taken from first case of the Tenth SPE Comparative Solution Project: A Comparison of Upscaling Techniques (SPE 72469). It is a heterogeneous reservoir, as shown in Figure 15. The permeability is correlated and distributed geostatistically over a small correlation length with the extensive size of shale strips acting as barrier in the model. The gas injection is used in this model for enhancing the ultimate recovery of the oil produced.

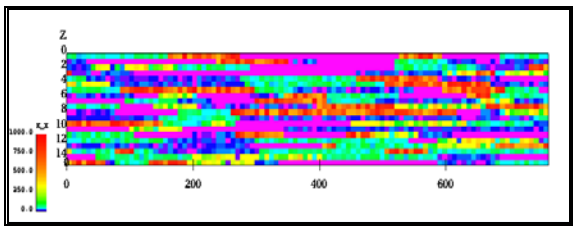

Figure 15 Permeability Model at a Fine Scale

For the comparison purposed, the above model will be coarsened from 100x1x20 cells (2000 cells) to 5x1x5 cells (25 cells). The reason being is that both lateral and vertical variability of the permeability are quite heterogeneous. In this experiment, finding the effective properties at any coarser scale will be required. Thus, testing the upscaling algorithm to represent 80 fine scale cells as a single coarse cell will use.

Result with Comparison to Various Upscaling Algorithms

The reservoir simulation results of using the new upscaling algorithms are summarised in this section. The comparison plots of the cumulative oil and gas production are shown in Figure 16 and Figure 17 respectively.

From the existed algorithms, the possible algorithms that can be used to represent the fine scale fluid flow behaviours are Arithmetic Harmonic and Diagonal Tensor. The upscaling with the Diagonal Tensor algorithm seems to better predict the gas breakthrough time of approximately 70 –80 days earlier than the fine scale's prediction, while the upscaling using the Arithmetic-Harmonic is better predicted the ultimate oil recovery at the end of the simulation. However, with the Arithmetic Harmonic, the predicted cumulative oil recovery has slightly different profile compared to the fine scale prediction. It predicted very closely prior to breakthrough, but the deviation is increased as it goes further from breakthrough point, which signifies slightly differences in the reservoir prediction.

Among those existed algorithms, Harmonic-Arithmetic seems to be the worst algorithm to represent the fluid flow behaviour at the coarser scales. It predicted later breakthrough and hence delayed the ultimate recovery time for the reservoir prediction, which can become quite significant in terms of reservoir management point of view.

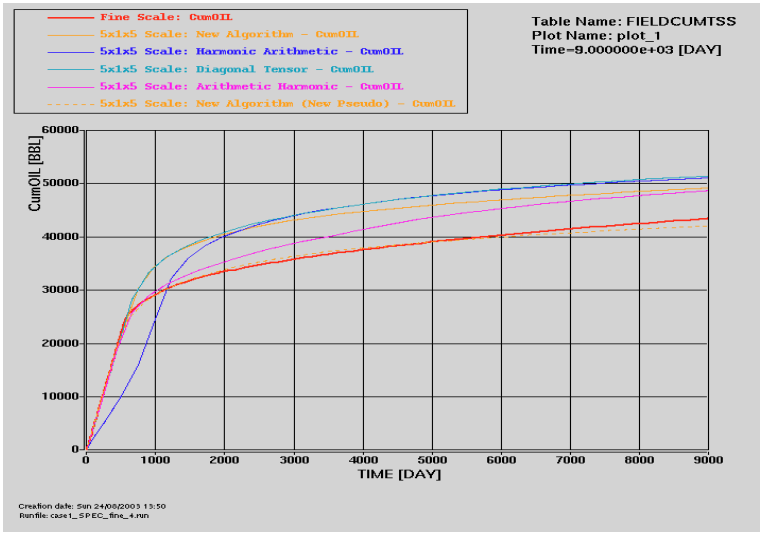

Figure 16 Comparison Plot of Cumulative Oil Production

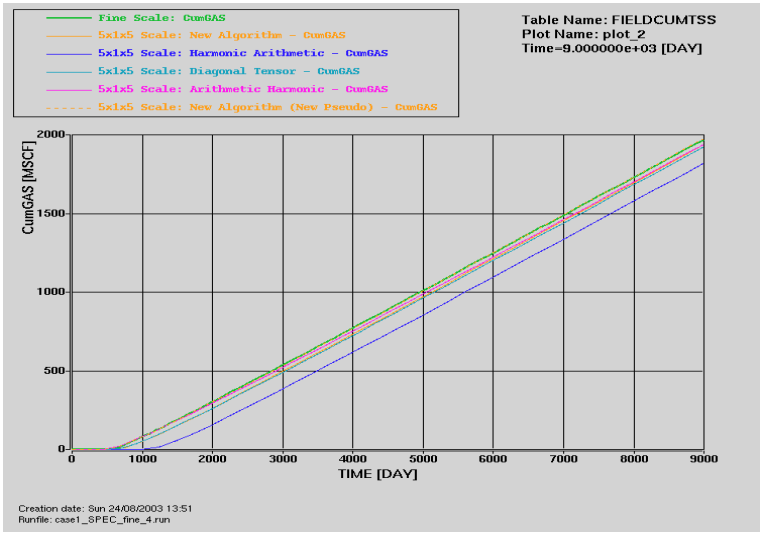

Figure 17 Comparison Plot of Cumulative Gas Production

Using the new upscaling algorithm, the prediction at the coarse scales has improved significantly. The breakthrough time of the gas injected fluid can be represented more accurately by approximately 20 to 30 days of the simulation time, while the ultimate recovered oil produced is similar to the best predicted algorithm which is Arithmetic Harmonic.

However, similar to most of the upscaling algorithms, the predictions at the coarse scale level seemed to have higher recovery of the oil produced in the reservoir, which is as expected due to unswept fluid remaining in the reservoir being produced at its coarser scale. The reservoir prediction with the new pseudo relative permeability by modifying its saturation to incorporate this unswept fraction of the fluid has indicated a much better improvement in the reservoir prediction at the coarser scale.

The fluid saturation profiles at the end of the simulation time are also compared as shown in Figure 18 and Figure 19 at its fine and coarser scales with the new algorithm respectively. They are found to be similar in profiles.

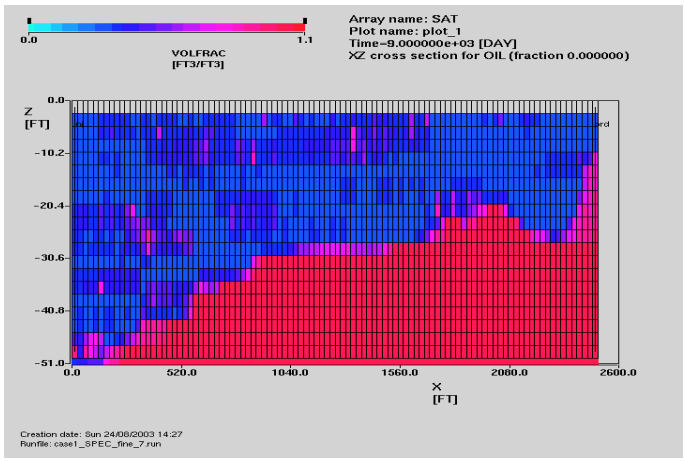

Figure 18 Fluid Saturation Plot at Fine Scale

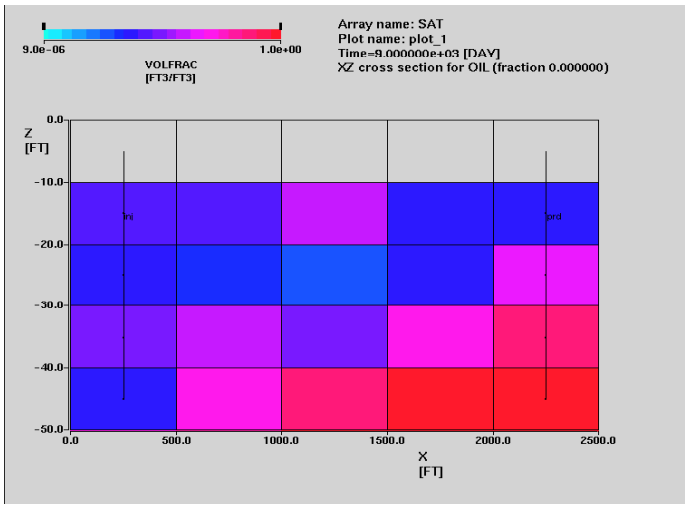

Figure 19 Fluid Saturation Plot at Coarse Scale (5x1x5 cells

Quality Check on the New Upscaling Algorithm with different scale (10x1.5 coarse cells)

For the quality checking for the new upscaling algorithm, the model at the fine scale is upscaled to 10x1x5 (50 cells) with the upscaling ratio of 10:1:4 (1 coarse cell = 40 fine cells).

The result of using different coarse scale with the new algorithm has concluded similar findings as discussed before for 5x1x5 coarse scale model.

Upscaled to 10x1x5	CumGas MMSCF	CumOil BBL	CumGasInj MMSCF
Fine Scale	**1.97**	**43434**	**2.21**
Arithmetic Harmonic	1.90 (-3.5%)	50534 (+16.3%)	2.19 (-1.3%)
Harmonic Arithmetic	1.78 (-9.90%)	50578 (+16.4%)	2.06 (-7.0%)
Diagonal Tensor	1.87 (-5.14%)	51166 (+17.8%)	2.16 (-2.6%)
Geometric	1.61 (-18.5%)	49468 (+13.9%)	1.89 (-14.9%)
New Algorithm	1.93 (-2.1%)	50399 (+16.0%)	2.22 (0.0%)
New Algorithm (Pseudo & Modified)	**1.97 (-0.0%)**	**43419 (-0.0%)**	**2.22 (0.0%)**

Table 2 Comparison Table for Oil & Gas Ultimate Recovery– 10x1x5 Coarse Cells

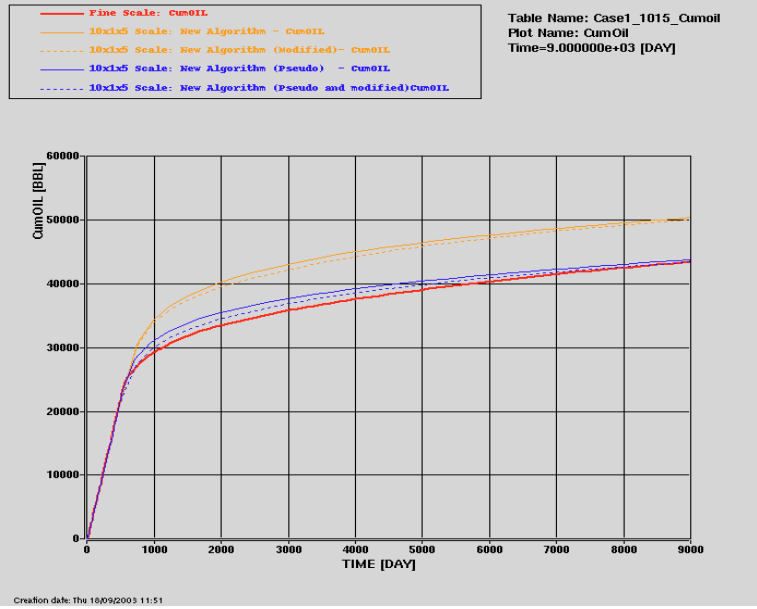

Figure 20 Comparison Plot of Cumulative Oil Produced with 10x1x5 Coarse Cells

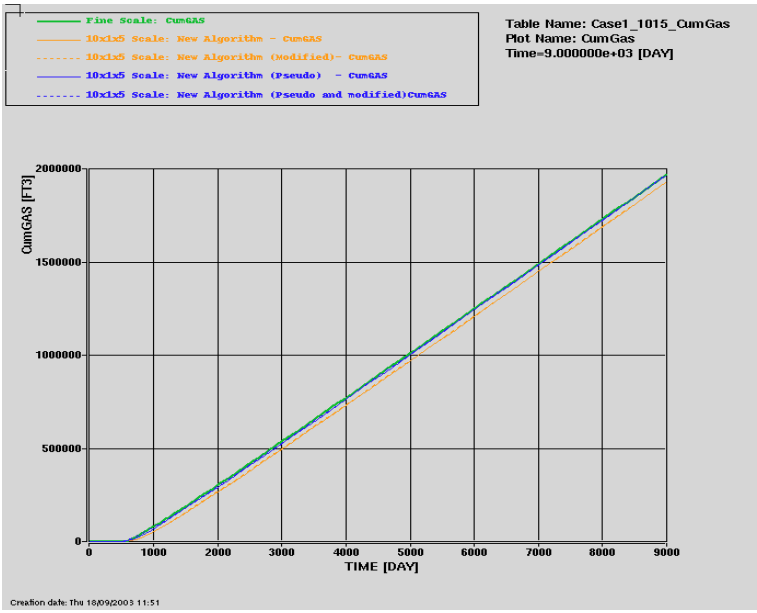

Figure 21 Comparison Plot of Cumulative Gas Produced with 10x1x5 Coarse Cells

Result with Comparison to Pseudo Upscaling (Kyte and Berry)

For comparison purposes, the reservoir prediction by using the new algorithm with the new pseudo method is also compared against the reservoir prediction by using the multi phase upscaling like Kyte & Berry method. It was found that the new algorithm is better predicted the cumulative oil produced compared to Kyte & Berry method, while the cumulative gas produced is similar in profile between the two upscaling methods.

Therefore, it can be concluded that the new algorithm has provided a significant improvement in upscaling theory. It is not only improving by better prediction of the reservoir fluid flow behaviour at the coarser scale, but is also improving the significant amount time for upscaling as it is compared to the multiphase upscaling like Kyte & Berry method.

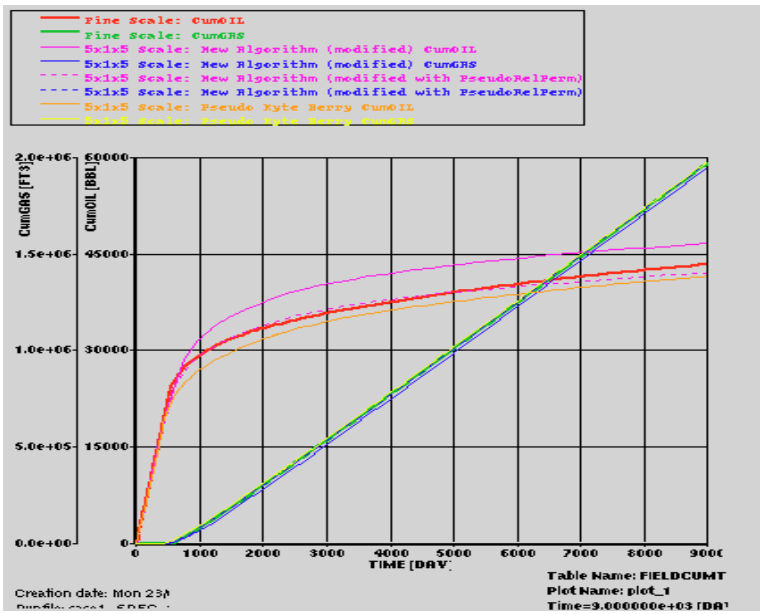

Figure 22 Comparison Plot of CumulativeOil & Gas Produced with Pseudo Upscaling

5 Conclusions & Recommendations

The following conclusions and recommendations are derived from the result.

- New upscaling algorithm has been successfully developed for providing better prediction of the fluid flow behaviour at its coarser scales compared to some existed upscaling algorithms like Diagonal tensor, arithmetic harmonic, harmonic arithmetic and/or multi phase upscaling like Kyte and Berry method.
- Identified improvement by using the new upscaling algorithm is better representation for the fluid breakthrough estimation for the reservoir field study and also better accurate prediction of the ultimate recovered of the fluid produced.
- Upscaling should be assessed individually from one case to another.
- Treatment on the undrained/unswept fluid within the reservoir model should be treated carefully. Net To Gross representation for undrainage flow path will need to be assessed individually in each model.
- Streamlines simulation may be useful for identifying the unswept fluid paths within the reservoir models.

Acknowledgement

The present work was carried out as part of the research titled "Different Scales and Integration of Data in Reservoir Simulation" for the Doctor of Philosophy at Curtin University of Technology, Bentley – Western Australia.

Nomenclature

k	permeability in fine cell
K	effective permeability in coarse cell
Q	the flow rate
A	cross sectional area
P	pressure
X	length in x direction
μ	Viscosity
V	electrical voltage
I	electrical current
R	electrical resistance
K_{rg}	relative permeability of gas
K_{rog}	relative permeability of gas in the presence of oil
K_{row}	relative permeability of water in the presence of oil
K_{rw}	relative permeability of water
K_{rg}*	K_{rg} at the end point
K_{rog}*	K_{rog} at the end point
K_{row}*	K_{row} at the end point
K_{rw}*	K_{rw} at the end point
h	reservoir thickness
L	reservoir length
$\Delta P/\Delta L$	pressure change across reservoir length

Subscript

n, m, p	number of blocks in x, y, z direction
i, j, k	block index
x, y, z	directional indication (x, y, z direction)
A	arithmetic average
AH	arithmetic harmonic average
G	geometric average
H	harmonic average
HA	harmonic arithmetic average
g	gas
gc	connate gas
w	water
wc	connate water
orw	residual oil
org	residual gas

References:

1. Aasum, Y, Kasap, E and Kelkar, M. (1993) SPE 25913 – Analytical Upscaling of Small – Scale Permeability Using a Full Tensor, Society of Petroleum Engineer, Denver, pp. 679 –92.
2. Begg, Kay, A., Gustason, ER and Angert, P.F. (1993) Characterization of a Complex Fluvial – Deltaic Reservoir for Simulation, The 4th Annual Archie Conference "Characterizing and Managing the Dynamic Reservoir – A multi disciplinary approach", Texas, pp. 143-8.
3. Christie, MA, Mansfield, M, King, PR, Barker, J.W. (1995) SPE 29127 – A

Renormalisation Based Upscaling Technique for WAG Floods in Heterogeneous Reservoirs, Society of Petroleum Engineers, Texas, pp. 353-61.

4. Christie, MA (1996) Upscaling for Reservoir Simulation, Journal of Petroleum Technology, Nov edn, London, pp. 1004-1010.
5. Del Toro, V. (1986) Electrical Engineering Fundamentals, Prentice-Hall, Englewood Cliffs.
6. Doyle, P.G and Snell, J.L. (1984) The Carus Mathematical Monographs Number Twenty Two – Random Walks and Electrical Networks, The Mathematical Association of America, Washington.
7. Durlofsky, L.J., Behrens, R.A., Jones, R.C., and Bernath, A. (1995) SPE 30709 – Scale up of Heterogeneous Three Dimensional Reservoir Descriptions, Society of Petroleum Engineers, Texas, pp. 53-66.
8. Durrett, R and Kesten, H (1991) Random Walks, Brownian motion and Interacting Particle Systems, Birkhäuser, Boston.
9. Hove, K., Olsen, G., Nilsson, S. and Tonnesen, M. (1992) SPE 24890 - From Stochastic Geological Description to Production Forecasting in Heterogeneous Layered Reservoirs, Society of Petroleum Engineers, Texas, pp. 311-325.
10. IRAP RMS User Manual (1999), Smedvig Technologies, pp. 331-48.
11. King, P.R and Edwards, Sir S. (1988) Mathematics in Oil Production - Effective Values in Averaging, Clarendon Press, Oxford, pp.217-34.
12. Lemouzy, P.M., Romeu, R.K (1993) SPE 26660 – A New Scaling-Up Method to Compute Relative Permeability and Capillary Pressure for Simulation of Heterogenous Reservoir, Society of Petroleum Engineers, Texas, pp. 1-8.
13. Renard, Ph & De Marsily, G., (1997) Calculating equivalent permeability: a review, Advanced in Water Resources, vol. 20, No. 5-6, pp. 253-278.
14. Tang, Z., Gaquerel, G. and Gawith, DE (1993) Integrating Geoscience and Engineering for Improved Field Management and Appraisal, The 4th Annual Archie Conference "Characterizing and Managing the Dynamic Reservoir – A multi disciplinary approach", Texas pp. 29 - 41.
15. Tchelep, H.A., Durlofsky, L.J., Chen, W.H. Bernath, A., and Chien, M.C.H. (1997) SPE 38886 – Practice Use of Scale Up and Parallel Reservoir Simulation Technologies in field Studies, Society of Petroleum Engineers, Texas, pp. 1-15.

Appendix C

New Upscaling Algorithm in IRAP RMS IPL Script

```
// File Name: Relax_3D_XYZ_Final_Apr03_LH.ipl
// Author: Lina Hartanto
//
// Capital letter represents the fine grid properties, while Lower case letter represents the coarse grid properties
//
// Declaration
Int NO_COL, NO_ROW, NO_LAY, no_col, no_row, no_lay, no_iter
Int I, J, K, i, j, k, tempI, tempJ, tempK, n
Int UPCELLi, UPCELLj, UPCELLk
Int tempi, tempj, tempk
Parameter Kl, Kr, Ku, Kd, Kf, Kb
Parameter KXl, KXr, KXu, KXd, KXf, KXb, WXl, WXr, WXu, WXd, WXf, WXb
Parameter KZl, KZr, KZu, KZd, KZf, KZb, WZl, WZr, WZu, WZd, WZf, WZb
Parameter KYl, KYr, KYu, KYd, KYf, KYb, WYl, WYr, WYu, WYd, WYf, WYb
Parameter KX, KY, KZ
Parameter WX, CurX, CurX2
Parameter WZ, CurZ, CurZ2
Parameter WY, CurY, CurY2
Parameter CurrX, KXeff
Parameter CurrZ, KZeff
Parameter CurrY, KYeff
//Parameter KXeffTEMP, KZeffTEMP, KYeffTEMP
Parameter ITER

Zone Z = @ZONES[32] //Zone Number for Fine Model
Zone z = @ZONES[33] //Zone Number for Coarse Model to be upscaled to.

NO_COL = Z.columns
NO_ROW = Z.rows
NO_LAY = Z.layers

no_col = z.columns
no_row = z.rows
no_lay = z.layers

// Assigning the Permeability Values
// Left hand side K_X
Kl = CreateContinuousParameter(Z, "Kleft")
KX = Z.K_X
tempk = 1
WHILE tempk <=no_lay DO
    tempj = 1
    WHILE tempj <=no_row DO
        tempi = 1
    WHILE tempi <= no_col DO
        UPCELLk = tempk*NO_LAY/no_lay
        K = (tempk-1)*UPCELLk/tempk +1
            WHILE K <=UPCELLk DO
                UPCELLj = tempj*NO_ROW/no_row
                J = (tempj-1)*UPCELLj/tempj+1
```

```
                WHILE J <=UPCELLj DO
                UPCELLi = tempi*NO_COL/no_col
                    I = (tempi-1)*UPCELLi/tempi + 1
                        Kl[I,J,K]=KX[I,J,K]*2
                        I = I + 1
                        WHILE I <=UPCELLi DO
                            tempI = I - 1
                            Kl[I,J,K] = 1/(1/(2*KX[I,J,K])+1/(KX[tempI,J,K]*2))
                        I = I+1
                        ENDWHILE
                J=J+1
                ENDWHILE
                K=K+1
                ENDWHILE
        tempi = tempi +1
        ENDWHILE
    tempj = tempj +1
    ENDWHILE
tempk = tempk + 1
ENDWHILE
Iconize(Kl)

//  RightHand Side K_X
Kr = CreateContinuousParameter(Z, "Kright")
KX = Z.K_X
tempk = 1
WHILE tempk <=no_lay DO
    tempj = 1
    WHILE tempj <=no_row DO
        tempi = 1
        WHILE tempi <= no_col DO
            UPCELLk = tempk*NO_LAY/no_lay
            K = (tempk-1)*UPCELLk/tempk +1
            WHILE K <=UPCELLk DO
                UPCELLj = tempj*NO_ROW/no_row
                J = (tempj-1)*UPCELLj/tempj+1
                WHILE J <=UPCELLj DO
                    UPCELLi = tempi*NO_COL/no_col
                    I = (tempi-1)*UPCELLi/tempi + 1
                    WHILE I <=UPCELLi DO
                        tempI = I + 1
                        IF tempI <=UPCELLi THEN Kr[I,J,K] =
1/(1/(2*KX[I,J,K])+1/(KX[tempI,J,K]*2)) ENDIF
                    I = I+1
                    ENDWHILE
                    Kr[UPCELLi,J,K]=KX[UPCELLi,J,K]*2
                J=J+1
                ENDWHILE
            K=K+1
            ENDWHILE
        tempi = tempi +1
        ENDWHILE
    tempj = tempj +1
    ENDWHILE
tempk = tempk + 1
ENDWHILE
Iconize(Kr)
```

```
// Front side K_Y
Kf = CreateContinuousParameter(Z, "Kfront")
KY = Z.K_Y
tempk = 1
WHILE tempk <=no_lay DO
    tempj = 1
    WHILE tempj <=no_row DO
        tempi = 1
        WHILE tempi <= no_col DO
            UPCELLk = tempk*NO_LAY/no_lay
            K = (tempk-1)*UPCELLk/tempk +1
            WHILE K <=UPCELLk DO
                UPCELLi = tempi*NO_COL/no_col
                I = (tempi-1)*UPCELLi/tempi+1
                WHILE I <=UPCELLi DO
                    tempJ = J - 1
                    UPCELLj = tempj*NO_ROW/no_row
                    J = (tempj-1)*UPCELLj/tempj + 1
                    Kf[I,J,K]=KY[I,J,K]*2
                    J = J + 1
                    WHILE J <=UPCELLj DO
                        Kf[I,J,K] = 1/(1/(2*KY[I,J,K])+1/(KY[I,tempJ,K]*2))
                    J = J+1
                    ENDWHILE
                I=I+1
                ENDWHILE
            K=K+1
            ENDWHILE
        tempi = tempi +1
        ENDWHILE
    tempj = tempj +1
    ENDWHILE
tempk = tempk + 1
ENDWHILE
Iconize(Kf)

//  Back Side K_Y
Kb = CreateContinuousParameter(Z, "Kback")
KY = Z.K_Y
tempk = 1
WHILE tempk <=no_lay DO
    tempj = 1
    WHILE tempj <=no_row DO
        tempi = 1
        WHILE tempi <= no_col DO
            UPCELLk = tempk*NO_LAY/no_lay
            K = (tempk-1)*UPCELLk/tempk +1
            WHILE K <=UPCELLk DO
                UPCELLi = tempi*NO_COL/no_col
                I = (tempi-1)*UPCELLi/tempi + 1
                WHILE I <=UPCELLi DO
                    UPCELLj = tempj*NO_ROW/no_row
                    J = (tempj-1)*UPCELLj/tempj+1
                    WHILE J <=UPCELLj DO
                        tempJ = J + 1
```

```
                        IF tempJ <= UPCELLj THEN Kb[I,J,K] =
1/(1/(2*KY[I,J,K])+1/(2*KY[I,tempJ,K])) ENDIF
                    J = J+1
                    ENDWHILE
                    Kb[I,UPCELLj,K]=KY[I,UPCELLj,K]*2
                I =I+1
                ENDWHILE
            K=K+1
            ENDWHILE
        tempi = tempi +1
        ENDWHILE
    tempj = tempj +1
    ENDWHILE
tempk = tempk + 1
ENDWHILE
Iconize(Kb)

// Up side K_Z
Ku = CreateContinuousParameter(Z, "Kup")
KZ = Z.K_Z
tempk = 1
WHILE tempk <=no_lay DO
    tempj = 1
    WHILE tempj <=no_row DO
        tempi = 1
        WHILE tempi <= no_col DO
            UPCELLi = tempi*NO_COL/no_col
            I = (tempi-1)*UPCELLi/tempi + 1
            WHILE I <=UPCELLi DO
                UPCELLj = tempj*NO_ROW/no_row
                J = (tempj-1)*UPCELLj/tempj+1
                WHILE J <=UPCELLj DO
                    UPCELLk = tempk*NO_LAY/no_lay
                    K = (tempk-1)*UPCELLk/tempk +1
                    Ku[I,J,K]=KZ[I,J,K]*2
                    K = K + 1
                    WHILE K <=UPCELLk DO
                        tempK = K - 1
                        Ku[I,J,K] = 1/(1/(2*KZ[I,J,K])+1/(KZ[I,J,tempK]*2))
                    K=K+1
                    ENDWHILE
                J=J+1
                ENDWHILE
            I = I+1
            ENDWHILE
        tempi = tempi +1
        ENDWHILE
    tempj = tempj +1
    ENDWHILE
tempk = tempk + 1
ENDWHILE
Iconize(Ku)

//  Down Side K_Z
Kd = CreateContinuousParameter(Z, "Kdown")
KZ = Z.K_Z
tempk = 1
```

```
WHILE tempk <=no_lay DO
    tempj = 1
    WHILE tempj <=no_row DO
        tempi = 1
        WHILE tempi <= no_col DO
            UPCELLi = tempi*NO_COL/no_col
            I = (tempi-1)*UPCELLi/tempi + 1
            WHILE I <=UPCELLi DO
                UPCELLj = tempj*NO_ROW/no_row
                J = (tempj-1)*UPCELLj/tempj+1
                WHILE J <=UPCELLj DO
                    UPCELLk = tempk*NO_LAY/no_lay
                    K = (tempk-1)*UPCELLk/tempk +1
                    WHILE K <=UPCELLk DO
                        tempK = K + 1
                        IF tempK <=UPCELLk THEN Kd[I,J,K] =
1/(1/(2*KZ[I,J,K])+1/(KZ[I,J,tempK]*2)) ENDIF
                        K=K+1
                    ENDWHILE
                    Kd[I,J,UPCELLk]=KZ[I,J,UPCELLk]*2
                J=J+1
                ENDWHILE
            I = I+1
            ENDWHILE
        tempi = tempi +1
        ENDWHILE
    tempj = tempj +1
    ENDWHILE
tempk = tempk + 1
ENDWHILE
Iconize(Kd)

// creating WX weighting Parameter Left
WXl = CreateContinuousParameter(Z, "WXleft")
WXr = CreateContinuousParameter(Z, "WXright")
WXu = CreateContinuousParameter(Z, "WXup")
WXd = CreateContinuousParameter(Z, "WXdown")
WXf = CreateContinuousParameter(Z, "WXfront")
WXb = CreateContinuousParameter(Z, "WXback")
WZl = CreateContinuousParameter(Z, "WZleft")
WZr = CreateContinuousParameter(Z, "WZright")
WZu = CreateContinuousParameter(Z, "WZup")
WZd = CreateContinuousParameter(Z, "WZdown")
WZf = CreateContinuousParameter(Z, "WZfront")
WZb = CreateContinuousParameter(Z, "WZback")
WYl = CreateContinuousParameter(Z, "WYleft")
WYr = CreateContinuousParameter(Z, "WYright")
WYu = CreateContinuousParameter(Z, "WYup")
WYd = CreateContinuousParameter(Z, "WYdown")
WYf = CreateContinuousParameter(Z, "WYfront")
WYb = CreateContinuousParameter(Z, "WYback")

Iconize(WXl)
Iconize(WXr)
Iconize(WXd)
Iconize(WXu)
Iconize(WXf)
```

```
Iconize(WXb)
Iconize(WZl)
Iconize(WZr)
Iconize(WZd)
Iconize(WZu)
Iconize(WZf)
Iconize(WZb)
Iconize(WYl)
Iconize(WYr)
Iconize(WYd)
Iconize(WYu)
Iconize(WYf)
Iconize(WYb)

// Creating the Permeability for X direction Calculation
KXl = CreateContinuousParameter(Z, "KXleft")
KXr = CreateContinuousParameter(Z, "KXright")
KXu = CreateContinuousParameter(Z, "KXup")
KXd = CreateContinuousParameter(Z, "KXdown")
KXf = CreateContinuousParameter(Z, "KXfront")
KXb = CreateContinuousParameter(Z, "KXback")
KXl=Z.Kleft
KXr=Z.Kright
KXu=Z.Kup
KXd=Z.Kdown
KXf=Z.Kfront
KXb=Z.Kback

tempk = 1
WHILE tempk <=no_lay DO
    tempj = 1
    WHILE tempj <= no_row DO
        tempi = 1
        WHILE tempi <= no_col DO
            UPCELLi = tempi*NO_COL/no_col
            I = (tempi-1)*UPCELLi/tempi + 1
            WHILE I <=UPCELLi DO
                UPCELLj = tempj*NO_ROW/no_row
                J = (tempj-1)*UPCELLj/tempj+1
                WHILE J <=UPCELLj DO
                    UPCELLk = tempk*NO_LAY/no_lay
                    K = (tempk-1)*UPCELLk/tempk +1
                    WHILE K <= UPCELLk DO
                        IF K = UPCELLk THEN KXd[I,J,K]=0 ENDIF
                        IF J = UPCELLj THEN KXb[I,J,K]=0 ENDIF
                        IF K = (tempk-1)*UPCELLk/tempk + 1 THEN KXu[I,J,K]=0 ENDIF
                        IF J = (tempj-1)*UPCELLj/tempj + 1 THEN KXf[I,J,K]=0 ENDIF
                        tempI=(tempi-1)*UPCELLi/tempi+1
                        WXl[tempI,J,K] = 1
                    K = K+1
                    ENDWHILE
                J=J+1
                ENDWHILE
            I=I+1
            ENDWHILE
        tempi = tempi +1
        ENDWHILE
```

```
    tempj = tempj +1
    ENDWHILE
tempk = tempk + 1
ENDWHILE
Iconize(KXl)
Iconize(KXr)
Iconize(KXu)
Iconize(KXd)
Iconize(KXf)
Iconize(KXb)

// creating Permeability Parameter for Z direction calculation
KZl = CreateContinuousParameter(Z, "KZleft")
KZr = CreateContinuousParameter(Z, "KZright")
KZu = CreateContinuousParameter(Z, "KZup")
KZd = CreateContinuousParameter(Z, "KZdown")
KZf = CreateContinuousParameter(Z, "KZfront")
KZb = CreateContinuousParameter(Z, "KZback")
KZl=Z.Kleft
KZr=Z.Kright
KZu=Z.Kup
KZd=Z.Kdown
KZf=Z.Kfront
KZb=Z.Kback

tempk = 1
WHILE tempk <=no_lay DO
    tempj = 1
    WHILE tempj <=no_row DO
        tempi = 1
        WHILE tempi <= no_col DO
            UPCELLk = tempk*NO_LAY/no_lay
            K = (tempk-1)*UPCELLk/tempk +1
            WHILE K <= UPCELLk DO
                UPCELLj = tempj*NO_ROW/no_row
                J = (tempj-1)*UPCELLj/tempj+1
                WHILE J <=UPCELLj DO
                    UPCELLi = tempi*NO_COL/no_col
                    I = (tempi-1)*UPCELLi/tempi + 1
                    WHILE I <= UPCELLi DO
                        IF I = UPCELLi THEN KZr[I,J,K]=0 ENDIF
                        IF J = UPCELLj THEN KZb[I,J,K]=0 ENDIF
                        IF I = (tempi-1)*UPCELLi/tempi +1 THEN KZl[I,J,K]=0 ENDIF
                        IF J = (tempj-1)*UPCELLj/tempj + 1 THEN KZf[I,J,K]=0 ENDIF
                        tempK=(tempk-1)*UPCELLk/tempk+1
                        WZu[I,J,tempK] = 1
                    I = I+1
                    ENDWHILE
                J=J+1
                ENDWHILE
            K=K+1
            ENDWHILE
        tempi = tempi +1
        ENDWHILE
    tempj = tempj +1
    ENDWHILE
tempk = tempk + 1
```

```
ENDWHILE

Iconize(KZr)
Iconize(KZl)
Iconize(KZf)
Iconize(KZb)
Iconize(KZu)
Iconize(KZd)

// Creating Permeability parameter for Y direction calculation
KYl = CreateContinuousParameter(Z, "KYleft")
KYr = CreateContinuousParameter(Z, "KYright")
KYu = CreateContinuousParameter(Z, "KYup")
KYd = CreateContinuousParameter(Z, "KYdown")
KYf = CreateContinuousParameter(Z, "KYfront")
KYb = CreateContinuousParameter(Z, "KYback")
KYl=Z.Kleft
KYr=Z.Kright
KYu=Z.Kup
KYd=Z.Kdown
KYf=Z.Kfront
KYb=Z.Kback

tempk = 1
WHILE tempk <=no_lay DO
    tempj = 1
    WHILE tempj <=no_row DO
        tempi = 1
        WHILE tempi <= no_col DO
            UPCELLi = tempi*NO_COL/no_col
            I= (tempi-1)*UPCELLi/tempi + 1
            WHILE I <= UPCELLi DO
                UPCELLk = tempk*NO_LAY/no_lay
                K = (tempk-1)*UPCELLk/tempk +1
                WHILE K <= UPCELLk DO
                    UPCELLj = tempj*NO_ROW/no_row
                    J = (tempj-1)*UPCELLj/tempj+1
                    WHILE J <=UPCELLj DO
                        IF I = UPCELLi THEN KYr[I,J,K]=0 ENDIF
                        IF K = UPCELLk THEN KYd[I,J,K]=0 ENDIF
                        IF I = (tempi-1)*UPCELLi/tempi +1 THEN KYl[I,J,K]=0 ENDIF
                        IF K = (tempk-1)*UPCELLk/tempk + 1 THEN KYu[I,J,K]=0 ENDIF
                        tempJ=(tempj-1)*UPCELLj/tempj+1
                        WYf[I,tempJ,K] = 1
                        J = J+1
                    ENDWHILE
                K=K+1
                ENDWHILE
            I=I+1
            ENDWHILE
        tempi = tempi +1
        ENDWHILE
    tempj = tempj +1
    ENDWHILE
tempk = tempk + 1
ENDWHILE
Iconize(KYl)
```

```
Iconize(KYr)
Iconize(KYu)
Iconize(KYd)
Iconize(KYf)
Iconize(KYb)

// Calculation for Iteration in X direction
WX = CreateContinuousParameter(Z,"newWX")
Iconize(WX)
ITER= CreateContinuousParameter(Z, "iter")
Iconize(ITER)
n = 1
no_iter = 25
WHILE n <= no_iter DO
tempk = 1
WHILE tempk <=no_lay DO
    tempj = 1
    WHILE tempj <= no_row DO
        tempi = 1
        WHILE tempi <= no_col DO
            UPCELLk = tempk*NO_LAY/no_lay
            K = (tempk-1)*UPCELLk/tempk +1
            WHILE K <=UPCELLk DO
                UPCELLj = tempj*NO_ROW/no_row
                J = (tempj-1)*UPCELLj/tempj + 1
                WHILE J <=UPCELLj DO
                    UPCELLi = tempi*NO_COL/no_col
                    I = (tempi-1)*UPCELLi/tempi +1
                    WHILE I <=UPCELLi DO
                        WX[I,J,K] = KXl[I,J,K]*WXl[I,J,K]+KXr[I,J,K]*WXr[I,J,K]
                        WX[I,J,K] = WX[I,J,K]+KXd[I,J,K]*WXd[I,J,K]+KXu[I,J,K]*WXu[I,J,K]
                        WX[I,J,K] = WX[I,J,K]+KXf[I,J,K]*WXf[I,J,K]+KXb[I,J,K]*WXb[I,J,K]
                        WX[I,J,K] =
WX[I,J,K]/(KXl[I,J,K]+KXr[I,J,K]+KXd[I,J,K]+KXu[I,J,K]+KXf[I,J,K]+KXb[I,J,K])
//                      updating values
                        tempI = I - 1
                        IF tempI >= (((tempi-1)*UPCELLi/tempi)+1) AND tempI<=UPCELLi THEN
WXr[tempI,J,K] = WX[I,J,K] ENDIF

                        tempI = I + 1
                        IF tempI <= UPCELLi THEN WXl[tempI,J,K] = WX[I,J,K] ENDIF

//                      Restoring original value
                        IF I =((tempi-1)*UPCELLi/tempi) +1 THEN WXl[I,J,K]= 1 ENDIF
                        IF I = UPCELLi THEN WXr[I,J,K] = 0 ENDIF

                        tempK = K + 1
                        IF tempK <= UPCELLk THEN WXu[I,J,tempK] = WX[I,J,K] ENDIF

                        tempK = K - 1
                        IF tempK >=(((tempk-1)*UPCELLk/tempk) +1) AND tempK <= UPCELLk
THEN WXd[I,J,tempK] = WX[I,J,K] ENDIF

                        IF K = ((tempk-1)*UPCELLk/tempk) +1 THEN WXu[I,J,K] = 0 ENDIF
                        IF K = UPCELLk THEN WXd[I,J,K] = 0 ENDIF

                        tempJ = J + 1
```

```
                    IF tempJ <= UPCELLj THEN WXf[I,tempJ,K] = WX[I,J,K] ENDIF

                    tempJ = J - 1
                    IF tempJ >=(((tempj-1)*UPCELLj/tempj) +1) AND tempJ <= UPCELLj THEN
WXb[I,tempJ,K] = WX[I,J,K] ENDIF

                    IF J = ((tempj-1)*UPCELLj/tempj) +1 THEN WXf[I,J,K] = 0 ENDIF
                    IF J = UPCELLj THEN WXb[I,J,K] = 0 ENDIF
                    SetParameter(Z,"iter",ITER)
                    SetParameter(Z,"WXleft",WXl)
                    SetParameter(Z,"WXright",WXr)
                    SetParameter(Z,"WXup",WXu)
                    SetParameter(Z,"WXdown",WXd)
                    SetParameter(Z,"WXfront",WXf)
                    SetParameter(Z,"WXback",WXb)
                    SetParameter(Z,"newWX",WX)
                I = I + 1
                ENDWHILE
            J=J+1
            ENDWHILE
        K=K+1
        ENDWHILE
    tempi = tempi +1
    ENDWHILE
tempj = tempj +1
ENDWHILE
tempk = tempk + 1
ENDWHILE
n = n+1
ENDWHILE

// Calculation for Iteration in Z direction
WZ = CreateContinuousParameter(Z,"newWZ")
Iconize(WZ)
n = 1
no_iter = 25
WHILE n <= no_iter DO
tempk = 1
WHILE tempk <=no_lay DO
    tempj = 1
    WHILE tempj <=no_row DO
        tempi = 1
        WHILE tempi <= no_col DO
            UPCELLk = tempk*NO_LAY/no_lay
            K = (tempk-1)*UPCELLk/tempk +1
            WHILE K <=UPCELLk DO
                UPCELLj = tempj*NO_ROW/no_row
                J = (tempj-1)*UPCELLj/tempj + 1
                WHILE J <=UPCELLj DO
                    UPCELLi = tempi*NO_COL/no_col
                    I = (tempi-1)*UPCELLi/tempi +1
                    WHILE I <=UPCELLi DO
                        WZ[I,J,K] = KZl[I,J,K]*WZl[I,J,K]+KZr[I,J,K]*WZr[I,J,K]
                        WZ[I,J,K] = WZ[I,J,K]+KZd[I,J,K]*WZd[I,J,K]+KZu[I,J,K]*WZu[I,J,K]
                        WZ[I,J,K] = WZ[I,J,K]+KZf[I,J,K]*WZf[I,J,K]+KZb[I,J,K]*WZb[I,J,K]
                        WZ[I,J,K] =
WZ[I,J,K]/(KZl[I,J,K]+KZr[I,J,K]+KZd[I,J,K]+KZu[I,J,K]+KZf[I,J,K]+KZb[I,J,K])
```

```
//                      updating values
                        tempK = K - 1
                        IF tempK >= (((tempk-1)*UPCELLk/tempk) +1) AND tempK <=UPCELLk
THEN WZd[I,J,tempK] = WZ[I,J,K] ENDIF
                        tempK = K + 1
                        IF tempK <= UPCELLk THEN WZu[I,J,tempK] = WZ[I,J,K] ENDIF

//                      Restoring original value
                        IF K =((tempk-1)*UPCELLk/tempk) +1 THEN WZu[I,J,K]= 1 ENDIF
                        IF K = UPCELLk THEN WZd[I,J,K] = 0 ENDIF

                        tempI = I + 1
                        IF tempI >=(((tempi-1)*UPCELLi/tempi) +1) AND tempI <=UPCELLi THEN
WZl[tempI,J,K] = WZ[I,J,K] ENDIF

                        tempI = I - 1
                        IF tempI >=(((tempi-1)*UPCELLi/tempi) +1) AND tempI <=UPCELLi THEN
WZr[tempI,J,K] = WZ[I,J,K] ENDIF

                        IF I = ((tempi-1)*UPCELLi/tempi) + 1 THEN WZl[I,J,K] = 0         ENDIF
                        IF I = UPCELLi THEN WZr[I,J,K] = 0 ENDIF

                        tempJ = J + 1
                        IF tempJ <= UPCELLj THEN WZf[I,tempJ,K] = WZ[I,J,K] ENDIF

                        tempJ = J - 1
                        IF tempJ >=(((tempj-1)*UPCELLj/tempj) +1) AND tempJ <= UPCELLj THEN
WZb[I,tempJ,K] = WZ[I,J,K] ENDIF

                        IF J = ((tempj-1)*UPCELLj/tempj) +1 THEN WZf[I,J,K] = 0 ENDIF
                        IF J = UPCELLj THEN WZb[I,J,K] = 0 ENDIF
                        SetParameter(Z,"iter",ITER)
                        SetParameter(Z,"WZleft",WZl)
                        SetParameter(Z,"WZright",WZr)
                        SetParameter(Z,"WZup",WZu)
                        SetParameter(Z,"WZdown",WZd)
                        SetParameter(Z,"WZfront",WZf)
                        SetParameter(Z,"WZback",WZb)
                        SetParameter(Z,"newWZ",WZ)
                    I = I + 1
                    ENDWHILE
                J=J+1
                ENDWHILE
            K=K+1
            ENDWHILE
        tempi = tempi +1
        ENDWHILE
    tempj = tempj +1
    ENDWHILE
tempk = tempk + 1
ENDWHILE
n = n+1
ENDWHILE

// Calculation for Iteration in Y direction
WY = CreateContinuousParameter(Z,"newWY")
Iconize(WY)
```

```
n = 1
no_iter = 20
WHILE n <= no_iter DO
tempk = 1
WHILE tempk <=no_lay DO
    tempj = 1
    WHILE tempj <=no_row DO
        tempi = 1
        WHILE tempi <= no_col DO
            UPCELLk = tempk*NO_LAY/no_lay
            K = (tempk-1)*UPCELLk/tempk +1
            WHILE K <=UPCELLk DO
                UPCELLj = tempj*NO_ROW/no_row
                J = (tempj-1)*UPCELLj/tempj + 1
                WHILE J <=UPCELLj DO
                    UPCELLi = tempi*NO_COL/no_col
                    I = (tempi-1)*UPCELLi/tempi +1
                    WHILE I <=UPCELLi DO
                        WY[I,J,K] =
KYl[I,J,K]*WYl[I,J,K]+KYr[I,J,K]*WYr[I,J,K]+KYd[I,J,K]*WYd[I,J,K]+KYu[I,J,K]*WYu[I,J,K]
                        WY[I,J,K] = WY[I,J,K]+KYf[I,J,K]*WYf[I,J,K]+KYb[I,J,K]*WYb[I,J,K]
                        WY[I,J,K] =
WY[I,J,K]/(KYl[I,J,K]+KYr[I,J,K]+KYd[I,J,K]+KYu[I,J,K]+KYf[I,J,K]+KYb[I,J,K])
//                      updating values
                        tempJ = J - 1
                        IF tempJ >= (((tempj-1)*UPCELLj/tempj) +1) AND tempJ <=UPCELLj THEN
WYb[I,tempJ,K] = WY[I,J,K] ENDIF
                        tempJ = J + 1
                        IF tempJ <= UPCELLj THEN WYf[I,tempJ,K] = WY[I,J,K] ENDIF

//                      Restoring original value
                        IF J =((tempj-1)*UPCELLj/tempj) +1 THEN WYf[I,J,K]= 1 ENDIF
                        IF J = UPCELLj THEN WYb[I,J,K] = 0 ENDIF

                        tempI = I + 1
                        IF tempI >=(((tempi-1)*UPCELLi/tempi) +1) AND tempI <=UPCELLi THEN
WYl[tempI,J,K] = WY[I,J,K] ENDIF

                        tempI = I - 1
                        IF tempI >=(((tempi-1)*UPCELLi/tempi) +1) AND tempI <=UPCELLi THEN
WYr[tempI,J,K] = WY[I,J,K] ENDIF
                        IF I = ((tempi-1)*UPCELLi/tempi) + 1 THEN WYl[I,J,K] = 0 ENDIF
                        IF I = UPCELLi THEN WYr[I,J,K] = 0 ENDIF

                        tempK = K + 1
                        IF tempK <= UPCELLk THEN WYu[I,J,tempK] = WY[I,J,K] ENDIF

                        tempK = K - 1
                        IF tempK >=(((tempk-1)*UPCELLk/tempk) +1) AND tempK <= UPCELLk
THEN WYd[I,J,tempK] = WY[I,J,K] ENDIF

                        IF K = ((tempk-1)*UPCELLk/tempk) +1 THEN WYu[I,J,K] = 0 ENDIF
                        IF K = UPCELLk THEN WYd[I,J,K] = 0 ENDIF
                        SetParameter(Z,"iter",ITER)
                        SetParameter(Z,"WYleft",WYl)
                        SetParameter(Z,"WYright",WYr)
                        SetParameter(Z,"WYup",WYu)
```

```
                    SetParameter(Z,"WYdown",WYd)
                    SetParameter(Z,"WYfront",WYf)
                    SetParameter(Z,"WYback",WYb)
                    SetParameter(Z,"newWY",WY)
                I = I + 1
                ENDWHILE
            J=J+1
            ENDWHILE
        K=K+1
        ENDWHILE
    tempi = tempi +1
    ENDWHILE
tempj = tempj +1
ENDWHILE
tempk = tempk + 1
ENDWHILE
n = n+1
ENDWHILE

// calculating the CurrentX through the system
CurX = CreateContinuousParameter(Z,"CurrentX")
CurX2 = CreateContinuousParameter(Z,"CurrentXright")
Iconize(CurX)
Iconize(CurX2)
tempk = 1
WHILE tempk <=no_lay DO
    tempj = 1
    WHILE tempj <=no_row DO
        tempi = 1
        WHILE tempi <= no_col DO
            UPCELLk = tempk*NO_LAY/no_lay
            K = (tempk-1)*UPCELLk/tempk +1
            WHILE K <=UPCELLk DO
                UPCELLj = tempj*NO_ROW/no_row
                J = (tempj-1)*UPCELLj/tempj+1
                WHILE J <=UPCELLj DO
                    UPCELLi = tempi*NO_COL/no_col
                    I = (tempi-1)*UPCELLi/tempi +1
                    WHILE I <=UPCELLi DO
                        IF I > (tempi-1)*UPCELLi/tempi +1 AND I < UPCELLi THEN
                            tempI = I - 1
                            CurX[I,J,K] = ((WX[tempI,J,K]- WX[I,J,K])*KXl[I,J,K])
                        ENDIF
                        IF I = (tempi-1)*UPCELLi/tempi +1 THEN CurX[I,J,K] = ((1 - WX[I,J,K])*
KXl[I,J,K]) ENDIF
                        tempI = I + 1
                        IF tempI <= UPCELLi THEN CurX2[I,J,K] = (WX[I,J,K]-
WX[tempI,J,K])*KXr[I,J,K] ENDIF
                        IF tempI >= UPCELLi THEN CurX2[I,J,K] = (WX[I,J,K])*KXr[I,J,K] ENDIF
                        SetParameter(Z,"CurrentX",CurX)
                        SetParameter(Z,"CurrentXright",CurX2)
                    I = I + 1
                    ENDWHILE
                J=J+1
                ENDWHILE
            K=K+1
            ENDWHILE
```

```
        tempi = tempi +1
        ENDWHILE
    tempj = tempj +1
    ENDWHILE
tempk = tempk + 1
ENDWHILE

// calculating the CurrentZ through the system
CurZ = CreateContinuousParameter(Z,"CurrentZ")
CurZ2 = CreateContinuousParameter(Z,"CurrentZdown")
Iconize(CurZ)
Iconize(CurZ2)
tempk = 1
WHILE tempk <=no_lay DO
    tempj = 1
    WHILE tempj <=no_row DO
        tempi = 1
        WHILE tempi <= no_col DO
            UPCELLi = tempi*NO_COL/no_col
            I = (tempi-1)*UPCELLi/tempi +1
            WHILE I <=UPCELLi DO
                UPCELLj = tempj*NO_ROW/no_row
                J = (tempj-1)*UPCELLj/tempj+1
                WHILE J <=UPCELLj DO
                    UPCELLk = tempk*NO_LAY/no_lay
                    K = (tempk-1)*UPCELLk/tempk +1
                    WHILE K <=UPCELLk DO
                        IF K = (tempk-1)*UPCELLk/tempk +1 THEN CurZ[I,J,K] = (1-
WZ[I,J,K])*KZu[I,J,K] ENDIF
                        IF K >(tempk-1)*UPCELLk/tempk+1 AND K< UPCELLk THEN
                            tempK = K - 1
                            CurZ[I,J,K] = (WZ[I,J,tempK]- WZ[I,J,K])*KZu[I,J,K]
                        ENDIF
                        tempK = K +1
                        IF tempK <= UPCELLk THEN CurZ2[I,J,K] = (WZ[I,J,K]-
WZ[I,J,tempK])*KZd[I,J,K] ENDIF
                        IF tempK >= UPCELLk THEN CurZ2[I,J,K] = (WZ[I,J,K])*KZd[I,J,K] ENDIF
                        SetParameter(Z,"CurrentZ",CurZ)
                        SetParameter(Z,"CurrentZdown",CurZ2)
                    K = K + 1
                    ENDWHILE
                J=J+1
                ENDWHILE
            I = I +1
            ENDWHILE
        tempi = tempi +1
        ENDWHILE
    tempj = tempj +1
    ENDWHILE
tempk = tempk + 1
ENDWHILE

// Calculating the CurrentY through the system
CurY = CreateContinuousParameter(Z,"CurrentY")
CurY2 = CreateContinuousParameter(Z,"CurrentYback")
Iconize(CurY)
Iconize(CurY2)
```

```
tempk = 1
WHILE tempk <=no_lay DO
    tempj = 1
    WHILE tempj <=no_row DO
        tempi = 1
        WHILE tempi <= no_col DO
            UPCELLi = tempi*NO_COL/no_col
            I = (tempi-1)*UPCELLi/tempi +1
            WHILE I <=UPCELLi DO
                UPCELLk = tempk*NO_LAY/no_lay
                K = (tempk-1)*UPCELLk/tempk+1
                WHILE K <=UPCELLk DO
                    UPCELLj = tempj*NO_ROW/no_row
                    J = (tempj-1)*UPCELLj/tempj +1
                    WHILE J <= UPCELLj DO
                        IF J = (tempj-1)*UPCELLj/tempj +1 THEN CurY[I,J,K] = (1-WY[I,J,K])*
KYf[I,J,K] ENDIF
                        IF J > (tempj-1)*UPCELLj/tempj +1 AND J < UPCELLj THEN
                            tempJ = J - 1
                            CurY[I,J,K] = (WY[I,tempJ,K]- WY[I,J,K])*KYf[I,J,K]
                        ENDIF
                        tempJ = J +1
                        IF tempJ <= UPCELLj THEN CurY2[I,J,K] = (WY[I,J,K]-
WY[I,tempJ,K])*KYb[I,J,K] ENDIF
                        IF tempJ >= UPCELLj THEN CurY2[I,J,K] = (WY[I,J,K])*KYb[I,J,K] ENDIF
                        SetParameter(Z,"CurrentY",CurY)
                        SetParameter(Z,"CurrentYback",CurY2)
                    J = J + 1
                    ENDWHILE
                K=K+1
                ENDWHILE
            I = I +1
            ENDWHILE
        tempi = tempi +1
        ENDWHILE
    tempj = tempj +1
    ENDWHILE
tempk = tempk + 1
ENDWHILE

// Parameter CurrentX
// For CurrentX calculation
CurrX = Z.CurrentX
KXeff = CreateContinuousParameter(z,"K_Xeff")
Iconize(KXeff)
// Setting the upscale k to the upscaled grid and calculation of K effective
tempk = 1
WHILE tempk <=no_lay DO
    tempj = 1
    WHILE tempj <=no_row DO
        tempi = 1
        WHILE tempi <= no_col DO
            KXeff[tempi,tempj,tempk] = 0
            UPCELLi = tempi*NO_COL/no_col
            I = (tempi-1)*UPCELLi/tempi +1
            WHILE I <=UPCELLi DO
                UPCELLj = tempj*NO_ROW/no_row
```

```
                J = (tempj-1)*UPCELLj/tempj+1
                WHILE J <=UPCELLj DO
                    UPCELLk = tempk*NO_LAY/no_lay
                    K = (tempk-1)*UPCELLk/tempk +1
                    WHILE K <= UPCELLk DO
                        KXeff[tempi,tempj,tempk]= KXeff[tempi,tempj,tempk]+ CurrX[I,J,K]
                    K = K + 1
                    ENDWHILE
                J=J+1
                ENDWHILE
            I=I+1
            ENDWHILE
            KXeff[tempi,tempj,tempk] = KXeff[tempi,tempj,tempk]/(NO_LAY/ no_lay)
            SetParameter(z,"K_Xeff",KXeff)
        tempi = tempi +1
        ENDWHILE
    tempj = tempj +1
    ENDWHILE
tempk = tempk + 1
ENDWHILE

// Parameter CurrentZ
// For CurrentZ calculation
CurrZ = Z.CurrentZ
KZeff = CreateContinuousParameter(z,"K_Zeff")
Iconize(KZeff)
// Setting the upscale k to the upscaled grid and calculation of K effective
tempk = 1
WHILE tempk <=no_lay DO
    tempj = 1
    WHILE tempj <=no_row DO
        tempi = 1
        WHILE tempi <= no_col DO
            KZeff[tempi,tempj,tempk] = 0
            UPCELLk = tempk*NO_LAY/no_lay
            K = (tempk-1)*UPCELLk/tempk +1
            WHILE K <= UPCELLk DO
                UPCELLj = tempj*NO_ROW/no_row
                J = (tempj-1)*UPCELLj/tempj+1
                WHILE J <= UPCELLj DO
                    UPCELLi = tempi*NO_COL/no_col
                    I = (tempi-1)*UPCELLi/tempi +1
                    WHILE I <= UPCELLi DO
                        KZeff[tempi,tempj,tempk] = KZeff[tempi,tempj,tempk]+CurrZ[I,J,K]
                    I = I + 1
                    ENDWHILE
                J=J+1
                ENDWHILE
            K=K+1
            ENDWHILE
            KZeff[tempi,tempj,tempk] = KZeff[tempi,tempj,tempk]/((NO_COL/ no_col))
            SetParameter(z,"K_Zeff",KZeff)
        tempi = tempi +1
        ENDWHILE
    tempj = tempj +1
    ENDWHILE
tempk = tempk + 1
```

```
ENDWHILE

// Parameter CurrentY
// For CurrentY calculation
CurrY = Z.CurrentY
KYeff = CreateContinuousParameter(z,"K_Yeff")
Iconize(KYeff)
// Setting the upscale k to the upscaled grid and calculation of K effective
tempk = 1
WHILE tempk <=no_lay DO
    tempj = 1
    WHILE tempj <=no_row DO
        tempi = 1
        WHILE tempi <= no_col DO
            KYeff[tempi,tempj,tempk] = 0
            UPCELLj = tempj*NO_ROW/no_row
            J = (tempj-1)*UPCELLj/tempj+1
            WHILE J <= UPCELLj DO
                UPCELLk = tempk*NO_LAY/no_lay
                K = (tempk-1)*UPCELLk/tempk +1
                WHILE K <= UPCELLk DO
                    UPCELLi = tempi*NO_COL/no_col
                    I = (tempi-1)*UPCELLi/tempi +1
                    WHILE I <= UPCELLi DO
                        KYeff[tempi,tempj,tempk] = KYeff[tempi,tempj,tempk]+CurrY[I,J,K]
                    I = I + 1
                    ENDWHILE
                K=K+1
                ENDWHILE
            J=J+1
            ENDWHILE
            KYeff[tempi,tempj,tempk] = KYeff[tempi,tempj,tempk]/((NO_LAY/ no_lay))
            SetParameter(z,"K_Yeff",KYeff)
        tempi = tempi +1
        ENDWHILE
    tempj = tempj +1
    ENDWHILE
tempk = tempk + 1
ENDWHILE
```